

**PREDICTION OF ULTIMATE SIDE SHEAR FOR DRILLED SHAFTS IN
MISSOURI SHALES**

**A Thesis
Presented to
The Faculty of the Graduate School
University of Missouri-Columbia**

**In Partial Fulfillment
Of the Requirements for the Degree
Master of Science**

**By
Alan D. Miller, PE.**

Dr. Erik Loehr, Thesis Supervisor

August 2003

ACKNOWLEDGEMENTS

I would like to take this opportunity to thank my supervising professor Dr. J. Erik Loehr for advising, sharing his thoughts, knowledge and experience with me while completing my research and thesis. I would also like to express my gratitude to Dr. John J. Bowders and Dr. Douglas E. Smith for reviewing this document as well as their valuable comments.

This thesis could not have been completed without the support and cooperation of many companies and individuals. I would like to thank Mr. Wayne Duryee from HNTB and Mr. Eric Neprud from Harrington and Cortelyou, Inc. for providing the use of their reports, pictures, illustrations, and guidance. I would like to thank Mr. Bill Ryan and Mr. Mike Ahrens from Loadtest Inc., for answering my many questions. Mr. Dave Smith from the Missouri Geologic Survey who helped me identify the geologic sections at the Lexington and the Waverly test sites. I would also like to thank Mr. Charles Rugg and Mr. Billie Tucker from Missouri Department of Transportation who where the construction inspectors for the Lexington and Waverly test sites respectively and helped with photographs and field information.

Finally I would like to thank the Missouri Department of Transportation, my boss (Mike Fritz), and my fellow employees for providing time and encouragement in the completion of this thesis.

TABLE OF CONTENTS

ACKNOWLEDGEMENTS	ii
LIST OF ILLUSTRATIONS	vi
LIST OF TABLES	xiv
ABSTRACT	xvi
CHAPTER	
1. INTRODUCTION	1
1.1 Problem Statement	1
1.2 Organization of Thesis	1
2. METHODS FOR PREDICTING SIDE SHEAR IN ROCK	4
2.1 Side Shear	4
2.2 Empirical Methods	6
2.2.1 Rosenberg and Journeaux	6
2.2.2 Horvath and Kenney	7
2.2.3 Williams et al. and Williams and Pells	9
2.2.4 Rowe and Armitage	11
2.2.5 Reese and O'Neill	11
2.2.6 Kulhawy and Phoon	12
2.2.7 Discussion of Empirical Methods	13
2.3 Factors Affecting Unit Side Shear for Drilled shafts in Rock	14
2.3.1 Interface roughness	15
2.3.2 Cleanliness of interface	17
2.3.3 Initial lateral concrete pressures	18
2.3.4 Length of time borehole remains open prior to concreting	19
2.3.5 Angle of internal friction and angle of interface dilation	19
2.3.6 Formation stiffness	19
2.3.7 Socket diameter	20
2.3.8 Loading Direction	22
2.4 Analytical methods	23
2.4.1 Kodikara et al.	24
2.4.2 McVay et al.	25
2.4.3 O'Neill and Reese	26
2.5 Summary	28
3. GENERAL OSTERBERG CELL TEST METHODS AND PROCEDURES	30
3.1 Description of Osterberg cell load test	30
3.2 Osterberg Load test Procedure	33
3.3 Instrumentation and data collection	34
3.4 Basic Interpretation of O-cell TM Tests	40
3.5 Determination of Creep Limit	45
3.6 Determination of Load-Transfer ((t-z) Curves	47
3.7 Determination of Unit Side Shear	52
3.8 Summary	53

4. LEXINGTON, MO. TEST SITE	56
4.1 Site Description	57
4.2 Geology of the Area	62
4.2.1 Fleming Formation	64
4.2.2 Croweburg Formation	64
4.2.3 Verdigris Formation	65
4.2.4 Bevier Formation	65
4.2.5 Lagonda Formation	66
4.2.6 Mulky Formation	66
4.3 Jar Slake Test of Shale Bedrock	67
4.4 Unconfined Compressive Strength of Bedrock at Piers 19 thru 24	68
4.5 Foundation Design	69
4.6 Construction of Test Shafts	70
4.6.1 Construction of Test Shafts TS-1 and TS-1A	71
4.6.2 Construction of Test Shaft TS-2	77
4.7 Load Test Setup and Procedures	82
4.7.1 Test Shaft TS-1A Setup and Procedure	82
4.7.2 Test Shaft TS-2 Setup and Procedure	84
4.8 General Test Results	85
4.8.1 Test Results for TS-1A	87
4.8.2 Test Results for TS-2	93
4.8.2.a Stage 1 Results	93
4.8.2.b Results for Stage 2 and 3	99
4.9 Practical Applications	106
4.10 Summary and Conclusions	107
5. GRANDVIEW TRIANGLE TEST SITE	108
5.1 Site Description	109
5.2 Geology of the Area	116
5.2.1 Cherryvale Formation	116
5.2.2 Drum Limestone Formation	119
5.2.3 Chanute Shale Formation	119
5.3 Unconfined Compressive Strength of Bedrock	120
5.4 Foundation Design	121
5.5 Construction of Test Shaft	123
5.6 Load Test Setup and Procedures	129
5.7 General Test Results	132
5.8 Practical Applications	140
5.9 Discussion	141
5.10 Summary and Conclusions	144
6. WAVERLY, MO. TEST SITE	146
6.1 Site Description	147
6.2 Geology of the Area	152
6.3 Unconfined Compressive Strength of Bedrock at Pier 11	156

6.4 Foundation Design	157
6.5 Construction of Test Shaft	157
6.6 Load Test Setup and Procedures	164
6.7 General Test Results	166
6.8 Practical Applications	172
6.9 Summary and Conclusions	173
7. EVALUATION OF DESIGN METHODS	175
7.1 Introduction	175
7.2 Summary of Test Results	175
7.3 Interpreted Alpha Factors	178
7.4 Evaluation of Design Methods	181
7.5 Summary	187
8. SUMMARY, CONCLUSIONS, AND RECOMMENDATIONS	191
8.1 Summary	191
8.2 Conclusions	193
8.3 Lessons Learned	195
8.4 Recommendations	196
APPENDICES	
A. Detailed data for load test and unconfined compressive strength of NX cores at Lexington site	198
B. Detailed data for load test and unconfined compressive strength of NX cores at Grandview site	218
C. Detailed data for load test and unconfined compressive strength of NX cores at Waverly site	233
D. SI units for Chapter 7 tables and figures	250
E. Construction and load test photographs for Lexington site (HNTB 1999)	262
F. Boring logs and core photographs for Lexington test site	278
G. Construction and load test photographs for Grandview site (HNTB 2000)	312
H. Boring logs and core photographs for Grandview test site	325
I. Construction and load test photographs for Waverly site	342
J. Boring logs and core photographs for Waverly test site	351
K. Geology for South abutment at Lexington site	367
REFERENCES	371

LIST OF ILLUSTRATIONS

Figure

2.1	Schematic of rock socket parameters (after Horvath et al. 1983).	8
2.2	Adhesion Factor α versus unconfined compressive strength (from Williams et al. 1980).	10
2.3	Side Resistance Reduction Factor β versus mass modulus factor (from Williams et al. 1980).	10
2.4	Model of Socket Roughness for Melbourne Mudstone where i_m = mean value of angle between face of the asperity or groove and the vertical, and h_m = mean double-amplitude height of the asperities (after Kodikara et al. 1992).	16
2.5	Sinusoidal interface pattern in clay shale (after O'Neill and Hassan 1993).	17
2.6	Unit side shear versus shear displacement for drilled shaft socket in rock of moderate roughness with $q_u = 3.0$ MPa (after Baycan 1996).	21
2.7	Comparison of side load versus displacement curve for top-down and O-cell TM loading test based on finite-element analyses (from Shi 2002).	23
2.8	$\alpha\beta$ versus borehole roughness where E_m is the estimated modulus or formation stiffness of the rock mass, σ_n is the initial radial pressure on the interface and can be taken as the estimated fluid pressure produced by the concrete (after Kodikara et al. 1992).	25
2.9	Adhesion factor α versus compressive strength q_u (from O'Neill et al. 1996).	27
3.1	Schematic of typical Osterberg cell load test.	32
3.2	Typical Osterberg load test load-displacement curves.	34
3.3	Typical instrumentation at the top of a drilled shaft.	35
3.4	Typical instrumentation at the top of a drilled shaft (from Loadtest).	36
3.5	Embedment strain gages (from Geokon).	37

3.6	Sister bars used to monitor stress within drilled shafts.....	38
3.7	Sister bar mounted on rebar cage.....	38
3.8	Embedded compression telltale (ECT) gage mounted in rebar cage.....	39
3.9	Schematic of embedded compression telltale.....	39
3.10	Typical Osterberg cell load displacement curves.....	40
3.11	Construction of “equivalent” top-down load-displacement curve from upward and downward load-displacement curves from O-cell™ test.....	42
3.12	Equivalent top-down load-displacement curve adjusted for additional elastic compression.....	45
3.13	Creep displacements from O-cell™ load tests as a function of applied load: (a) upper portion of shaft and (b) lower portion of shaft.....	48
3.14	Osterberg cell load-displacement curves showing creep limit displacements.....	49
3.15	Equivalent top-down load-displacement curve with creep limit.....	49
3.16	Load distribution curves determined from strain gage data.....	51
3.17	Typical load distribution from a top-down load test on a drilled shaft (from Reese 1984).....	52
3.18	Distribution of load with depth for top-down load test (after Kyfor et al. 1992).....	54
3.19	Unit side shear versus O-cell displacement relationship for several segments of a drilled shaft.....	55
4.1	Location sketch of Lexington bridge site.....	58
4.2	Plan view of Lexington bridge showing location of bridge bents and test shafts.....	59
4.3	Elevation view of bridge showing piers 19- 24 and test shafts TS-1A and TS-2.....	61
4.4	Stratigraphy of Lexington test site.....	63

4.5	Jar slake index test results for Croweburg Formation: Elev. 172.27 m , slake index (2).	64
4.6	Range of jar slake index test results for Verdigris Formation: (a) Elevation 176.75 m, slake index (1); (b) elevation 175.27 m, slake index (2).	65
4.7	Range of jar slake index test results for Bevier Formation: (a) Elevation 183.95 m, slake index (6); (b) elevation 180.45 m, slake index (5).	66
4.8	Manitowoc 4100 series crane with drill assembly.	71
4.9	Schematic of test shaft TS-1A.	73
4.10	Sonar caliper prior to placement in test shaft excavation.	74
4.11	Preparing to lower carrying frame and O-cell™ into test shaft TS-1A.	74
4.12	Carrying frame and instrumentation for test shaft TS-1A.	75
4.13	Sonar caliper log of rock socket for test shaft TS-1A.	76
4.14	Schematic of test shaft TS-2.	78
4.15	Carrying frame and two Osterberg load cells for test shaft TS-2.	79
4.16	Lowering carrying frame and O-cells for test shaft TS-2.	79
4.17	Sonar caliper log of rock socket for test shaft TS-2 (81-98 ft from top of casing).	80
4.18	Sonar caliper log of rock socket for test shaft TS-2 (98.5-117.5 ft from top of casing).	81
4.19	Schematic of test shaft TS-1A showing location of instrumentation.	83
4.20	Schematic of test shaft TS-2 showing location of instrumentation.	86
4.21	Measured load-displacement curves for downward and upward loading of test shaft TS-1A.	87
4.22	Equivalent top-down load-displacement curve for TS-1A.	88
4.23	Distribution of axial force for test shaft TS-1A.	89

4.24 Mobilized unit side shear versus O-cell TM movement for test shaft TS-1A.....	91
4.25 Mobilized unit side shear values calculated from strain gage data for test shaft TS-1A.....	92
4.26 Creep displacement for upper portion of test shaft TS-1A.....	92
4.27 Creep displacement for lower portion of test shaft TS-1A.....	93
4.28 Measured load-displacement curves for lower O-cell TM in test shaft TS-2, Stage 1.....	94
4.29 Equivalent top-down load-displacement curves for test shaft TS-2, Stage 1....	94
4.30 Distribution of axial force for test shaft TS-2, Stage 1.....	96
4.31 Unit side shear versus lower O-cell TM movement for test shaft TS-2, Stage 1..	96
4.32 Mobilized unit side shear values calculated from strain gage data for test shaft TS-2, Stage 1.....	97
4.33 Creep displacement for upper portion of test shaft TS-2, Stage 1.....	98
4.34 Creep displacement for lower portion of test shaft TS-2, Stage 1.....	99
4.35 Measured load-displacement curves for downward and upward loading of O-cell TM in test shaft TS-2, Stages 2 & 3.....	100
4.36 Equivalent top-down load-displacement curves for test shaft TS-2, Stages 2 and 3.....	101
4.37 Distribution of axial force for test shaft TS-2, Stages 2 & 3.....	102
4.38 Unit side shear versus upper O-cell TM movement for test shaft TS-2, Stages 2 & 3.....	103
4.39 Mobilized unit side shear values calculated from strain gage data for test shaft TS-2, Stages 2 & 3.....	104
4.40 Creep displacements for upper segment of shaft for test shaft TS-2, Stages 2 & 3.....	105
4.41 Creep displacements for middle segment of shaft for test shaft TS-2, Stage 2.....	105

5.1	Roadmap of Grandview Triangle are in Metropolitan Kansas City.....	110
5.2	Grandview Triangle (from HNTB 2002).....	111
5.3	Grandview Triangle bridges and Osterberg cell load test site (from HNTB 2002).....	112
5.4	Kansas City Stratigraphy (from URS 2001).....	114
5.5	Kansas City Stratigraphy (from URS 2001).....	115
5.6	Elevation view of Pier 3 thru 7 for bridge A6252.....	117
5.7	Range of jar slake index test results for Wea Shale Member: (a) elevation 986.0 ft, slake index (3), (b) elevation 880.8 ft, slake index (6).....	118
5.8	Range of jar slake index test results for Quivira Shale Member: (a) elevation 905.7 ft., slake index (1), (b) elevation 910.0 ft., slake index (4).	119
5.9	Range of jar slake index test results for Chanute Shale Member: (a) elevation 920.0 ft., slake index (1), (b) elevation 916.2 ft., slake index (4).....	120
5.10	Grandview Triangle load test site (from HNTB 2002).....	122
5.11	Schematic of Grandview Triangle test shaft and various shale strata.....	125
5.12	Compressible end-bearing device.....	126
5.13	Watson 3100 drill rig.....	126
5.14	Sonic caliper log of Grandview Triangle test shaft (from HNTB 2002).....	127
5.15	Lowering load frame into Grandview Triangle test shaft.....	128
5.16	Placing shaft concrete using tremie and pump truck.....	129
5.17	Schematic of Grandview test shaft instrumentation.....	131
5.18	Measured load displacement curves for upward and downward loading of test shaft at the Grandview Triangle site.....	133

5.19	Equivalent top-down load-displacement curves for Grandview Triangle test shaft.....	134
5.20	Distribution of axial force curves for the Grandview Triangle test shaft.....	135
5.21	Mobilized unit side shear versus O-cell displacement for various geologic strata at the Grandview Triangle test site.....	136
5.22	Mobilized unit side shear calculated from strain gage data for Grandview Triangle test shaft.....	138
5.23	Zone of influence for level 2 and 3 strain gages.....	138
5.24	Creep displacement for upper portion of Grandview Triangle test shaft.....	139
5.25	Creep displacement for lower portion of Grandview Triangle test shaft.....	140
5.26	Influence of strain gage positioning (after Hayes and Simmonds 2002).....	142
5.27	Adjusted axial load curve based on assumed unit side shear value for Quivira Shale.....	143
6.1	Location sketch at Waverly bridge site.....	148
6.2	Plan and elevation view Waverly bridge site.....	149
6.3	Elevation view of bridge showing Piers 9 thru 12 and the location of the test shaft.....	151
6.4	Range of jar slake index test results for Zone A Weir Formation: (a) elevation 606.1 ft., slake index (2), (b) elevation 602.6 ft., slake index (2).....	153
6.5	Range of jar slake index test results for Zone B Weir Formation: (a) elevation 597.1 ft., slake index (1), (b) elevation 590.6 ft., slake index (3).....	154
6.6	Range of jar slake index test results for Zone C Weir Formation: (a) elevation 581.9 ft., slake index (5), (b) elevation 578.5 ft., slake index (6).....	155
6.7	Range of jar slake index test results for Zone D Weir Formation: (a) elevation 565.2 ft., slake index (3), (b) elevation 571.5 ft., slake index (5).....	155
6.8	Pier 11 at Waverly site.....	158

6.9	Schematic of the test shaft at Pier 11.	159
6.10	American 9270 Series crane with a Hain twin drill, drilling rock socket at Pier 12, existing bridge in background.	160
6.11	Temporary outer casing, inner permanent casing, and casing clamp at Pier 12 (Pier 11 is in the background).	160
6.12	Bullet tooth rock auger used to excavate rock socket at Waverly test site.	161
6.13	Core Barrel used to excavate rock socket at Waverly test site.	162
6.14	Miniature shaft inspection device (Mini-SID) used to inspect bottom of rock socket at Waverly bridge site.	162
6.15	Rebar cage with Osterberg load cell.	163
6.16	Schematic of test shaft showing location of instrumentation.	165
6.17	Measured load-displacement curves for test shaft at Waverly site.	167
6.18	Equivalent top-down load-displacement curves for Waverly test shaft.	168
6.19	Distribution of axial force for the Waverly test shaft.	169
6.20	Mobilized unit side shear versus O-cell TM displacement for Waverly test shaft.	170
6.21	Mobilized unit side shear values calculated from strain gage data for the Waverly test shaft.	170
6.22	Creep displacements for the upper portion of the Waverly test shaft.	171
6.23	Creep displacements for the lower portion of the Waverly test shaft.	172
7.1	Unit side shear versus average q_u .	177
7.2	Back-calculated alpha factor (α) versus the average q_u for test sites in shale.	179

7.3	Back-calculated alpha factor (α) versus average q_u :	
	(a) q_{u-avg} . plus one standard deviation,	
	(b) q_{u-avg} . minus one standard deviation.....	183
7.4	Comparison of measured unit side shear data to predicted unit side shear by several methods.....	185
7.5	Factor M versus concrete slump (after O'Neill et al. 1996).....	185
7.6	Modified Rowe and Armitage method.....	186
7.7	Comparison of measured and predicted unit side shear value using the Horvath and Kenney (1979) method.....	188
7.8	Comparison of measured and predicted unit side shear value using the Rowe and Armitage (1987) method.....	189
7.9	Comparison of measured and predicted unit side shear value using the modified Rowe and Armitage (1987) method.....	190

LIST OF TABLES

Table	
2.1	Roughness classification (after Pells et al. 1980)..... 11
2.2	Characterization of borehole roughness (from Kodikara et al. 1992)..... 24
2.3	Adjustment factor for soft seams and joints (O'Neill & Reese 1999)..... 27
3.1	Available O-cell TM sizes and capacities..... 33
3.2	Comparison of the maximum mobilized unit side shear (after Shi 2002)..... 55
4.1	Summarized of jar slake index tests results for shale formations at Lexington site. 67
4.2	Unconfined compressive strengths for rock cores at Lexington site..... 68
4.3	Unit side shear values calculated from strain gage data for test shaft TS-1A... 91
4.4	Unit side shear values calculated from strain gage data for test shaft TS-2, Stage 1..... 97
4.5	Unit side shear values calculated from strain gage data for test shaft, TS-2, Stages 2 & 3..... 103
4.6	Costs for Osterberg cell load tests for test shafts TS-1A and TS-2..... 106
4.7	Anticipated cost savings for drilled shafts..... 106
5.1	Results of jar slake index tests of shale formations at the Grandview Triangle site..... 120
5.2	Unconfined compressive strengths of rock strata at the Grandview Triangle site..... 121
5.3	Unit side shear values calculated from strain gage data for the Grandview Triangle test shaft..... 137
6.1	Drilled shaft parameters for Piers 10, 11, and 12..... 150
6.2	Summary of jar slake tests index test results of Weir Formation at Waverly site..... 153

6.3	Unconfined compressive strengths for Pier 11.....	156
6.4	Mobilized unit side values calculated from strain gage data for the Waverly test shaft.....	171
7.1	Summary of measured unit side shear values and unconfined compressive strength (q_u) values of shale at test sites.....	176
7.2	Summary of back-calculated alpha values for shale at Missouri test sites.....	180
7.3	Comparison of measured and predicted unit side shear determined by various methods.....	184

PREDICTION OF ULTIMATE SIDE SHEAR FOR DRILLED SHAFTS IN MISSOURI SHALES

Alan D. Miller, PE.

Dr. Erik Loehr, Thesis Supervisor

ABSTRACT

Bridges crossing major rivers in the State of Missouri have relied heavily on drilled shafts socketed into bedrock as the principal means of achieving bearing capacity of the foundation elements. Rock sockets in shales and weak rocks are designed to develop axial capacity in side shear. End bearing is usually neglected. The current procedures used by the Missouri Department of Transportation (MoDOT) to estimate the ultimate unit side shear follow procedures in the 1996 AASHTO and FHWA-IF-99-025 manuals. The methods provided in these manuals roughly predict the ultimate unit side shear to be equal to 0.15 times the unconfined compressive strength (q_u) of the shale core. These design methods have lead to the design of rock sockets 1.5 to 2.5 meters (5 to 8 ft) in diameter and as long as 15 meters (50 ft) to support loads in the range of 112 to 169 MN (1000 to 1500 tons). In order to achieve more economical designs and to take some of the uncertainty out of the prediction of the ultimate unit side shear, MoDOT conducted four full-scale Osterberg cell (O-cell) load tests at three different sites.

Analysis of the load test data indicated that the ultimate unit side shear may be conservatively estimated as 0.3 times the unconfined compressive strength of the shale. Design methods proposed by Rowe and Armitage (1987) and Kulhawy and Phoon (1993) produced almost identical results and most closely predicted the ultimate unit side shear measured in the load tests. Because the Rowe and Armitage (1987) method slightly over-

estimates the ultimate unit side shear for shale with low compressive strengths, a minor modification of the method is proposed to produce slightly more conservative values. Finally, the analysis of the load test data will lead to significant increases in the predicted ultimate unit side shear over current methods followed by MoDOT.

CHAPTER ONE INTRODUCTION

1.1 Problem Statement

Design of foundations for bridges in the State of Missouri have relied heavily on drilled shafts socketed into bedrock as the principal means of achieving bearing capacity of the foundation elements. Rock sockets in shales and weak rocks are designed to develop axial capacity in side shear. End bearing is usually neglected. Current procedures used by the Missouri Department of Transportation (MoDOT) to estimate the ultimate unit side shear capacity in weak rock often lead to exceedingly long rock sockets. As a result, MoDOT has conducted four Osterberg Load cell tests on large drilled shafts at three different bridge sites. These load tests and the results they have produced are the subject of this thesis. The objective of this thesis is to document the load tests and to present an evaluation of several design methods based on the results of these tests.

1.2 Organization of Thesis

Existing empirical and analytical methods for predicting the ultimate unit side shear capacity for drilled shafts socketed into weak rock are presented in Chapter 2. Empirical methods are generally based on results of full-scale load tests while analytical methods attempt to model the soft rock-drilled shaft interface numerically, often using the finite-element method.

All load tests presented in this thesis were performed using the Osterberg cell (O-cellTM) method of loading, invented by Dr. Jorj Osterberg. The general procedures used to perform and interpret O-cell load tests are described in Chapter 3, along with

associated instrumentation such as strain gages and telltales used to determine end bearing and side shear capacities of drilled shafts.

The results of the four load tests are presented in Chapters 4, 5, and 6. In each of these chapters, the general geology of the site area is first described followed by more thorough descriptions of the specific strata involved in the load tests. The procedures followed to construct the test shafts and perform the load tests are then described along with presentation of the shaft layout and associated instrumentation. Finally, the results of each load test are presented.

In Chapter 4, load tests performed on two full-scale drilled shafts for a proposed bridge across the Missouri River at Lexington, Missouri are described. The bedrock at the Lexington site consists of Pennsylvanian Age shales, siltstones, sandstones, limestones, and scattered coal beds. The shafts were tested to maximum loads of 13.3 MN (1,495 tons) and 17.5 MN (1,968 tons) in May and June of 1999. The Osterberg cell load tests were successful in allowing MoDOT to develop a more economical design for the drilled shafts for the proposed bridge.

Chapter 5 presents the results of a load test performed on a full-scale drilled shaft as part of the reconstruction of an interchange in the Kansas City metropolitan area known as the Grandview Triangle. The bedrock at the Grandview Triangle site consists of horizontally bedded layers of limestones and shales known as the Kansas City Group. The shaft was loaded to 34.3 MN (3,856 tons) on June 3, 2002. Data from the Osterberg cell load test would allow the 2.3 m (7.5 ft) diameter rock sockets at bridge A6252 to be shortened a total of 65.2 m (214 ft) for a net savings of \$19,000.

A load test on a “production” drilled shaft for a proposed bridge across the Missouri River at Waverly, Missouri is described in Chapter 6. The bedrock at the Waverly site consists of Pennsylvanian Age shales, siltstones, sandstones, limestones, and scattered coal beds. The production shaft was tested to a maximum load of 22.5 MN (2,525 tons), on September 30, 2002. The Osterberg cell load test was successful in testing the shaft to twice the design load and assuring the foundation engineers that the main river pier would be safe.

In Chapter 7, the results of all four tests are summarized with particular focus on values of unit side shear determined from the load tests for various strata. The measured unit side shear values are then compared to values predicted by several current design methods and a method to more accurately predict ultimate unit side shear in Missouri shales is proposed. Finally, Chapter 8 includes a summary of this thesis, conclusions reached from the four load tests described, and several recommendations for further work.

CHAPTER TWO

METHODS FOR PREDICTING SIDE SHEAR IN ROCK

Empirical and analytical methods for predicting the unit side shear capacity of drilled shafts socketed into weak rock are presented in this chapter. Empirical methods are generally based on results from full-scale load tests while analytical methods attempt to model the soft rock-drilled shaft interface numerically, often using finite-element solutions.

Rock socketed drilled shafts transfer axial load through upper non-competent strata to competent bedrock, which can sustain the load. The load is transferred to the bedrock through two basic load bearing mechanisms, end bearing and side shear (Kiehne 1997). Drilled shafts designed to carry load in end bearing require construction and inspection techniques that guarantee the cleanliness of the base (Pells 1980). This may be difficult to achieve, particularly for deep sockets that use a drilling fluid such as water or slurry. Rock socketed end bearing drilled shafts normally require competent rock which can support large loads for at least two shaft diameters below the base of the rock socket. For weak rocks such as shales that cannot carry large loads in end bearing, rock socketed drilled shafts are designed to carry axial load primarily in side shear. The ultimate unit side shear may be related to factors created by construction technique such as interface roughness and cleanliness, properties of the weak rock, such as cohesion and angle of internal friction, and the geometry of the rock socket.

2.1 Side Shear

Many designers prefer to design drilled shafts to take load in side shear only versus combined side shear and end bearing because the amount of movement required to

mobilize side shear is relatively small, while that required to mobilize end bearing is relatively large (Osterberg 2000). Side shear is generally fully mobilized when shaft movement is 6 to 13 mm (1/4 to 1/2 inch) while end bearing is not fully mobilized until the movement is on the order of centimeters (inches).

Both empirical and analytical methods have been used to predict the ultimate unit side shear of rock sockets (Carruba 1997). Empirical methods are generally based on full-scale load tests in which the ultimate unit side shear is back-calculated from instrumentation. The ultimate unit side shear (f_{\max}) is then related to the unconfined compressive strength of the soil/rock (q_u) using an empirical constant, usually denoted α , as

$$f_{\max} = \alpha \cdot q_u \quad (2.1)$$

Other researchers have attempted to address drilling parameters such as rock socket roughness by adding a second constant, β . In this case the empirical relation takes the form

$$f_{\max} = \alpha \cdot \beta \cdot q_u \quad (2.2)$$

Still other researchers believe the true expression relating unit side shear to unconfined compressive strength is a power function of the form

$$f_{\max} = \alpha \cdot (q_u)^c \quad (2.3)$$

Analytical methods are often based on finite element methods and are generally similar in form to equations 2.1 through 2.3 with additional factors to address roughness, initial normal stress at the shaft rock interface, stiffness and cohesion of the rock mass,

and the presence of joints or seams in the rock mass. Specific empirical methods are described in Section 2.2; analytical methods are described in Section 2.4.

2.2 Empirical Methods

The following empirical methods have been developed based on data from the geographic area and/or rock formations of interest to the authors. As with all empirical methods, additional calibration should be performed using full-scale load tests for geographic areas or rock formations that are significantly different than those used to develop the methods.

2.2.1 Rosenberg and Journeaux

The Rosenberg and Journeaux (1979) method is based on a top-down load test performed on a 457 mm (18 in) diameter rock socket in highly fractured Andesite with an unconfined compressive strength of 10.3 MPa (108 tsf) and a pullout test on a 203 mm (8 in) diameter rock socket in shale with an unconfined compressive strength of 20.7 MPa (216 tsf). A 0.1 m (4 in) styrofoam isolating pad was placed at the base of the 560 mm (22 in) long rock socket for the top-down load test to eliminate end bearing. Rosenberg and Journeaux correlated their test data with tests performed by Moore (1964), Matich and Kozicki (1967), Thorburn (1966), Seychuck (1970), Gibson and Deveny (1973), and Jackson et al. (1974) in shales and sandstones in Canada. They found that the ultimate unit side shear was best predicted as

$$f_{\max} = 1.11 (q_u)^{0.51} \quad (2.4)$$

where f_{\max} and q_u are given in tsf.

2.2.2 Horvath and Kenney

Horvath and Kenney (1979) developed a method based on data from 50 sites in Australia, Canada, England, and the U.S. They found that ultimate unit side shear was best predicted as

$$f_{\max} = \alpha (q_u)^{0.5} \quad (2.5)$$

where α is 2.5 to 3 for shafts greater than 16 inches in diameter and f_{\max} and q_u are given in psi. For SI units, α is 0.2 to 0.25 for shafts greater than 406 mm (16 in) in diameter and f_{\max} and q_u are given in MPa.

Horvath et al. (1983) subsequently proposed a modification to address borehole roughness for artificially roughened boreholes by evaluating α based on the depth of the grooves in the rock socket as shown in Figure 2.1. They found that the coefficient α could be computed as

$$\alpha = RF^{0.45} = 0.8 \left[\Delta r / r (L_t / L_s) \right]^{0.45} \quad (2.6)$$

where RF is a dimensionless roughness factor, Δr is the average height of the asperities or grooves, r is the nominal socket radius to the base of the grooves, L_t is total distance along the socket wall profile, and L_s is the nominal socket length.

Socket roughness may be determined approximately in the field with either mechanical or electronic calipers. Sonic calipers may be used in dry holes while sonar calipers are available for drilled shafts constructed using either water or drilling slurry. Recently, a laser bore-hole caliper has been developed in Australia (Seidel 1998). Reese and O'Neill (1988) define a socket as rough if the roughness factor, RF, exceeds 0.10.

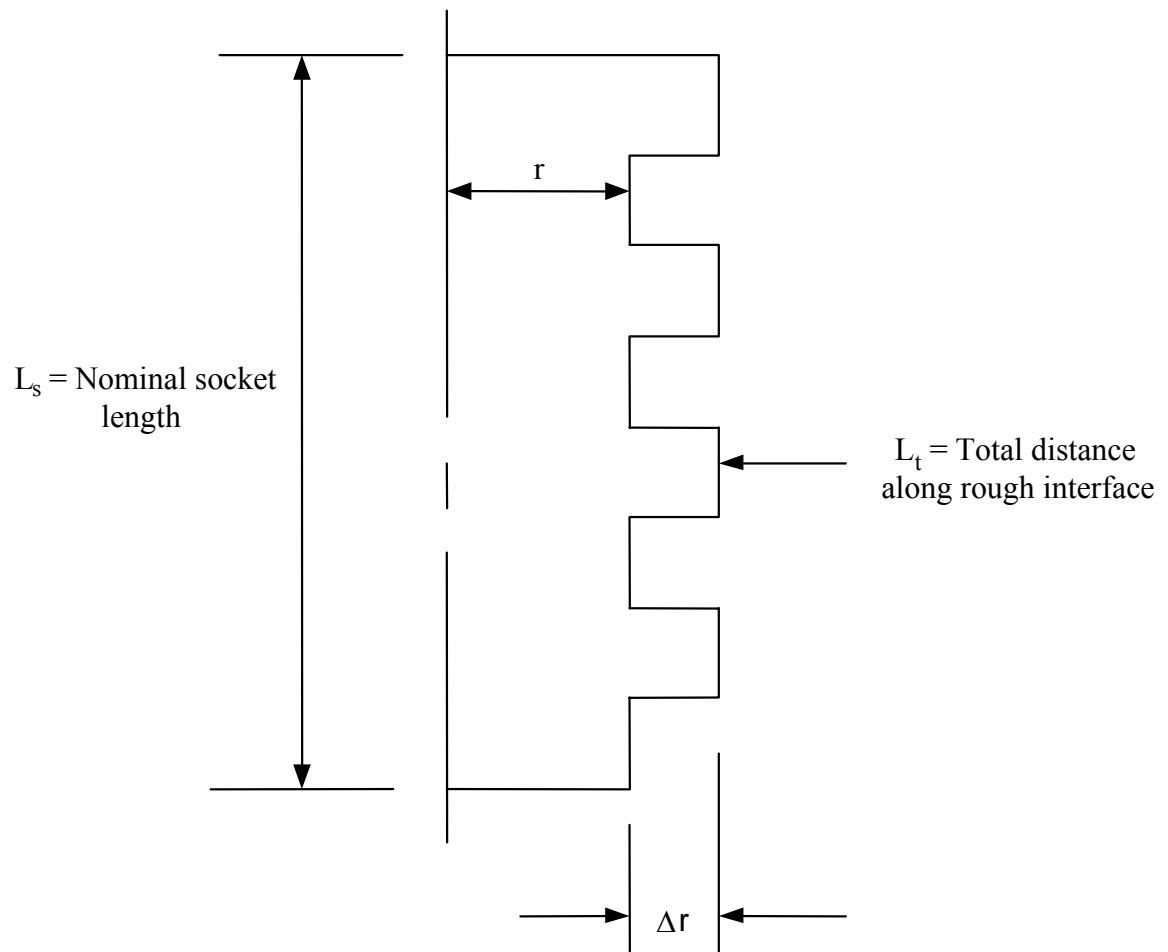


Figure 2.1- Schematic of rock socket parameters (after Horvath et al. 1983).

2.2.3 Williams et al. and Williams and Pells

Williams and his colleagues (Williams et al. 1980; Williams and Pells 1981) developed a semi-empirical method based on 15 load tests on shafts with diameters ranging from 335 to 1580 mm (13 to 62 in) founded in the Silurian-aged Mudstone in Melbourne, Australia and 27 load tests on drilled shafts with diameters ranging from 64 to 710 mm (2.5 to 28 in) in the Hawkesbury sandstone in Sydney. They found that f_{\max} could be estimated as

$$f_{\max} = \alpha \cdot \beta \cdot q_u \quad (2.7)$$

where α reflects variations in the intact strength of the rock only and can be obtained from Figure 2.2, and β is an adjustment factor to account for seams of softer material in the rock. If laminations are closed tightly, β is taken to be 1.0. Otherwise β is obtained from Figure 2.3, where

$$E_m / E_c = \frac{L_c}{(E_c / E_s) \sum t_s + \sum t_c} \quad (2.8)$$

where E_m is Young's modulus of the rock mass, E_c is Young's modulus of intact rock cores, and E_s is the Estimated Young's modulus of the material in seams (all given in MPa) L_c is the length of core, t_s is the thickness of each seam, and t_c is the thickness of intact rock (all given in either mm or meters).

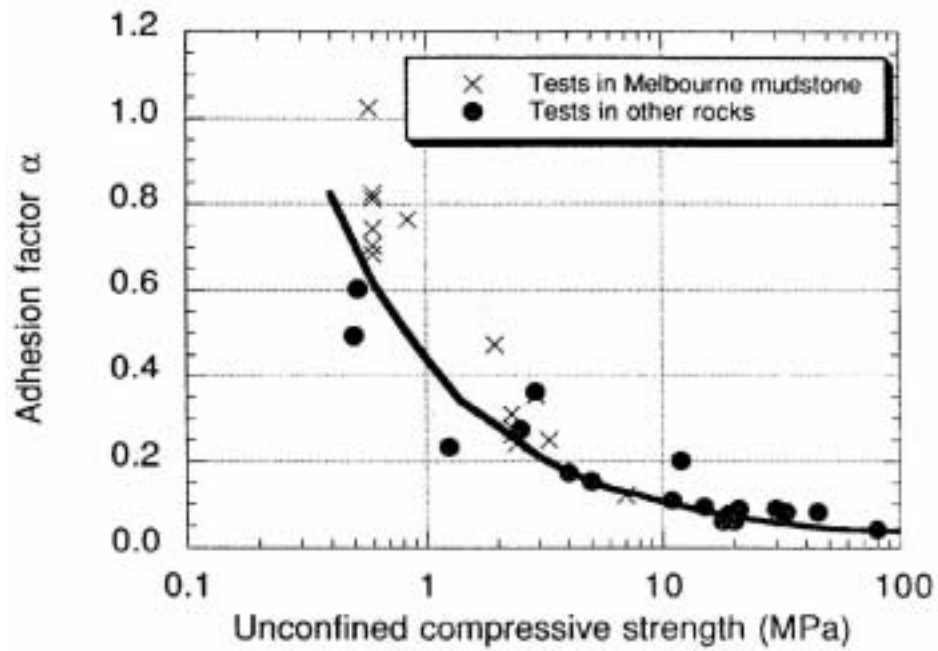


Figure 2.2- Adhesion factor α versus unconfined compressive strength (from Williams et al. 1980).

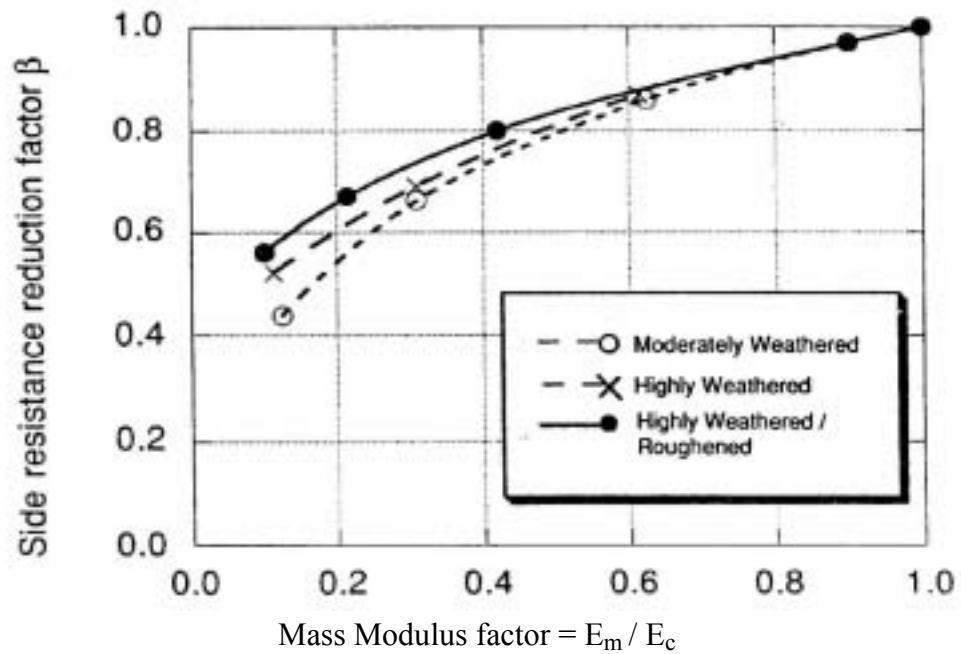


Figure 2.3- Side resistance reduction factor β versus mass modulus factor (from Williams et al. 1980).

2.2.4 Rowe and Armitage

Rowe and Armitage (1987) proposed a method that assumes the interface is clean and the side of the shaft is in either a natural state or artificially roughened. This method was confirmed based on load tests on drilled shafts with relatively smooth interfaces in Ordovician aged shales in southern Ontario Canada. The equations they proposed are based on a shaft roughness classification by Pells et al.(1980) as defined in Table 2.1.

For roughness classes R1, R2, and R3, they propose computing f_{\max} as

$$f_{\max} = 0.45 (q_u)^{0.5} \quad (2.9)$$

where f_{\max} and q_u are in MPa. For roughness class R4, the equation is

$$f_{\max} = 0.6 (q_u)^{0.5} \quad (2.10)$$

Table 2.1= Roughness Classification (after Pells et al. 1980).

Roughness Class	Description
R1	Straight, smooth sided socket, grooves or indentions less than 1 mm deep.
R2	Grooves of depth 1 to 4 mm, width greater than 2 mm, at spacing 50 – 200 mm.
R3	Grooves of depth 4 to 10 mm, width greater than 5 mm, at spacing 50 – 200 mm.
R4	Grooves or undulations of depth greater than 10 mm, width greater than 10 mm, at spacing 50 – 200 mm.

2.2.5 Reese and O'Neill

Reese and O'Neill (1988) proposed a method for the Federal Highway Administration (FHWA) that is derived from a method developed by Kulhawy (1983) in an earlier FHWA publication on drilled shafts. The 1988 FHWA method conservatively recommends assuming that the load is carried entirely in side shear or entirely in end bearing, depending on whether or not the computed settlement is more or less than 10

mm (0.4 in). Based on load tests in three clay-shale formations, Reese and O'Neill recommended using Equation 2.5, developed by Horvath and Kenney (1979), for rock with an unconfined compressive strength greater than 2.01 MPa (21 tsf). For rock with an unconfined compressive strength of 1.72 MPa to 2.01 MPa (18 to 21 tsf) they recommended that an equation developed by Carter and Kulhawy (1987) be used to determine the ultimate unit side shear. The Carter and Kulhawy relationship is given as

$$f_{\max} = 0.15 q_u \quad (2.11)$$

where q_u is in the range of $2.01 \geq q_u \geq 1.72$ MPa ($21 \geq q_u \geq 18$ tsf). For rock with an unconfined compressive strength less than 0.38 MPa (4 tsf) they recommended that ultimate unit side shear be calculated as

$$f_{\max} = 0.275 q_u \quad (2.12)$$

where $q_u \leq 0.38$ MPa (4 tsf). Values of the ultimate unit side shear for q_u between 0.38 MPa and 1.72 MPa (4 tsf and 18 tsf) may be determined by interpolation between equations 2.11 and 2.12.

2.2.6 Kulhawy and Phoon

Kulhawy and Phoon (1993) used the database developed by Rowe and Armitage (1984), which consisted of 67 load tests at 18 different sites, supplemented by 47 load tests from 23 sites in Florida Limestone (McVay 1992) to develop an expression for f_{\max} involving socket roughness. They plotted unit side resistance (f_s) versus average soil and rock strength normalized by atmospheric pressure (P_a) on a log-log plot for smooth sockets in soil and for rough sockets in rock as defined by Rowe and Armitage (1987) in Table 2.1. The results were interpreted as linear, giving the exponential relationship

$$f_{\max} = P_a \psi (q_u / 2P_a)^{0.5} \quad (2.13)$$

where ψ is a dimensionless factor that reflects variations in the intact strength of the rock and roughness of rock socket. They found the mean value of ψ in rock may be taken as equal to 2, with a standard deviation of 0.17. They further found that an extreme lower bound for rock would be 0.5, while 1.0 is a better working lower bound. The apparent upper bound for ψ is 3, which could be used for very rough or artificially roughened drilled shafts in rock but should not be used without load tests. Rowe and Armitage (1984) suggest a mean ψ value of 2 and a value of 2.7 for roughened shafts.

2.2.7 Discussion of Empirical Methods

According to Zhang (1998), relationships for relating the ultimate side shear to the unconfined compressive strength of the rock follow two major groups. The first is a simple linear expression of the form

$$f_{\max} = \alpha \cdot q_u$$

While the other is a power function of the form

$$f_{\max} = \alpha \cdot (q_u)^c$$

Whether the relation between f_{\max} and q_u is better represented by a power function or a linear function depends mainly on the range of q_u considered (O'Neill et al. 1996). The linear function proposed by Carter and Kulhawy (1987) is only applicable for q_u between 1.7 and 2 MPa (18 to 21 tsf), whereas the power function of Horvath and Kenny (1979) applies over a wider range. Zhang (1998) concluded that “Extensive studies of load test

data by Williams and Pells (1981) and Kulhawy and Phoon (1993) indicated that the power-curve relationship is closer to the real case.”

O’Neill et al. (1996) analyzed a database of 139 loading tests and came to the conclusion that a unique value of α does not exist and more parameters than just q_u are required to make accurate predictions of f_{max} . Williams and his colleagues, (Williams et al. 1980; Williams and Pells 1981) developed a semi-empirical method where α reflects variations in the intact strength of the rock and β is an adjustment factor to account for seams of softer material in the rock (Eq. 2.7). Due to the difficulty in isolating these different variables with empirical data, much of the work to evaluate additional factors has utilized numerical methods as described in the following sections.

2.3 Factors Affecting Unit Side Shear for Drilled shafts in Rock

O’Neill (1996) has noted the ultimate side shear capacity of drilled shafts socketed into rock is dependent on a number of factors including factors related to construction technique such as

- interface roughness
- cleanliness of interface
- initial lateral concrete pressure
- length of time borehole remains open prior to concreting
- destroyed or intact base resistance

factors related to the properties of the rock such as

- angle of internal friction of the rock
- angle of interface dilation

- formation stiffness
- initial coefficient of lateral earth pressure

factors related to the load test method such as

- pull out test
- top-down loading
- jacking upward from the base (O-cellTM)

and factors related to socket geometry such as

- length
- diameter

The following sections summarize the current understanding of the effects of these parameters.

2.3.1 Interface roughness

Research conducted by Williams and Pells (1981) and Horvath et al. (1983) indicated that the ultimate unit side shear resistance in drilled shaft sockets in soft cohesive rock is controlled by the interface roughness as much as, or more than rock strength. In general, shafts with rougher side-walls are expected to have higher unit side shear than shafts with smooth side walls. Kulhawy and Phoon (1993) found that the ratio of maximum unit side shear to unconfined compressive strength (f_{\max} / q_u) could be four times higher for a rough socket than for a smooth socket. Williams and Pells (1981) and Kodikara (1992) have modeled the borehole roughness by assuming clean triangular interface joints as shown in Figure 2.4. Williams and Pells used a finite element analysis to corroborate their field load test. Kodikara uses a rational mathematical model to account for borehole roughness, strength of the rock, and dilatancy at the shaft-rock

interface. The height of the asperities or grooves (h_m) and the angle of the asperities with the vertical side of the borehole (i_m) are needed for the model.

In clay shale, the interface is generally not clean due to disturbance by the auger, perched groundwater or seeps, or even water introduced into the hole by drillers to facilitate the removal of the cuttings which can produce a smear zone several millimeters thick (O'Neill and Hassan 1993). Research by O'Neill and Hassan (1993) in the Eagle Ford Shale in Texas indicates that the borehole sidewalls can be modeled as a sinusoidal interface pattern as shown in Figure 2.5, particularly for clay shale.

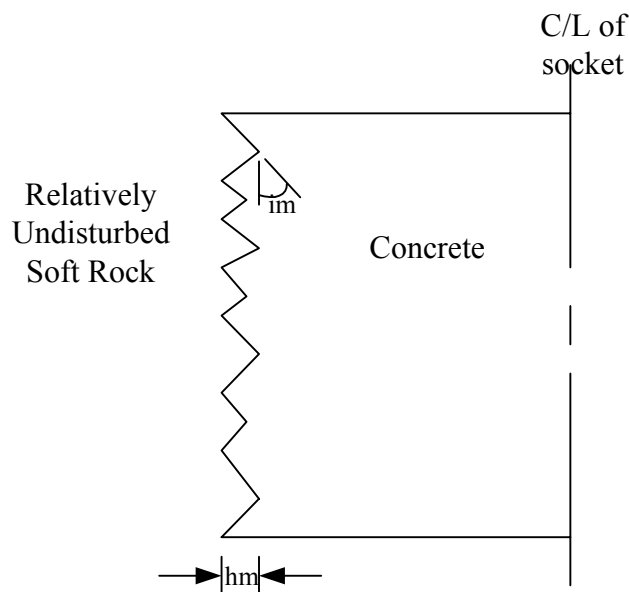


Figure 2.4- Model of socket roughness for Melbourne Mudstone, where i_m = mean value of angle between face of the asperity or groove and the vertical and h_m = mean double-amplitude height of the asperities (after Kodikara et al. 1992).

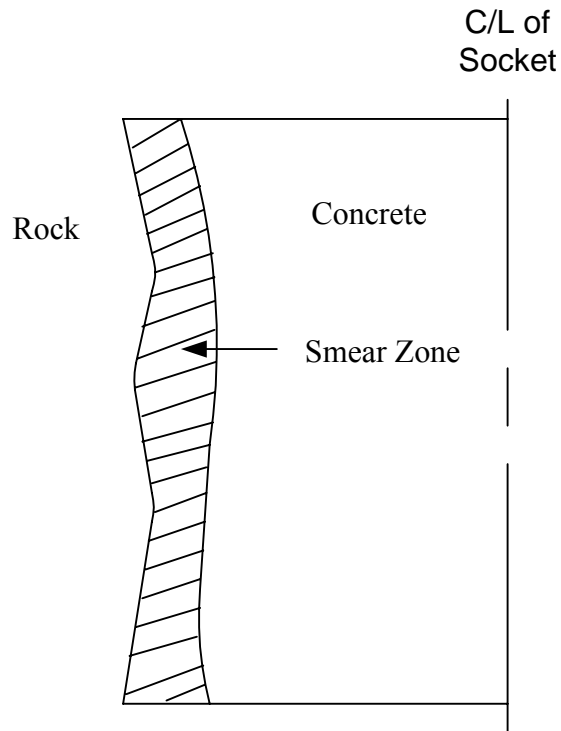


Figure 2.5- Sinusoidal interface pattern in clay shale (after O'Neill and Hassan 1993).

2.3.2 Cleanliness of interface

Hassan and O'Neill (1997) have found that smearing of argillaceous intermediate geomaterials (IGMs) caused by construction technique has a significant negative effect on load transfer. The smearing of the interface is believed to account for large differences observed in f_{\max} in full-scale loading tests in IGMs of similar strength. IGMs or intermediate geomaterials are defined by O'Neill (1996) as argillaceous geomaterials including heavily overconsolidated clays, clay shales, saprolites, and mudstones that are prone to smearing when drilled and have an unconfined compressive strength (q_u) in the range of 0.5 to 5.0 MPa (5 to 50 tsf). Osterberg (1992) found that a thin grease like layer is formed, for drilled shafts constructed in shale using water as the drilling fluid, which can greatly reduce the shaft friction. Hassan and O'Neill (1997) have

recommended that if smearing can occur during the drilling process the shaft be designed as smooth.

Horvath (1980) found that the loss of unit side shear due to smear is not as great in rough sockets, particularly in artificially roughened sockets. Osterberg (1992) reported that drilling methods used in weaker rocks, and even hard sandstones, provide sufficient roughness and there seems to be no effect of smoothness. Shear rings or grooving of the socket has been recommended by Hummert (1988) to increase unit side shear in the Pierre Shale in Colorado.

2.3.3 Initial lateral concrete pressures

Initial lateral concrete pressures due to the depth of concrete in shaft may have a significant influence on the unit side shear for both rough and smooth sockets. The initial normal stress, σ_n , on the concrete-rock/soil interface at the mid-depth of the socket can be taken as being equal to the pressure of the fluid concrete. Failure at the interface of a smooth socket is primarily a function of the modulus of the rock mass, E_m , the angle of sliding resistance at the interface, ϕ_{rc} , and the initial normal stress at the interface, σ_n . As σ_n increases f_{max} increases significantly (Hassan and O'Neill 1997). A finite element study performed by Hassan and O'Neill (1997) found that the unit side shear in the elastic range increases with increasing values of σ_n , but that there is no major difference in the ultimate unit side shear, f_{max} , when settlement approaches an infinite value. The ultimate unit side shear value tends to be equal to the undrained shear strength (s) of the soft rock or $q_u / 2$ when the angle of internal friction of the soft rock is equal to zero, ($\phi = 0$).

2.3.4 Length of time borehole remains open prior to concreting

For argillaceous geomaterials such as clay shales it is generally believed that the unit side shear is reduced as the time of exposure of the rock socket to drilling fluids is increased. This is primarily caused by softening of the side-walls of the socket. Osterberg (1992) has noted a reduction in unit side shear for shale with rock sockets that were drilled dry and which rapidly deteriorate when exposed to air.

2.3.5 Angle of internal friction and angle of interface dilation

In rough sockets, failure often takes places at the base of the asperities or grooves, by shearing off the asperities, whereas in a smooth socket failure takes place due to slip along the interface between the shaft and rock. As the angle of internal friction (ϕ) of the weak rock increases, the ultimate unit side shear, f_{\max} , increases for rough sockets while there is virtually no effect of ϕ for smooth sockets (Hassan and O'Neill 1997). In contrast, since failure occurs at the base of the asperities for rough sockets, the angle of interface dilation (ϕ_{rc}) has little effect on the ultimate unit side shear. For smooth sockets however, where sliding takes place along the interface, the angle of interface dilation can significantly affect the ultimate unit side shear with f_{\max} increasing with increasing ϕ_{rc} .

2.3.6 Formation stiffness

The formation stiffness E_m (and by inference q_u) has a significant effect on load transfer in side shear for smooth sockets (Hassan and O'Neill 1997). Goeke (1979) and Osterberg (1999) have concluded that the lab strength of rock cores is lower than the insitu or formation strength. Goeke attributes the erratic lab data partially to swelling of the shale in the core barrel during coring and to partial drying of samples, which result in

development of micro fissures in the sample. Naturally occurring laminations in shales also cause low unconfined compressive strengths in the lab. Insitu, the weight of the overburden increases the shear strength between the laminations (Osterberg 1999). For weak rocks with naturally occurring laminations, O'Neill (1996) has proposed testing undrained rock cores in compression using a triaxial cell with a confining pressure to more appropriately represent field conditions.

Based on published test data, Osterberg (1992) has found that as the unconfined compressive strength, increases the ultimate unit side shear decreases as a fraction of the rock strength. For weak rocks, such as shales with q_u in the range of 2.4 to 3,447 kPa (3.6 to 36 tsf), the ultimate side shear is 0.3 to 0.5 times q_u . For rocks with strengths in the range of 3.4 to 13.8 MPa (36 to 144 tsf), the ultimate unit side shear is 0.1 to 0.3 times q_u . Finally for rocks such as hard limestone and granite with strengths in the range 13.8 to 55.2 MPa (144 to 576 tsf), the ultimate unit side shear is 0.03 to 0.1 times q_u . This data would again reaffirm that the power-curve relationship for the ultimate unit side shear is closer to the real case.

2.3.7 Socket diameter

The diameter of rock sockets can also affect the unit side shear values. It is generally believed that as the diameter of the socket increases the ultimate unit side shear decreases, but very little comparative load testing has been done on large shafts. A study of existing test data by Horvath and Kenny (1979) indicates the ultimate unit side shear decreases with increasing diameter but for socket diameters larger than 380 mm (15 inches) the effect of socket diameter appears negligible. Expanding cavity theory which

can be used to compute radial stresses caused by dilation of the socket during axial loading suggests that there is an effect of diameter on load transfer (Hassan and O'Neill 1997). Analysis by Hassan and O'Neill showed that unit side shear is reduced with increasing diameter regardless of length but experimental evidence suggests that the effect is small for diameters greater than 610 mm (2 feet). Baycan (1996) used a computer program (ROCKET 95) developed by Seidel and Haberfield (1995) to model the behavior of a rough socket. He found that roughness and diameter have a major effect on unit side shear. As the diameter increases radial stresses in the rock surrounding the shaft decrease and thus the maximum unit side shear decreases as show in Figure 2.6.

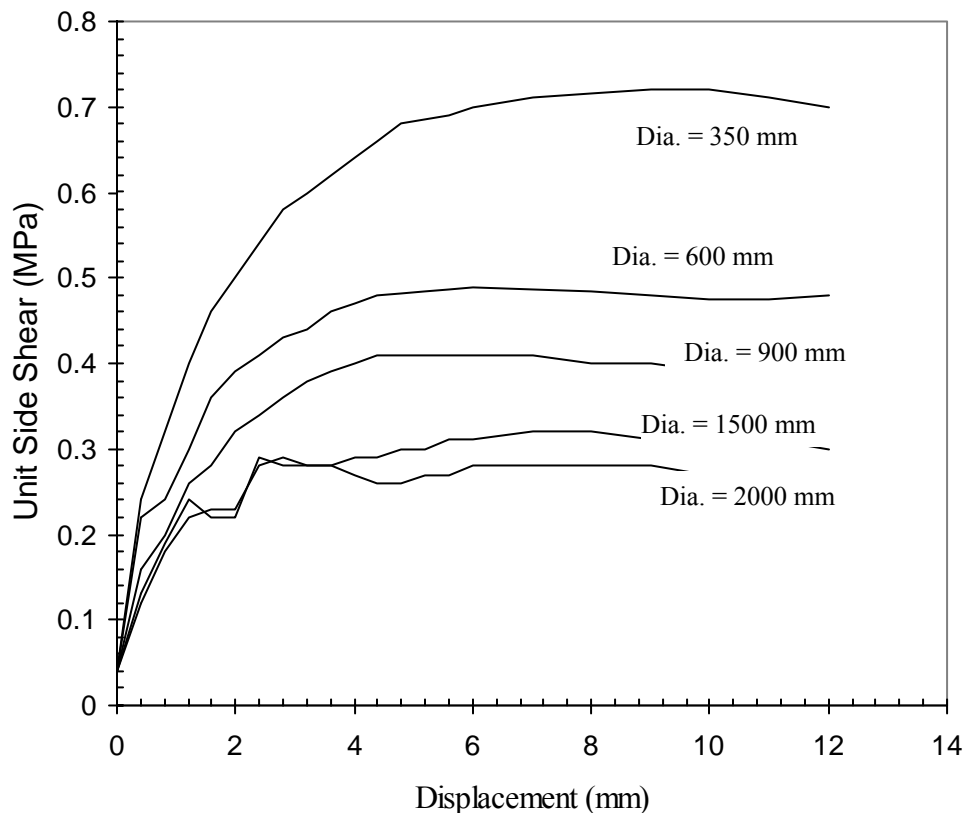


Figure 2.6- Unit side shear versus shear displacement for drilled shaft sockets in rock of moderate roughness with $q_u = 3.0$ MPa (after Baycan 1996).

2.3.8 Loading Direction

One issue directly affecting results from Osterberg load cell tests is the issue of loading direction since unit side shear values are often determined from the portion of the shaft that is loaded upwards while the actual field loading is generally downwards. Data by Kulhawy and Phoon (1993) shows no significant difference in the unit side shear as a function of loading direction, as has been noted previously by Rowe & Armitage (1984). Ogura (1996) tested three, 1.2 m (3.9ft) diameter shafts in soft soil in Osaka, Japan one using top-down loading and two loaded with an O-cellTM placed near the base of the 38.5m (126.3 ft) shafts. The measured unit side shear was the same although the shafts tested with the O-cellsTM failed in end bearing and the side shear was not fully mobilized. Shi (2002) used a finite element model (ABAQUS) to compare the effects of loading direction on the load taken up in side shear. Shi found that, in soil with a modulus several orders of magnitude less than that of the concrete, there was only a slight difference in the predicted side load with the O-cellTM type (upward) loading being slightly less than for top-down loading. However, Shi found that the difference between loads taken up by side shear for top-down and O-cellTM loading became more pronounced for rock socketed shafts as shown in Figure 2.7, with the difference in the side load for the two methods increasing with increasing modulus of the rock. The O-cellTM loading produced conservative values for side shear in all cases but Shi's finite element model showed the need for further research comparing top-down loading and loading from the bottom of the shaft using the O-cellTM.

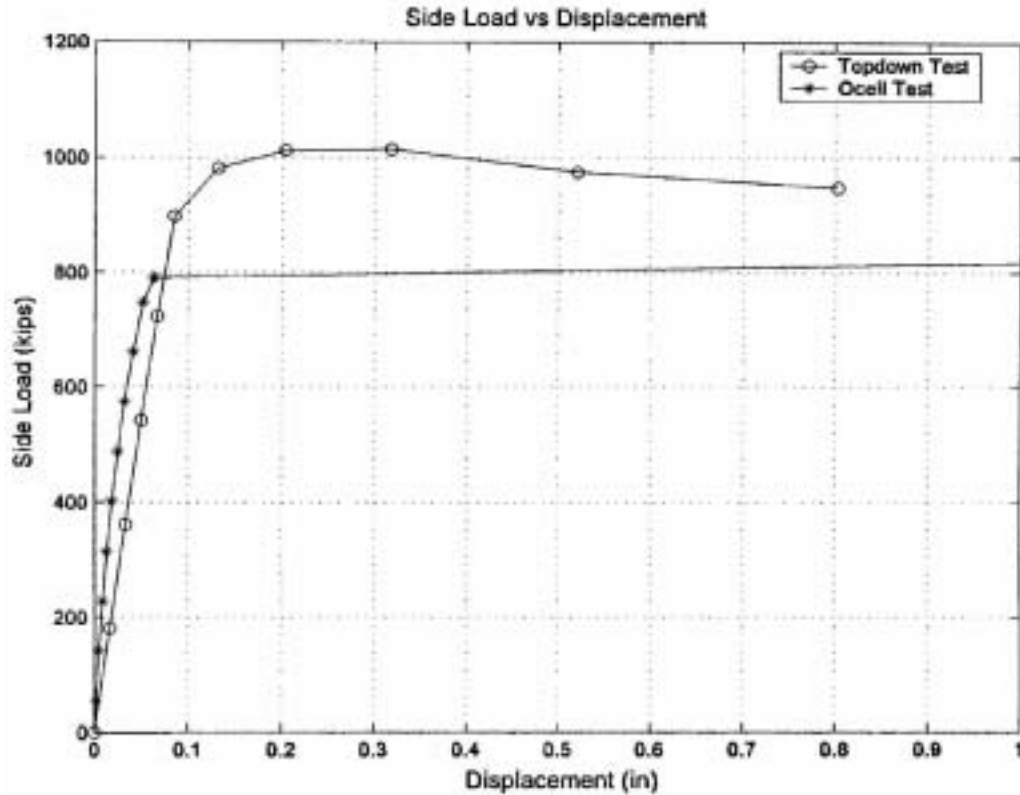


Figure 2.7- Comparison of side load versus displacement curves for top-down and O-cellTM loading based on finite element analyses (from Shi 2002).

2.4 Analytical methods

Because of the difficulty in addressing all of the factors affecting the unit side shear capacity of drilled shafts using empirical methods, a number of analytical methods have been developed to predict capacity as a function of these factors. Analytical methods proposed by Kodikara et al. (1992), McVay et al. (1992), and O'Neill and Reese (1999) attempt to model the soft rock shaft interface by considering interface roughness, cleanliness of interface, initial lateral concrete pressure, properties of the weak rock such as angle of internal friction ϕ' and cohesion c' , angle of interface dilation ϕ_{rc} , and the formation stiffness E_m . The following sections describe these methods in more detail.

2.4.1 Kodikara et al.

Kodikara et al. (1992) used a rational mathematical model to account for borehole roughness, initial normal stress on the interface, and stiffness of the soft rock during interface dilation. This method is an extension of finite element analyses (elasto-plastic, c' , ϕ') performed by Williams et al. (1980). In the method, f_{\max} is predicted as

$$f_{\max} = \alpha \cdot \beta \cdot q_u \quad (2.14)$$

where the product $\alpha \cdot \beta$ is determined from Figure 2.8, and is a function of the uniaxial compressive strength of the rock (q_u), the initial radial pressure on the interface (σ_n), the ratio of the modulus of the rock (E_m) to q_u , and the roughness of the interface. Figure 2.8 was developed for the ratio of E_m / q_u equal to 300 which is appropriate for many weak rocks. Figures for other values of E_m / q_u are also available (Kodikara et al. 1992). The roughness of the shaft interface is determined from Table 2.2 using roughness measures defined previously in Section 2.3.1 and shown in Figure 2.4. I_{sd} , which was not previously defined, is defined as the standard deviation of the angle between face of the asperity or groove and the vertical (i_m).

Table 2.2-Characterization of borehole roughness (from Kodikara et al.1992).

Parameter	Range of Values of Sockets in Melbourne Mudstone		
	Smooth	Medium	Rough
i_m (°)	10-12	12-17	17-30
I_{sd} (°)	2-4	4-6	6-8
h_m (mm)	1-4	4-20	20-80

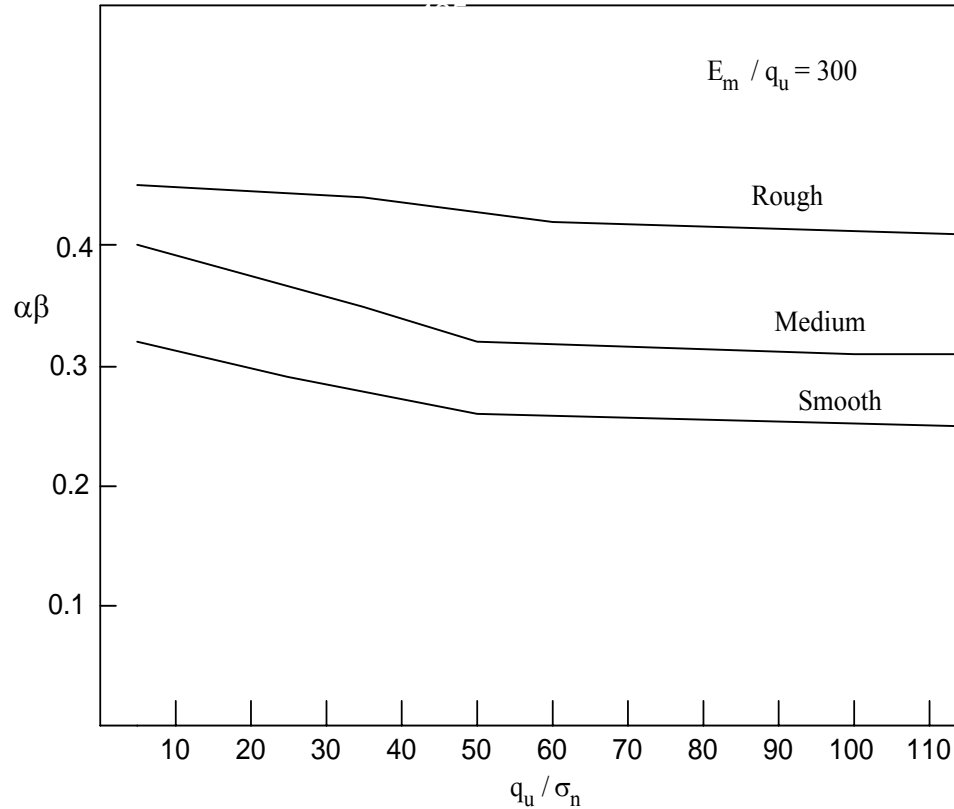


Figure 2.8- $\alpha\beta$ versus borehole roughness, where E_m is the estimated modulus or formation stiffness of the rock mass and σ_n is the initial radial pressure on the interface which can be taken as the estimated fluid pressure produced by the concrete (after Kodikara et al.1992).

2.4.2 McVay et al.

McVay et al.(1992) performed numerical analyses using a parametric finite element method to more closely examine the maximum unit side shear at the shaft-rock interface. McVay et al. found that the unit side shear is in close approximation to the cohesion value of the rock and that more than a single laboratory specimen is required to accurately determine the cohesion value. McVay et al. used both the uniaxial compression test and the splitting tensile (ASTM D3967) test to determine the cohesion

of the rock. Using Mohr's circle and several trigonometric functions, McVay et al. found that the maximum unit side shear was best predicted as

$$f_{\max} = 0.5 (q_u)^{0.5} (q_t)^{0.5} \quad (2.15)$$

Where q_t is the splitting tensile strength of the rock and f_{\max} , q_u , and q_t are given in tsf. McVay et al. found excellent agreement with the unit side shear computed by equation 2.15 and a database consisting of 53 pullout tests and 7 load tests at 14 different sites in Florida. The rock encountered at these test sites was a weak limestone.

2.4.3 O'Neill and Reese

O'Neill and Reese (1999) expand on finite element modeling of the Eagle Ford clay shale performed by Hassan and O'Neill in 1993 to develop the method currently recommended by the Federal Highway Administration (FHWA) for the calculation of f_{\max} for smooth sockets in intermediate geomaterials with unconfined compressive strengths (q_u) in the range of 0.5 to 5.0 MPa (5 to 50 tsf). The FHWA recommends rock sockets for drilled shafts be designed as smooth unless they are artificially roughened. For smooth rock sockets or sockets drilled using slurry, FHWA recommends the following expressions to predict f_{\max}

$$f_{\max} = \alpha \cdot \phi \cdot q_u \quad (2.16)$$

where α is an adhesion factor estimated from Figure 2.9, ϕ is a factor to account for the presence of open joints estimated from Table 2.3, and f_{\max} and q_u are given in MPa. In Figure 2.9, σ_n is the pressure of the fluid concrete at the middle of the layer assuming the slump of the concrete is at or above 175 mm (7 in.) and the concrete is placed at a rate of

12 m (40 feet) per hour and p_a is the atmospheric pressure in the units in which σ_n is calculated. The fluid pressure of the concrete is estimated as

$$\sigma_n = 0.65 \gamma_c Z_i \quad (2.17)$$

where γ_c is the unit weight of concrete in kN/m^3 and Z_i is the depth to middle of layer in meters with a maximum depth of 12 m (40 feet).

Table 2.3 - Adjustment factor for soft seams and joints (from O'Neill & Reese 1999).

RQD %	ϕ	
	Closed Joints	Open or gouge filled Joints
100	1.00	0.85
70	0.85	0.55
50	0.60	0.55
30	0.50	0.50
20	0.45	0.45

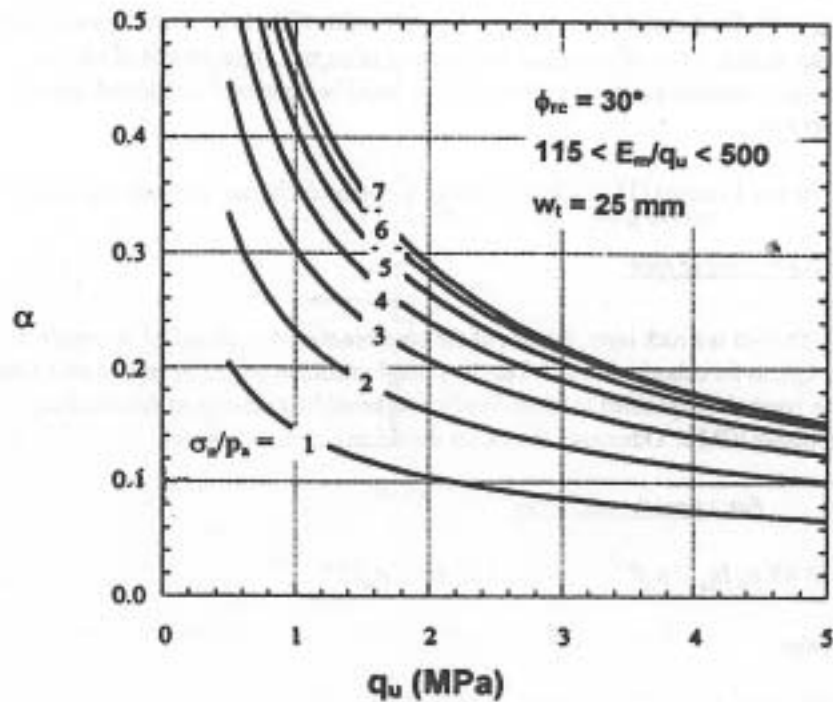


Figure 2.9- Adhesion factor α versus compressive strength q_u (from O'Neill et al. 1996).

For drilled shafts with smooth sockets and unconfined compressive strengths greater than 5.0 MPa (50 tsf) O'Neill and Reese (1999) recommend using Horvath and Kenney's (1979) method (Equation 2.5) normalized with respect to atmospheric pressure (P_a) by Carter and Kulhawy (1988). The expression takes the form;

$$f_{\max} = 0.65 P_a (q_u / P_a)^{0.5} \leq 0.65 P_a (f'_c / P_a)^{0.5} \quad (2.18)$$

where f'_c is the 28-day compressive strength of the concrete and P_a is the atmospheric pressure in the units of f_{\max} and q_u ($P_a = 0.1013 \text{ MPa} = 1.058 \text{ tsf}$). For rough sockets in rock, O'Neill and Reese recommended using the relationship proposed by Horvath (1983) and given in Equation 2.6.

2.5 Summary

Empirical and analytical methods for predicting the maximum side shear capacity of drilled shaft socketed into weak rock have been presented in this chapter. Empirical methods are generally based on full-scale load tests while analytical methods attempt to model the soft rock-drilled shaft interface behavior numerically.

Many of the methods for predicting ultimate unit side shear are based on empirical correlations with the unconfined compressive strength of rock cores. These relationships fall in two major groups: linear functions of q_u involving one or more coefficients and power functions of q_u involving one or more coefficients and the exponent for q_u . Many authors now believe the power-curve relationship is closer to the real case, or at least applicable over a broader range of q_u .

Other authors have related ultimate unit side shear to factors created by construction technique, properties of the rock mass, and geometry of the socket using numerical models. Linear relationships to address these additional factors were proposed by Kodikara et al. (1992) and O'Neill and Reese (1999). McVay et al. (1992) proposed a power function relationship.

CHAPTER THREE

GENERAL OSTERBERG CELL TEST METHODS AND PROCEDURES

A new test method for full-scale load testing of drilled shafts has recently been developed that uses an Osterberg load cell (O-cellTM) invented by Dr. Jorj Osterberg. The Osterberg cell, along with instrumentation such as strain gages and telltales, can be used to determine end bearing and side shear capacities of drilled shafts and piles. This chapter includes a general description of the Osterberg cell load test method and the general procedure used to perform O-cellTM load test. Methods for analysis and interpretation are then described followed by the procedure used to determine ultimate unit side shear values from O-cellTM load test results.

3.1 Description of Osterberg cell load test

The Osterberg load cell (O-cellTM) is a sacrificial, jack-like device that is used to test the axial capacity of drilled shafts. The O-cellTM may be attached either to the rebar cage or a carrying frame and is usually positioned at the base of the shaft or some distance above the base as shown in Figure 3.1. As the O-cellTM is expanded under hydraulic pressure, it simultaneously exerts an upward force against the portion of the shaft above the cell and an equal downward force against the portion of the shaft and/or bearing strata below the cell. The O-cellTM has the advantage of being able to apply large loads on drilled shafts without the need for a large reaction system.

Dr. Jorj Osterberg, Professor Emeritus at Northwestern University developed and patented the test. The O-cellTM was first used on a bored pile in 1984. The O-cellTM evolved from a bellows type expansion cell to the current design which is very similar to the piston type jack commonly used on conventional load tests, except that the piston

extends downward instead of upwards (Schmertmann 1997). Approximately 400 tests have been performed in the United States and Southeast Asia (Osterberg 1999).

LoadTest, Inc. of Gainesville, Florida is currently the exclusive distributor of the O-cellTM and provides installation and test support services.

O-cellTM test capacities have increased steadily over recent years. A 1993 test performed for the Kentucky Transportation Cabinet for a bridge across the Ohio River at Owensboro, reached a load of 54 MN (6000 + tons) in each direction (Goodwin 1993). In 1997, a test for the Florida Department of Transportation (FDOT) across the Apalachicola River reached a load of 133 MN (14950 tons) in both directions (Schmertmann 1998). The Florida test used three 864 mm (34 in.) diameter O-cellsTM in a 2.75 m (9.0 ft.) diameter shaft socketed 13.7 m (50 ft.) into limestone. On January 30, 2001, an O-cellTM load test was performed in Tucson, Arizona for the Arizona Department of Transportation (ADOT) that reached a load of 151 MN (17,000 tons) in both directions. The O-cellTM load test was performed on a 2.43 m (8.0 ft) diameter shaft 41.3 m (135.5 ft) deep. Three 864 mm (34 in.) diameter O-cellsTM were installed 8.7 m (28.5 ft) above the base of the shaft. The drilled shaft was constructed by drilled shaft contractors, Anderson Drilling (Lakeside, CA) and Case Foundation (Rosedelle, IL). Anderson Drilling used “Big Stan”, the world’s largest truck-mounted drill rig to excavate the shaft. The available O-cellTM sizes and capacities are shown in Table 3.1.

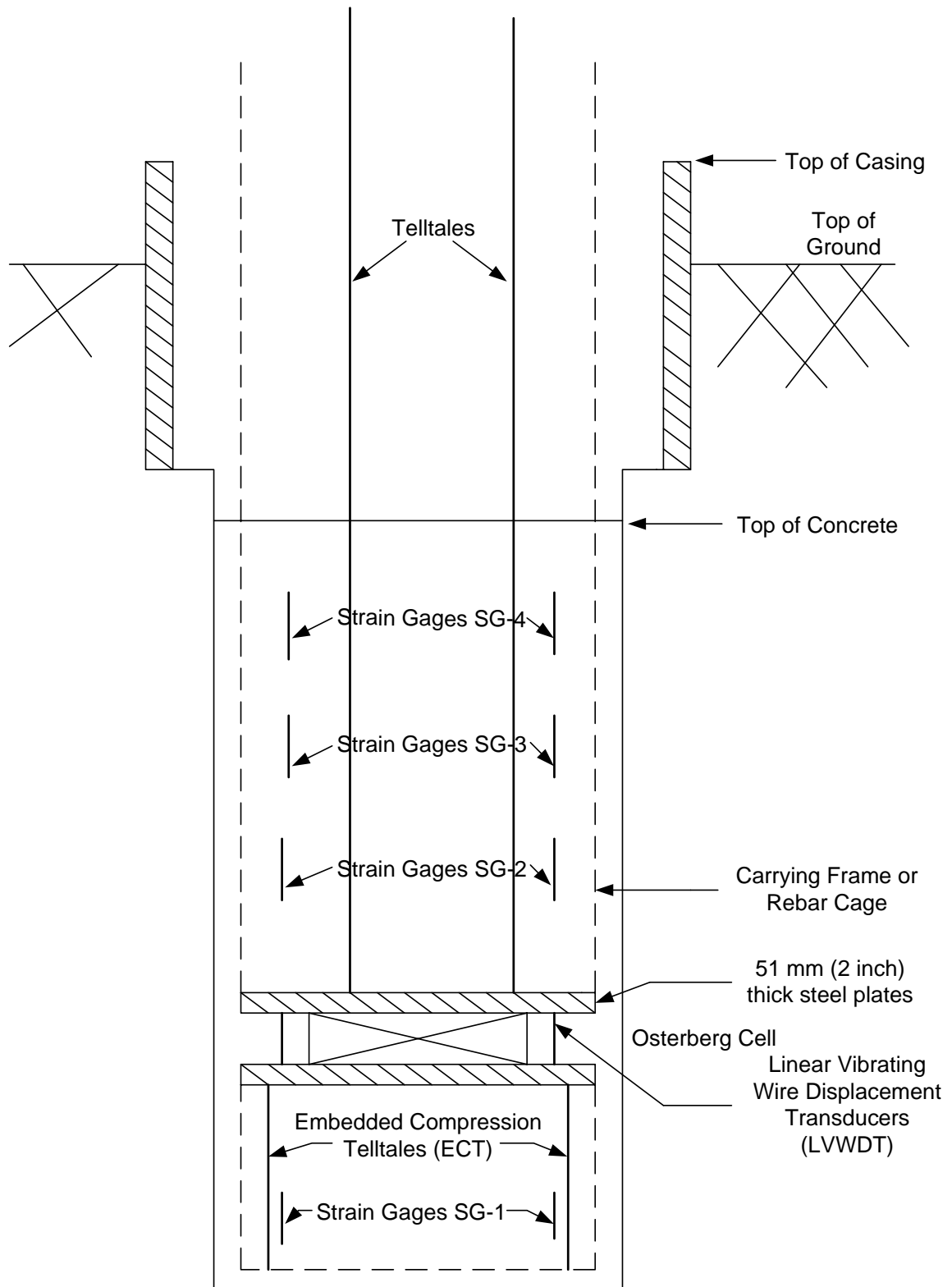


Figure 3.1-Schematic of typical Osterberg cell load test.

Table 3.1-Available O-cellTM sizes and capacities.

Nominal Diameter		Nominal Capacity	
(mm)	(in)	(MN)	(tons)
230	9	1.8	200
330	13	3.6	400
540	21	8.9	1000
660	26	16.0	1800
870	34	27.0	3000

3.2 Osterberg Load Test Procedure

O-cellTM load tests are generally performed by pressurizing the O-cellTM in increments and monitoring displacements at the top and bottom of the shaft and strains at various points along the shaft. The O-cellTM is usually pressurized following the ASTM Quick Test Method (ASTM D1143), although other methods may be used. The Quick Test Method stipulates that small increments of load be applied every four minutes. As the O-cellTM expands, the side shear (f_s) developed above the O-cellTM, between the concrete of the shaft and the walls of the rock socket, serves as the reaction to develop the end bearing (q) below the O-cellTM, or end bearing and side shear if the O-cellTM is set some distance above the bottom of the rock socket. Simultaneously, the end bearing and any side shear derived below the O-cellTM serve as the reaction to apply load to the upper part of the shaft above the O-cellTM. By loading in this manner, load-displacement curves for both the upper and lower portions of the shaft are obtained simultaneously as shown in Figure 3.2. The test is continued until the shaft fails in end bearing or side shear, the capacity of the O-cellTM is exceeded, or in some cases, until two to three times the design load is achieved. The objective of the O-cellTM test is to position the O-cellTM so that failure in side shear and end bearing occurs simultaneously.

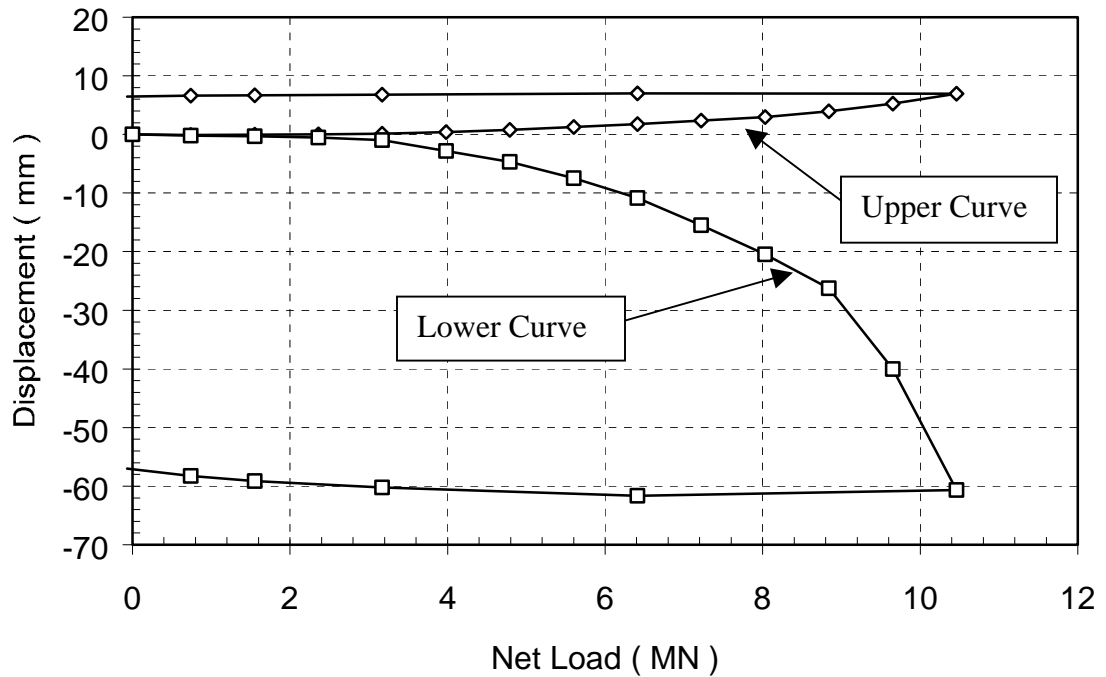


Figure 3.2-Typical Osterberg load test load-displacement curves.

3.3 Instrumentation and Data Collection

Displacements and strains that take place during an O-cellTM test are typically measured by electronic gages connected to a computerized data acquisition system. Figure 3.1 shows a schematic indicating the various types of instruments commonly used. The opening or extension between the top and bottom plates of the O-cellTM is measured by two, or sometimes three Linear Vibrating Wire Displacement Transducers (LVWDTs) attached to the bottom plate of the cell. Upward movement of the top of the shaft is measured using dial gages or Linear Voltage Displacement Transducers (LVDT) mounted on a reference beam set over the top of the shaft. The upward movement of the O-cellTM is measured using a pair of steel telltales that extend from the top of the O-cellTM to the top of the shaft. The telltales also provide for measurement of the

compression of the shaft if the displacement of the top of the shaft is monitored. The downward movement of the bottom plate is determined by subtracting the upward movement of the top of the O-cellTM from the total extension of the O-cellTM. The reference beam is in turn monitored by a surveyor's level. Typical instrumentation of the top of shaft is shown in Figures 3.3 and 3.4. The load applied by an O-cellTM is calibrated versus hydraulic pressure before installation and pressure to the cell is measured during the test using a Bourdon gage or vibrating wire pressure transducer.

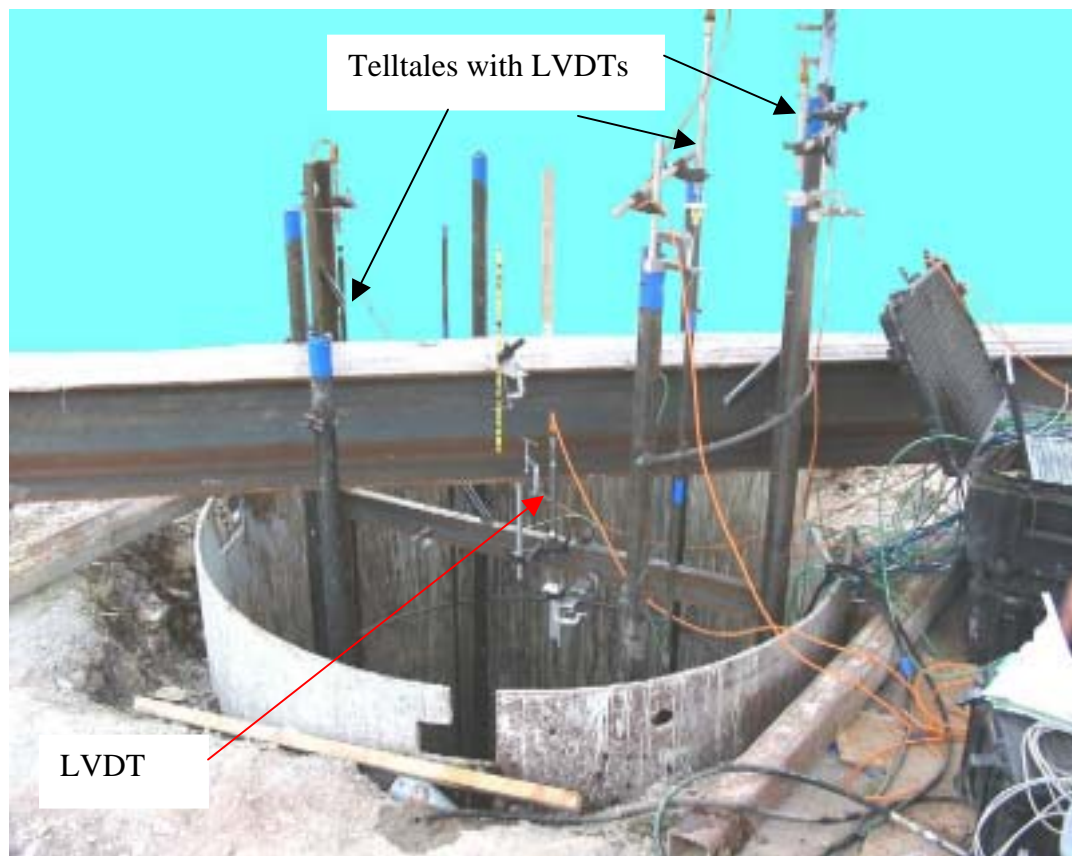


Figure 3.3- Typical instrumentation at the top of a drilled shaft with telltales monitored with LVDTs to determine shaft compression and a LVDT attached to a reference beam to monitor movement of the top of the shaft. The LVDT on the middle telltale is monitoring movement of the bottom plate of the O-cellTM assembly. The LVWDTs used to monitor top of shaft movement are not visible.



Figure 3.4-Typical instrumentation at the top of a drilled shaft, telltales monitored with digital dial gages. The 25 mm (1 in) stroke dial gages are used to monitor compression of the shaft and are shown. The 100 mm (4 in) stroke dial gages are used to monitor top of shaft movement and are hidden behind the reference beam, although the magnetic base of the right one is visible (from Loadtest).

In addition to the basic instrumentation described above, strain gages are often installed at various positions along the shaft as shown in Figure 3.1 to facilitate determination of load transfer along the length of the shaft. Two types of embedment strain gages are commonly used in drilled shafts to monitor strain and shaft compression of the concrete. The first type is a concrete embedment strain gage with large flanges at both ends to provide anchorage into the concrete as shown in Figure 3.5. The second type of gage is a “sister bar” consisting of strain transducer mounted on the central portion of a length of reinforcing steel as shown in Figure 3.6 and 3.7. Both concrete

embedment gages and sister bars are available with vibrating wire and fiber optic strain sensors. Sister bars are, at times, used with inexpensive foil resistance type strain gages, although these types of gages are not nearly as robust as vibrating wire or fiber optic gages. The advantage of using vibrating wire strain gages over more conventional electric resistance gages is the sensor output, which is frequency rather than a voltage or resistance. The frequency output is easier to transmit over long cables and is unaffected by voltage drops that may be caused by corrosion, moisture, or temperature effects. The frequency signal is also not affected by changes in the length of the sensor cables (Hayes 2002). Fiber optic gages have similar advantages and are not affected by temperature (“self compensating”).

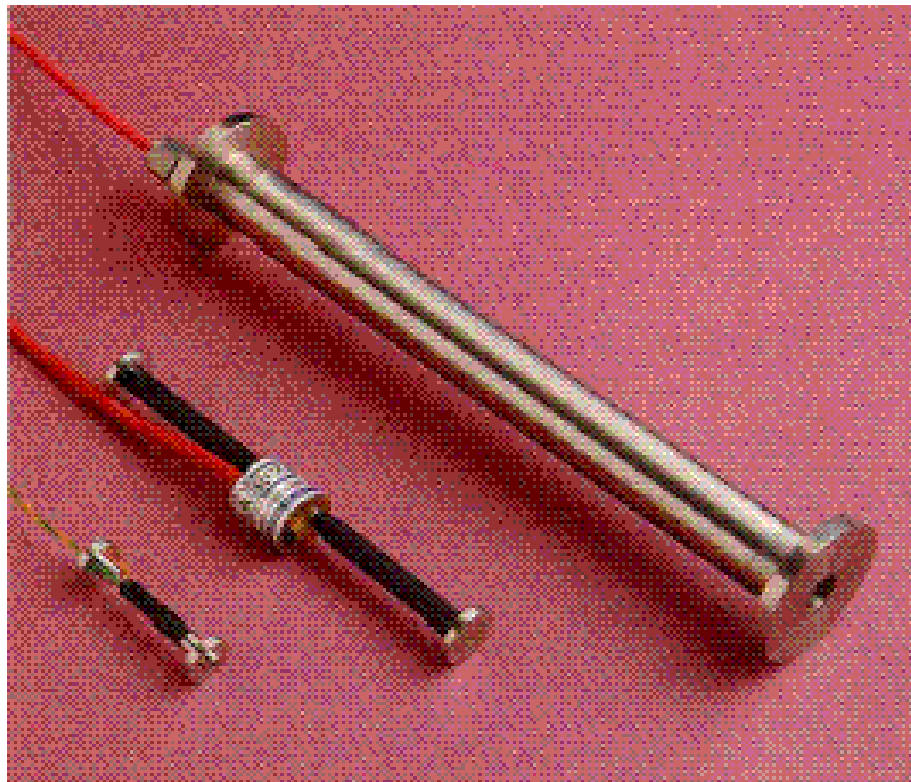


Figure 3.5- Embedment strain gages (from Geokon).



Figure 3.6- Sister bars used to monitor strains within drilled shafts.



Figure 3.7- Sister bar mounted on rebar cage.

Compression of the shaft concrete may also be measured by using an Embedded Compression Telltales (ECT) as shown in Figures 3.8 and 3.9. The ECT assemblies generally consist of a 13 mm (1/2 inch) steel casing with an inner 6 mm (1/4 inch) steel rod. A linear vibrating wire displacement transducer is attached to the 6 mm steel rod to monitor displacements.



Figure 3.8- Embedded compression telltale (ECT) gage mounted in rebar cage.

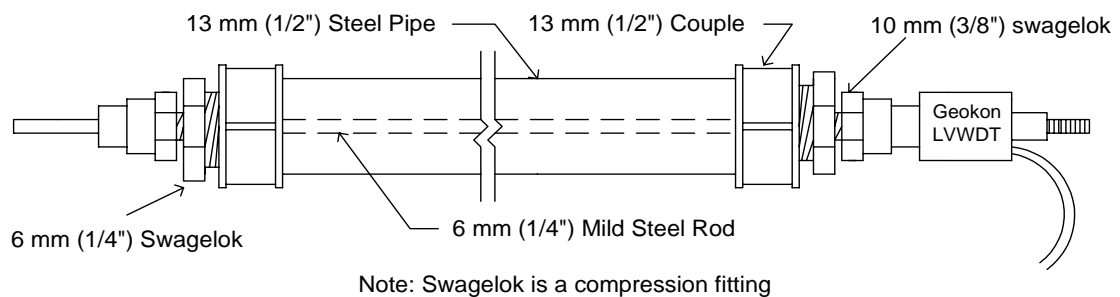


Figure 3.9- Schematic of embedded compression telltale.

3.4 Basic Interpretation of O-cellTM Tests

The O-cellTM test provides two separate load-displacement curves as shown in Figure 3.10. One curve, referred to as the “upper” curve, describes the upward displacement of the shaft above the O-cellTM versus applied load. This curve represents the resistance provided by side shear above the O-cellTM plus the buoyant weight of the shaft above the O-cellTM as a function of displacement (Schmertmann 1998). The other, “lower” curve describes the downward displacement of the shaft below the O-cellTM as a function of the load, which represents the resistance derived from end bearing plus any upward side shear between the O-cellTM and the base of the shaft.

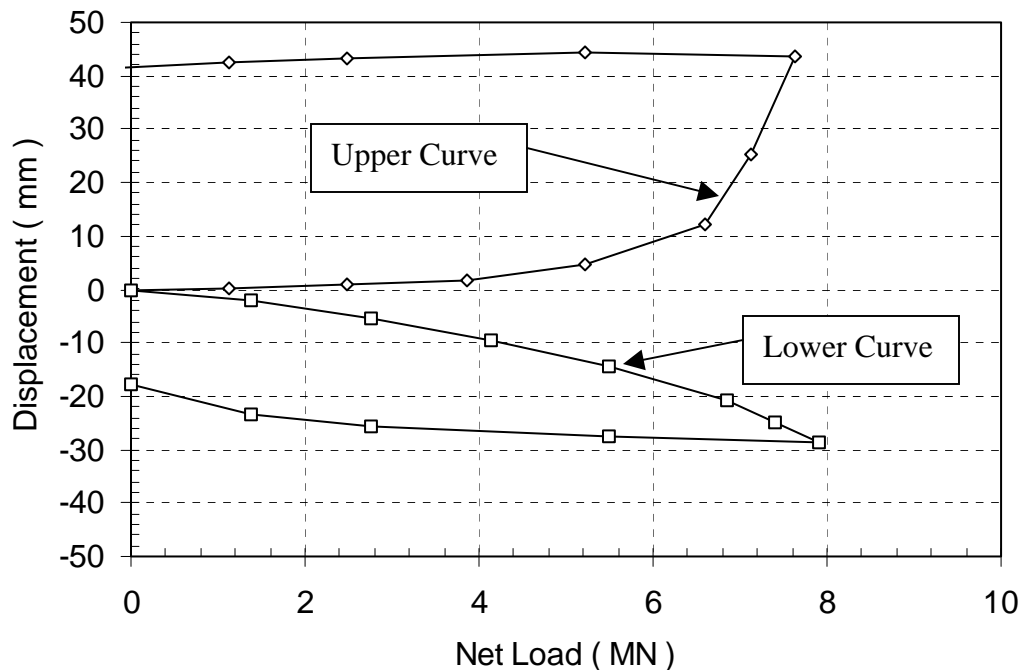


Figure 3.10- Typical Osterberg cell load-displacement curves.

Based on the measured upward and downward responses from an O-cellTM test, an equivalent “top-down” load-displacement curve can be developed using a procedure described by Osterberg (1998). The procedure consists of first picking a value of

displacement and determining the corresponding loads from the upward and downward response curves. The loads for the upward and downward response curves are then added together and plotted versus the selected value of displacement. This procedure is illustrated in Figure 3.11 for a displacement of 10 mm. In this case the load from the upper curve is 6.4 MN and the load from the lower curve is 4.2 MN, which results in an equivalent top-down load of 10.6 MN. Another value of displacement is then selected and the process repeated until a complete top-down load-displacement curve is generated.

A problem often arises with the equivalent top-down procedure in that often the shaft will fail in upward side shear before the end bearing is fully developed (or vice-versa). When this occurs, there is not enough data on the lower curve to define loads at larger displacements and the equivalent top-down load-displacement curve cannot be completely generated. To remedy this problem, Osterberg (1998) has proposed applying a hyperbolic extrapolation to the downward load-displacement curve to generate enough points to complete the equivalent top-down load-displacement curve. This process may be reversed if the downward portion of the shaft fails before the upward portion of the shaft.

Several basic assumptions must be made in order to construct the equivalent top-down load-displacement curve. These assumptions include:

1. The load-displacement curve resulting from the upward displacement of the top of the shaft is identical to the downward displacement of the shaft in a conventional, top-down compression load test.

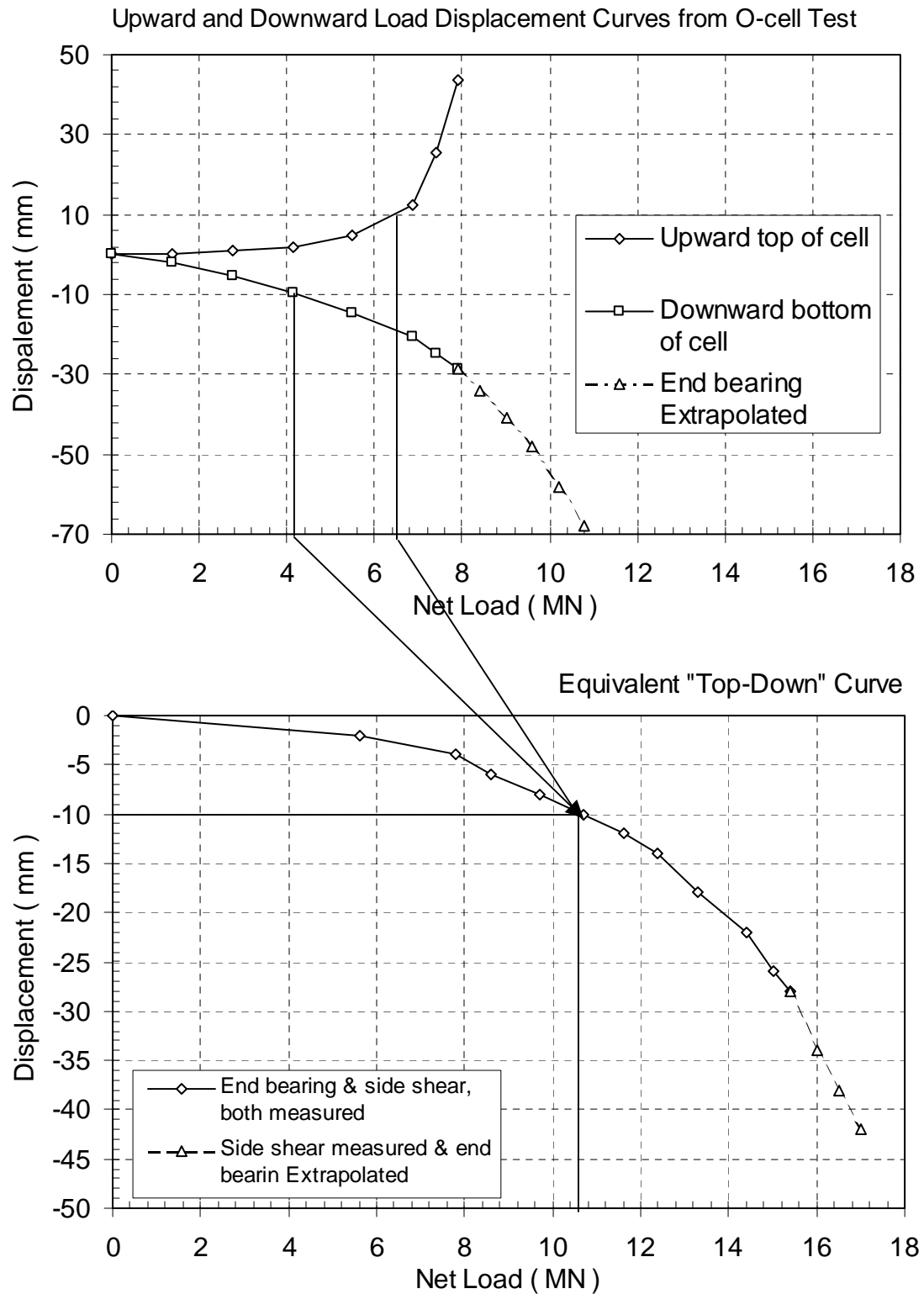


Figure 3.11- Construction of equivalent "top-down" load-displacement curve from upwards and downwards load-displacement curves from O-cellTM test.

2. The load-displacement curve resulting from the downward displacement of the bottom of the O-cellTM is identical to the downward bottom-of-shaft displacement in a conventional top-down load test.
3. The compression of the shaft is considered negligible.

Based on finite element analyses and a search of literature, engineers at LoadTest Inc. and researchers at the University of Florida and elsewhere have indicated that the O-cellTM test produces slightly lower values of the ultimate unit side shear than obtained from conventional top-down load tests. Data from Kulhawy and Phoon (1993) shows no significant difference as a function of loading direction; similar observations were noted previously by Rowe & Armitage (1984). Ogura (1996) tested 1.2 m (3.9ft) diameter shafts in soil in Osaka, Japan using both top-down loading and loading with an O-cellTM placed near the base of the 38.5m (126.3 ft) shafts. The measured unit side shear was similar for both tests. However, the shafts tested with the O-cellsTM failed in end bearing prior to side shear being fully mobilized. Engineers at Loadtest Inc. compared the predicted equivalent displacement to measured displacement for drilled shaft load tests performed in Japan by Kisida et al. (1992) and Ogura et al. (1995). The ratio of predicted equivalent displacement to measured displacement, averaged 1.03 with a coefficient of variation of 9.4 percent.

Shi (2002) used a finite element model (ABAQUS) to compare the effects of loading direction on the load taken up in side shear. Shi found that for a soil with a modulus several orders of magnitude less than that of the concrete, there was only a slight difference in the predicted side loads from top-down and bottom-up loading and that the Osterberg cell load test produced results that were slightly conservative. Shi also found

that the difference between load taken up by side shear in top-down and bottom-up loading is more pronounced for rock socketed shafts where the modulus of the rock is similar to or greater than that of the concrete. Shi further found that the difference in the side load for top-down and bottom-up loading increases with increasing modulus of the rock. The Osterberg cell load test was found to produce conservative values for unit side shear, but Shi's finite element analyses demonstrate the need for further research comparing top-down loading and shafts loaded from the bottom-up using the Osterberg load cell.

To construct the equivalent top-down load-displacement curve from the O-cellTM test results, the drilled shaft is initially assumed to behave as a rigid body and the real elastic compression that is part of the movement data obtained from an O-cellTM load test is included in the construction of the equivalent top-down load-displacement curve. However, the elastic compression in the equivalent top-down test always exceeds the elastic compression in an O-cellTM load test. This assumption is based on the premise that soil strength typically increases with depth and as the load is dissipated through side shear the elastic compression decreases. In a top-down test, load is applied where the soil unit side shear is the weakest and the elastic compression is greatest whereas in the O-cellTM test the load is applied at the base of the shaft where the unit side shear is the greatest and the elastic compression is the least. Loadtest presents an approximate solution for determining the additional elastic compression of a top-down loaded shaft in their procedures for the construction of equivalent top-down load-displacement curves (August 2000). The procedure consists of first assuming a load distribution along the shaft and then determining the elastic compression or deflection (δ_{OLT}) for a shaft

loaded with either one or two Osterberg load cells and the elastic deflection (δ_{TLT}) of an equivalent top-down loaded shaft. The additional elastic compression or deflection ($\Delta\delta$) is determined as

$$\Delta\delta = \delta_{TLT} - \delta_{OLT} \quad (3.1)$$

The additional elastic compression or deflection $\Delta\delta$ is added to the “rigid” top-down load displacement curve previously constructed to obtain the final corrected equivalent top-down load-displacement curve as shown in Figure 3.12.

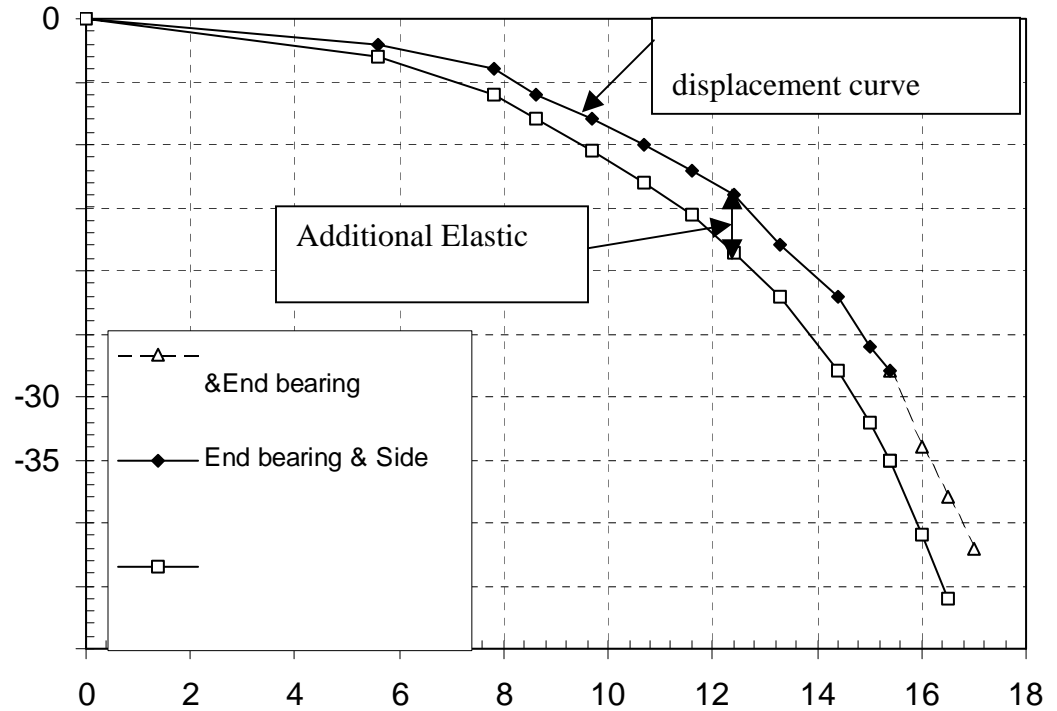


Figure 3.12- Equivalent top-down load-displacement curve adjusted for additional elastic compression.

3.5 Determination of Creep Limit

The creep limit is generally defined as the load at which further loading of the shaft will cause displacement of the shaft to occur freely. The creep limit is determined

by plotting the displacement that may occur over the time interval between 2 to 4 minutes after applying a load, while the load is maintained constant as shown in Figures 3.13a and b. A break in the curve of displacement versus load indicates the creep limit-the point at which displacement begins to accelerate under constant load. In Figure 3.13 the creep limit for the upper portion of the shaft occurs at a load of 4.7 MN. At an applied load of 4.7 MN the upper segment of the shaft has displaced a total of 3.4 mm as determined from the overall load-displacement curves as shown in Figure 3.14. The creep limit for the combined end bearing and side shear from the lower portion of the shaft occurs at a load of 1.6 MN and a total displacement of 3.3 mm.

In a top-down loaded shaft, creep cannot begin to occur freely until the overall load exceeds a combined creep limit. Although the creep limit is generally defined as the load at which further loading of the shaft will cause displacement of the shaft to occur freely, it is usually determined as the displacement corresponding to the limiting load. A conservative approach would be to set the combined creep limit equal to the lesser displacement for the creep limits determined in Figures 3.13 and 3.14. However, Loadtest recommends setting the combined creep limit to be the equivalent top-down load where the total displacement is equal to the larger of the displacements determined from Figures 3.13 and 3.14. They believe this procedure more nearly matches the actual case. Application of the recommended procedure to determine the combined creep limit for the data shown in Figures 3.13 and 3.14 for an equivalent top-down load-displacement curve is as follows. For a loading of 4.7 MN the upper segment of the shaft displaces 3.4 mm while for a loading of 1.6 MN the lower segment of the shaft displaces 3.3 mm as determined from Figure 3.14. The maximum displacement of 3.4 mm is

plotted on the “rigid” equivalent top-down load-displacement curve as shown in Figure 3.15 to determine the combined creep limit of 7.9 MN. If a creep limit cannot be determined for either the upper or load displacement curve, the maximum displacement recorded is used to determine the combined creep limit for the equivalent top-down load-displacement curve.

3.6 Determination of Load Transfer (t-z) Curves

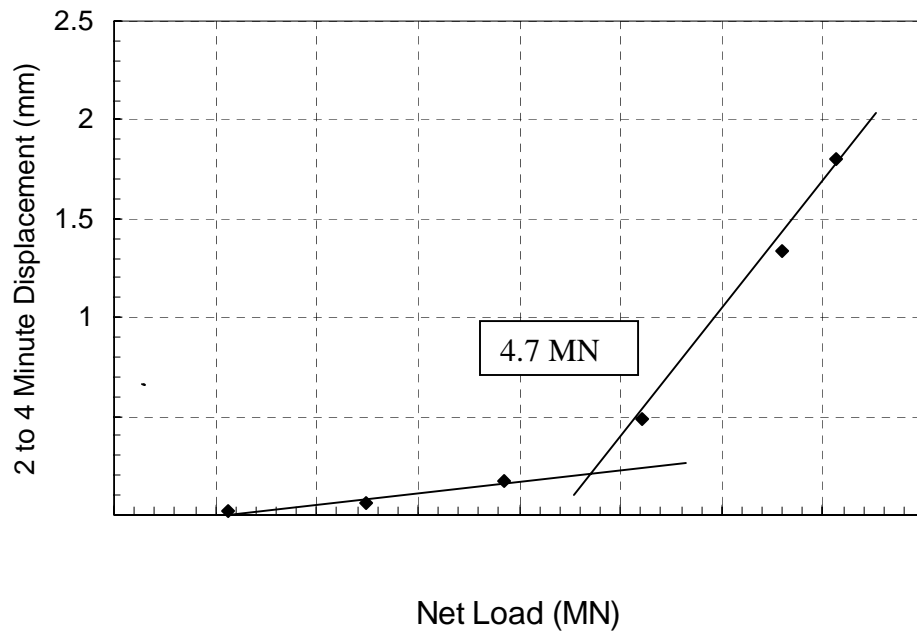
Load transfer curves showing the distribution of force in the shaft versus depth may be obtained from the strain gage data in a manner identical to that used for top-down load tests. Several levels of strain gages are typically installed in the shaft at strata changes or at other points of interest. The modulus of the shaft concrete is determined from concrete cylinders prepared from the original shaft concrete and tested on the day of the O-cellTM test. The modulus of the concrete in the shaft (E_c) may be calculated by applying the ACI formula to the compressive strength of concrete (f'_c)

$$E_c = 4700 f'_c{}^{0.5} \quad (3.2)$$

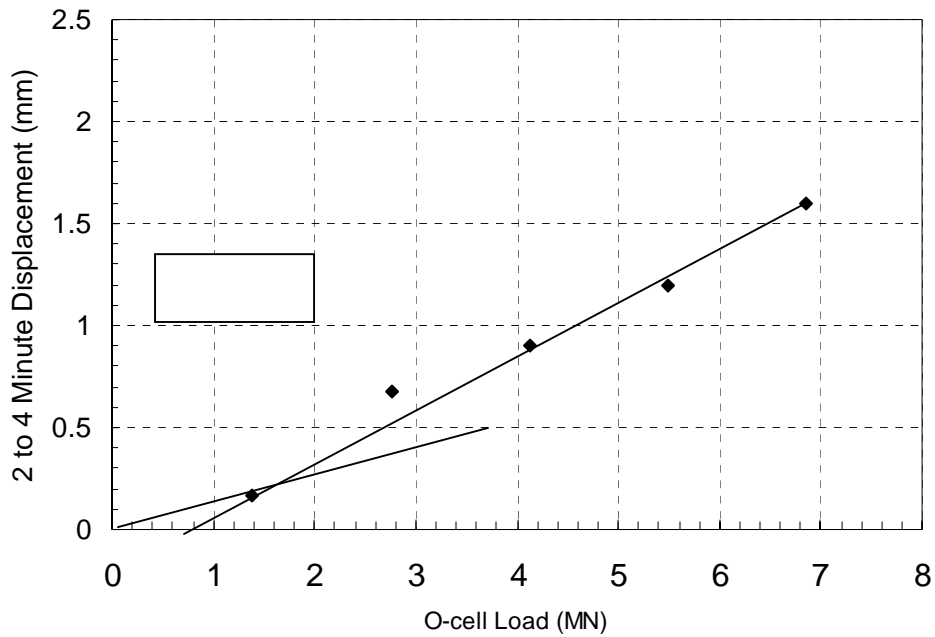
where E_c is the modulus of the concrete in MPa and f'_c is the 28-day compressive strength of the concrete in MPa. Equation 3.2 is applicable for concrete with a unit weight (γ_c) greater than or equal to 14 kN/m³ and less than or equal to 25 kN/m³. In English units the expression is given as:

$$E_c = 57000 f'_c{}^{0.5} \quad (3.3)$$

where E_c and f'_c are given in psi and Equation 3.3 applies to concrete with a unit weight γ_c greater than or equal to 90 pcf and less than or equal to 155 pcf.



a. Upper portion of shaft.



b. Lower portion of shaft.

Figure 3.13- Creep displacements from O-cellTM load tests as a function of applied load:
(a) upper portion of shaft and (b) lower portion of shaft.

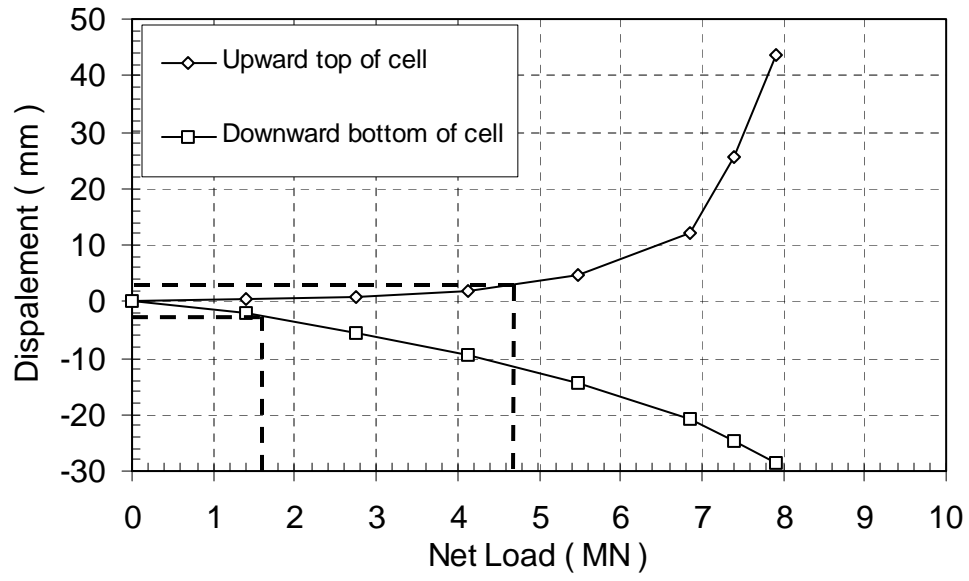


Figure 3.14- Osterberg cell load-displacement curves showing creep-limit displacements.

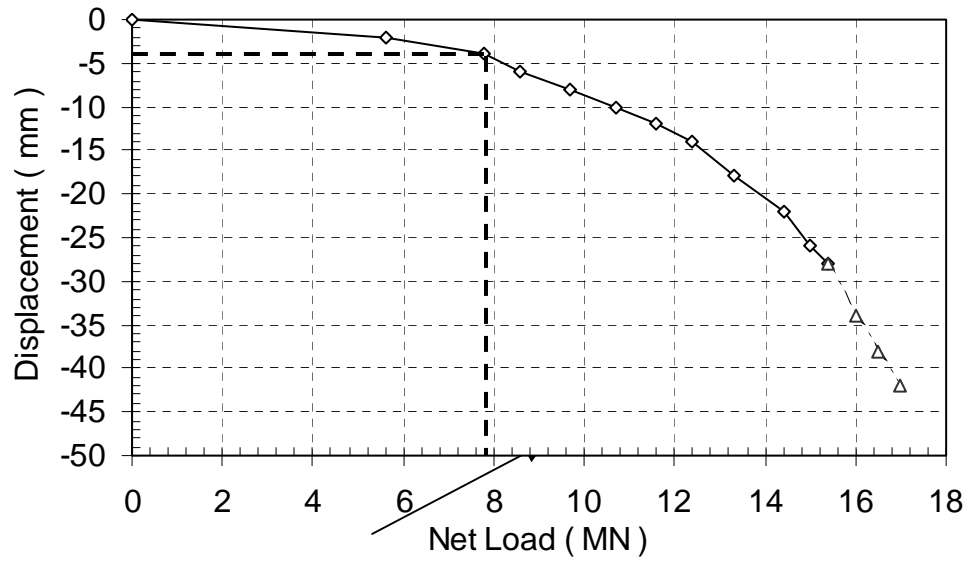


Figure 3.15- Equivalent top-down load-displacement curve with creep limit.

Knowing the modulus of the concrete, the area of the steel, and the area of concrete in the shaft, an “equivalent” shaft modulus (E_p) can be determined as

$$E_p = \frac{E_c A_c + E_s A_s}{A_p} \quad (3.4)$$

where A_c is the area of the concrete, A_s is the area of the reinforcing steel, A_p is the total cross sectional area of the drilled shaft at the point of interest, and E_s is the modulus of the reinforcing steel. The diameter of the drilled shaft may be obtained by using either a mechanical caliper or sonar methods. Sonic calipers are also available and a new method developed in Australia uses a laser. Using the “equivalent” shaft modulus calculated in Equation 3.4, the average axial stress at a given elevation (σ_i) can be computed as

$$\sigma_i = E_{pi} * \epsilon_{axial-i} \quad (3.5)$$

where $\epsilon_{axial-i}$ is the axial strain determined from strain gages within the shaft.

Strain gages are generally installed at various elevations along the length of the shaft with two to four strain gages installed at each elevation of interest. Typically the average strain at elevation i is determined from the average of the strain gages at that elevation. The axial force at elevation i (F_i) is then computed as

$$F_i = \sigma_i A_{pi} = A_{pi} E_{pi} \epsilon_{axial-i} \quad (3.6)$$

where A_{pi} is the shaft area at elevation i . The distribution of axial force with elevation or depth can then be calculated and plotted as shown in Figure 3.16. In the figure, the notation used to indicate each load is as follows: 1L-4 denotes the first loading event,

load increment number 4. The curve for 1L-4 indicates that 5.5 MN is applied at the elevation of the Osterberg cell. The load at the level 1 strain gages for this applied load is about 2.35 MN. This means that 3.15 MN of axial load has been taken up in side shear between the O-cellTM and SG-1 ($5.5 - 2.35 = 3.15$). The maximum applied load for an Osterberg cell load test occurs at the elevation of the O-cellTM. This is contrary to a top-down load test where the maximum load is applied at the top of the shaft as seen in Figure 3.17.

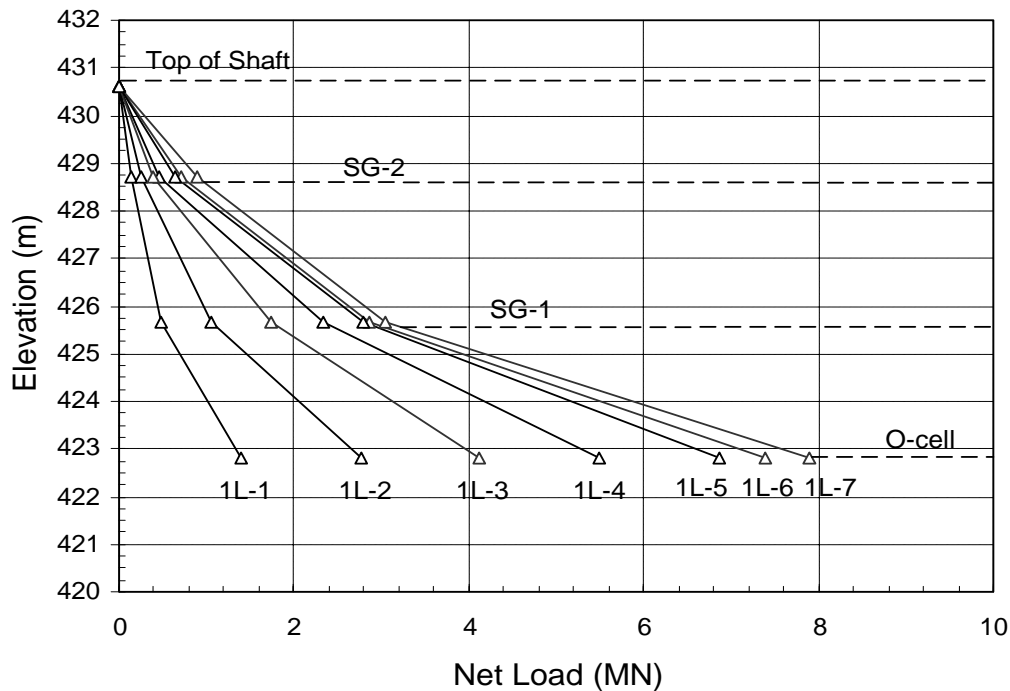


Figure 3.16- Load distribution curves determined from strain gage data.

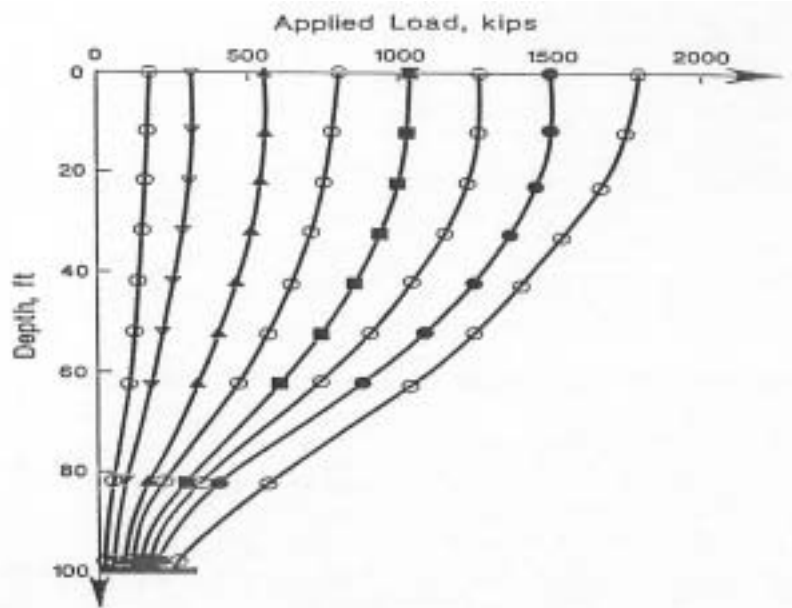


Figure 3.17- Typical load distribution from a top-down load test on a drilled shaft (from Reese 1984).

3.7 Determination of Unit Side Shear

Once the distribution of load along the shaft is known, the value of the average unit side shear for a particular segment of the shaft is calculated as

$$f_s = \Delta F_i / (\text{Shaft Perimeter} * \Delta z_i) \quad (3.7)$$

where f_s is the unit side shear for the shaft segment, ΔF_i is the change in axial force over the length of the shaft segment, and Δz_i is the length of the shaft segment. This procedure is shown graphically for a conventional top-down load test in Figure 3.18 where Q_b and Q_s are axial loads resisted by end bearing and side shear, respectively. The values of the average unit side shear for each segment are generally plotted versus the O-cellTM displacement as shown in Figure 3.19 to help determine if the maximum unit side shear was achieved.

Shi (2002) used a finite element model to compare the maximum unit side shear that would be determined from a top-down load test with that of the bottom loaded Osterberg cell load test for a test shaft constructed in Wilsonville Alabama as shown in Table 3.2. The 812mm (32 in) diameter shaft was socketed 5.6 meters (18.5 ft) into shale with an unconfined compressive strength of 8.96 MPa (93.6 tsf). The shaft was tested by Loadtest Inc. on February 9, 1994 to a maximum load of 4.75 MN (534 tons). At this load the upward displacement was 17 mm (0.66 in) and the downward displacement was 61 mm (2.384 in). Although overall the average unit side shear along the length of the shaft is similar for the top-down load test compared to the O-cellTM load test, the O-cellTM load test method has a tendency to have higher values of unit side shear closer to the bottom of the shaft or closer to the O-cellTM.

3.8 Summary

A new test method for full-scale load testing of drilled shafts and piles has been presented in this chapter. This method consists of placing an Osterberg load cell (O-cellTM) at or near the base of a drilled shaft or pile to test the axial capacity of the shaft or pile. The Osterberg load cell along with instrumentation such as strain gages and telltales can be used to determine end bearing and side shear capacities of drilled shafts and piles. This chapter includes a general description of the Osterberg cell load test method and the general procedure used to perform O-cellTM load tests. Methods for analysis and interpretation are then described followed by the procedure used to determine ultimate unit side shear values from O-cellTM load test results.

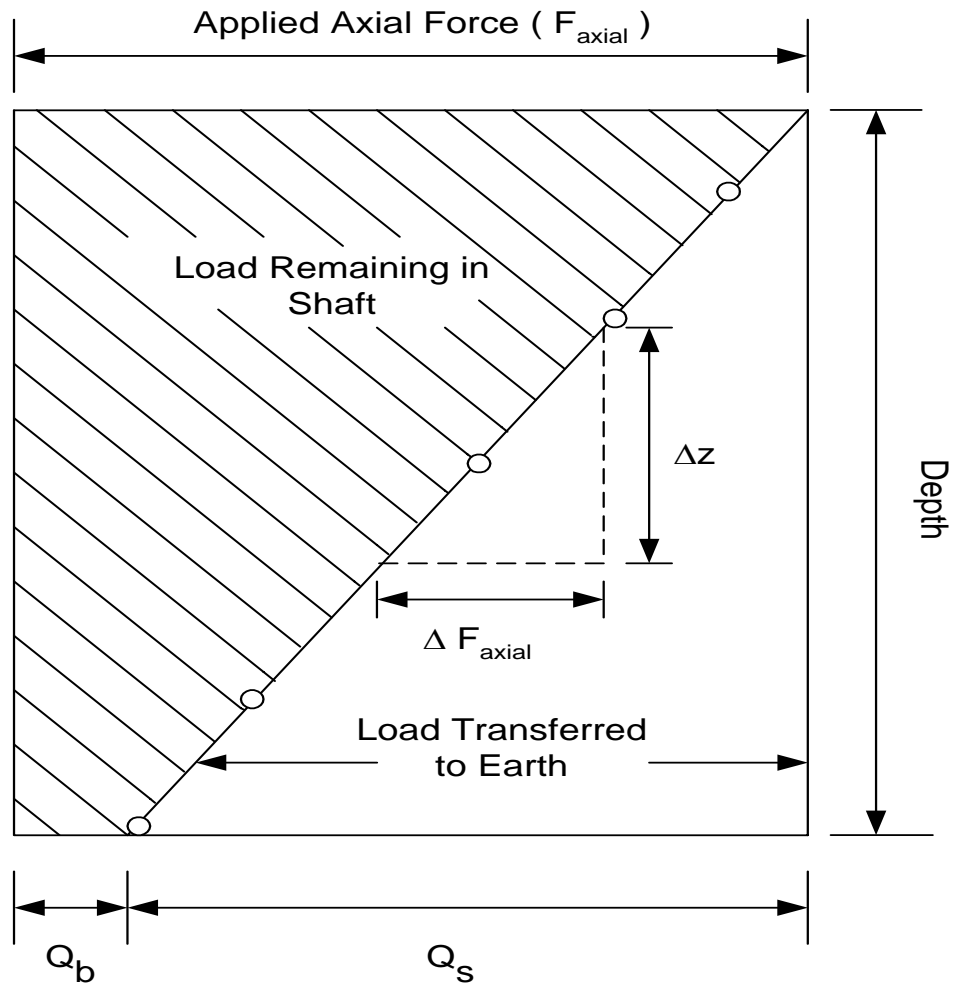


Figure 3.18- Distribution of load with depth for top-down load test (after Kyfor et al. 1992).

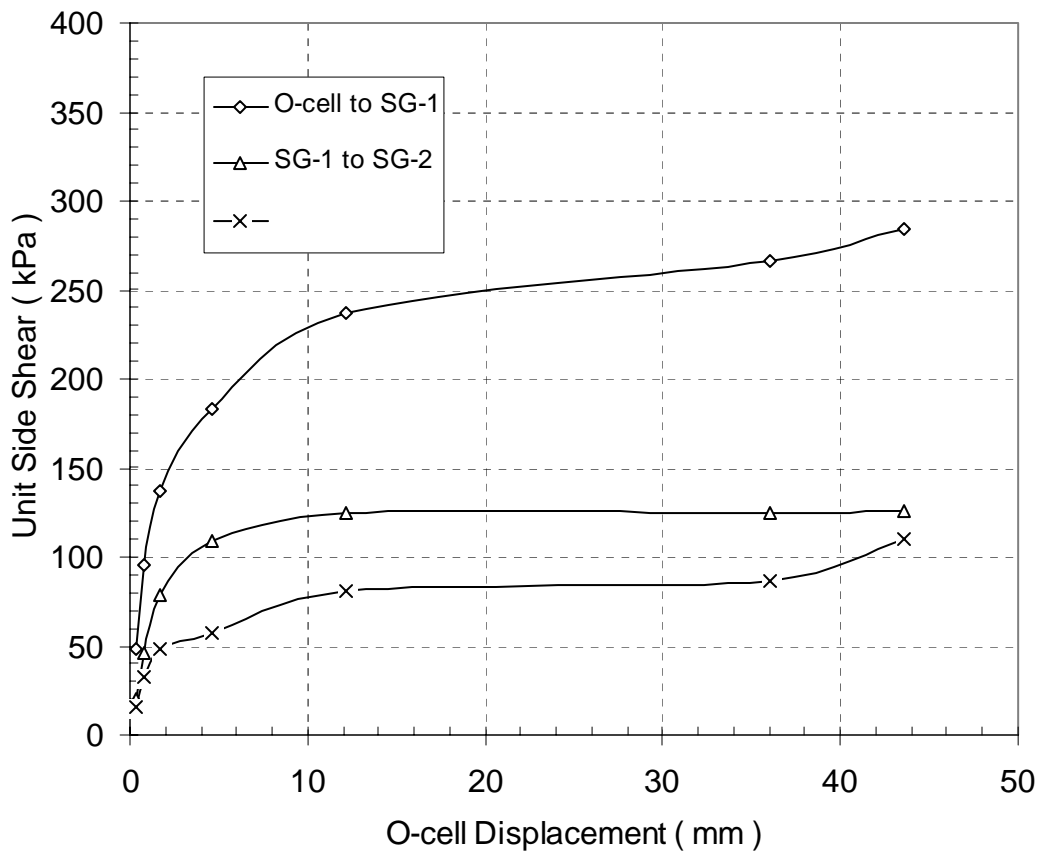


Figure 3.19- Unit side shear versus O-cell displacement relationships for several segments of a drilled shaft.

Table 3.2- Comparison of the maximum mobilized unit side shear (after Shi 2002)

Depth Interval	Measured		FE Model		FE Model	
	O-cell TM Test		O-cell TM Test		Top Down Test	
	kPa	tsf	kPa	tsf	kPa	tsf
O-cell TM to SG-1	746.9	7.8	536.3	5.6	344.7	3.6
SG-1 to SG-2	411.8	4.3	459.6	4.8	392.6	4.1
SG-2 to SG-3	363.9	3.8	392.6	4.1	402.2	4.2
SG-3 to SG-4	124.5	1.3	162.8	1.7	430.9	4.5

CHAPTER FOUR

LEXINGTON, MO. TEST SITE

A new bridge is proposed across the Missouri River in central Missouri.

Foundation elements chosen for the piers in the river are to be drilled shafts socketed into bedrock. The bedrock at the bridge site consists of Pennsylvanian Age shales, siltstones, sandstones, limestones, and scattered coal beds. The unconfined compressive strength of this material varies from about 150 to 16,460 kPa (1.6 to 172 tsf). Present design methods used by MoDOT would dictate that axial load be carried in side shear only for drilled shafts socketed into bedrock. The ultimate side shear was calculated using methods developed by Horvath and Kenny (1979) or Reese and O'Neill (1988). These calculations showed that rock sockets with a diameter of 1.67 m (5.5 ft) would need to be as long as 18.3 m (60 ft) in order to carry the anticipated axial load. In order to develop a more economical design, it was decided to perform two Osterberg cell load tests at sites in the river close to the proposed bridge alignment. The Osterberg cell load tests were performed by Loadtest Inc. in May and June of 1999 and indicated that the bedrock had higher load capacities than estimated in the original design and that cost savings of around 1.8 million dollars could be realized.

A general geologic description of the Lexington test site is presented in this chapter followed by a summary of the engineering characteristics of the most pertinent strata. The construction and testing procedures for the two test shafts are then described, followed by presentation of the results from each load test. Because the bridge was designed, and load test results reported in SI units, all figures and tables are shown in SI units. Dual units are reported throughout the text.

4.1 Site Description

The Missouri Department of Transportation (MoDOT) is planning a realignment of Route 13 at Lexington, Missouri. The realignment includes a new bridge across the Missouri River, Section 19 and 22, Township 51 North, Range 26 West, about 3.9 km (2.4 miles) east or downstream of the present structure, which was opened to traffic in 1925.

The project is situated in the Missouri River alluvial plain in the central part of the state of Missouri as shown in Figure 4.1. The alluvial plain is mostly flat with some earthen levees constructed to protect row crop production. Currently, the river channel is located adjacent to the bluff on the southern limit of the plain. The Missouri River alluvial plain is about 1.1 kilometers (3350 feet) wide in the project area and the alluvial material consists of 1 to 2 meters (3.3 to 3.5 ft) of cohesive soil overlying sand with scattered gravel layers. The thickness of the alluvial materials in the floodplain North of the river varies from 26.5 to 33.3 meters (86.9 to 109.3 ft). Within the river, the alluvial sand and gravel layers range in thickness from 8.5 to 16 meters (27.9 to 52.5 ft) (HNTB 1998). The total length of the bridge is to be 1244.5 meters (4083 feet) with 25 spans of various lengths. The two main river spans will be 144 and 122 m (472 and 400 feet) in length as shown in Figure 4.2. The bridge will extend from the north abutment located in the flood plain southeast across the flood plain and river to the south abutment located on the bluff on the south side of the river.



Figure 4.1- Location sketch of Lexington bridge site.

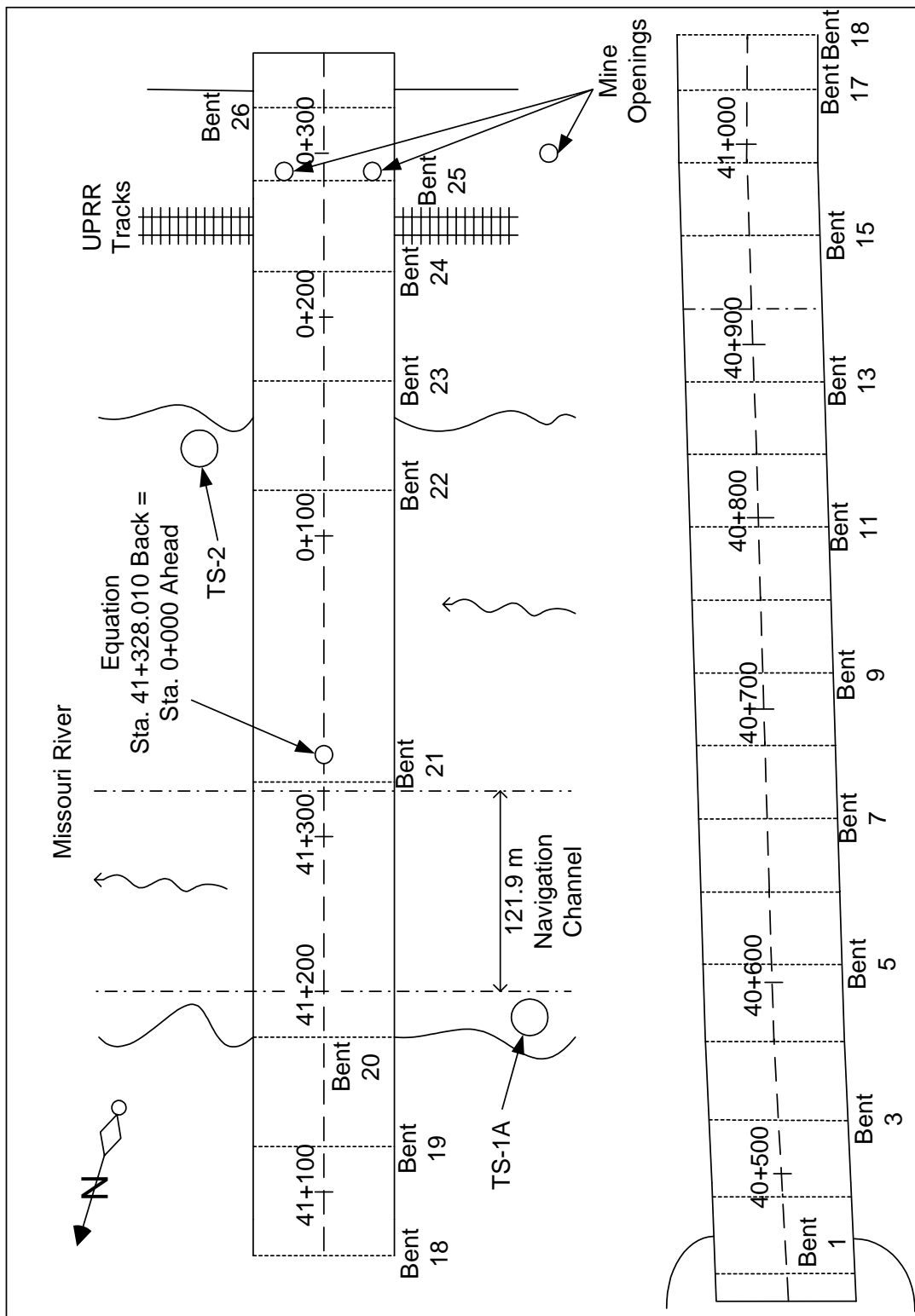


Figure 4.2- Plan view of Lexington bridge showing locations of bridge bents and test shafts

Foundation elements for Piers 1 through 18 were anticipated to be H-piles driven to bedrock. Drilled shafts socketed into the shale bedrock were anticipated for Piers 19 through 24, which included the three piers in the river (21, 22 and 23). Foundations for Piers 25 and 26 were anticipated to be H-piles driven in pre-bored holes in the shale bedrock. An elevation view of Piers 19 through 24 with anticipated rock sockets and test shafts TS-1A and TS-2 is provided in Figure 4.3. Piers 19, 23, and 24 will have 6 six shafts in a group; Piers 20 and 22 will have eight; and the mid-river pier, Pier 21, will have 15 shafts in a group. Rock sockets for Piers 19 through 21 will encounter from the base upwards the Croweburg Formation 4m (13.1 ft) thick, Verdigris Formation 3.4 m (11.2 ft) thick, and the Bevier Formation 10.6 m (34.8 ft) thick. Additionally, test shaft TS-1A would encounter the Fleming Formation below the Croweburg. Rock sockets at Pier 22 would encounter the Bevier Formation and the Lagonda Formation 10.8 m (35.4 ft) in thickness. Rock sockets for Piers 23 and 24 would encounter the Lagonda and the Mulky Formation 3.2 m (10.5 ft) in thickness. At Pier 25, the Higginsville Limestone was not continuous over the full footing and it was decided to prebore to about elevation 208.75 m and seat H-piles into the Little Osage Formation. At Pier 26, piles were anticipated to be pre-bored through the loess overburden and Altamont Formation and seated into the Bandera Formation. The geology of the site is described in the following paragraphs using the *Stratigraphic Succession in Missouri* (Thompson 1995) as a guide.

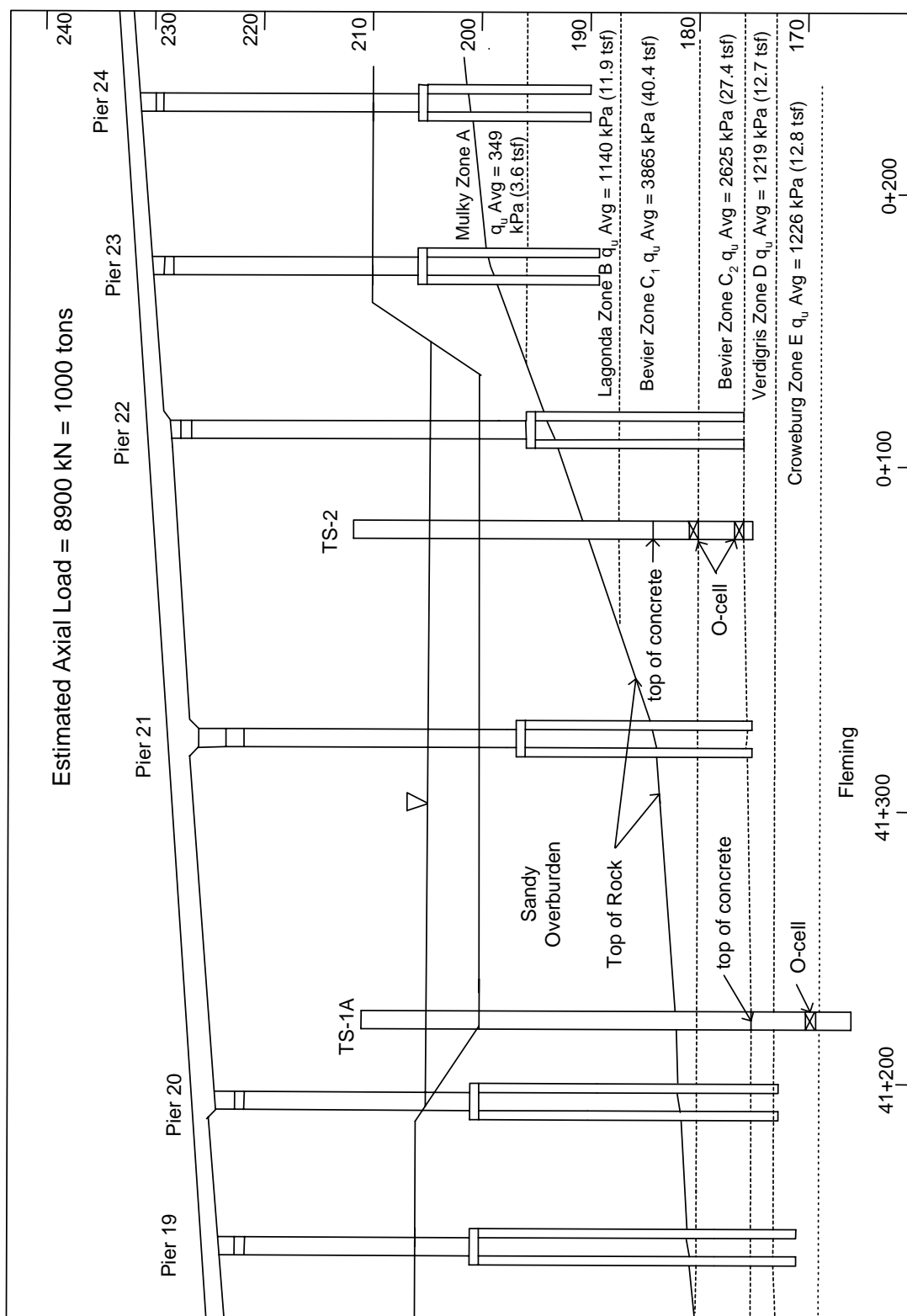


Figure 4.3- Elevation view of bridge showing piers 19 -24 and test shafts TS-1A and TS-2.

4.2 Geology of the Area

The underlying bedrock at the test site is of lower Pennsylvanian Age, Desmoinesian Series, and is assigned to the Cherokee and Marmaton Groups. The Cherokee and Marmaton Groups are horizontally bedded and dip slightly in a northwesterly direction. The Cherokee Group contains most of the mineable coal beds in Missouri and is divided into the Krebs and Cabaniss Subgroups. Rock sockets for the drilled shafts are planned in the upper part of the Cabaniss Subgroup.

The Cabaniss Subgroup consists of sandstone, siltstone, underclay, limestone, and coal beds. Underclay is usually a very compact clay to claystone that underlies coal beds and commonly contains the roots of coal plants. The underclay may range from a few centimeters to several meters in thickness. The underclay is noted in MoDOT's drilling logs as a clay shale, poorly laminated. The subsurface investigation for the river piers encountered six of the eleven widely recognized successions of the Cabaniss Subgroup of the Cherokee Group. These are from the base upward: the Fleming Formation, the Croweburg Formation, the Verdigris Formation, the Bevier Formation, the Lagonda Formation, and the Mulky Formation. Each of these formations is described in the following paragraphs and the location of the rock sockets for the test shafts with respect to the formations is shown in Figure 4.4.

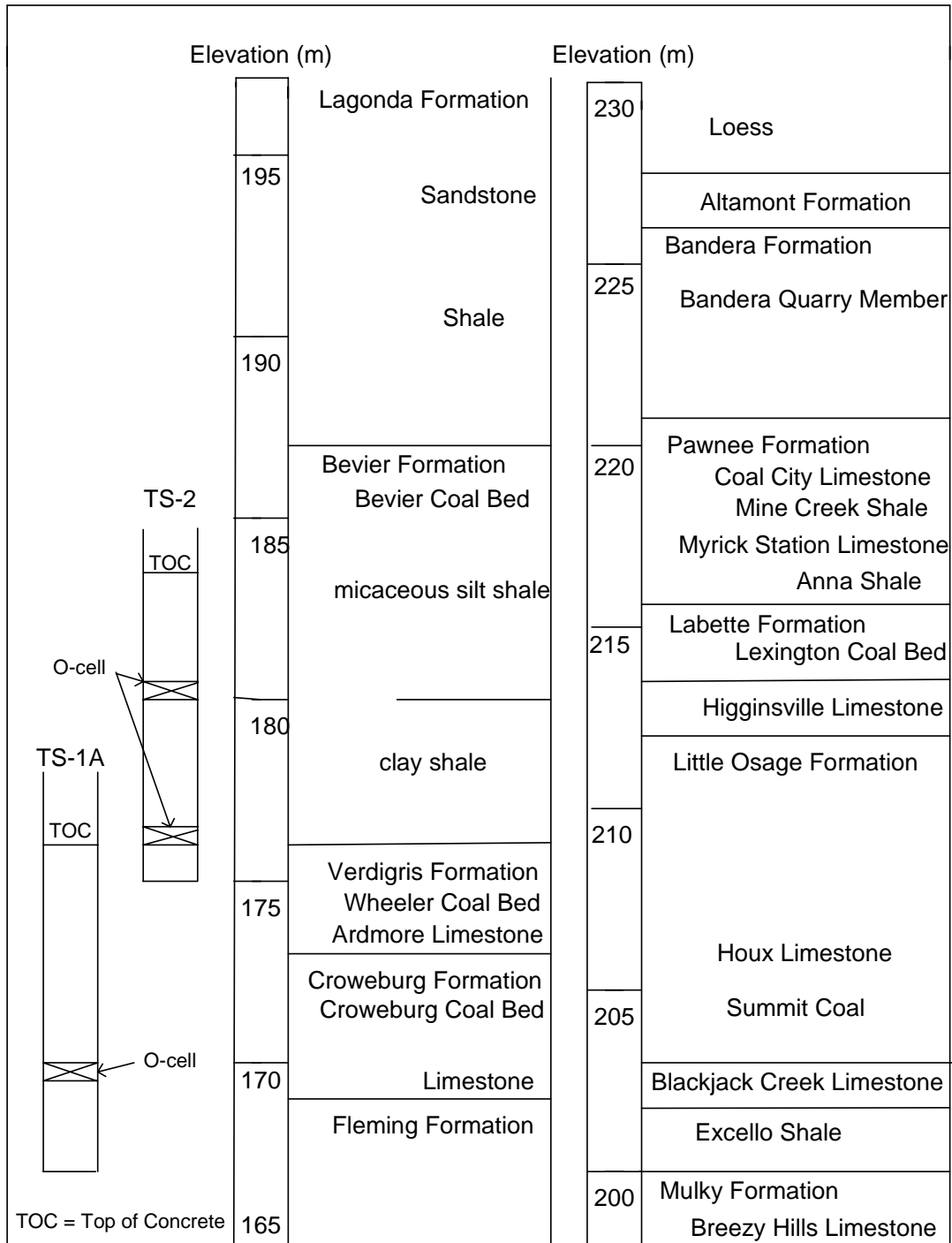


Figure 4.4- Stratigraphy of Lexington test site.

4.2.1 Fleming Formation

The Fleming Formation includes (from the base upward) a thin dark-gray fossiliferous limestone, a dark gray to black fissile shale, lenses of fine-grained sandstone and siltstone, an underclay, and the Fleming Coal Bed (Thompson 1995). This formation was encountered from about elevation 165.5 to 169.0 m and averages about 3.5 m (11.5 ft) in thickness. SPT blow counts in the Fleming Formation averaged 100 blows in 6 cm (2.4 in).

4.2.2 Croweburg Formation

The Croweburg Formation includes (from the base upward) a fossiliferous limestone, a gray-green calcareous clay shale, underclay, and the Croweburg Coal bed (Thompson 1995). This formation was encountered from about elevation 169 to 173 m and averages about 4 m (13.1 ft) in thickness. SPT blow counts in the Croweburg Formation averaged 100 blows in 8 cm (3.1 in). Liquid limits varied from 46 to 27 and the PI varied from 23 to 11. A jar slake test (Wood and Deo 1975 and Lutten 1977) performed on the gray clay shale indicated a jar slake index of 2 as shown in Figure 4.5.



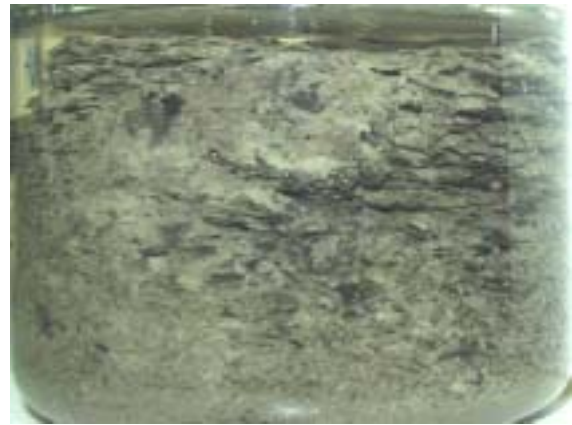
Figure 4.5- Jar slake index test results for Croweburg Formation: Elev. 172.27 m, slake index (2).

4.2.3 Verdigris Formation

The Verdigris Formation includes (from the base upward) gray-green clay shale to mudstone, a black fissile shale, gray thick bedded shaly limestone, (Ardmore Limestone Member), poorly laminated gray clay shale, (probably underclay), and the Wheeler coal bed (Thompson 1995). The Ardmore Limestone was encountered at about elevation 173.4 m. This formation was encountered from about elevation 173 to 176.4 m and averages about 3.4 m (11.2 ft) in total thickness. SPT blow counts in the Verdigris Formation averaged 100 blows in 12 cm (4.7 in). Liquid limits varied from 37 to 34 and the PI varied from 16 to NP. Jar slake tests performed on the gray clay shale varied from a jar slake index of 1 to 2 as shown in Figure 4.6.



(a) Slake Index (1)



(b) Slake Index (2)

Figure 4.6- Range of jar slake index test results for Verdigris Formation: (a) Elevation 176.75 m, slake index (1); (b) elevation 175.27 m, slake index (2).

4.2.4 Bevier Formation

The Bevier Formation includes (from the base upward) a gray clay shale, a micaceous silt shale to siltstone, a clay shale, and the Bevier coal bed (Thompson 1995). This formation was encountered from about elevation 176.4 to 187 m and averaged about

10.6 m (34.8 ft) in thickness. SPT blow counts in the Bevier Formation averaged 100 blows in 9 cm (3.5 in). Liquid limits varied from 25 in the upper Bevier (zone C1) to 39 in the lower Bevier (zone C2) and the PI varied from 2 to 16. Jar slake tests performed on the dark gray to black shale varied from a jar slake index of 5 to 6 as shown in Figure 4.7.



(a) Slake Index (6) Bevier Zone C1

(b) Slake Index (5) Bevier Zone C2

Figure 4.7- Range of jar slake index test results for Bevier Formation: (a) Elevation 183.95 m, slake index (6); (b) elevation 180.45 m, slake index (5).

4.2.5 Lagonda Formation

The Lagonda Formation includes a shale and siltstone or sandstone (Thompson 1995). This formation was encountered from about elevation 187 to 197.8 m and averages about 10.8 m (35.4 ft) in thickness. SPT blow counts in the Lagonda Formation averaged 100 blows in 13 cm (5.1 in).

4.2.6 Mulky Formation

The Mulky Formation includes an underclay, the Breezy Hills Limestone Member, and the Mulky coal bed (Thompson 1995). The Breezy Hills Limestone was

encountered at about elevation 197.9 m. The formation was encountered from about elevation 197.8 to 201.0 m and averages about 3.2 m (10.5 ft) in thickness.

4.3 Jar Slake Test of Shale Bedrock

The jar slake test is performed by immersing an oven dried sample of core in water as described by Wood and Deo (1975) and Lutten (1977). The sample is observed continuously for the first 10 minutes and carefully during the first 30 minutes. When a reaction occurs, it happens primarily during this time frame. A final observation is made after 24 hours. The condition of the piece is categorized as follows:

1. Degrades to a pile of flakes or mud
2. Breaks rapidly, forms many chips or both
3. Breaks slowly, forms many chips or both
4. Breaks rapidly, develops several fractures or both
5. Breaks slowly, develops few fractures or both
6. No Change

Jar slake index values for the shale formations at the Lexington site are summarized in Table 4.1.

Table 4.1- Summary of jar slake index tests results for shale formations at Lexington site.

Formation	Zone	Elevation (m)	Jar Slake Index
Bevier	C1	183.95	6
Bevier	C1	181.15	6
Bevier	C2	180.45	5
Bevier	C2	178.57	5
Verdigris	D	177.77	1
Verdigris	D	176.75	1
Verdigris	D	175.27	2
Croweburg	D	172.75	2

4.4 Unconfined Compressive Strength of Bedrock at Piers 19 thru 24

Bedrock samples were taken with a standard split spoon sampler and a NX-sized double-wall core barrel. The core was logged with the amount of core recovered and the RQD being noted although MoDOT does not record RQD's in shale. Samples of the NX core were returned to the laboratory for further testing. Unconfined compressive strengths of the rock cores for Piers 19 through 24 varied from 140 kPa (1.5 tsf) to 25,830 kPa (269 tsf) with an overall average unconfined compressive strength of 2828 kPa (29.5 tsf). The bedrock profile was divided into six zones based on strata and trends in material strengths, as shown in Table 4.2. The unconfined compressive strength of the rock core varied considerably, influenced by the difficulty of obtaining representative samples of the shale and the presence of scattered limestone layers. Unreasonably low values for the unconfined compressive strength were not used to calculate the average strengths for the layers. Higher values caused by scattered limestone layers were also discounted.

Table 4.2- Unconfined compressive strengths for rock cores at Lexington site.

Zone	Elevation	Formation	Avg. q_u		Range	Std. Dev.
			kPa	tsf		
	Meters				kPa	kPa
A	197.7-201	Mulky	225	2.3	110 - 340	117
B	187-197.7	Lagonda	1,570	16.4	140 - 7,520	1,775
C ₁	180.4-187	Bevier	3,811	39.8	1020 - 8,105	2,210
C ₂	176.4-180.4	Bevier	3,001	31.3	311 - 7,130	2,565
D	173.0-176.4	Verdigris	1,212	12.7	218 - 4,482	1,244
E	169-173.0	Croweburg	1,716	17.9	253 - 5,590	1,552
F	165.5-169	Fleming	544	5.7	150-1241	404

4.5 Foundation Design

Drilled shafts socketed into bedrock were chosen for the foundations of the piers immediately adjacent to the river and the river piers. Drilled shafts were chosen due to the thickness of the alluvium and the potential depth of scour. Scour is predicted to extend as much as 3 to 8 meters below the top of the shale bedrock.

Due to the alternating layers of shale, sandstone, siltstone, coal, and underclays, the rock socket design was based entirely on side resistance; potential resistance from end bearing was ignored. The ultimate unit side shear was determined by using Equations 2.11 and 2.18 presented in Chapter 2. The allowable unit side shear was determined by dividing the ultimate unit side shear by a safety factor of 2.5 as required by the American Association of State Highway and Transportation Officials (AASHTO 1996) manual on Standard Specifications for Highway Bridges. AASHTO allows the safety factor to be reduced to a value of 2.0 if a load test is performed. For a design load estimated to be about 8900 kN (1000 tons) and 1.68 meter (5.5 feet) diameter rock sockets, the required socket lengths would vary from 25.5 to 29 meters (83.6 to 95 feet). Rock sockets of this length would be very costly (HNTB 1996). The possibility of using larger diameter sockets, or increasing the number of sockets in a footing, was investigated but these alternatives were found to increase the footing size, which would in turn increase the potential scour depth and costs (HNTB 1996). In order to reduce the costs and allow for a practical design, it was decided to perform Osterberg cell load tests on two test shafts founded in various strata of the shale bedrock to better quantify available side shear resistance from the rock socket with the hope of producing more economical designs.

4.6 Construction of Test Shafts

Due to the difficulty with access to the sites by land and to avoid hindering river traffic, the two test shafts were located in the river but near the river banks. Test shaft one (TS-1) was planned to be located adjacent to the North river bank to evaluate side shear in Zones D, E, and F (Table 4.2) to provide design data for Piers 19 through 22. Test shaft two (TS-2) was to be constructed adjacent to the South river bank to evaluate side shear in Zones C₁, C₂, and D to provide design data for Piers 21 and 22, and possibly 23 and 24 (HNTB 1996). The location of the test shafts is shown in Figures 4.2 and 4.3. Test shaft one (TS-1) was located near the North bank of the river immediately west of Pier 20 and Test shaft two (TS-2) was located near the South bank immediately east of Pier 22 (Figure 4.2).

The two test shafts were constructed by Massman Construction using a Manitowoc 4100 series crane with drill assembly mounted on a barge as shown in Figure 4.8. Both shafts were permanently cased through the overburden soils with the permanent casing seated into the shale bedrock. The rock sockets were drilled using a bullet tooth rock auger. The drilling fluid used was water and concrete was poured using a tremie. The slump of the concrete was about 203 mm (8 in) when it left the concrete plant and about 102 mm (4 in) when it was pumped into the shafts. The concrete mix included a four-hour retarder. Loadtest Inc. provided the Osterberg cells, instrumentation, and gages and performed the load tests. Both test shafts were impacted by high river levels and scheduling conflicts. As described in more detail below, test shaft TS-1 had to be abandoned due to caving of the shale bedrock, and was subsequently replaced by another test shaft denoted as TS-1A.



Figure 4.8- Manitowoc 4100 series crane with drill assembly.

4.6.1 Construction of Test Shafts TS-1 and TS-1A

The contractor mobilized to the site and began driving sheet piling for a work platform and ice deflector on February 15, 1999. The overburden soils for shaft TS-1 were excavated and 31 m (102 ft) of casing was set into the shale bedrock on March 30, 1999. The excavation of the rock socket was completed on April 13, 1999. The river subsequently rose above the construction platform and inundated the shaft. The river subsided below the work platform on April 19, 1999. The O-cellTM was removed and the rock socket was over-reamed on April 22nd in an attempt to freshen the sidewalls of the socket. The river then rose above the platform on April 23rd for a second time. Work resumed on May 12, 1999 when an additional sonar caliper test of the rock socket was performed. Sonar results indicated that the socket had caved to more than double the

original diameter at some depths. TS-1 was therefore abandoned and a new test shaft, TS-1A, was drilled 15 meters upstream of TS-1. The collapse of test shaft TS-1 has led to a specification change that requires rock sockets to be excavated and the shaft concrete to be placed within 3 days for shafts constructed in shales. Further specification changes require the use of polymer slurry in drilled shafts constructed in shale that cannot be constructed “in the dry.”

The rock socket for test shaft TS-1A was drilled on June 15th through 16th, 1999. Figure 4.9 shows a schematic of TS-1A. The shaft was calipered on June 17, 1999 using a sonar caliper as shown in Figure 4.10. The carrying frame with one 660 mm (26 in) O-cellTM and various instrumentation was then placed into the rock socket as shown in Figure 4.11. The carrying frame was constructed from C-4 channel section as shown in Figure 4.12. The shaft concrete was also placed into the rock socket on June 17, 1999. A sonar caliper log for TS-1A is presented in Figure 4.13. Loadtest personnel arrived on the site on June 22, 1999 and started the test at 10:35 am. The test was completed at 2:00 pm.

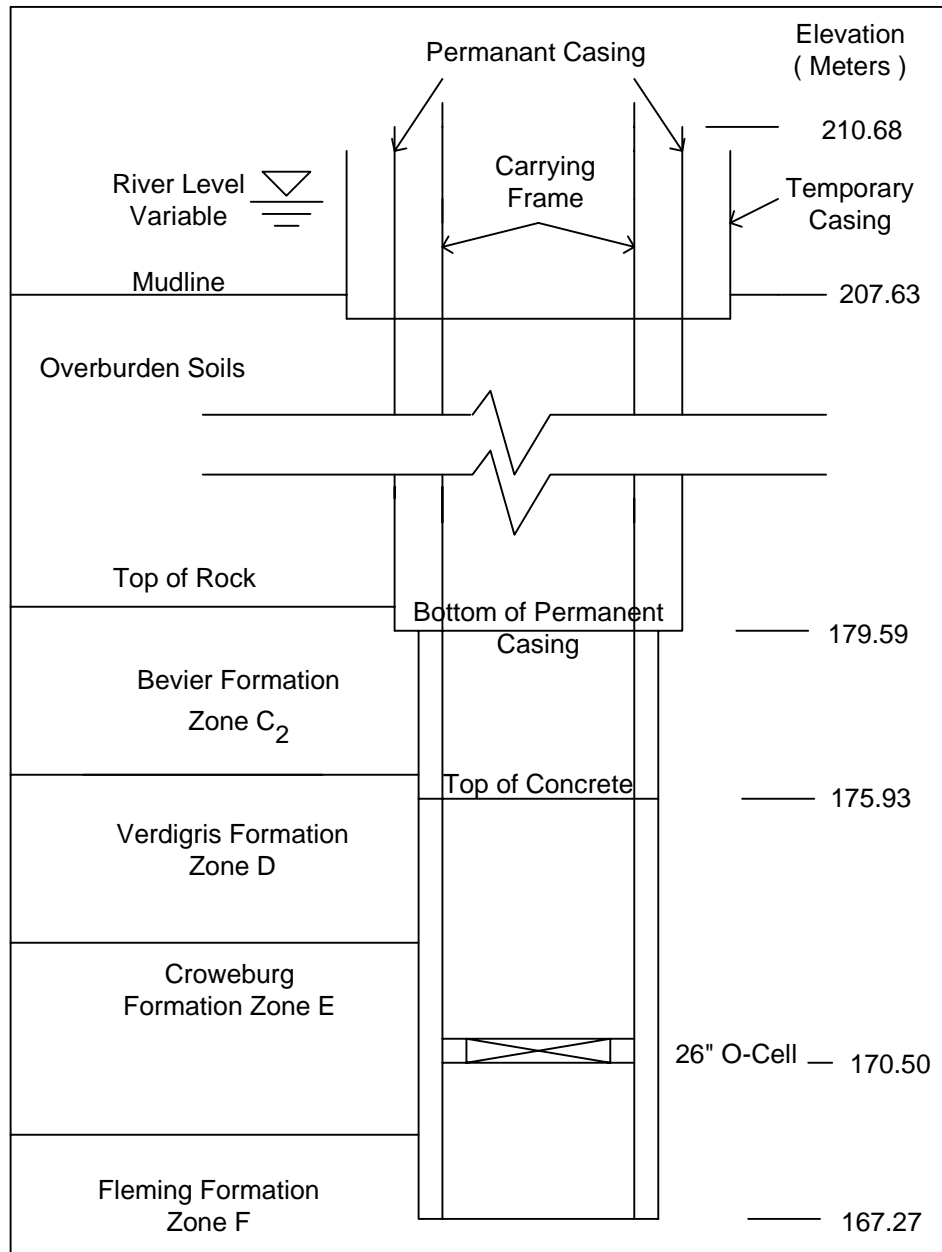


Figure 4.9- Schematic of test shaft TS-1A.



Figure 4.10- Sonar caliper prior to placement in test shaft excavation.



Figure 4.11- Preparing to lower carrying frame and O-cellTM into test shaft TS-1A.



Figure 4.12- Carrying frame and instrumentation for test shaft TS-1A.

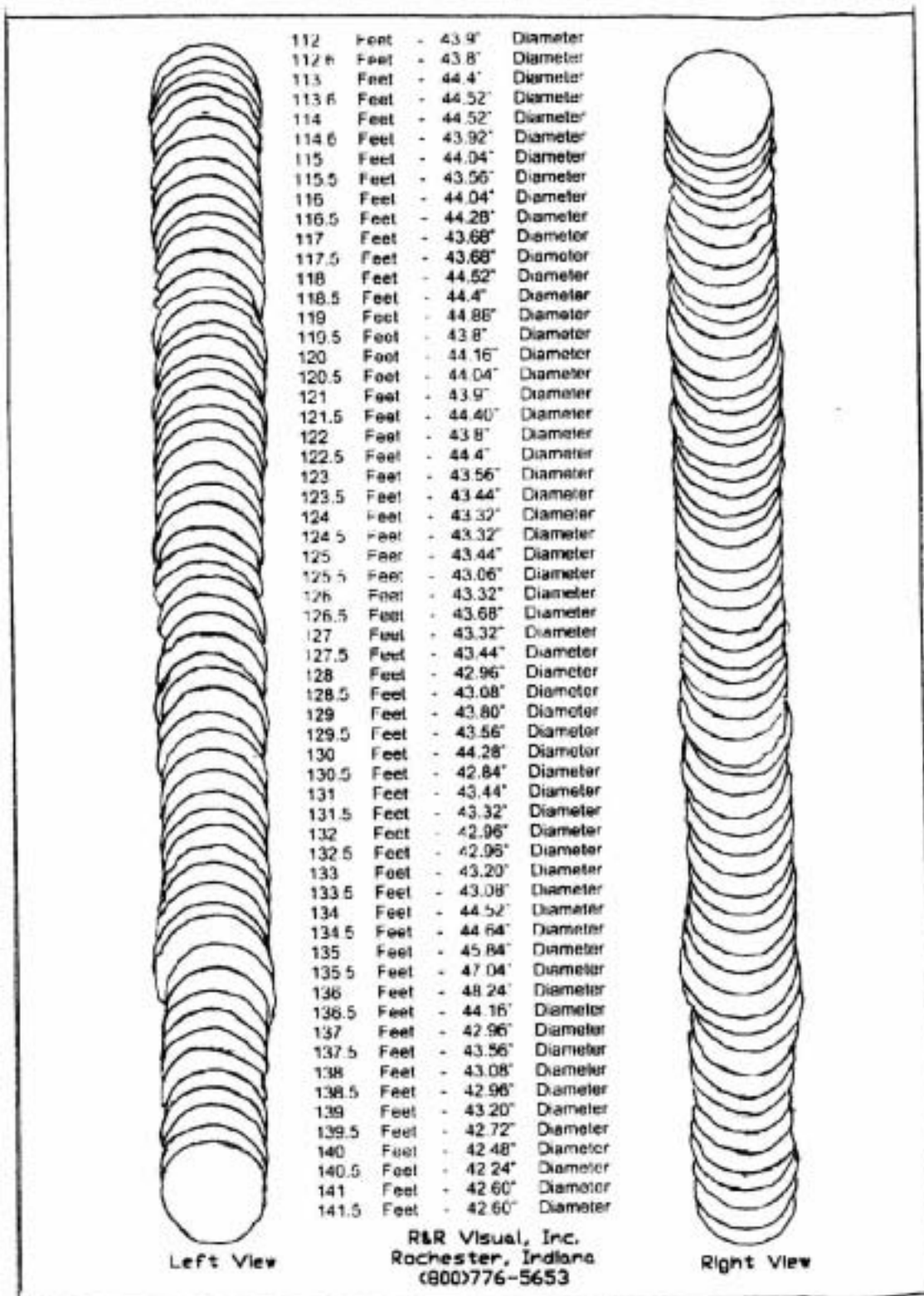


Figure 4.13- Sonar caliper log of rock socket for test shaft TS-1A.

4.6.2 Construction of Test Shaft TS-2

Test shaft TS-2 included two Osterberg load cells to allow evaluation of unit side shear in separate strata. Figure 4.14 shows a schematic of test shaft TS-2. The contractor mobilized and began driving sheet piling for the work platform and ice deflector on February 18, 1999. Temporary casing was set on April 1, 1999. The overburden soils were excavated and 17.1 m (56 ft) of permanent casing was set into the shale bedrock on April 2nd. The rock socket was drilled to about 1.5 m (5ft) above the planned top of the rock socket concrete (Elev. 184.4 m) on April 6, 1999. Completion of the shaft was then delayed due to scheduling conflicts. On April 14, 1999 the socket was drilled to about 1 meter below the location for the upper Osterberg cell (Elev. 180.17 m). During the following days, the river level rose above the construction platform and likely topped the permanent casing. When the river level dropped below the platform on April 21, 1999, TS-2 was drilled to the planned depth and cleaned by airlifting. The socket was calipered with a sonar unit and the carrying frame with two O-cellsTM was set on April 22nd as shown in Figures 4.15 and 4.16. Sonar caliper logs for TS-2 are presented in Figures 4.17 and 4.18.

Since the test shafts were located in the river, the delivery of concrete to the site involved a 2.5 kilometer (1.5 mile) barge trip. Delays occurred in placing concrete in TS-2 due to clogging of the tremie pipe and, by the end of the day on April 22nd, only the bottom cell was encased in concrete. This caused a cold joint at an elevation of approximately 178.5 meters. The permanent casing was capped as the river rose above the platform on April 23rd. On April 26th air and water were pumped to the cold joint to

attempt to suspend the dirt and debris that had accumulated and a second attempt to complete the pour was made. The slump of the concrete was about 102 mm (4 in). Problems with the concrete pump and tremie again delayed the pour. The cold joint was again flushed on April 27th and the concrete pour was completed. Loadtest personnel arrived on the site and completed the test on May 3, 1999.

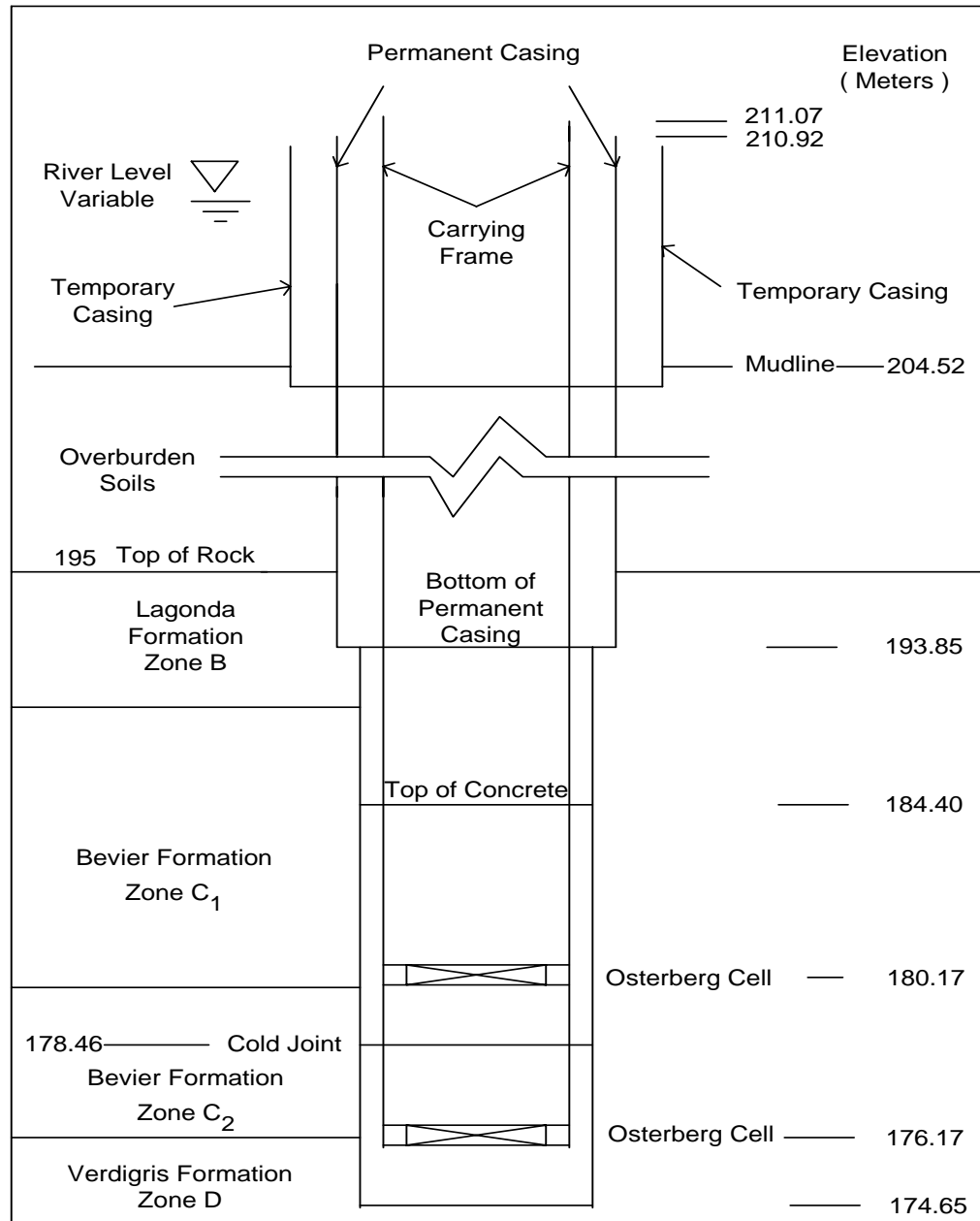


Figure 4.14- Schematic of test shaft TS-2.



Figure 4.15- Carrying frame with two Osterberg load cells for test shaft TS-2.



Figure 4.16- Lowering carrying frame and O-cells for test shaft TS-2.

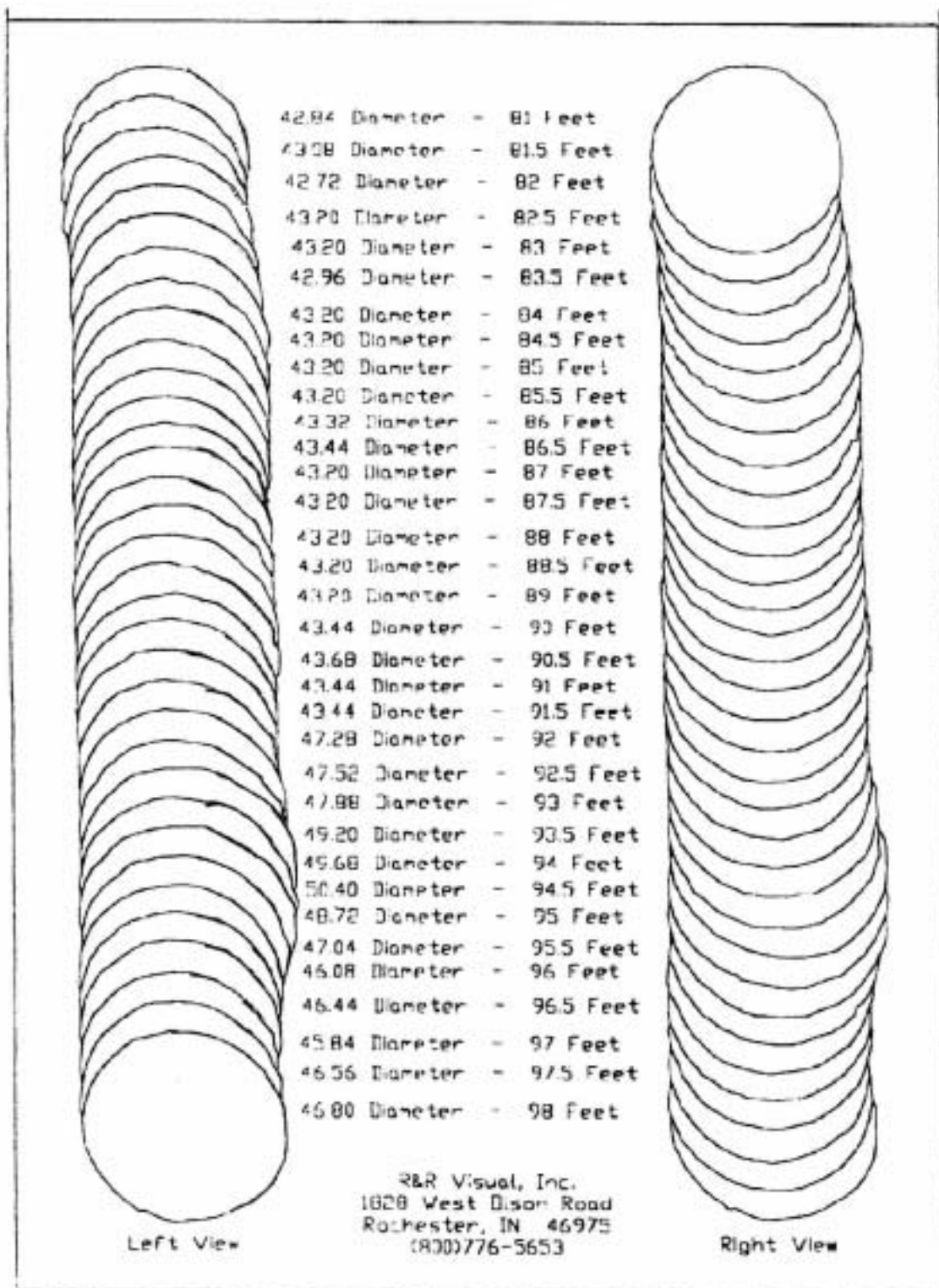


Figure 4.17- Sonar caliper log of rock socket for test shaft TS-2 (81-98 ft from top of casing).

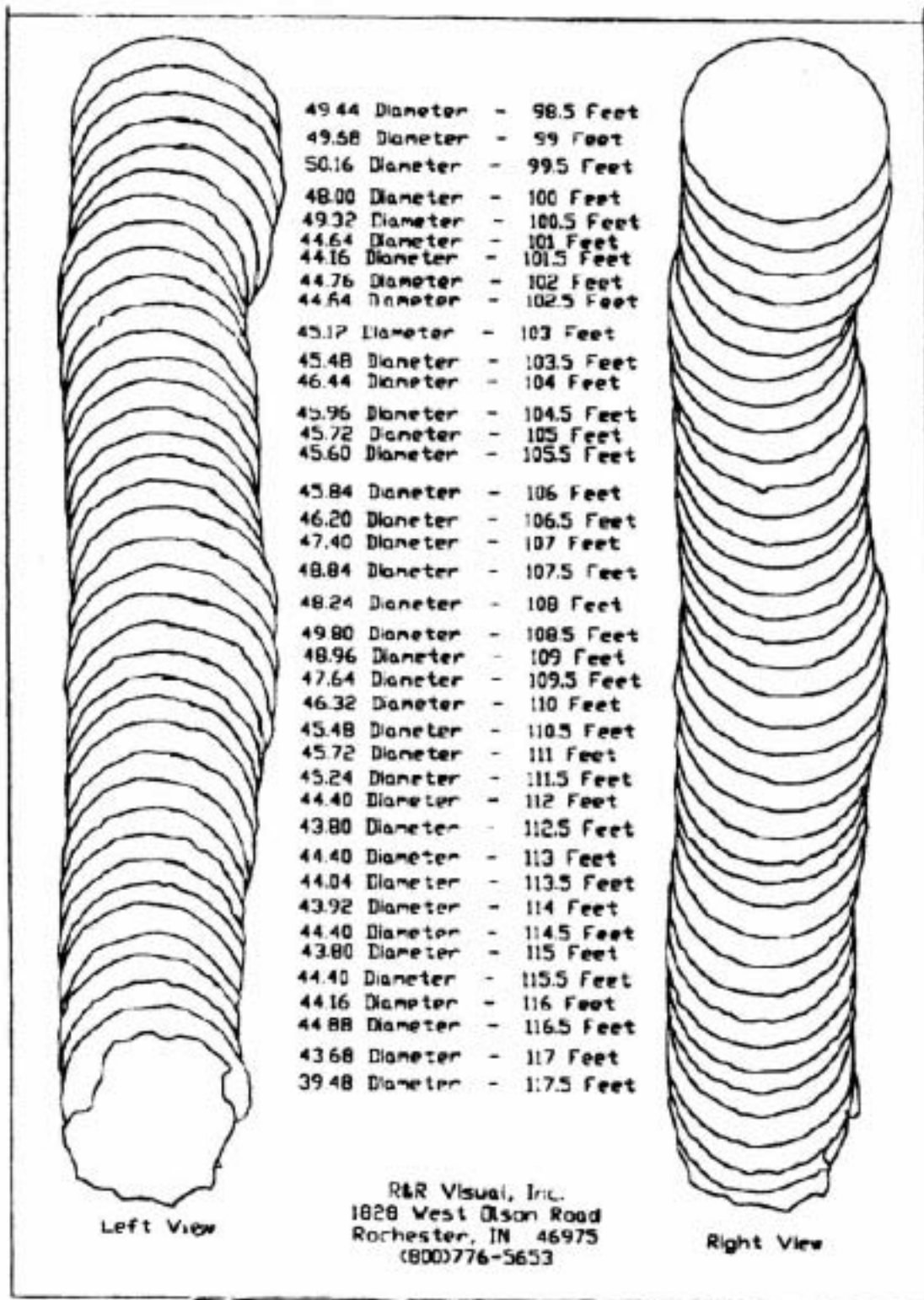


Figure 4.18- Sonar caliper log of rock socket for test shaft TS-2 (98.5-117.5 ft from top of casing).

4.7 Load Test Setup and Procedures

Load tests for test shafts TS-1A and TS-2 were performed by Loadtest Inc. on June 22, 1999 and May 3, 1999, respectively. The test setup and instrumentation for each test are described in the following sections along with the loading procedure utilized for each test.

4.7.1 Test Shaft TS-1A Setup and Procedure

The 660 mm (26 in) diameter O-cellTM, with its base located 3.23 m (10.6 ft) above the tip of the rock socket was pressurized to assess the combined end bearing and side shear below the O-cellTM and side shear above the cell. The O-cellTM was pressurized in 36 equal increments of 0.48 MN (54.3 tons) to a maximum load of 17.39 MN (1955 tons). The loading increments are denoted as 1L-1, 1L-2, 1L-3, etc. and the unloading events are denoted as 1U-1, 1U-2, 1U-3, etc. Although the capacity of the cell was not reached, the capacity of the available pressure gage was reached at a load of 17.39 MN (1955 tons) and the test had to be stopped. The O-cellTM was then unloaded in 7 equal increments and the test was concluded. Other than the problem with the gage capacity no significant problems were encountered in performing the test.

Expansion of the O-cellTM was measured by three LVWDTs positioned between the lower and upper plates of the O-cellTM. Test shaft TS-1A instrumentation is shown in Figure 4.19 and a summary of test shaft dimensions is given in Table A.1 in Appendix A. Compression of the shaft above the O-CellTM was measured by a pair of embedded compression telltales (ECTs). Two digital dial gages attached to a reference beam monitored the top of shaft (carrying frame) movement. Four levels of three sister bar

vibrating wire strain gages were installed in the shaft: one level below the cell and three above. The strain gages were used to assess load transfer in the shaft.

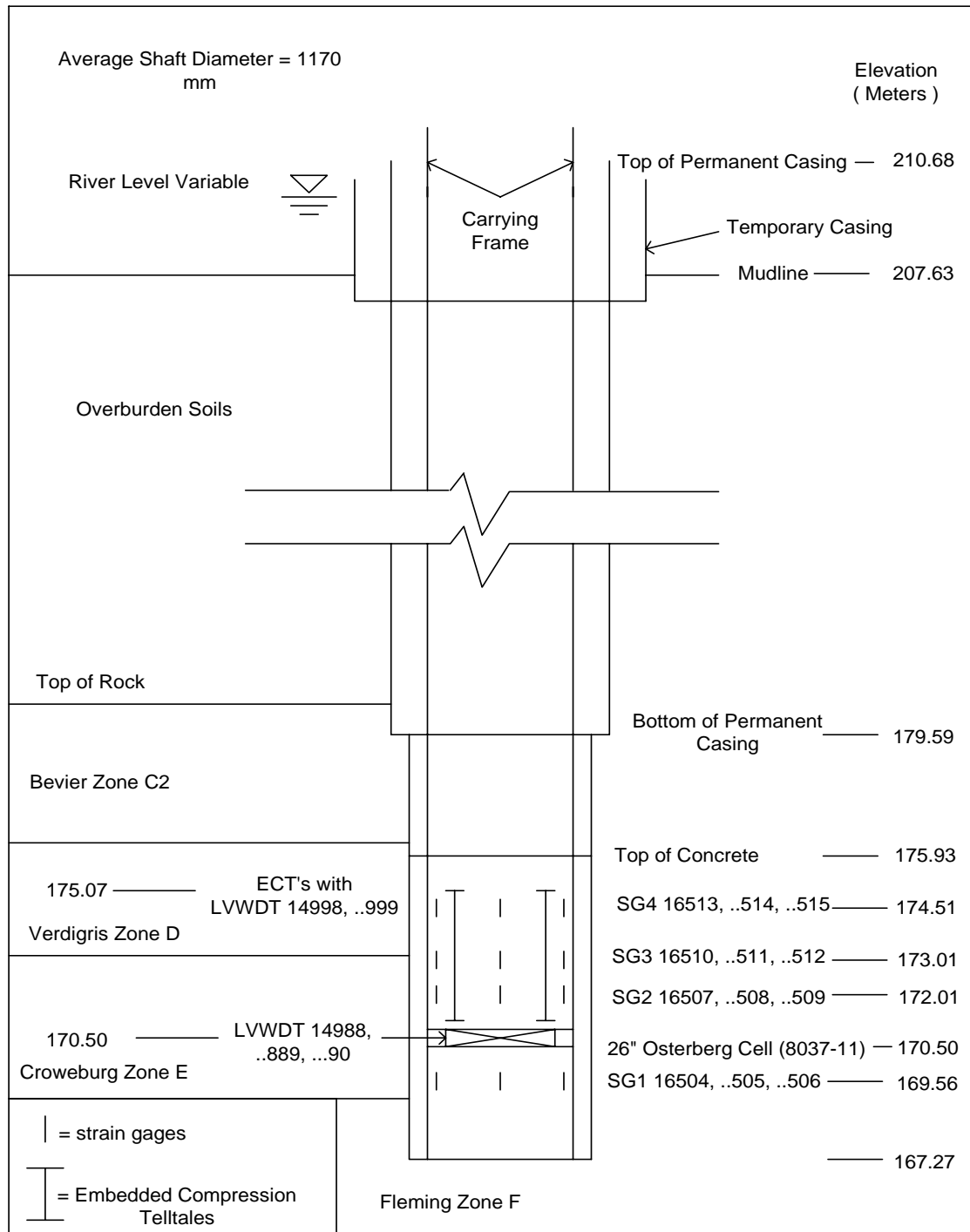


Figure 4.19- Schematic of test shaft TS-1A showing location of instrumentation.

4.7.2 Test Shaft TS-2 Setup and Procedure

The load test for test shaft TS-2 was performed in three stages to evaluate load transfer in different segments of the shaft. The three stages are as follows:

Stage 1: In Stage 1, the lower 660 mm (26 in) diameter O-Cell™, with its base located 1.52 m (5 ft) above the tip of the rock socket, was pressurized to assess the combined end bearing and side shear below the lower O-Cell™ using the side shear above the lower and upper cells as the reaction. The lower O-Cell™ was pressurized in 13 even increments of 0.8 MN (90 tons) to a maximum load of 10.59 MN (90 tons), at which point the combined end bearing and side shear below the cell were approaching ultimate capacity. The lower O-Cell™ was then unloaded in 5 increments and Stage 1 was concluded.

Stage 2: In Stage 2, the hydraulic line to the lower O-cell™ was left open to allow compression of the cell. The upper 660 mm (26 in) diameter O-cell™ was then pressurized to assess side shear of the shaft between the upper and lower O-cells™ using the side shear above the upper O-cell™ as the reaction. By allowing the lower O-Cell™ to drain, no end bearing resistance was provided below the lower O-cell™. The upper O-cell™ was pressurized in 13 even increments of 0.8 MN (90 tons) to a maximum load of 10.59 MN (1190 tons). The upper O-cell™ was not unloaded.

Stage 3: In Stage 3, the hydraulic line to the lower cell was closed (therefore providing end bearing resistance) before the next loading increment was applied to the upper O-cell™. The combined end bearing and side shear below the upper O-cell™ were then used to assess the side shear above the upper O-cell™. The upper O-cell™ was loaded in four additional increments of 0.8 MN (90 tons) to a maximum load of

13.35 MN (1500 tons), at which point the upper O-cellTM reached its maximum stroke and depressurized.

Expansion of the O-CellsTM was measured by three LVWDTs positioned between the lower and upper plates of the O-CellsTM. Test shaft TS-2 instrumentation is shown in Figure 4.20 and a summary of test shaft dimensions is given in Table A.5 in Appendix A. Compression of the shaft between the two levels of O-CellsTM was measured by a pair of embedded compression telltales (ECTs). Compression of the shaft above the upper O-cellTM was also measured by a pair of ECTs. Two digital dial gages attached to a reference beam monitored the top of shaft (carrying frame) movement. Four levels of three sister bar vibrating wire strain were installed in the shaft, two levels above the lower O-CellTM and two levels above the upper O-cellTM. The strain gages were used to assess load transfer in the shaft.

4.8 General Test Results

The results of the Osterberg cell load tests are presented in the following sections for test shafts TS-1A and TS-2. Detailed load test data is presented in Appendix A. Load- displacement plots are presented from which an “equivalent” top-down load-displacement curve is constructed. Creep is plotted versus the O-cellTM load to determine the creep limit. The distribution of axial force with depth or elevation for various load increments, generated from the strain gage data, is then presented along with unit side shear values calculated for various segments of the shaft. Plots of unit side shear versus O-cellTM movement are used to determine if the maximum unit side shear was achieved.

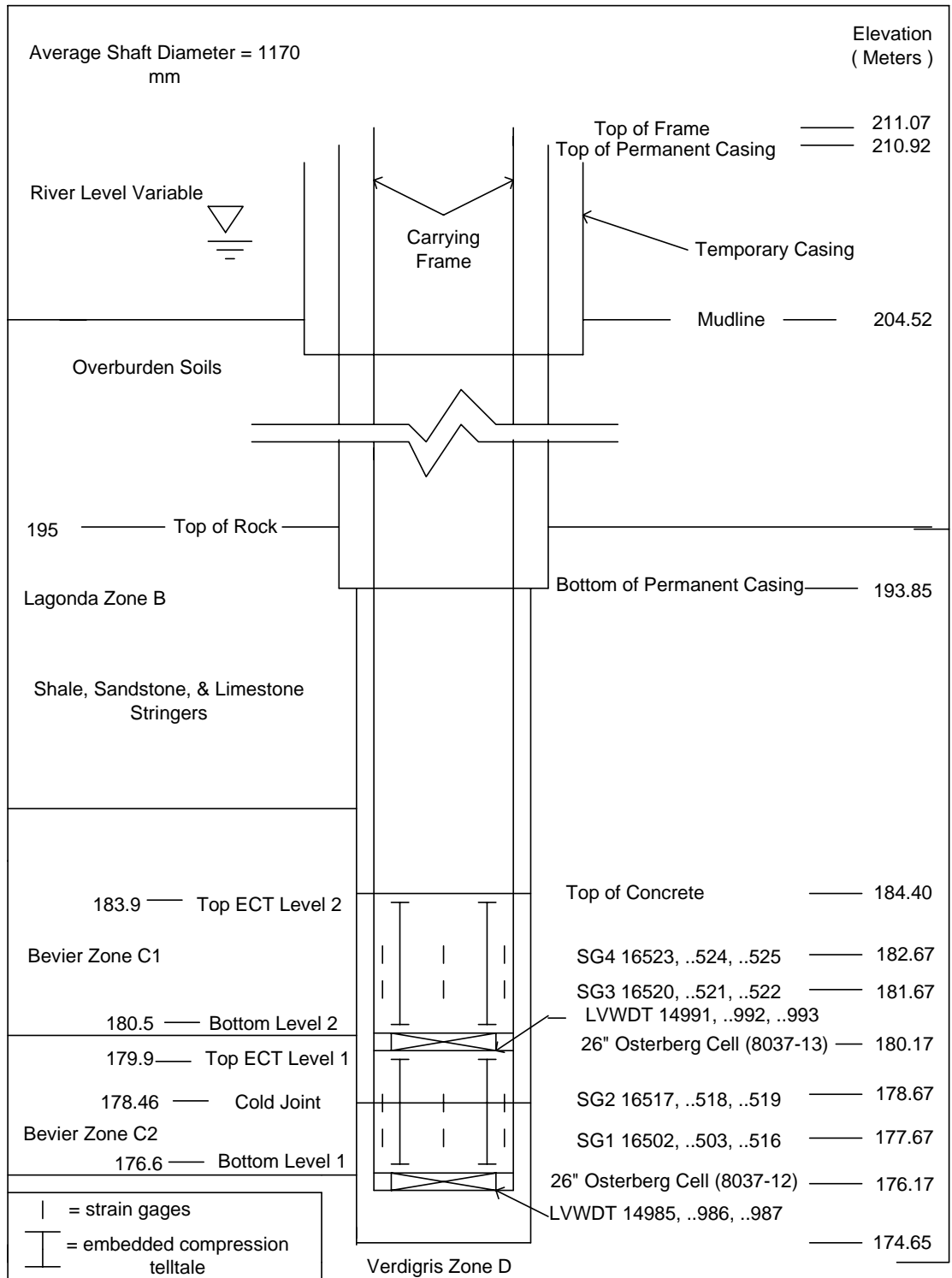


Figure 4.20- Schematic of test shaft TS-2 showing location of instrumentation.

4.8.1 Test Results for TS-1A

The measured load-displacement response for the load test on test shaft TS-1A is shown in Figure 4.21. The maximum applied load occurred at the 36th increment of load for the first and only load interval (1L-36). The maximum load was equal to 17.5 MN minus the buoyant weight of the shaft above the O-CellTM (0.11 MN), for a net applied load of 17.39 MN (1955 tons). At this load, the O-CellTM had expanded 19.1 mm (0.75 in) with 5.5 mm (0.22 in) of upward displacement and 13.6 mm (0.54 in) of downward displacement. The ultimate capacity was not reached in the rock socket either above or below the O-CellTM although the downward loading appears nearer to failure than the upward loading.

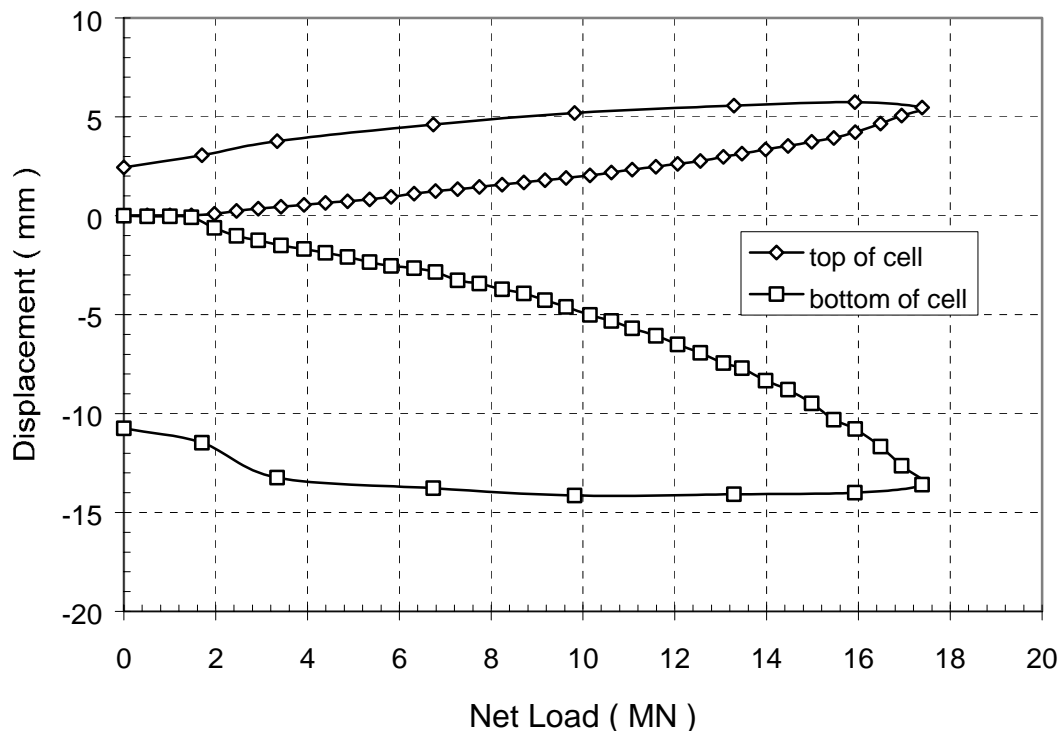


Figure 4.21- Measured load-displacement curves for downward and upward loading of test shaft TS-1A.

Equivalent top-down load-displacement curves were determined as described in Chapter 3. The equivalent top-down load-displacement curves for shaft TS-1A are shown in Figure 4.22. One of the curves shown was computed assuming a rigid shaft, while the other accounts for additional elastic compression that would occur in a top-down test as described in Chapter 3. The curve is extended out to a displacement of 13.6 mm (0.54 in) by extrapolating the O-Cell™ data for the upper portion of the shaft as described in Chapter 3.

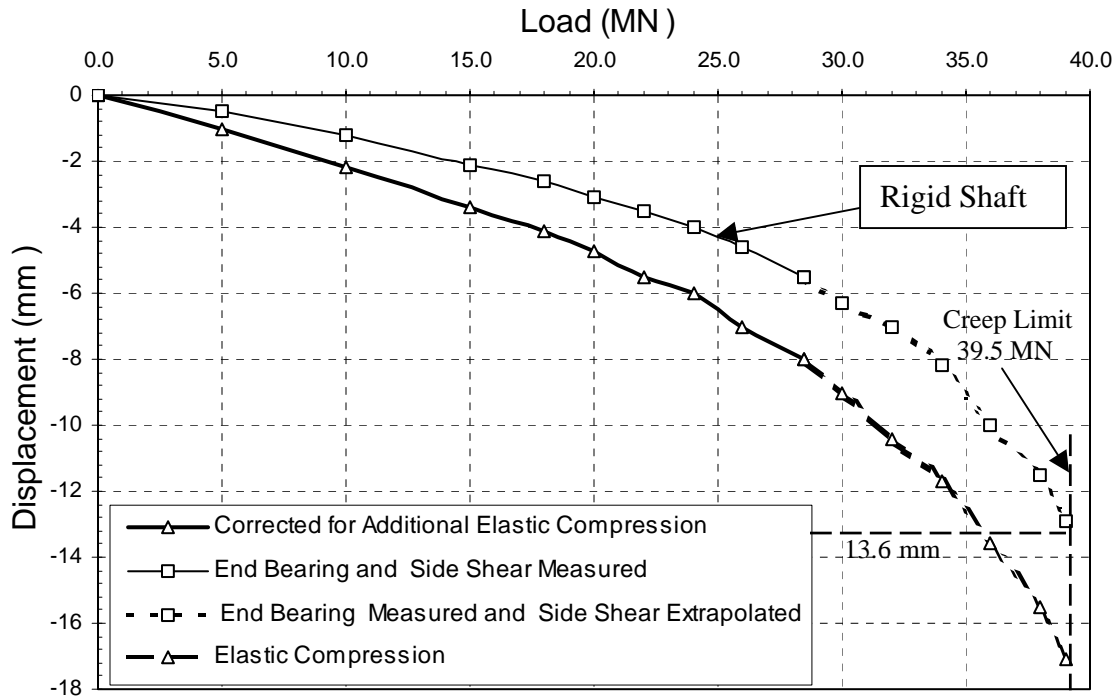


Figure 4.22- Equivalent top-down load-displacement curve for test shaft TS-1A.

The distribution of axial force with depth or elevation at various load increments is generated from strain gage data, the equivalent modulus of the shaft, and the cross-sectional area of the shaft as described in Chapter 3 (Eq. 3.7). The distribution of axial force determined for several load increments applied to TS-1A is shown in Figure 4.23. The strain gage data is provided in Appendix A. On the day of the test, the compressive

strength of test cylinders made from the shaft concrete was 28.1 MPa (4075 psi). This combined with the area of reinforcing steel and shaft diameter, was used to determine an average shaft stiffness (AE) of 25,506 MN (5,730,000 kips).

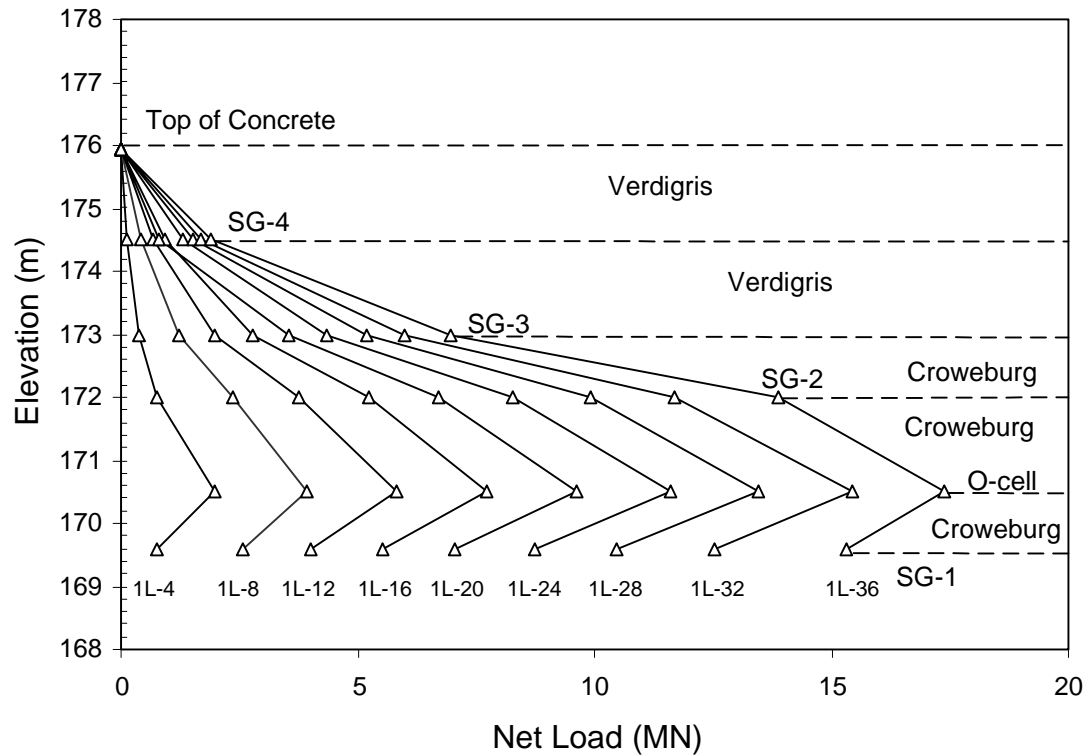


Figure 4.23- Distribution of axial force for test shaft TS-1A.

The magnitude of the unit side shear mobilized for a segment of the shaft is calculated as the change in axial force, ΔF_i , over the length of the segment divided by the surface area of the shaft segment. The average unit side shear above the O-CellTM was found to be 873 kPa (9.1 tsf). Average unit side shear mobilized in the socket below the O-CellTM cannot be estimated directly since an unknown amount of end bearing resisted the load. If the unit side shear value for the segment of shaft below the O-CellTM is assumed to be equal to the unit side shear between the O-cellTM and the level 1 strain gages (SG-1), the unit end bearing value is computed to be 9622 kPa (100.5 tsf).

The mobilized unit side shear for each load increment is plotted versus O-cellTM movement in Figure 4.24. The mobilized unit side shear curves indicate that the side shear has been fully mobilized in the shaft segments immediately adjacent to the O-cellTM (between the O-cellTM and SG-1 and the O-cellTM and SG-2). The mobilized unit side shear curves for the other segments are still increasing, which indicates that the unit side shear values determined for these strata are less than ultimate values. The maximum values of unit side shear determined for each strata are shown in Table 4.3 and plotted in Figure 4.25. The overall maximum value of unit side occurred in the segment of the socket between the level 2 (SG-2) and level 3 (SG-3) strain gages in the Croweburg Formation and was equal to 1983 kPa (20.7 tsf). However, the unit side shear was not the ultimate value (Figure 4.24).

The creep limit is determined by plotting the displacement that occurs over the time interval 2 to 4 minutes after application of a load while the load is maintained constant as shown in Figures 4.26 and 4.27. As shown in the figures, a creep limit was not reached for either the upper side shear or the combined lower side shear and end bearing. A maximum displacement of 13.6 mm (0.54 in) occurred in the lower segment of the shaft during the O-cellTM load test. This data indicates that since a creep limit was not determined, significant creep would not occur for a top loaded shaft until a displacement greater than 13.6 mm (0.54 in) is exceeded by some unknown amount. The displacement of 13.6 mm (0.54 in) correlates to a load of 39.5 MN (4440 tons) on the rigid top-down load-displacement curve as shown in Figure 4.22.

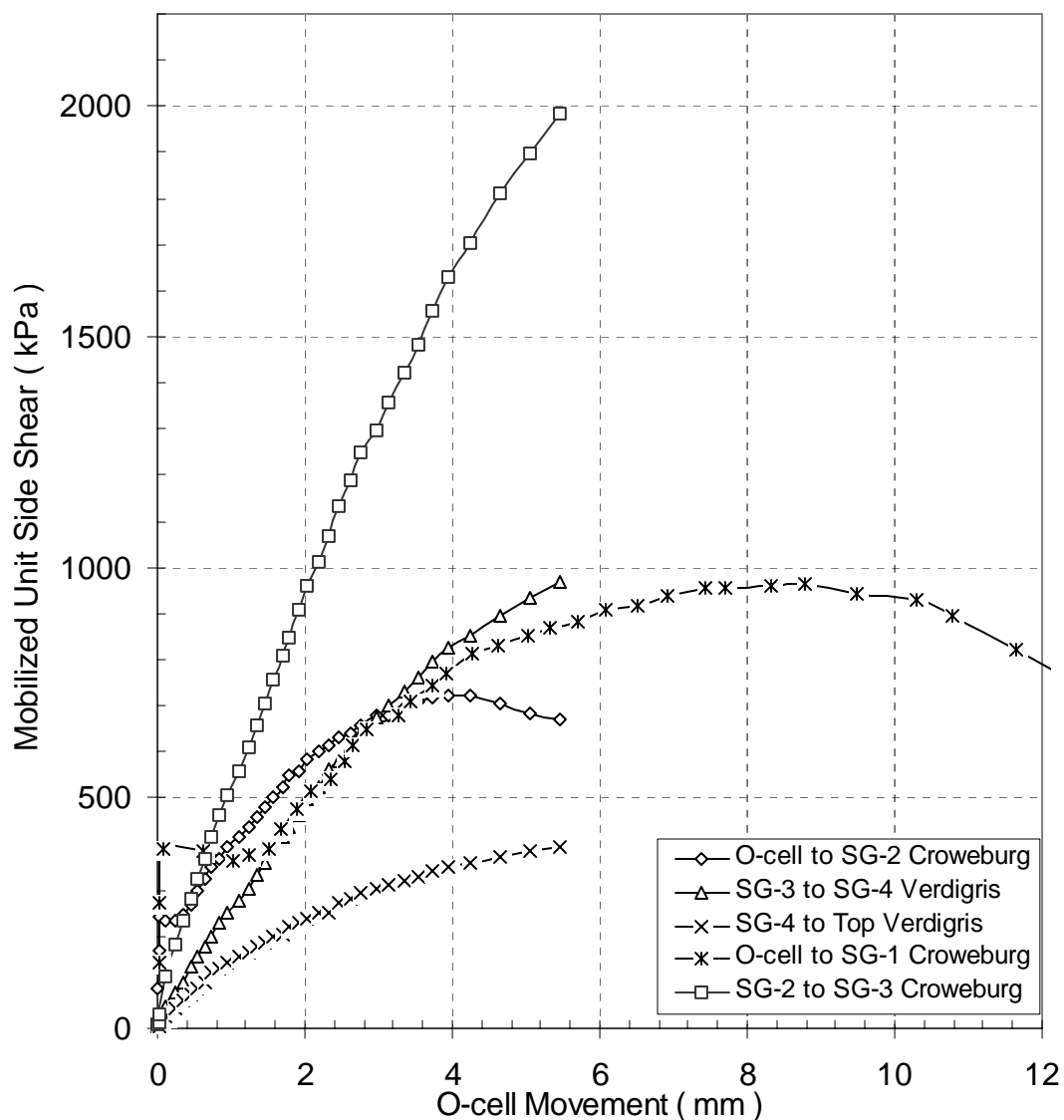


Figure 4.24- Mobilized unit side shear versus O-cellTM movement for test shaft TS-1A.

Table 4.3- Unit side shear values calculated from strain gage data for test shaft TS-1A.

Load Transfer Zone	Strata	Elevation (m) From – To	Unit Side Shear	
			kPa	tsf
SG-4 to Top of Shaft	Verdigris	174.51 – 175.93	391	4.1
SG-3 to SG-4	Verdigris	173.01 – 174.51	968	10.1
SG-2 to SG-3	Croweburg	172.01 – 173.01	1983	20.7
O-Cell TM to SG-2	Croweburg	170.5 – 172.01	723	7.6
SG-1 to O-Cell TM	Croweburg	169.56 – 170.5	963	10.1

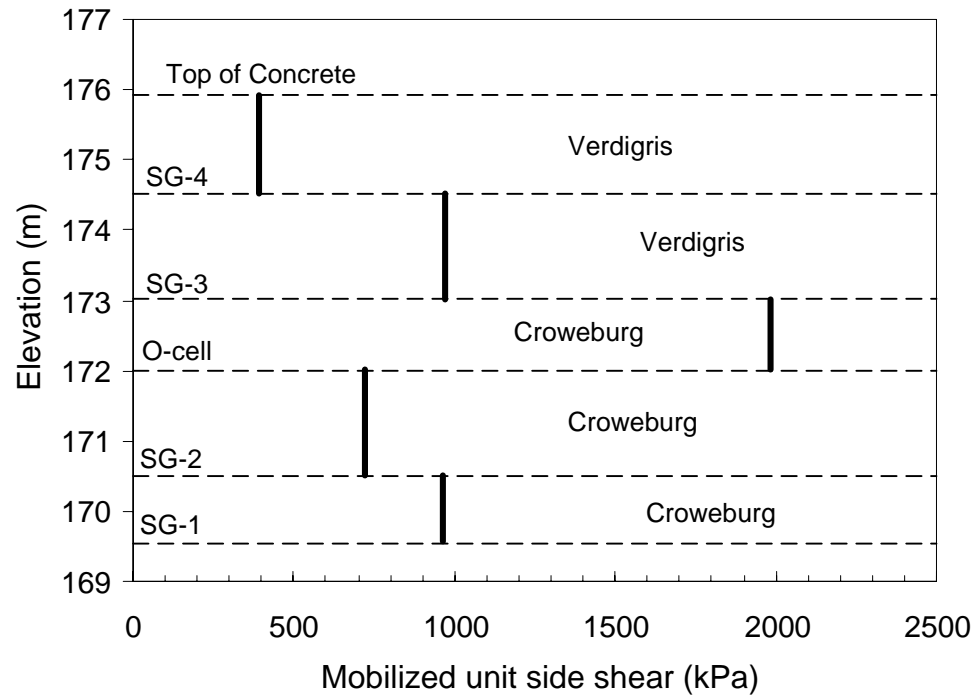


Figure 4.25- Mobilized unit side shear values calculated from strain gage data for test shaft TS-1A.

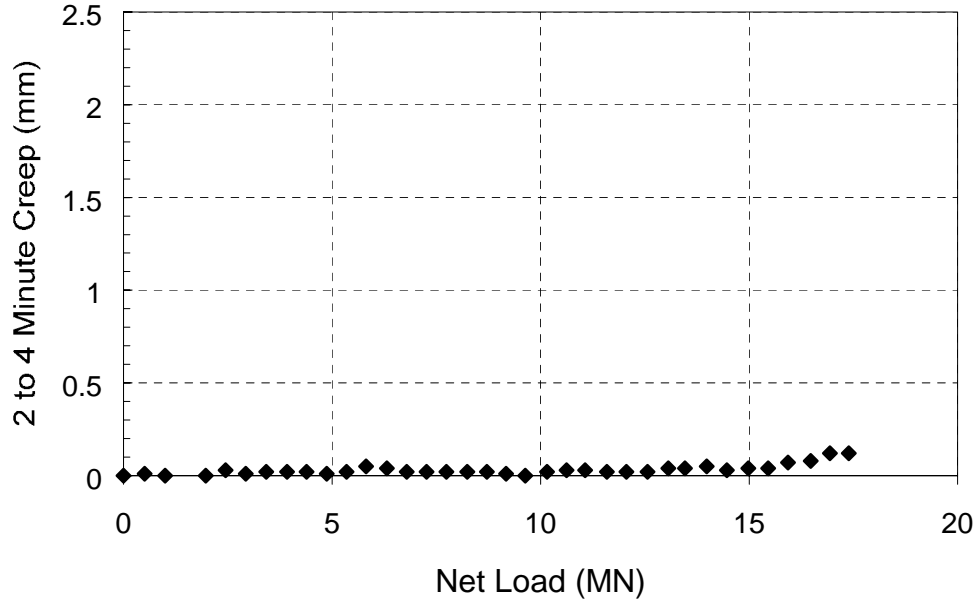


Figure 4.26- Creep displacement for the upper portion of test shaft TS-1A.

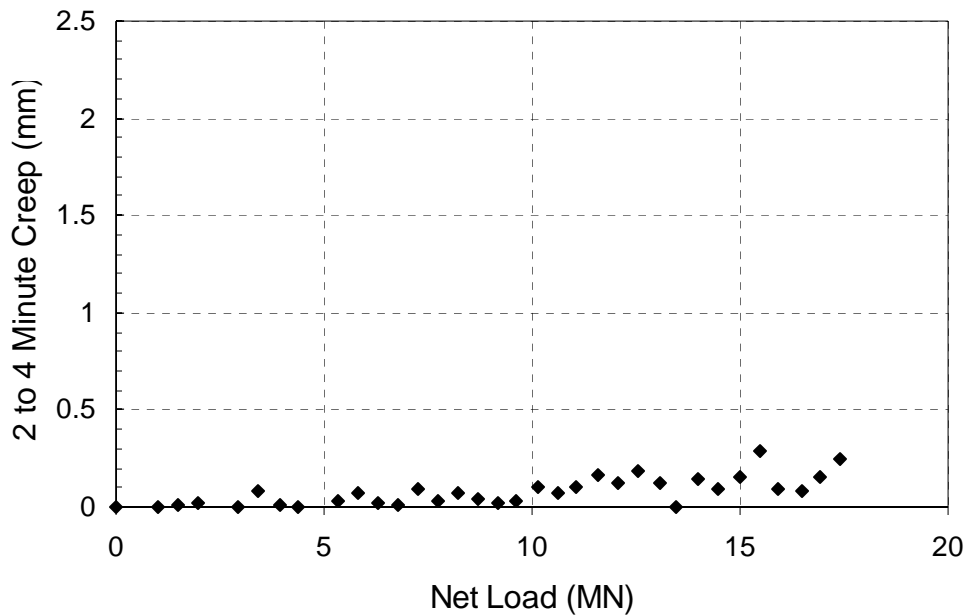


Figure 4.27- Creep displacement for the lower portion of test shaft TS-1A.

4.8.2 Test Results for TS-2

4.8.2.a Stage 1 Results: In stage 1, the lower O-cellTM was pressurized to determine the combined end bearing and side shear below the O-CellTM using the side shear above the cell as the reaction. The upward and downward load-displacement curves determined from the first stage of the load test on shaft TS-2 are plotted in Figure 4.28. In this stage, the lower O-CellTM was incrementally pressurized to a maximum net load of 10.46 MN (1175 tons), which occurred at load level 1L-13. At this loading, 60.7 mm (2.39 in) of downward movement below the lower O-CellTM had occurred and the socket segment below the O-CellTM had reached ultimate capacity. The lower O-CellTM was then unloaded in 5 increments and Stage 1 was concluded.

The equivalent top-down load-displacement curves for Stage 1 loading are shown in Figure 4.29. Again, one curve shown was computed assuming a rigid shaft; the other curve contains an adjustment for additional elastic compression that would occur in a top-

down load test. The curve is extended out to a displacement of 50 mm (2 in) by extrapolating the side shear response above the O-Cell™ as described in Chapter 3.

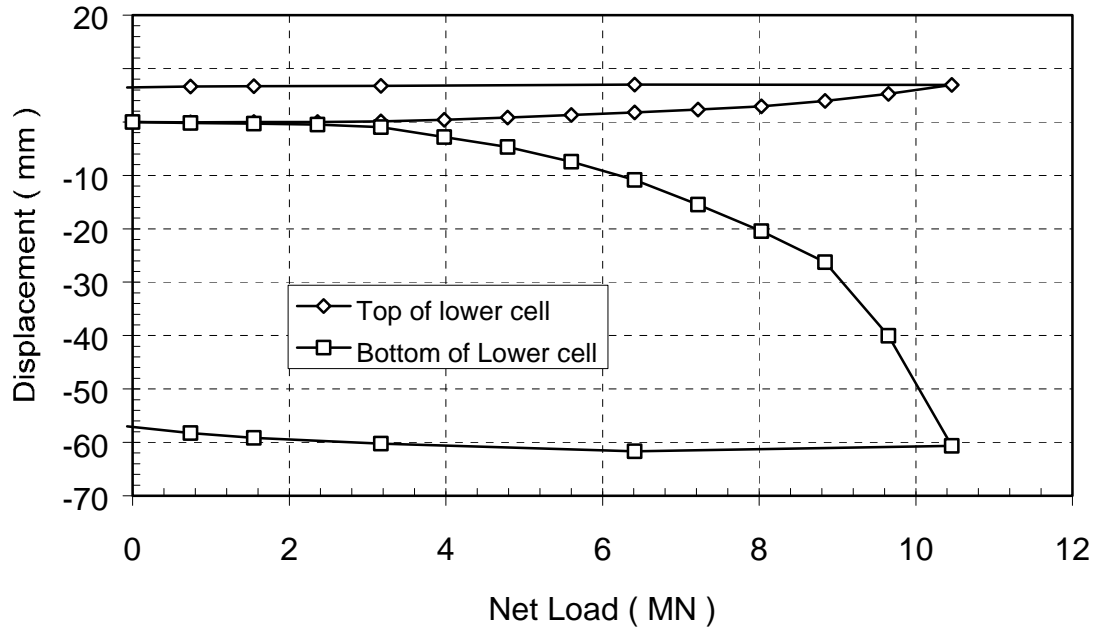


Figure 4.28- Measured load-displacement curves for lower O-cell™ in test shaft TS-2, Stage 1.

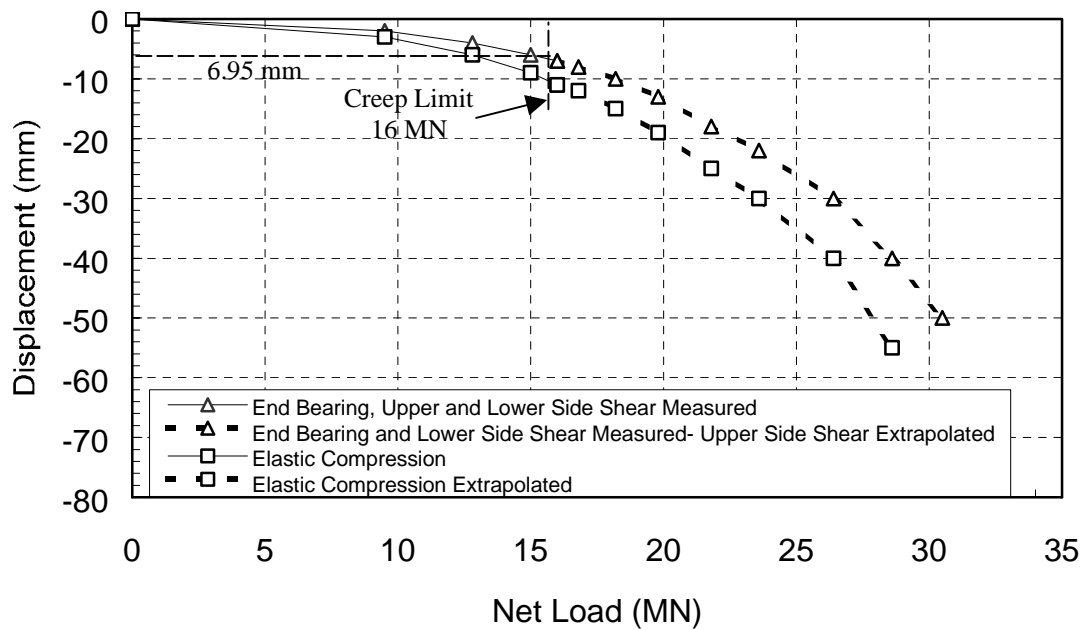


Figure 4.29- Equivalent top-down load-displacement curves for test shaft TS-2, Stage 1.

The distribution of axial force with elevation determined from the strain gage data at various loads is shown in Figure 4.30. The strain gage data used to calculate these distributions appear in Appendix A. On the day of the test, the concrete compressive strength was reported to be 33.7 MPa (4,890 psi) below elevation 178.46 m and 28.1 MPa (4070 psi) above. Elevation 178.46 m is the elevation of the cold joint. This, combined with the area of reinforcing steel and shaft diameter, was used to determine an average shaft modulus of 28.0 GPa (4060 ksi) above the upper-cell, 28.8 GPa (4170 ksi) between the upper and lower O-CellTM, and 26.9 GPa (3900 ksi) below the lower O-CellTM. The average shaft stiffness (AE) of the upper segment of shaft is 30,724 MN (6,895,000 kips), the middle segment is 30,805 MN (6,930,000 kips), and the lower segment is 25,890 MN (5,823,000 kips).

The mobilized unit side shear for each load increment is plotted versus O-cellTM movement in Figure 4.31. The unit side shear curves indicate that the maximum side shear has been reached in only the shaft segment between the lower O-cellTM and level 2 strain gages. The maximum side shear for this shaft segment was about 885 kPa (9.2 tsf). Very little load was transferred in side shear above strain gage level SG-2, although some load was transferred between strain gage levels SG-2 and SG-3 near the end of the test as the side shear between the O-cellTM and the level 2 strain gages dropped off.

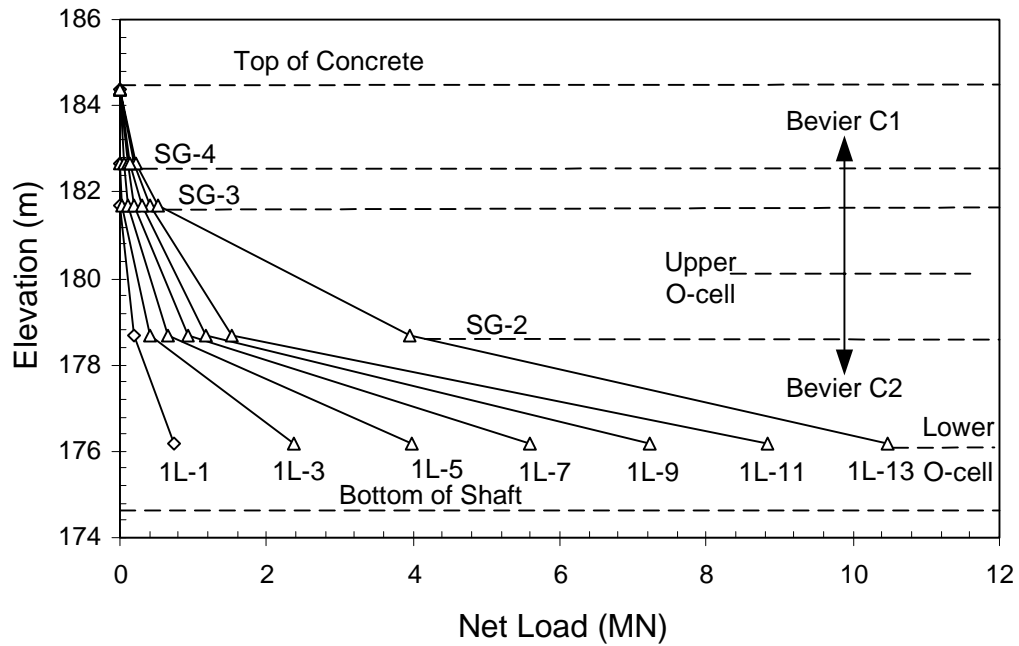


Figure 4.30-Distribution of axial force for test shaft TS-2, Stage 1.

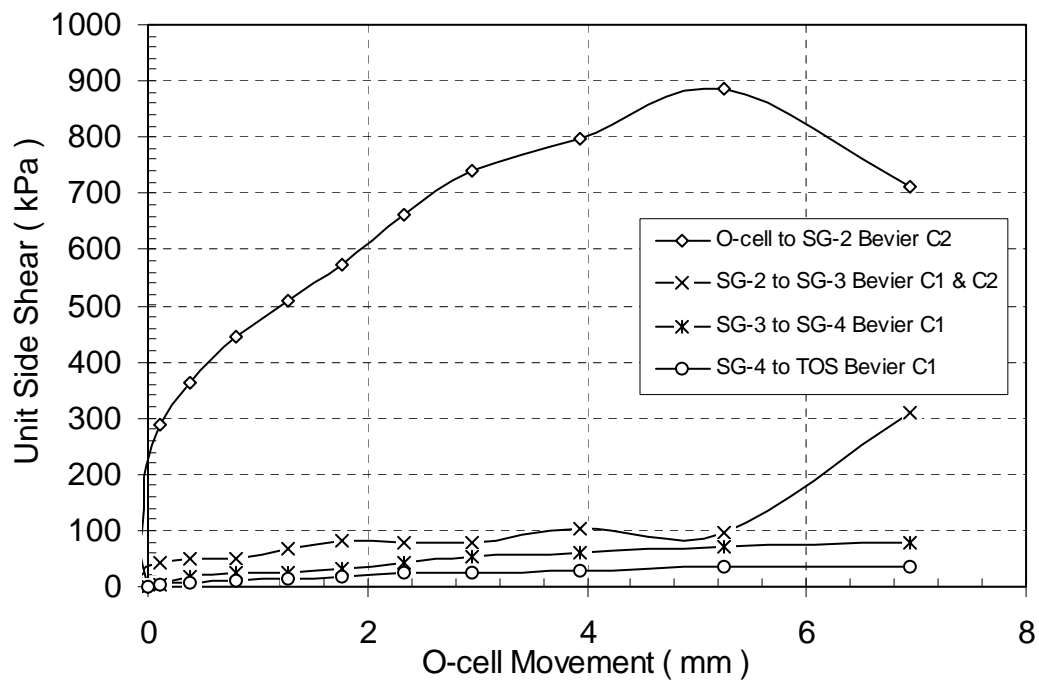


Figure 4.31- Unit side shear versus lower O-cell™ movement for test shaft TS-2, Stage 1.

The maximum mobilized unit side shear values determined for various segments of the shaft for Stage 1 are shown in Table 4.4 and plotted in Figure 4.32. Only the side shear value for the segment of socket between the O-cell and strain gage level SG-2 is an ultimate value. Strain gages at level SG-1 were located too close to the O-cellTM and gave negative readings, which indicated tension in the shaft. These readings were ignored. The unit side shear below the lower O-cellTM could not be determined. Assuming a unit side shear value of 918 kPa (9.6 tsf) for the segment of shaft below the lower O-cellTM based on values for the Verdigris Formation for shaft TS-1A, a unit end bearing value of 5826 kPa (61 tsf) may be calculated.

Table 4.4- Unit side shear values calculated from strain gage data for test shaft TS-2, Stage 1.

Load Transfer Zone	Strata	Elevation (m)	Unit Side Shear	
			kPa	tsf
SG-4 to Top of Shaft	Bevier C ₁	182.67 – 184.40	34	0.36
SG-3 to SG-4	Bevier C ₁	181.67 – 182.67	78	0.81
SG-2 to SG-3	Bevier C ₁ & C ₂	178.67 – 181.67	311	3.2
Lower O-Cell to SG-2	Bevier C ₂	176.17 – 178.67	885	9.2

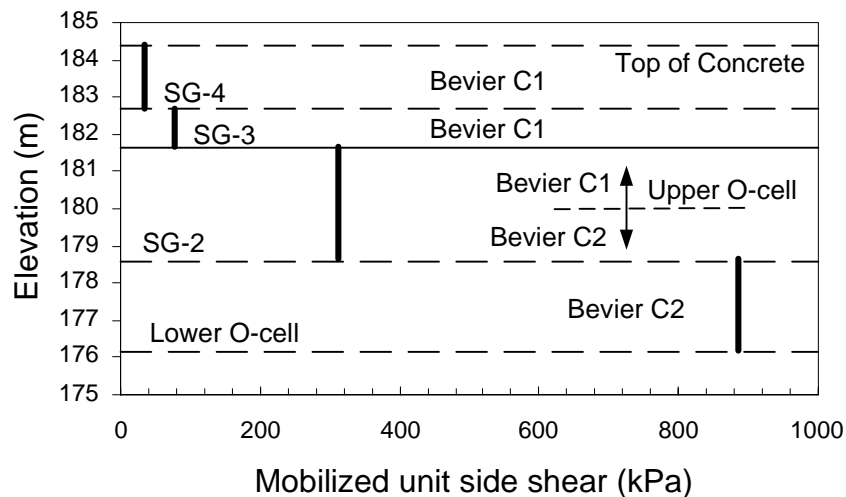


Figure 4.32- Mobilized unit side shear values calculated from strain gage data for test shaft TS-2, Stage 1.

The displacement that occurred over the interval from 2 to 4 minutes after application of a load under a constant load is plotted versus the load in Figures 4.33 and 4.34 for the upper and lower portions of the shaft, respectively. No apparent creep limit was reached for the upper side shear for a maximum displacement of 6.95 mm (0.27 in). For the combined lower side shear and end bearing, a creep limit of 3.3 MN (370 tons) was reached at a displacement of 1.3 mm (0.05 in). The 6.95 mm displacement shown on the rigid top-down load-displacement curve in Figure 4.29 to indicates a combined creep limit of about 16 MN (1800 tons).

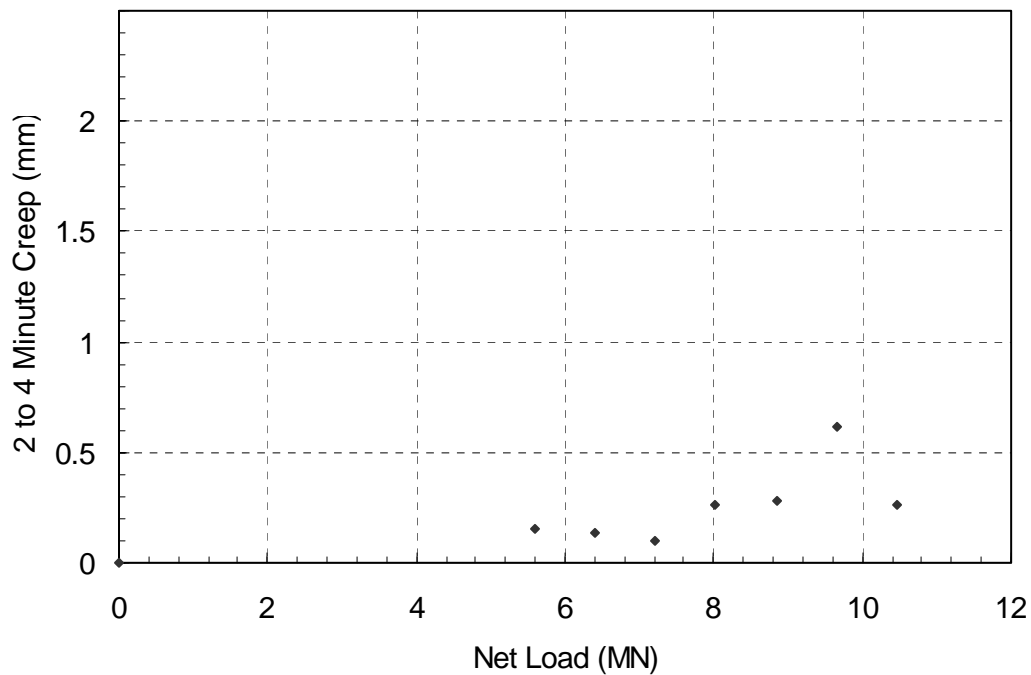


Figure 4.33- Creep displacement for the upper portion of test shaft TS-2, Stage 1.

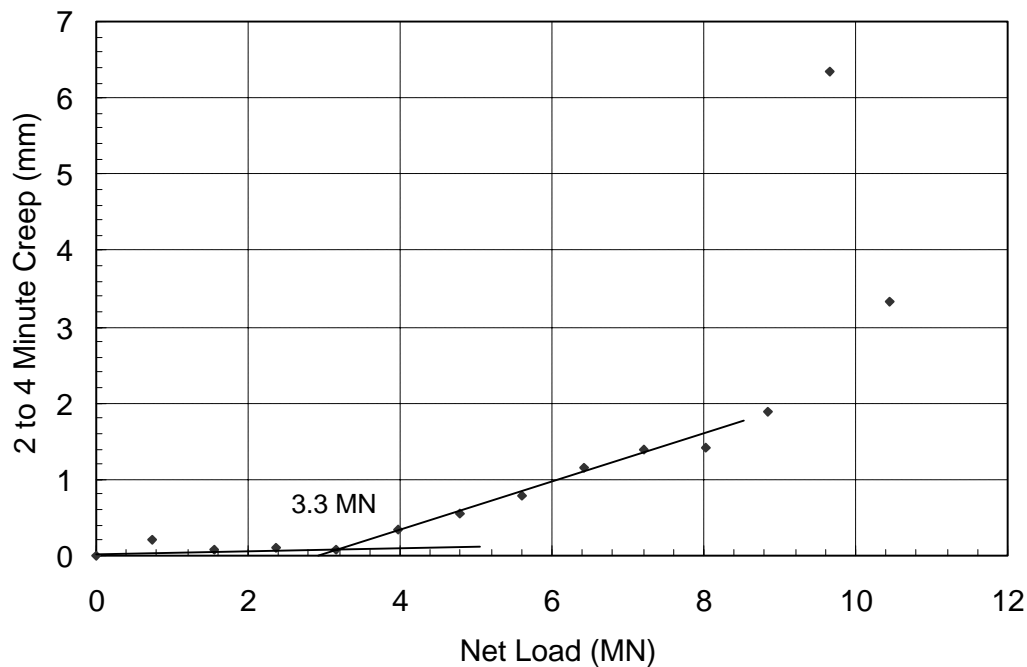


Figure 4.34- Creep displacements for the lower portion of test shaft TS-2, Stage 1.

4.8.2.b Results for Stage 2 and 3: In Stage 2, the lower O-cellTM was vented to serve as a compressible inclusion (zero reaction) while the upper load cell was pressurized to measure the side shear between the upper and lower cells using the side shear above the upper cell as the reaction. In Stage 3, the lower O-cellTM was first sealed while maintaining pressure in the upper load cell. The pressure in the upper load cell was then incrementally increased to measure the side shear above the upper load cell using the combined side shear and end bearing below the upper load cell as the reaction.

The combined upper and lower load-displacement curves for Stages 2 and 3 are shown in Figure 4.35. In Stage 2, the upper O-CellTM was incrementally pressurized to a net load of 10.65 MN (1197 tons). At this load, the downward movement below the upper cell was 12.4 mm (0.49 in) and the upward movement above the cell was 3.5 mm

(0.14 in). The lower cell was closed and stage 2 was concluded. In Stage 3, predominantly downward movement below the upper cell continued despite closing the lower O-CellTM. The socket segment above the upper cell did not reach ultimate capacity before the upper cell reached its maximum extension and depressurized. At the final load of 13.3 MN (1495 tons), upward movement was 7.7 mm (0.31 in) while downward movement was 140.4 mm (5.5 in). The equivalent top-down load-displacement curve is shown in Figure 4.36. The curve is extended out to a settlement of 13.1 mm (0.52 in) by extrapolating the side shear data above the upper cell.

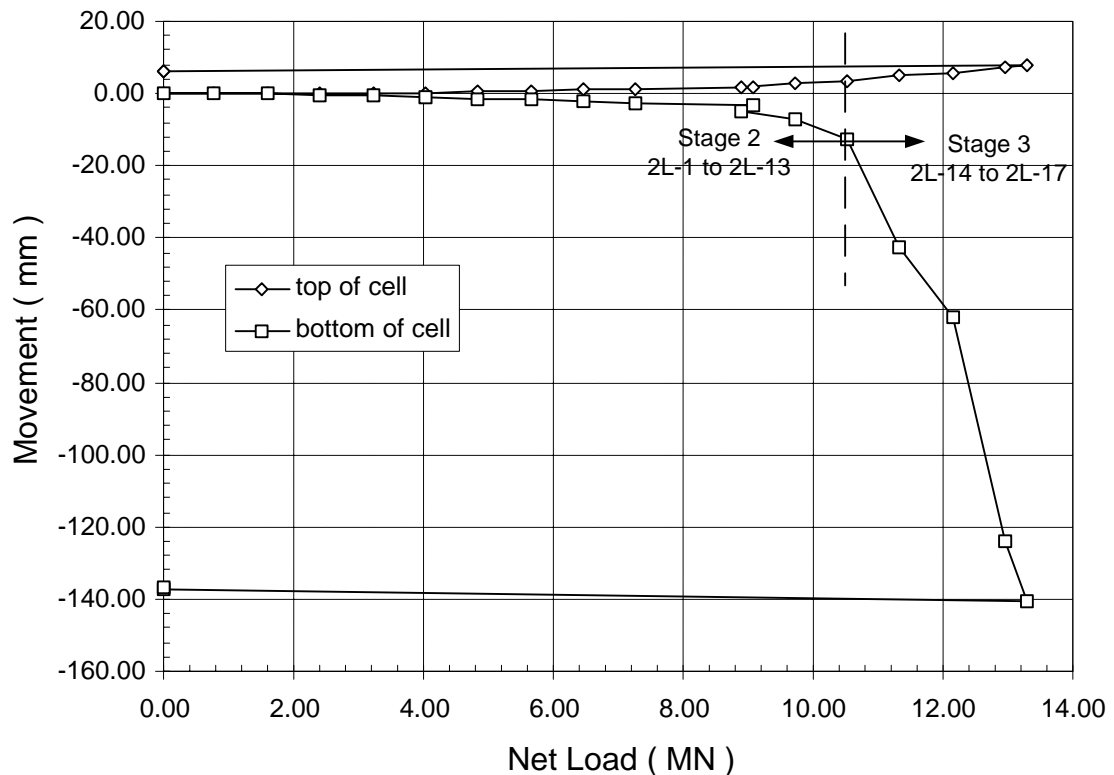


Figure 4.35- Measured load-displacement curves for downward and upward loading of upper O-cellTM in test shaft TS-2, Stages 2 & 3.

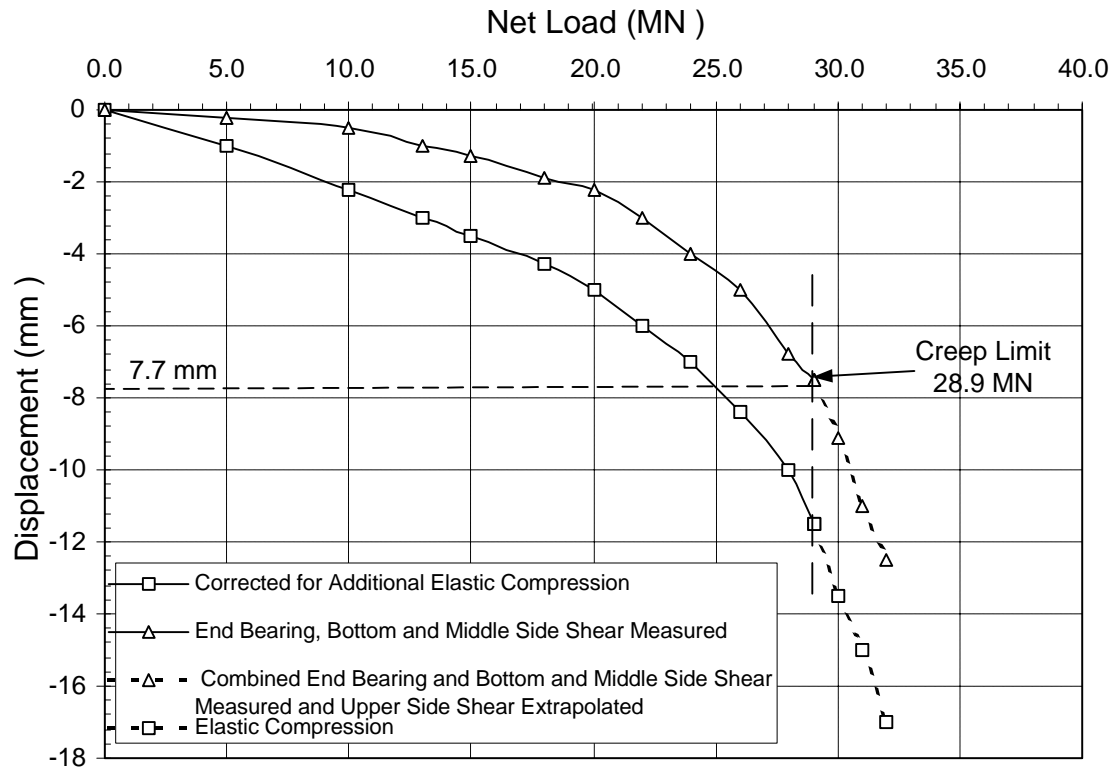


Figure 4.36- Equivalent top-down load-displacement curves for test shaft TS-2, Stages 2 and 3.

The distribution of axial force with elevation at various load increments is shown in Figure 4.37. The strain gage data is presented in Appendix A. The values of average shaft stiffness (AE) used to determine the distribution of axial force were 30,724 MN (6,895,000 kips) for the upper segment of shaft, 30,805 MN (6,930,000 kips) for the middle segment of shaft, and 25,890 MN (5,823,000 kips) for the lower segment of shaft.

The mobilized unit side shear versus load determined for loading in Stages 2 and 3 are plotted as a function of O-cell™ displacement in Figure 4.38. Strain gages at levels SG-1 and SG-2 were affected by layers of questionable concrete and their proximity to the cold joint (Loadtest 1999). As a result, the strain gage data at these levels was ignored and the mobilized unit side shear in the middle section of the shaft was

determined from the relative pressures in the upper and lower O-cellsTM. Based on the data shown in Figure 4.38, only the segment of shaft between the upper and lower O-cellsTM clearly reached an ultimate unit side shear, although all the curves appear to near ultimate values at the end of loading. Values of mobilized unit side shear determined for the final load increment for the shaft segments are shown in Table 4.5 and plotted in Figure 4.39. The socket segment between the O-CellsTM reached an ultimate unit side shear of 726 kPa (7.6 tsf). The average measured unit side shear in the 4.23 m (13.9 ft) shaft section above the upper O-CellTM was 846 kPa (8.8 tsf). An average ultimate unit side shear value of 976.8 kPa (10.2 tsf) was determined for shaft section above the upper O-CellTM by extrapolating and curve fitting the upper load displacement curve.

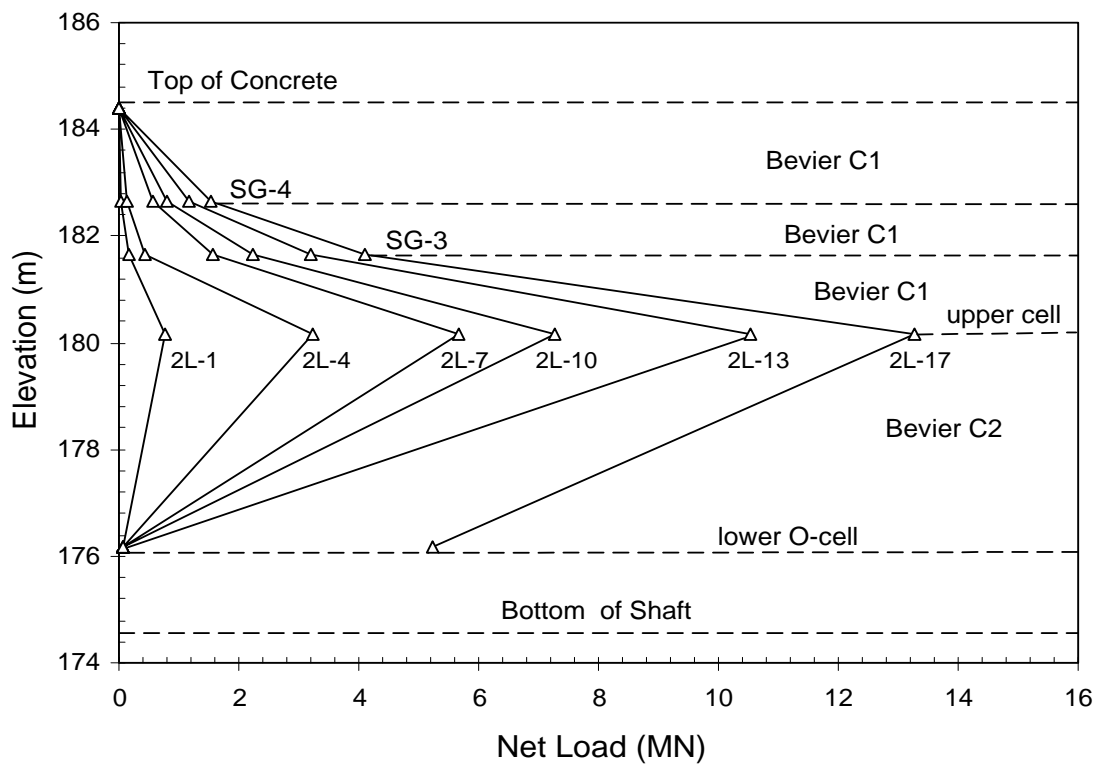


Figure 4.37- Distribution of axial force for test shaft TS-2, Stages 2 & 3.

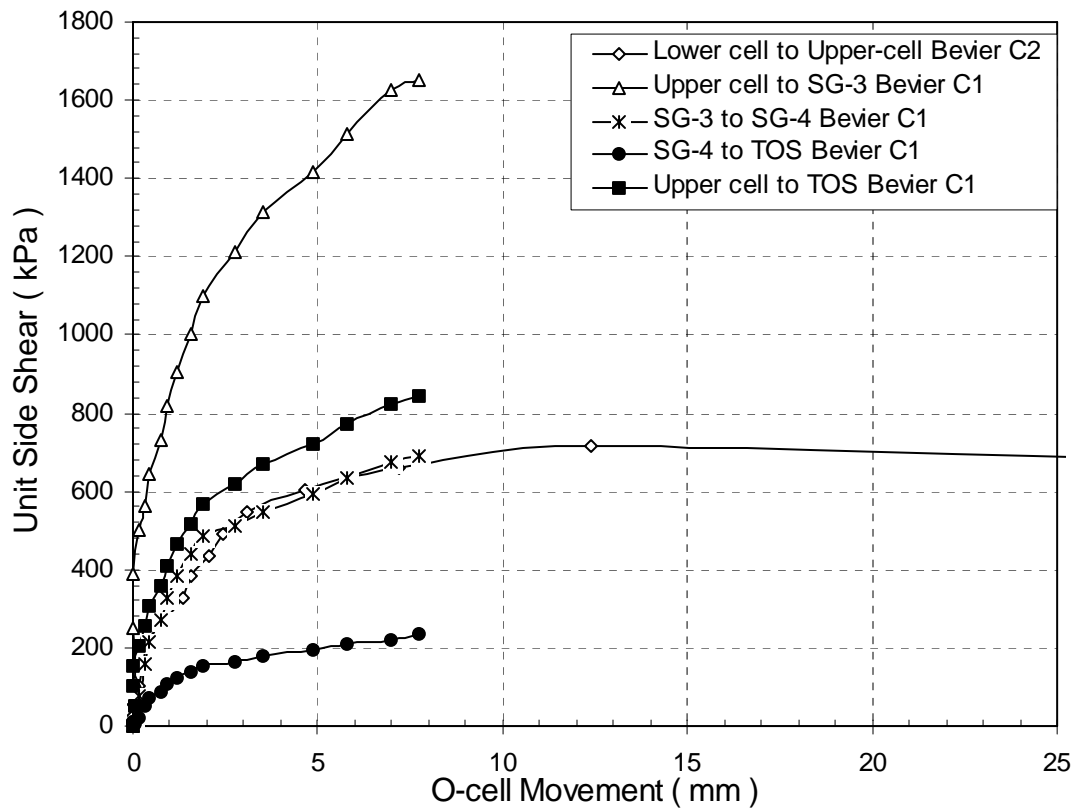


Figure 4.38-Unit side shear versus upper O-cellTM movement for test shaft TS-2, Stages 2 & 3.

Table 4.5-Unit side shear values calculated from strain gage data for test shaft TS-2, Stages 2 & 3.

Load Transfer Zone	Strata	Elevation (m) From – To	Unit Side Shear	
			kPa	tsf
upper cell to Top of Shaft	Bevier C ₁	180.17 to 184.40	846	8.8
SG-4 to Top of Shaft	Bevier C ₁	182.67 – 184.40	236	2.45
SG-3 to SG-4	Bevier C ₁	181.67 – 182.67	694	7.3
upper cell to SG-3	Bevier C ₁	180.17 – 181.67	1653	17.3
lower to upper cell	Bevier C ₂	176.17 - 180.17	726	7.6

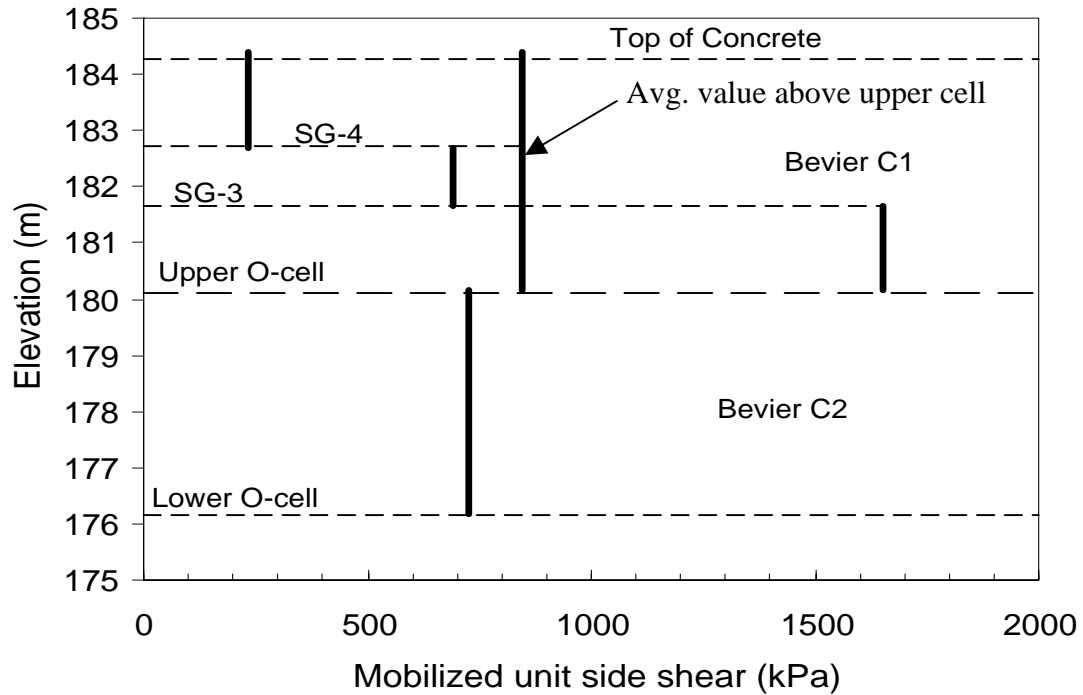


Figure 4.39- Mobilized unit side shear values calculated from strain gage data for test shaft TS-2, Stages 2 & 3.

Figures 4.40 and 4.41 show the creep displacements during stages 2 and 3 for the upper and middle portions of the shaft as a function of net loads. A creep limit was not reached for the upper side shear at a maximum displacement of 7.7 mm (0.31 in) during stages 2 and 3. The middle side shear creep data indicated that a creep limit of 8.0 MN (900 tons) was reached at a displacement of 2.9 mm (0.12 in) during Stage 2. The combined end bearing and lower side shear data from Stage 1 indicated that a creep limit of 3.3 MN (370 tons) was reached at a displacement of 1.3 mm (0.05 in) for the lower segment of the shaft. Since a top-loaded shaft will not begin to creep significantly until all the components begin creep movement, significant creep will not begin until top loading exceeds 28.9 MN (3245 tons) at a displacement of 7.7 mm (0.31 in) by some unknown amount (Figure 4.36).

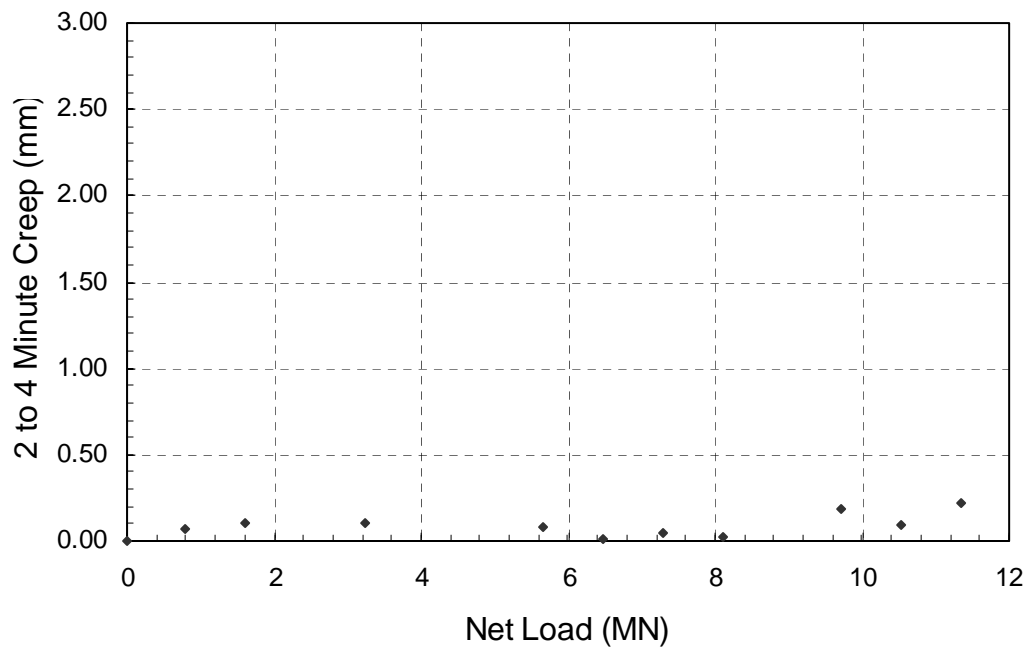


Figure 4.40- Creep displacement for upper segment of shaft for test shaft TS-2, Stages 2 & 3.

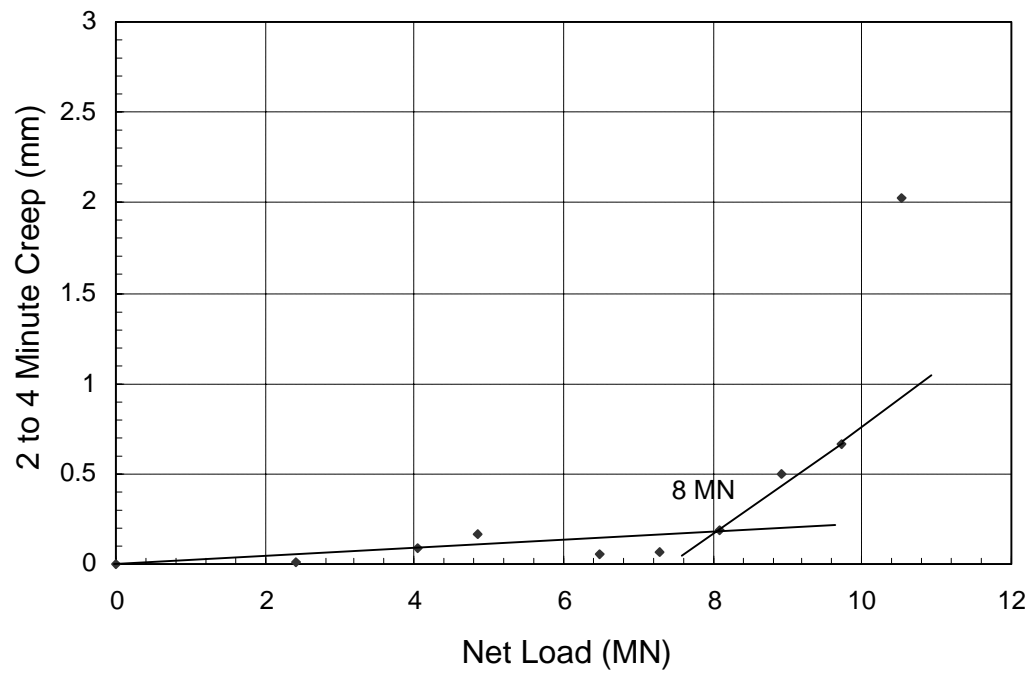


Figure 4.41- Creep displacement for middle segment of shaft for test shaft TS-2, Stage 2.

4.9 Practical Applications

The Osterberg cell load tests were successful in allowing MoDOT to develop a more economical design for the drilled shafts for the proposed bridge alignment. Table 4.6 shows a cost break down for the two Osterberg cell load tests and Table 4.7 shows the anticipated cost savings. The anticipated cost savings were based on the drilling costs of the rock socket and did not include shaft concrete or reinforcing steel. There would also be a reduction in the amount of cross-hole sonic logging and verification coring of selected shafts. Finally this cost did not include additional geotechnical investigation that would be required if the rock sockets could not be shortened. The additional geotechnical investigation would cost about \$150,000.

Table 4.6- Costs of Osterberg cell load tests for test shafts TS-1A and TS-2.

Mobilization	\$45,000	
Drilling Overburden	\$89,000	46 m (12220 mm Dia.)
Steel Casing	\$16,000	48 m (1220 mm ID)
Drilling Rock Socket	\$63,000	32.5 m (1067 mm Dia.)
Drilled Shaft Concrete	\$ 2,000	14.3 Cu. Meter
Load Test (one cell)	\$75,000	
Load Test (two cells)	\$142,000	
Design Cost	\$60,000	

Table 4.7- Anticipated cost savings for drilled shafts.

Pier	Length of Socket		Length Saved	No. of Shafts	Amount Saved
	Before Test	After Test			
	(m)	(m)	(m)		
19	25.6	7.3	18.3	6	\$360,250
20	31.0	6.9	24.1	8	\$632,580
21	23.2	7.5	15.7	15	\$772,680
22	21.2	14.8	6.4	8	\$167,990
23	16.8	8.5	8.3	6	\$163,390
24	21.1	10.2	10.9	6	\$214,580
				Total	\$2,311,470
				Test Costs	-\$492,000
				Cost Savings	\$1,819,470

4.10 Summary and Conclusions

The Missouri DOT proposed to build a new bridge across the Missouri River in central Missouri. The proposed foundation design for the piers in the vicinity of the river consisted of drilled shafts socketed into bedrock. The bedrock at this location consisted of alternating layers of clay shale, siltstone, coal, and underclay with scattered layers of limestone and sandstone. Since the shales could not support large axial loads in end bearing it was decided to design the rock sockets based side shear only. Current design methods used by MoDOT would require exceedingly long rock sockets that would be very expensive. In order to reduce costs and to better quantify the available unit side shear capacity of bedrock, two Osterberg cell load tests were performed in May and June of 1999 between periods of high water.

A general geologic description of the Lexington test site was presented in this chapter followed by a summary of the engineering characteristics of the most pertinent strata. The construction and testing procedures for the two test shafts were described, followed by presentation of the results from each load test. The values of unit side shear determined from the Osterberg cell load tests exceeded the anticipate values and allowed the shafts to be designed more economically.

CHAPTER FIVE

GRANDVIEW TRIANGLE TEST SITE

The Missouri Department of Transportation (MoDOT) is currently in the process of “untangling the triangle” in metropolitan Kansas City, Missouri. The intersection, known as the Grandview Triangle, is located in southern Jackson County and handles about 250,000 vehicles per day on three major interstate routes and 7 local routes. The 250 million dollar make over of the triangle is to be phased in over 7 to 8 years with the total replacement of all bridges and pavement. The completed project is projected to accommodate more than 400,000 vehicles per day and increase the size of the triangle from the present 284 acres to more than 376 acres. All work is being done while maintaining current traffic volumes.

The construction of new bridges and walls alongside the existing bridges has presented many challenges to bridge and geotechnical engineers. A twelve span structure (A6252) and a thirteen span structure (A6254) will cross US 71 and will require the construction of footings in the median of US 71. The use of conventional spread footings or pile caps would require a detour to allow room for the footing excavation. Drilled shafts socketed into bedrock would not require a detour and were investigated as the preferred foundation type. Previously constructed drilled shafts in the triangle have been assumed to carry axial load in end bearing only. Since the closest limestone layer thick enough to support the axial loads in end bearing only is about 80 feet (24.4 m) below the top of the shaft, an Osterberg cell load test was performed to investigate the unit side shear characteristics of the bedrock to determine if adequate axial capacity could be achieved in shallower strata by considering side shear only.

In this chapter, the general conditions at the site are described followed by descriptions of the engineering characteristics of the soil/rock of most importance to this site. The construction and loading of the test shaft is then described, followed by presentation of the results from the load test. The reconstruction of the Grandview Triangle was designed using English units. All results are therefore reported using English units or dual units.

5.1 Site Description

The Grandview Triangle site is located in metropolitan Kansas City, Missouri. The area is known to local residents as the Grandview Triangle because three major interstate routes (US71, I-470, and I-435) and 7 local routes converge in this area. A map of the southern Kansas City metropolitan area is shown in Figure 5.1. A plan view of the overall project is shown in Figure 5.2 and the location of the test shaft is shown in Figure 5.3.

The project is situated on moderate to steeply sloping rolling hills that border Hickman Mills Creek. The project soils originated from residuum of the weathering of limestone and shales. About 70 per cent of the ground surface is covered by Snead soils of the Snead-Urban land complex. The remaining 30 per cent is covered by the Urban land portion of the complex, which consists of residential and commercial development including roadways and bridges. The Liquid Limits ranged from 40 to 64 for the Snead soil. The Plasticity Index (PI) varied from 18 to 38 and the Snead is predominately a CH soil by ASTM classification.

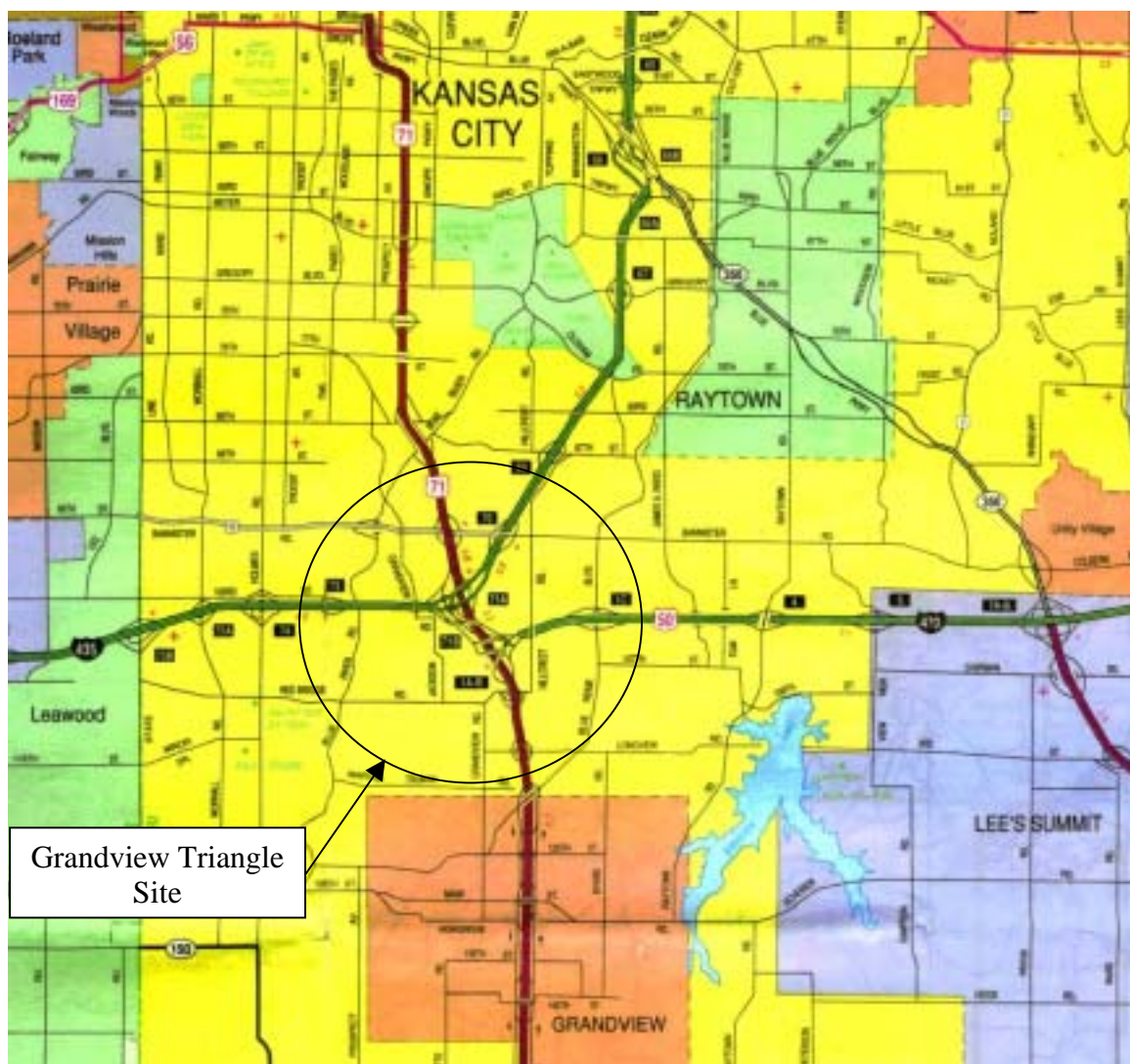


Figure 5.1- Roadmap of Grandview Triangle area in Metropolitan Kansas City.

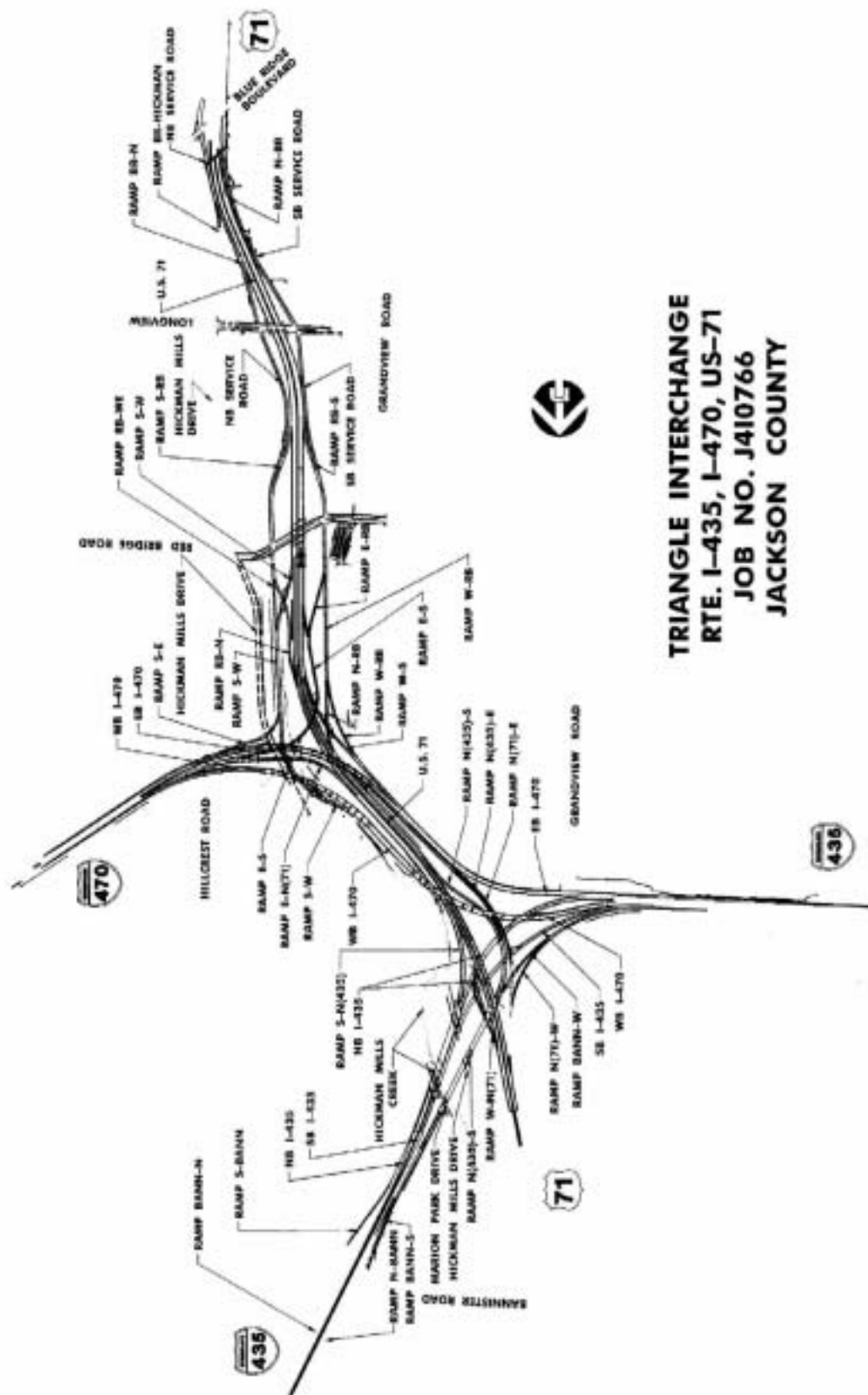
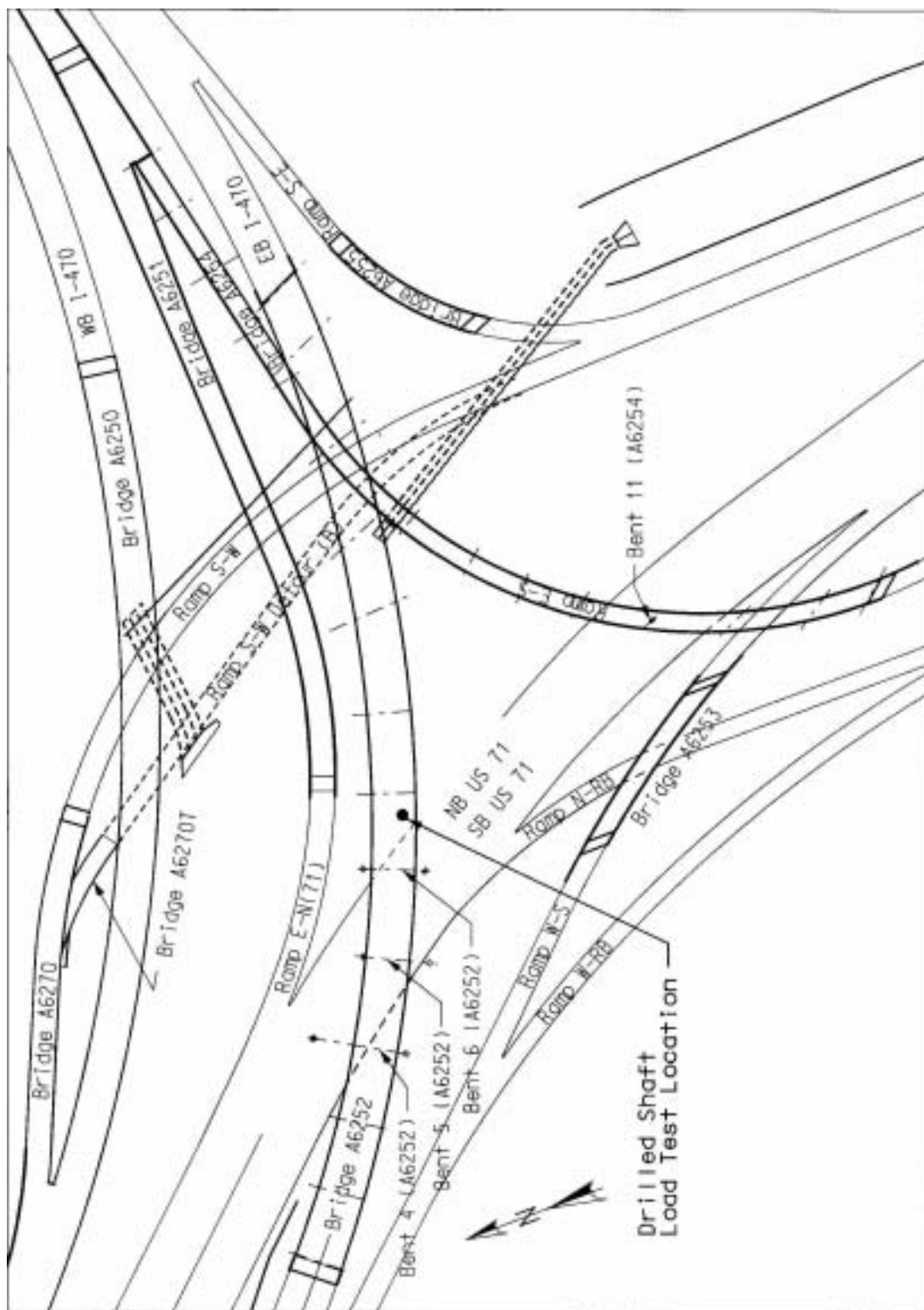


Figure 5.2 Grandview Triangle (from HNTB 2002).



Geologic units of the Kansas City Group are exposed within the limits of the project. The Kansas City Group is a Pennsylvanian Age deposit consisting predominately of alternating sequences of horizontally bedded limestones and shales as shown in Figures 5.4 and 5.5 (in descending order). Shale units may be very hard to calcareous in nature or clay-like in the form of claystones and siltstones. Geologic units exposed in various road cuts and encountered during the subsurface investigation in descending order varied from the Argentine Limestone Member of the Wyandotte Formation to the Bethany Falls Limestone Member of the Swope Formation. The Argentine Limestone was encountered at about elevation 973.7 ft. and the Bethany Falls Limestone was encountered at about elevation 826 ft.

All of the existing bridges, ramps, and pavement at the site will be replaced with 25 new bridges and more than 40 retaining walls. The bridges will consist of simple 3 span plate girder structures to large multiple span structures. Foundations for most bridges in the project area include drilled shafts and spread footings. Drilled shafts for most of the large bridge structures were socketed into either the Winterset Limestone or the Bethany Falls Limestone. These shafts were designed to carry axial load in end bearing only with an allowable end bearing pressure of 30 to 40 tsf (2.87 to 3.83 MPa). However, for bridges A6252 and A6254 shown in Figure 5.3, these strata were excessively deep and, since several piers were located in the median of US 71, spread footings would have required excessive traffic closures. An O-cell test was therefore planned to evaluate if the design load could be supported in side shear from shallower strata. A more detailed geologic description of the Osterberg cell load test site is presented in the following section.



Figure 5.4 Kansas City Stratigraphy (from URS 2001).

GEOLOGIC COLUMNAR SECTION IN THE KANSAS CITY AREA

GROUP	FORMATION	MEMBER	COLUMN	THICKNESS (FT) AVG. RANGE No.
ZARAH	LANE SHALES			
LINN SUB - GROUP	IOLA LIMESTONE	RAYTOWN (CALICO LEDGE) LIMESTONE		6' 5.2' - 8'
		MUNCE CREEK SH PAOLA LIMESTONE		2' 0.1' - 5'
	CHANUTE SHALES			19' 14' - 24.3'
	DRUM (BUILDING LEDGE) LIMESTONE	CEMENT CITY LIMESTONE		9' 4' - 13.5'
	CHERRY- VALE SHALES	QUIVIRA SHALES		8' 3' - 26'
		(REEF LEDGE) WESTERVILLE (ODOLIC LEDGE) LIMESTONE (BULL LEDGE)		12' 3' - 23.2'
	FORMATION	WEA SHALES		21' 14' - 30'
		BLOCK LIMESTONE		6' 0.8' - 7.8'
		FONTANA SHALES		5' 1' - 13'
KANSAS CITY GROUP	DENNIS LIMESTONE	WINTerset (CHERT LEDGE) LIMESTONE		29' 26' - 35'
	FORMATION	STARK SHALES		3.5' 2.5' - 9'
	GALESBURG SHALES			3' ±
	SWOPE LIMESTONE	BETHANY FALLS (CEMENT ROCK) LIMESTONE		20' 15' - 26'
		HUSHPUCNEY SHALES		4' 2' - 7'
	FORMATION	MIDDLE CREEK LIMESTONE		3' 1.4' - 5.3'
BRONSON SUB - GROUP	LADORE SHALES			4' 1' - 15'
	HERTHA LIMESTONE	SNABAR LIMESTONE		3-14'
		MOUND CITY SH		3-4' 3.4' - 13.8'
		CRITZER L.S.		0-3'

- DESCRIPTION**
- 17) Lane Shale - Dark bluish-gray shale and gray and yellowish-brown sandy shale. Weathers light green to tan or yellow. It contains a channel sandstone near Hickman Mills. The Lane is thin in the southern part of Kansas City, thickens in the north part of the city and in southern Jackson County. It also thins to the east of the city but thickens near Lees Summit.
- 18) Raytown Limestone - The color is irregular gray, blue, buff and reddish, the texture is quite variable. The limestone is wavy bedded to massive and may have shale breaks. Weathering causes stains and blotches and produces a rough surface.
- 19) Muncie Creek Shale - Gray or gray-green clay shale in the upper and black fissile shale in the lower part. The shales are often separated by a thin shaley limestone. Water bearing.
- 20) Paola Limestone - Dark bluish-gray unit bedded limestone, weathers bluish-gray.
- 21) Chanute Shale - Variable. Dark gray to green, platy to blocky shale and/or yellowish brown sandy shale and highly variable sandstone (usually in the upper portion). A red or maroon zone occurs locally near the middle. The lower portion is usually lighter in color and may be limy. Weathers to a fat clay.
- 22) Drum Limestone - Blue-gray to gray green, massive to slabby limestone. Weathers light gray to tan to nearly white with deep yellow staining along bedding planes and joints.
- 23) Quivira Shale - Variable. Blue-gray to olive shale, locally has about one foot of black sub-fissile or maroon shale near the middle, weathers light olive green. The combined average thickness of the Quivira Shale and underlying Westerville Limestone is 18 feet. This shale weathers to clay rapidly and is not too sound for engineering purposes.
- 24) Westerville Limestone - Highly variable in the upper part, which may be represented by cross bedded oolitic limestone, by shale or by an interbedded combination of the two in any proportion. Where this part is composed entirely of shale it is not distinguishable from the overlying Quivira Shale and is assigned to that member. The limestone is generally gray to blue-gray, fairly thin bedded and weathers nearly white. The separating shales are usually blue-gray and weather olive. In the Parkville area the upper limestone is cherty. The complete range of variation in this zone can take place within a very short distance. The lower part is a very consistent light gray, usually unit bedded limestone which ranges from 2 to 6 feet in thickness but averages 3 to 4 feet.
- 25) WEA Shale - Dark blue-gray to gray green shale, locally may be sub-fissile, may have a thin zone of maroon silty shale in the upper part, weathers olive. It usually has several thin impure limestone or silstone zones in the lower few feet. This shale is usually wet and weathers rapidly to fat clay.
- 26) Block Limestone - Variable. Usually two blue-gray limestones separated by blue-gray shale. The lower limestone is consistent, averaging 1 to 2 feet in thickness. The upper bed may be absent locally.
- 27) Fontana Shale - Dark blue-gray shale, may have a black sub-fissile zone in the middle or lower part. Weathers gray-green to buff.
- 28) Winterset Limestone - The upper part is blue gray to dark gray slabby to massive limestone with abundant nearly black chert nodules and numerous irregular shale breaks. A 1 to 3 foot very dark gray shale is present near the middle. The lower part is light gray irregularly bedded limestone with some light gray chert and shale seams.
- NOTE #3 - The Canville Limestone, lowest member of the Dennis Limestone Formation, is usually absent in the Kansas City Area.
- 29) Stark Shale - Gray and yellow shale in the upper and black fissile shale in the lower part. This shale is water bearing.
- 30) Galesburg Shale - An under-clay like relatively structureless soft light gray nodular calcareous shale.
- 31) Bethany Falls Limestone - Except for the uppermost 1 to 3 feet, which is commonly a fairly soft, clayey, nodular limestone similar to the overlying Galesburg shale, the upper part is gray, mottled, massive algal or nearly white oolitic limestone which may be cross bedded. A fairly thin shale bed may be present locally near the middle. The lower portion is light gray, dense, thin bedded limestone. The entire unit weathers nearly white. The 20 foot thickness is fairly consistent, but the bed attains a maximum of 26 feet southeast of Independence. Vertical joints are prominent and outcrops usually exhibit large detached rocks.
- 32) Hushpuckney Shale - Bluish-gray clay shale in the upper and black fissile shale in the lower part. This shale is water bearing.
- 33) Middle Creek Limestone - One or two dark bluish-gray, vertical joints.
- 34) Ladore Shale - Variable. Gray to buff clayey to sandy shale. May locally be replaced by algal limestone which is assigned to Snabar.
- 35) Snabar Limestone - 1 or 3 beds of gray limestones. Weathers brown.
- 36) Mound City Shale - Gray calcareous shale in the upper and dark calcareous in the lower part.
- 37) Critzer Limestone - Brownish-gray, nodular, impure limestone which grades into red or green shale.

DRAWING NO. 3

Compiled by James P. Garber; Originally Drawn by L.A. Cunningham; Converted to Computer File by Dr. Charles H. Cammack

Figure 5.5 Kansas City Stratigraphy (from URS 2001).

5.2 Geology of the Area

The underlying bedrock in the project area is of upper Pennsylvanian Age, Missourian Series, Kansas City Group. The Kansas City Group is divided into three subgroups (in ascending order): the Bronson, Linn, and Zarah. Rock sockets for drilled shafts to support Piers 4, 5, and 6 for bridge A6252 and Pier 11 for bridge A6254 are planned for location in shales and limestones of the Linn Subgroup as shown in Figure 5.6.

The Linn Subgroup consists of horizontally bedded shales and limestones. The Linn Subgroup consists of (from the base upwards): the Cherryvale Formation, the Drum Formation, the Chanute Formation, and the Iola Formation (Thompson 1995). The relevant strata from these formations are described in more detail below.

5.2.1 Cherryvale Formation

The Cherryvale Formation is composed of five members (from the base upwards): the Fontana Shale Member, the Block Limestone Member, the Wea Shale Member, the Westerville Limestone Member, and the Quivira Shale Member. The Fontana Shale Member and Block Limestone Member were significantly below the base of the rock socket and were not included in the analysis. The Fontana Shale Member was encountered from about elevation 852 to 862 ft and averages about 10 feet (3.3 m) in thickness. The Block Limestone Member was encountered from about elevation 862 to 864 ft and averages about 2 feet (0.6 m) in thickness.

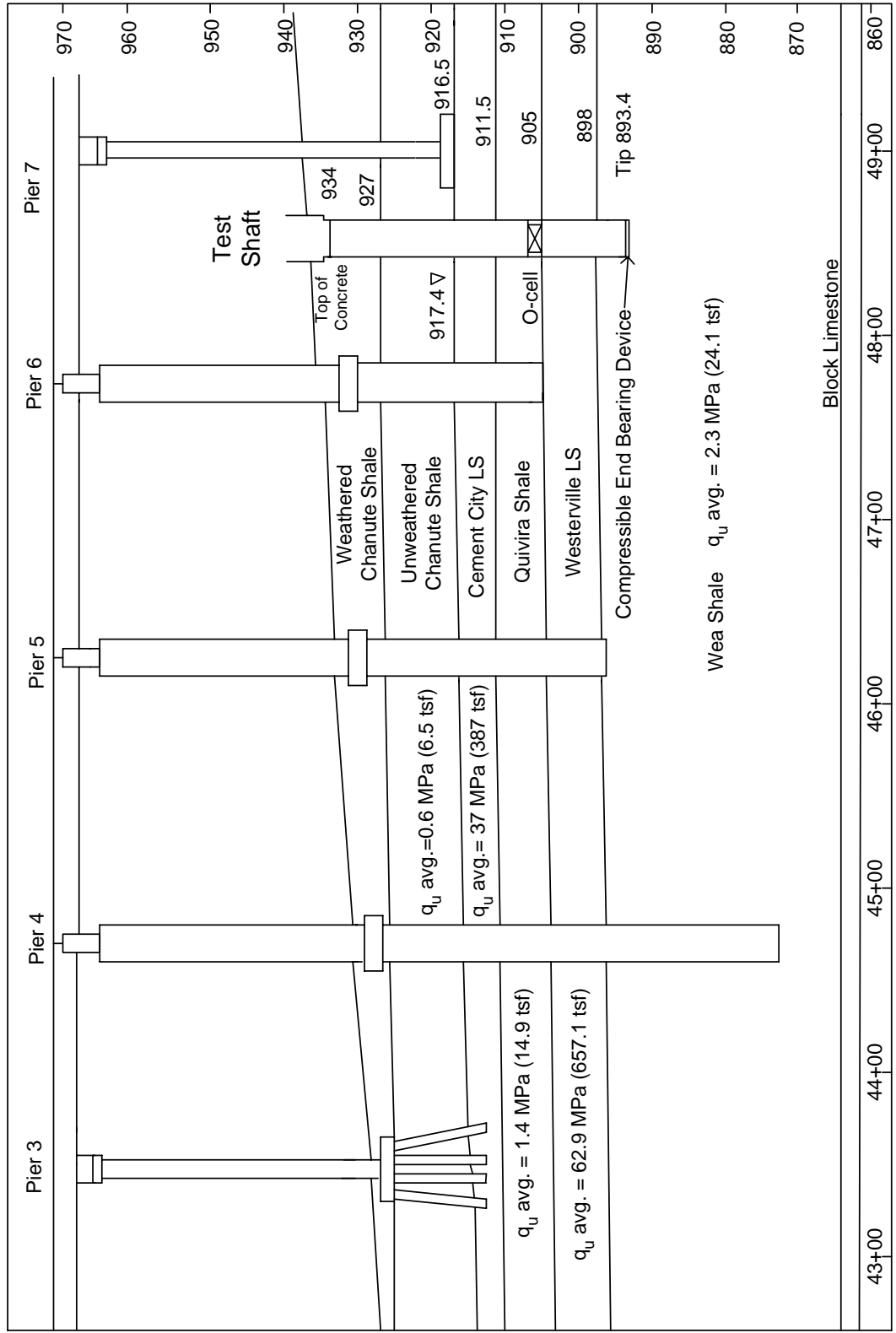
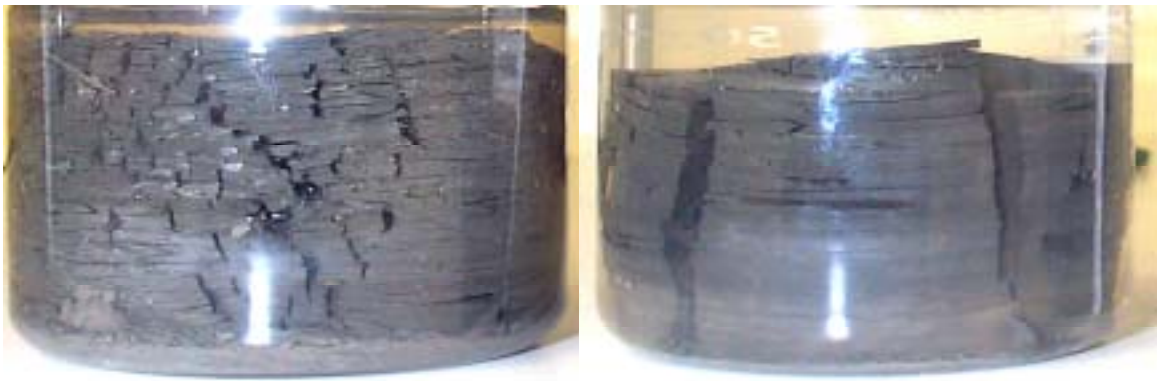


Figure 5.6 - Elevation view of Piers 3 thru 7 for bridge A6252.

Wea Shale Member: The Wea Shale Member of the Cherryvale Formation is a bluish-gray, silty, micaceous shale. This member was encountered from about elevation 864.0 to 898.1 ft and averages about 34.1 feet (10.4 m) in thickness. Standard Penetration Test blow counts in the Wea Shale Formation averaged 100 blows in 12 inches (30 cm). Jar slake tests performed on this material produced jar slake indices from 3 to 6 as shown in Figure 5.7 and summarized in Table 5.1.



(a) Slake Index (3)

(b) Slake Index (6)

Figure 5.7- Range of jar slake index test results for Wea Shale Member: (a) elevation 986.0 ft, slake index (3), (b) elevation 880.8 ft, slake index (6).

Westerville Limestone Member: The Westerville Limestone Member consists of a lower, even-bedded limestone and an upper, oolitic limestone. This member was encountered from about elevation 898.1 to 904.8 ft. and averages about 6.7 feet (2.04 m) in thickness. RQD values for this stratum varied from 34 to 100 percent.

Quivira Shale Member: The Quivira Shale Member includes a gray shale in the lower and middle parts, a thin clay in the upper part, and a overlying slightly fissile dark gray shale. This member was encountered from about elevation 904.8 to 911.3 ft and averages about 6.5 feet (1.98 m) in thickness. Jar slake tests performed on this material produced jar slake indices of 1 to 4 as shown in Figure 5.8 and summarized in Table 5.1.



a. Slake Index (1)

b. Slake Index (4)

Figure 5.8- Range of jar slake index test results for Quivira Shale Member: (a) elevation 905.7 ft., slake index (1), (b) elevation 910.0 ft., slake index (4).

5.2.2 Drum Limestone Formation

The Drum Limestone Formation contains two limestone members (from the base upwards): the Cement City Limestone Member and the Corbin City Limestone Member. In Missouri, only the lower limestone member (Cement City) has been recognized to date. The Cement City Limestone Member is a gray to buff limestone. This member was encountered from about elevation 911.3 to 916.5 ft and averages about 5.2 feet (1.58 m) in thickness. RQD values varied from 22 to 100 percent.

5.2.3 Chanute Shale Formation

The Chanute Shale Formation consists of a silty, gray or maroon claystone in the lower part, overlain by a silty to sandy shale. An un-weathered portion of this formation was encountered from about elevation 916.5 to 927.2 ft. This portion averages about 10.7 feet (3.26 m) in thickness. Above elevation 927.2 ft to the base of the Raytown Limestone Member of the Iola Formation, at about elevation 938.8 ft, the Chanute Shale was weathered. Standard Penetration Test blow counts in the Chanute Shale Formation averaged 100 blows in 8.8 inches (22 cm) above elevation 927.2 ft and 100 blows in 3

inches (7.6 cm) below elevation 927.2 ft. Jar slake indices for this material varied from 1 to 4 as shown in Figure 5.9 and summarized in Table 5.1.



a. Slake Index (1)



b. Slake Index (4)

Figure 5.9- Range of jar slake index test results for Chanute Shale Member: (a) elevation 920.0 ft., slake index (1), (b) elevation 916.2 ft., slake index (4).

Table 5.1- Results of jar slake index tests of shale formations at the Grandview Triangle site.

Formation	Elevation	2	5	10	30	1440
	(ft)	(min)	(min)	(min)	(min)	(min)
Chanute	920.0	2	2	2	1	1
Chanute	918.2	3	4	4	4	4
Quivira	909.6	4	4	4	4	4
Quivira	905.9	2	1	1	1	1
Wea	895.7	4	4	4	3	3
Wea	892.2	5	5	5	4	4
Wea	890.4	4	4	4	4	4
Wea	887.4	5	5	5	5	5
Wea	880.8	6	6	6	6	6
Wea	878.8	3	5	5	5	5
Wea	874	5	5	5	5	5
Wea	869.7	6	6	6	6	6

5.3 Unconfined Compressive Strength of Bedrock

The bedrock profile was divided into five layers based on strata. Average values and ranges of the unconfined compressive strength for each layer are summarized in Table 5.2. The bedrock was sampled by split spoon (SPT) and cored. The core was

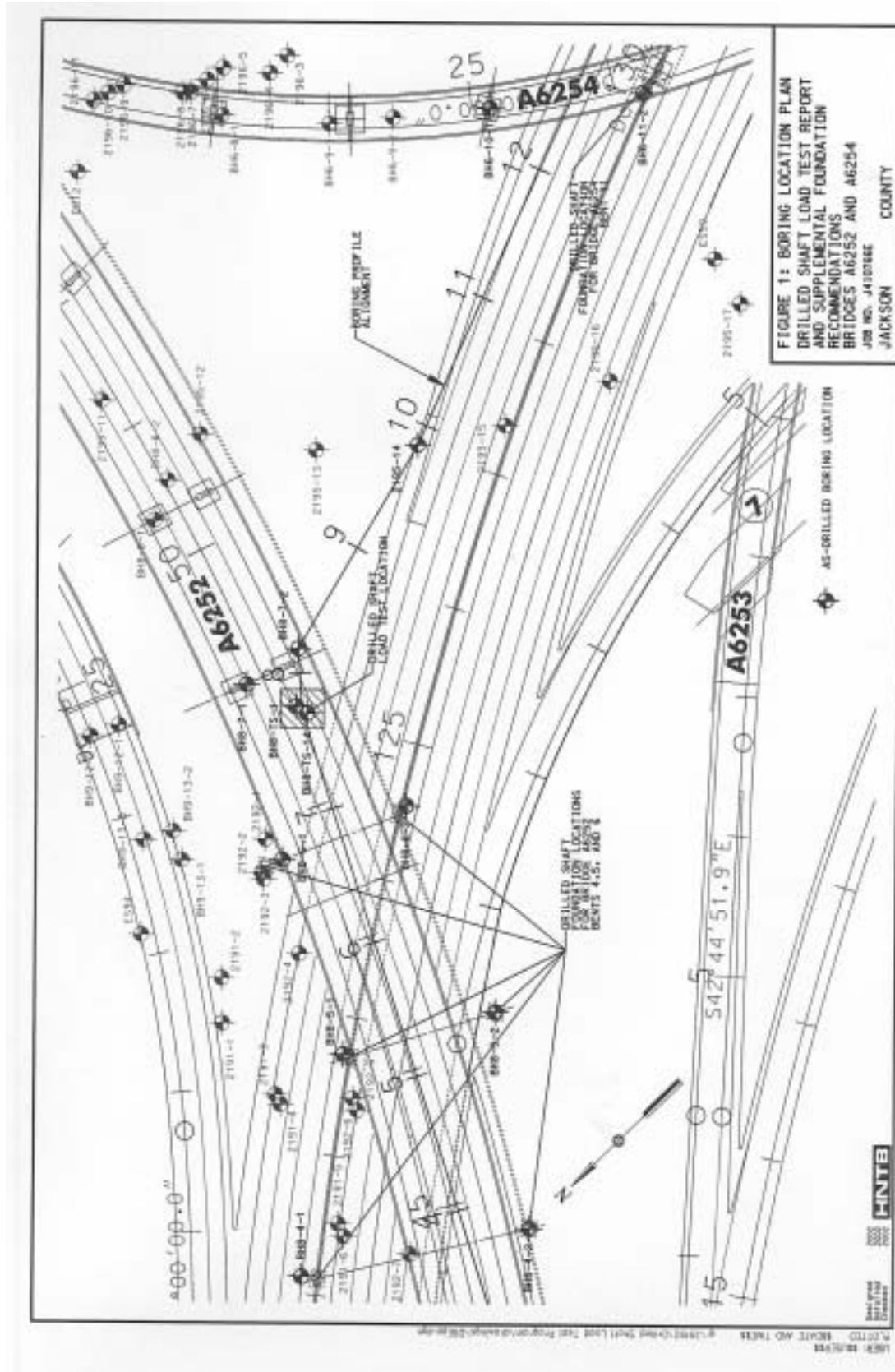
logged with the amount of core recovered and the RQD being noted. Samples of the NX core were returned to the laboratory for further testing. As shown in the table, the unconfined compressive strengths of the limestones are significantly higher than the shales and will take most of the axial load. The strength of the limestones exceeds the strength of 4000 psi = 288 tsf (27.6 MPa) concrete and the strength of concrete would control the ultimate side shear capacity. The strength of the shales ranges from 6.5 to 24.1 tsf (0.6 to 2.3 MPa) and generally increases with the depth of the stratum.

Table 5.2- Unconfined compressive strengths of rock strata at the Grandview Triangle site.

Strata	Elev. ft.	Avg. q_u		Range tsf	Std. Dev. tsf
		MPa	tsf		
Chanute	916.5 - 927.2	0.6	6.5	2.7 - 10.1	3.3
Cement City	911.3 - 916.5	37.0	386.6	118.6 - 588.0	179.8
Quivira	904.8 - 911.3	1.4	14.9	11.1 - 18.2	3.0
Westerville	898.1 - 904.8	62.9	657.1	164.8 - 1104	311.9
Wea	< 898.1	2.3	24.1	8.4 - 33.1	8.7

5.4 Foundation Design

Proposed bridge A6252 will cross US 71 at an angle as shown in Figure 5.10. Piers 4, 5, and 6 will each be supported by one column in the median of US 71. One column of proposed bridge A6254, Pier 11, will also be located in the median. Construction of spread footing or pile caps in the median of US 71 would likely require a detour to allow room for the footing excavation including the use of sheet piling. Drilled shafts socketed into bedrock would not require a detour and were therefore investigated as the preferred foundation type.



Since the closest limestone member (Winterset Limestone at about elevation 852 ft) thick enough to support drilled shafts and axial loads in end bearing is about 80 feet (24.4 m) below the top of the drilled shaft elevation, an Osterberg cell load test was recommended by HNTB (2002) to investigate side shear characteristics of the alternating layers of shale and limestone at shallower depths. The test shaft location was selected to be adjacent to Pier 6 on Bridge A6252 as shown in Figures 5.6 and 5.10.

5.5 Construction of Test Shaft

The test site was located on the east side of U.S. Highway 71 between proposed bridges A6252 and A6254 at Station 125+05, 90 ft. left of centerline. This site provided access for construction equipment and avoided existing roadways, utilities, and planned foundations. The site was also as close as possible to the planned production shafts.

A 34 inch (870 mm) diameter O-CellTM was selected to evaluate the side shear capacities of the different strata of shale and limestone as shown in Figure 5.11. To focus the test on the unit side shear capacities, a compressible inclusion was placed at the base of the rock socket as shown in Figure 5.12. The compressible end-bearing device, consisting of 3 inches (76 mm) of styrene foam sandwiched between two one half inch (12.5 mm) thick steel plates was placed at the base of the carrying frame and lowered into the shaft prior to concrete placement.

The test shaft was constructed by Clarkson Construction and their drilling subcontractor, Hayes Drilling, using a Watson 3100 drill rig shown in Figure 5.13. Work began on May 28, 2002 with drilling of the weathered limestone and shales at the surface with a double-flight 84 inch (2.1 m) bullet tooth rock auger. Temporary casing

was seated into the Chanute shale. The remainder of the rock socket was excavated alternating between a 72 inch (1.8 m) rock auger and core barrel. The last 2.5 foot long (0.76 m) piece of Westerville Limestone core fell out of the core barrel while attempting to remove it. The core fell back into the hole sideways. Unsuccessful attempts were made to remove the misaligned core with a couple of different sizes of core barrels and the 72 inch (1.8 m) rock auger. At this point, the hole had filled to the top of the Cement City Limestone with seepage water and had to be pumped dry before further attempts to remove the core could proceed. The core was eventually broken up using a 36 inch (914 mm) core barrel and the pieces removed using the rock auger. The excavation of the rock socket was completed on May 31, 2002.

Water was observed entering the excavation from cracks in the Cement City Limestone at a rate of 3 feet (0.9 m) per hour. The hole was pumped dry and both sonic caliper and down-hole camera inspections were performed. The sonic caliper log is shown in Figure 5.14. The camera was used with a tape to determine exact elevations of the bedrock layers. After inspection, the hole was again pumped dry and the load frame was lowered into the hole as shown in Figure 5.15. Figure 5.16 shows the placement of the shaft concrete using a tremie line and pump truck on May 31, 2002. The slump of the concrete varied from 7 inches (178 mm) for the first truck to 5.5 inches (140 mm) for the last truck. The Osterberg cell load test was performed by Loadtest Inc. on June 3, 2002.

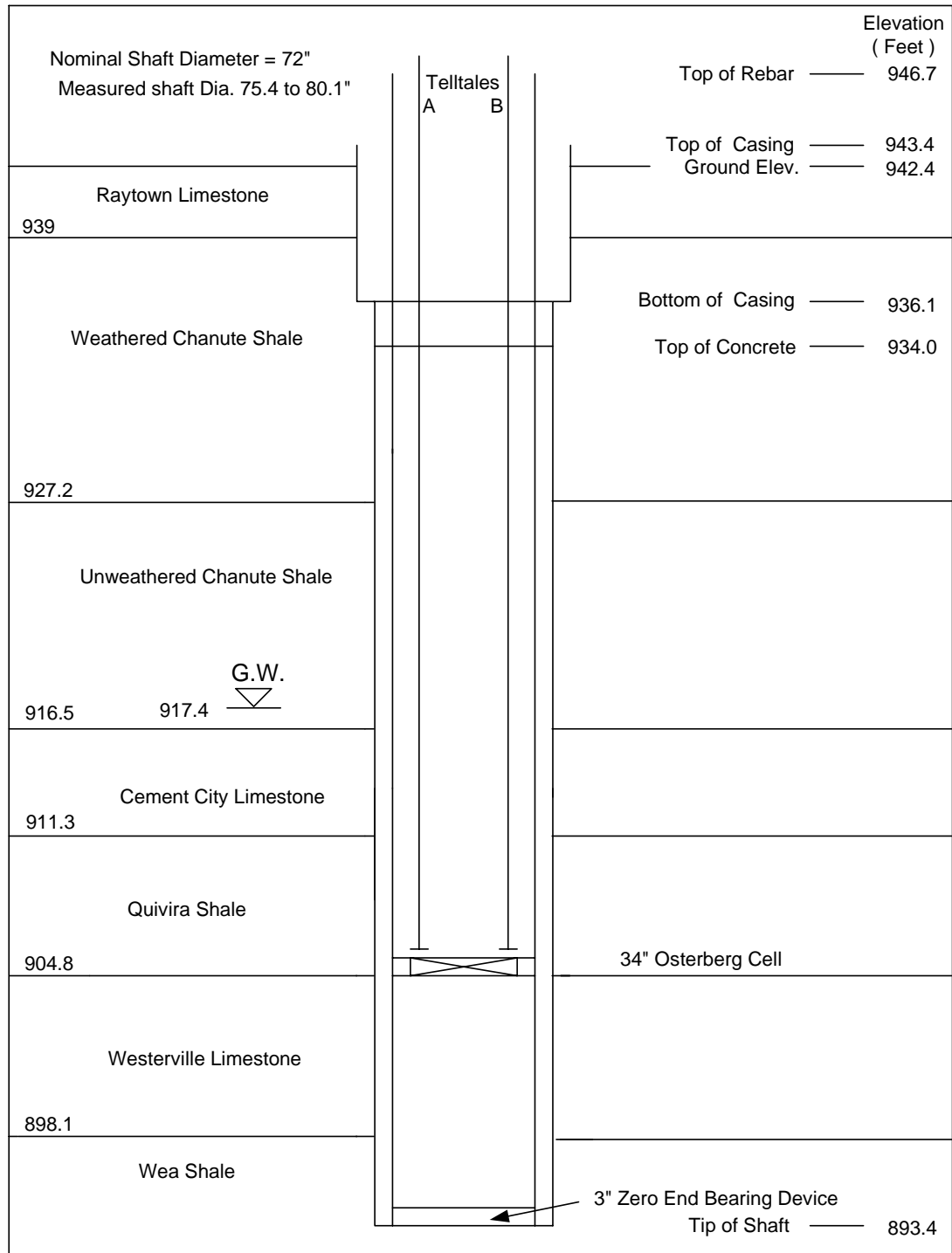


Figure 5.11- Schematic of Grandview Triangle test shaft and various shale strata.



Figure 5.12- Compressible end-bearing device.



Figure 5.13- Watson 3100 drill rig.

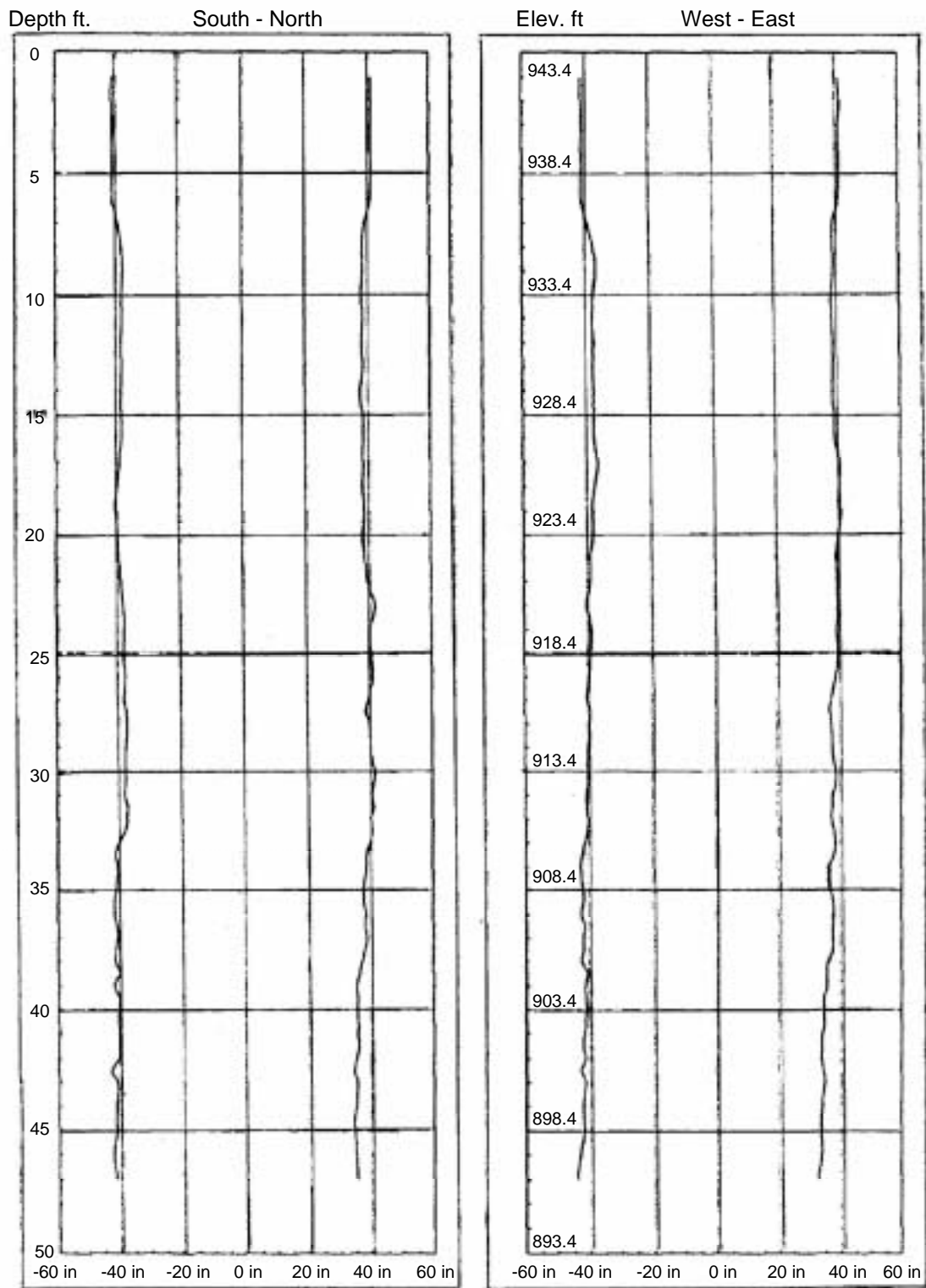


Figure 5.14- Sonic caliper log of Grandview Triangle test shaft (from HNTB 2002).



Figure 5.15- Lowering load frame into Grandview Triangle test shaft.



Figure 5.16- Placing shaft concrete using tremie and pump truck.

5.6 Load Test Setup and Procedures

The 34 inch (870 mm) diameter O-CellTM, with its base located 11.6 feet (3.54 m) above the tip of the rock socket, was pressurized to assess the combined end bearing and side shear below the O-CellTM and side shear above the cell. Initial assessments of the side shear capacities indicated that the segment of shaft below the O-CellTM would fail in side shear first. After determination of the side shear in the lower segment of the shaft, continued loading would completely compress the end-bearing device and begin mobilizing end-bearing. The combined end-bearing and side shear below the O-CellTM

would then be used as a reaction to assess the side shear above the O-CellTM.

The O-CellTM was pressurized in 21 equal increments of 600 psi (4,137 kPa) to a maximum O-cellTM pressure of 12,610 psi (86.9 MPa), which corresponds to a load of 3,856 tons (34.3 MN) in each direction. The loading increments are denoted as 1L-1, 1L-2, and 1L-3, etc.; the unloading events are denoted as 1U-1, 1U-2, 1U-3, etc. At the maximum load of 3,856 tons (34.3 MN) the upper segment of the shaft was displacing rapidly and higher loads could not be achieved. The O-CellTM was then unloaded in 5 equal increments and the test was concluded. The applied load increments followed procedures in ASTM D1143- Standard Test Method for Piles Under Static Axial Compressive Load.

Test shaft instrumentation is shown in Figure 5.17 and a summary of dimensions is given in Table B.1 in Appendix B. Expansion of the O-CellTM was measured by three LVWDTs (Geokon Model 4450 Series) positioned between the lower and upper plates of the O-CellTM. Compression of the shaft between the O-CellTM and the compressible end-bearing device at the base of the shaft was measured by a pair of embedded compression telltales (ECTs). Telltale casings were attached to the carrying frame and the upper plate of the O-CellTM to monitor top of shaft movement and top of cell movement, respectively.

Strain gages were used to assess the load transfer in side shear of the shaft above and below the O-CellTM. Six levels of two sister bar vibrating wire strain gages were installed in the shaft - four levels above the cell and two below. Final positioning of the strain gages was determined by the down-hole camera, which was used to determine exact elevations of the bedrock layer interfaces.

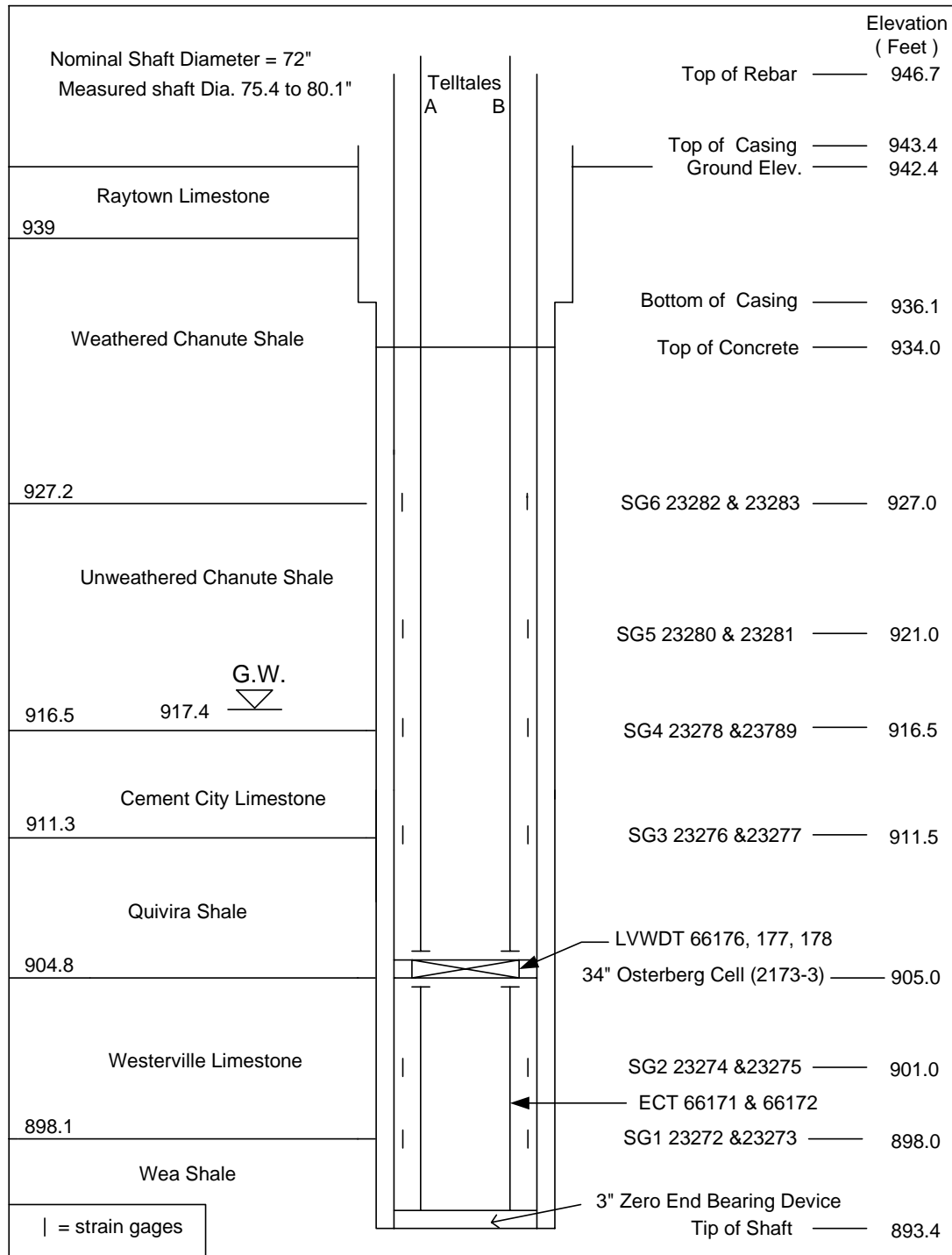


Figure 5.17- Schematic of Grandview test shaft instrumentation.

5.7 General Test Results

Results of the Osterberg cell load test at the Grandview Triangle site are presented in this section. Detailed load test data, including a summary of test shaft dimensions, load-displacement data, strain gage data, and computed unit side shear data is presented in Appendix B.

Upward and downward load displacement curves determined from the load test at the Grandview Triangle test site are shown in Figure 5.18. The maximum gross load applied to the base of the shaft occurred at load interval 1L-21 and equaled 3,856 tons (34.3 MN) in each direction. At this loading, the O-CellTM had expanded 1.63 inches (41.45 mm) with 1.41 inches (35.8 mm) of upward movement and 0.22 inches (5.67 mm) of downward movement. At the maximum load, the ultimate capacity of the rock socket above the O-CellTM was reached and additional load could not be applied to the rock socket below the O-CellTM.

The maximum net load applied to the upper portion of the shaft was equal to 3,856 tons (34.30 MN) minus the buoyant weight of the shaft, 59 tons (0.53 MN), for a net applied load of 3,797 tons (33.78 MN). The maximum net load applied to the shaft segment below the O-CellTM was equal to 3,856 tons (34.30 MN). Due to the minimal downward displacement and the use of the compressible end-bearing device, the entire load below the cell was assumed to be carried by side shear only.

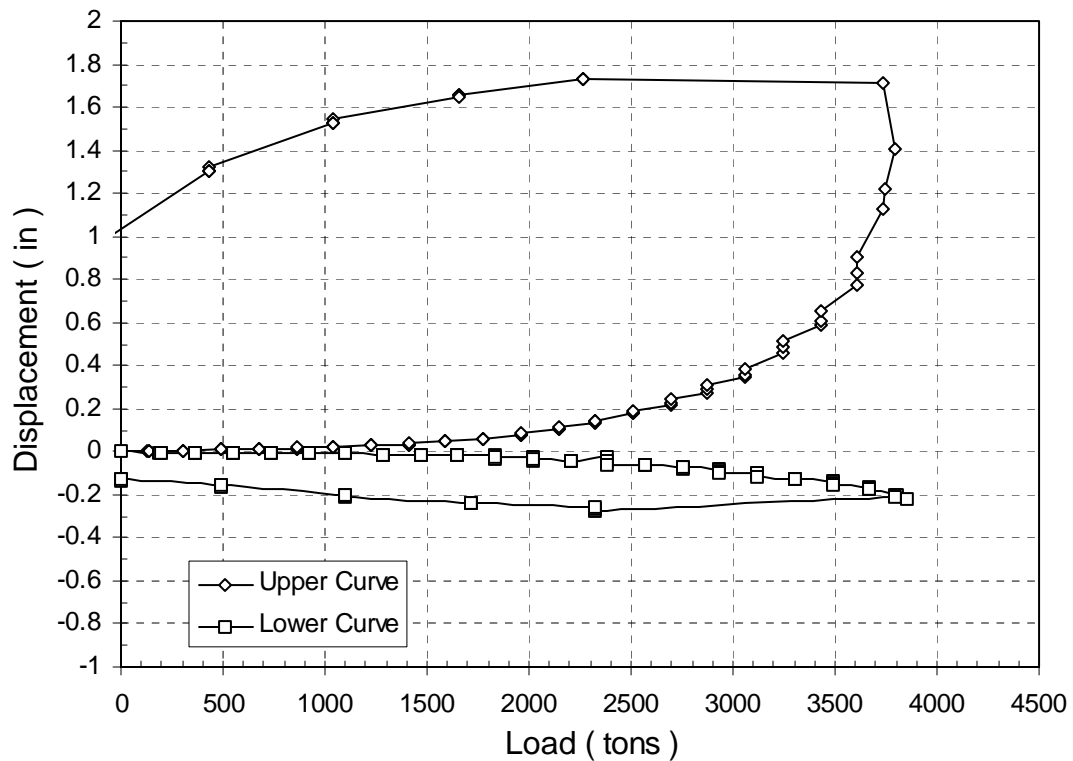


Figure 5.18- Measured load-displacement curves for upward and downward loading of test shaft at the Grandview Triangle site.

The equivalent top-down load-displacement curves are shown in Figure 5.19.

None of the load was transferred in end bearing and the equivalent top-down load-displacement curve does not include end bearing. The equivalent top-down load-displacement curve adjusted for additional elastic compression indicates that a shaft loaded from the top with a load of 5,463 tons (48.6 MN) would settle about 0.25 inches (6.4 mm), of which 0.15 inches (3.9 mm) is estimated to be from elastic compression of the shaft.

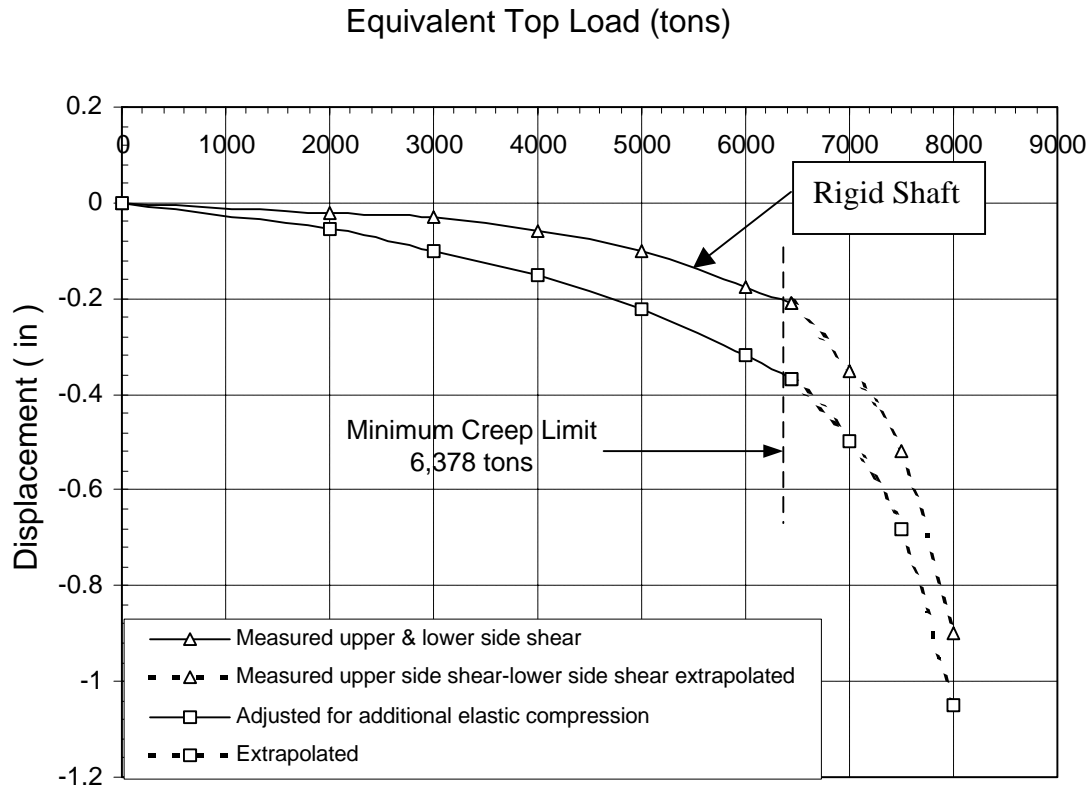


Figure 5.19- Equivalent top-down load-displacement curves for the Grandview Triangle test shaft.

The distribution of axial force with depth or elevation at various load increments is generated from strain gage data, the equivalent modulus of the shaft, and the cross-sectional area of the shaft as described in Chapter 3. The distribution of axial force with elevation for the Grandview Triangle test is shown in Figure 5.20 for different loading levels. Detailed strain gage data used to compute these forces is given in Appendix B.

On the day of the test, the concrete compressive strength, as determined from concrete test cylinders, was 6000 psi (41.37 MPa). Equation 3.3 was used to calculate an elastic modulus for the concrete of 4,415,000 psi (30,230 MPa). This, combined with the area of reinforcing steel and shaft diameters- 77.8 inches (1976 mm) above the O-Cell™ and 76.3 inches (1938 mm) below- was used to determine an average shaft stiffness (AE) of 21,000,000 kips (93,853 MN).

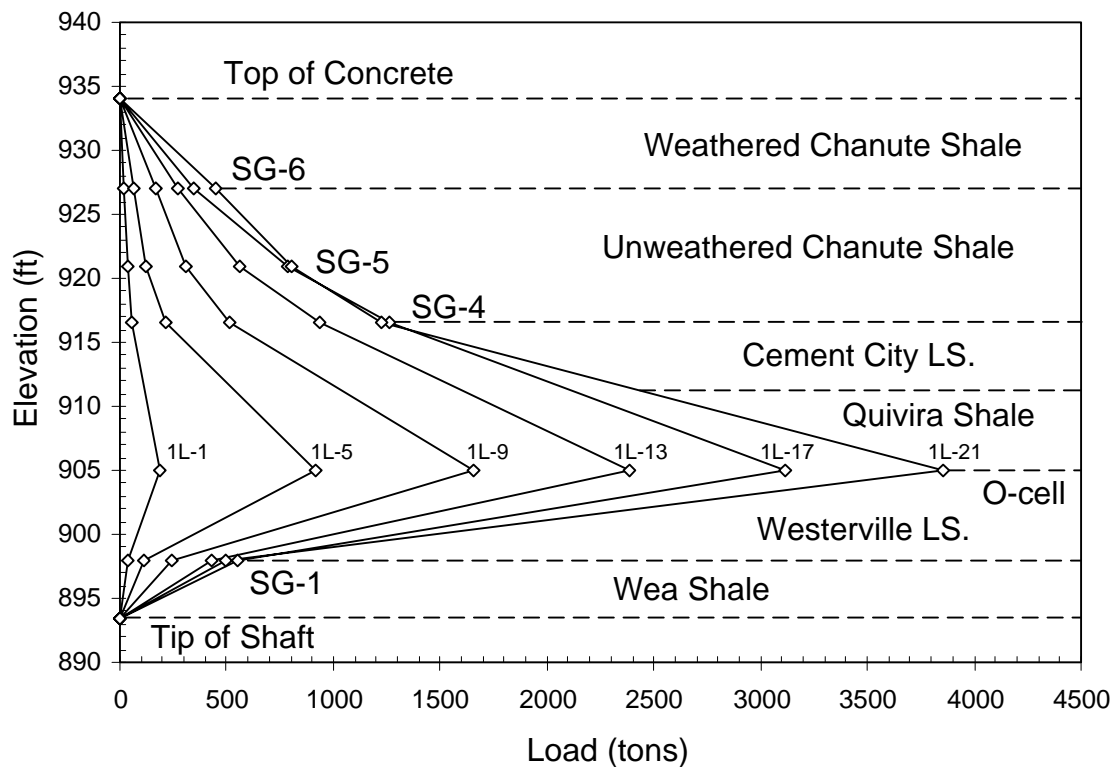
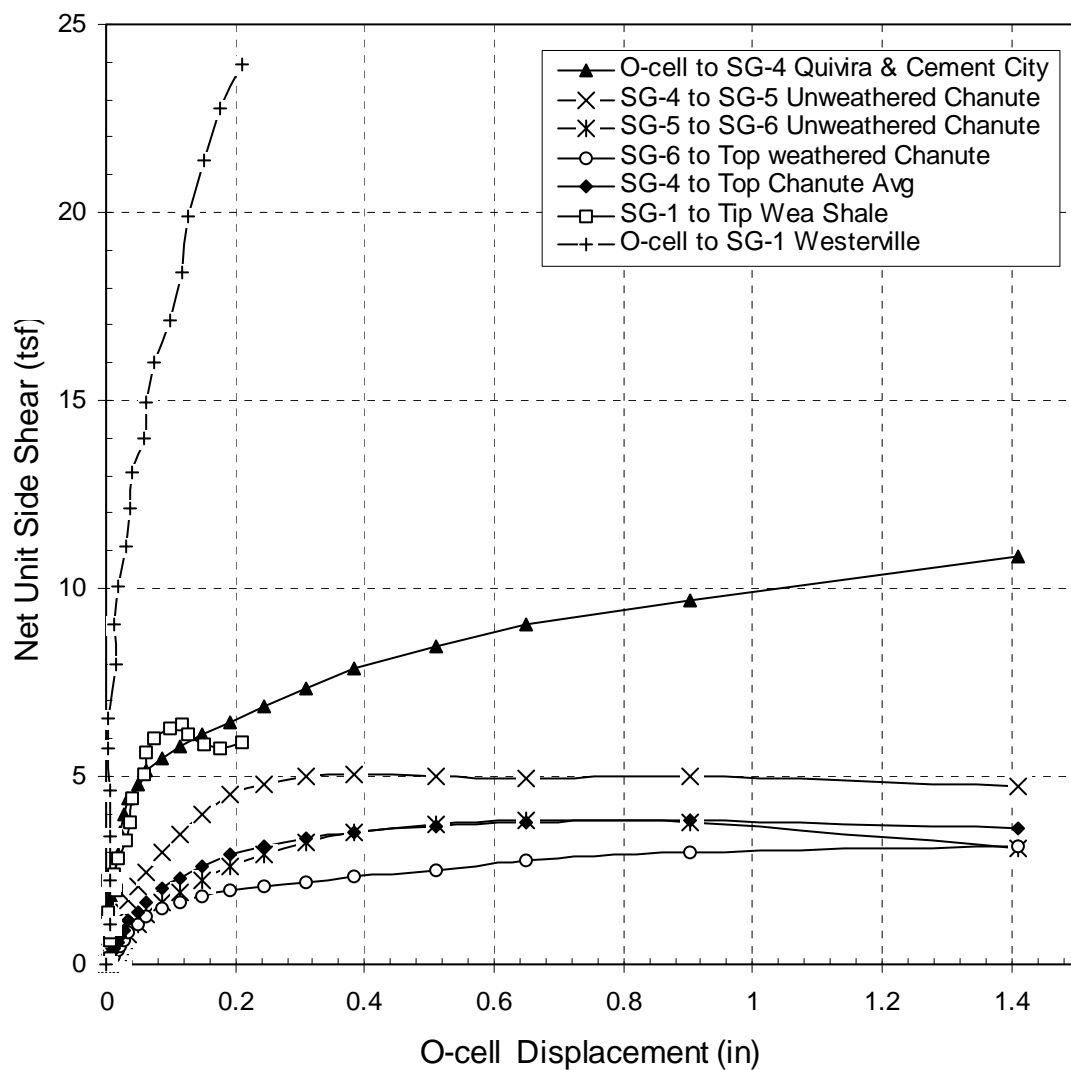


Figure 5.20- Distribution of axial force for the Grandview Triangle test shaft.

Figure 5.21 shows the mobilized unit side shear plotted versus O-cellTM displacements for the different strata encountered at the Grandview test site. As shown in Figure 5.21, the ultimate unit side shear was mobilized in the weathered and unweathered Chanute Shale strata and the Wea Shale strata. No clear peak in the unit side shear was observed in the Quivira Shale and Cement City strata or in the Westerville Limestone stratum. The maximum mobilized unit side-shear values for the shaft based on strain gage data are shown in Table 5.3 and plotted in Figure 5.22. The ultimate unit side shear of the unweathered Chanute Shale varied from 3.1 to 4.8 tsf (296.9 to 407.6 kPa). The weathered Chanute Shale had an ultimate side shear of 3.2 tsf (301 kPa). The average

ultimate side shear for the entire thickness of Chanute Shale was 3.6 tsf (346.8 kPa). The ultimate unit side shear for the combined Cement City Limestone and Quivira Shale was 10.9 tsf (1039.4 kPa). The Wea Shale had an ultimate side shear value of 6.4 tsf (612.9 kPa). The Westerville Limestone did not achieve an ultimate side shear during this load test. A maximum unit side shear of 24 tsf (2,298 kPa) was achieved for the Westerville Limestone before the Osterberg cell load test was concluded.



5.21- Mobilized unit side shear versus O-cell displacement for various geologic strata at the Grandview Triangle test site.

Level 2 and level 3 strain gages were too close to the O-CellTM and did not produce reliable data. Because the steel plates above and below the O-cellTM are not infinitely stiff, a cone of compression is believed to develop above and below the O-cellTM, as shown in Figure 5.23, that distributes the applied load out to the sides of the socket. The level 2 and 3 strain gages were located near the sides of the rock socket, in a transition zone where material at the sides of the socket is believed to be in tension. Since the level 3 strain gages did not function properly, unit side shear values for the Cement City Limestone and Quivira Shale could not be determined directly from the strain gage data. A value of unit side shear of 4.8 tsf (460 kPa) was therefore assumed for the Quivira Shale in order to calculate the unit side shear of the Cement City Limestone. The assumed unit side shear value was determined by a comparison of calculated unit shear values and unconfined compressive strength data for all shale formations at the site.

Table 5.3-Unit side shear values calculated from strain gage data for the Grandview Triangle test shaft.

Load Transfer Zone	Strata	Elevation (ft)	Unit Side Shear	
			kPa	tsf
Top of Shaft to SG-6	Weathered Chanute	934 - 927	301	3.2
SG-6 to SG-5	Chanute	927 - 921	295	3.1
SG-5 to SG-4	Chanute	921 - 916.5	453	4.8
SG-6 to SG-4	Chanute	927 - 916.5	363	3.8
SG-4 to O-Cell TM	Combined Quivira & Cement City	916.5 - 905.0	>1,039	>10.9
SG-4 to SG-3	Cement City	916.5 - 911.5	>1,651*	>17.2*
SG-3 to SG-2	Quivira	911.5 - 905.0	460*	4.8*
O-Cell TM to SG-1	Westerville	905.0 - 898.0	>2,293	>24.0
SG-1 to Tip of Shaft	Wea	898.0 - 893.4	565	5.9

* The value for the Quivira was assumed in order to calculate the unit side shear of the Cement City Limestone.

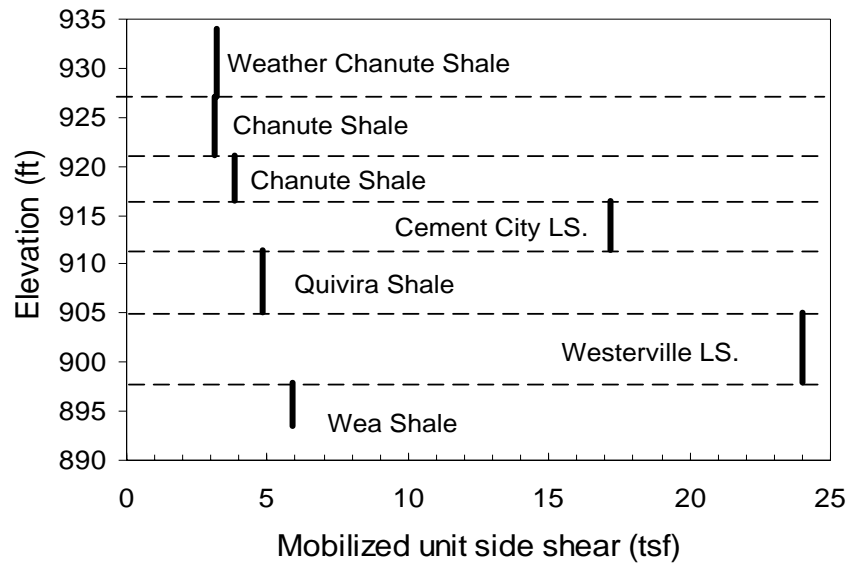


Figure 5.22- Mobilized unit side shear calculated from strain gage data for Grandview Triangle test shaft.

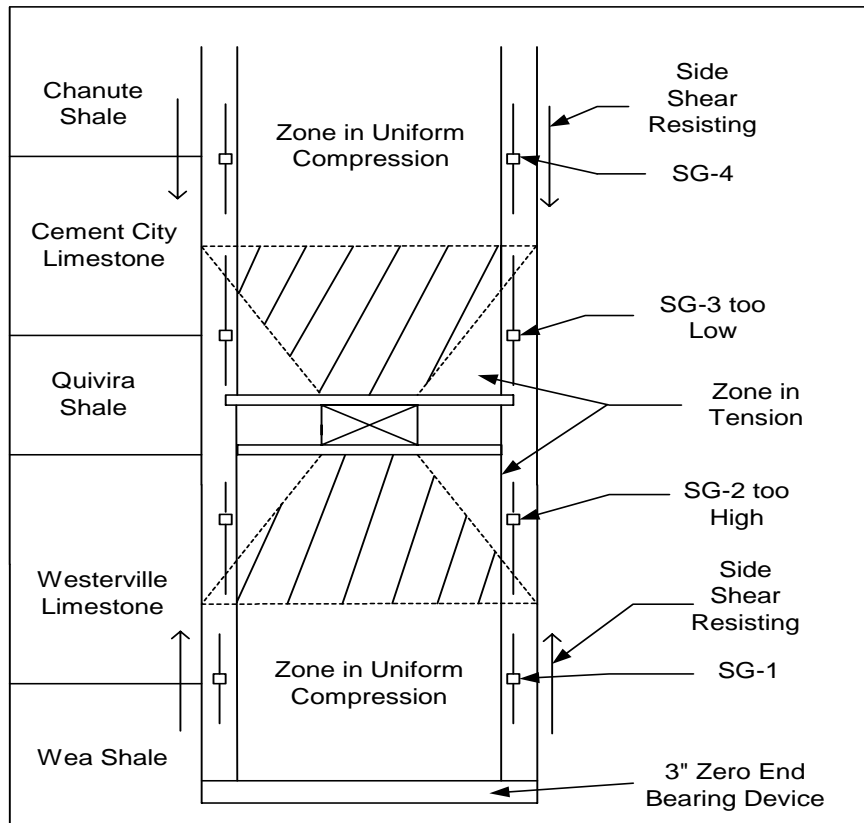


Figure 5.23- Zone of influence for level 2 and 3 strain gages.

As described in Chapter 3, the creep limit is determined by plotting the additional displacement that occurs over the time interval 2 to 4 minutes after application of the load while the load is maintained as shown in Figures 5.24 and 5.25. A creep limit of 2,600 tons (23.13 MN) was reached for the upper portion of the shaft at a displacement of 0.217 inches (5.51 mm). At a maximum loading of 3,856 tons (34.3 MN), no apparent creep limit was reached for the lower portion of the shaft with a displacement of 0.223 inches (5.67 mm). Based on these results, Loadtest recommended that significant creep would not occur for a top loaded shaft until a load greater than 6,378 tons (56.73 MN) is exceeded by some unknown amount.

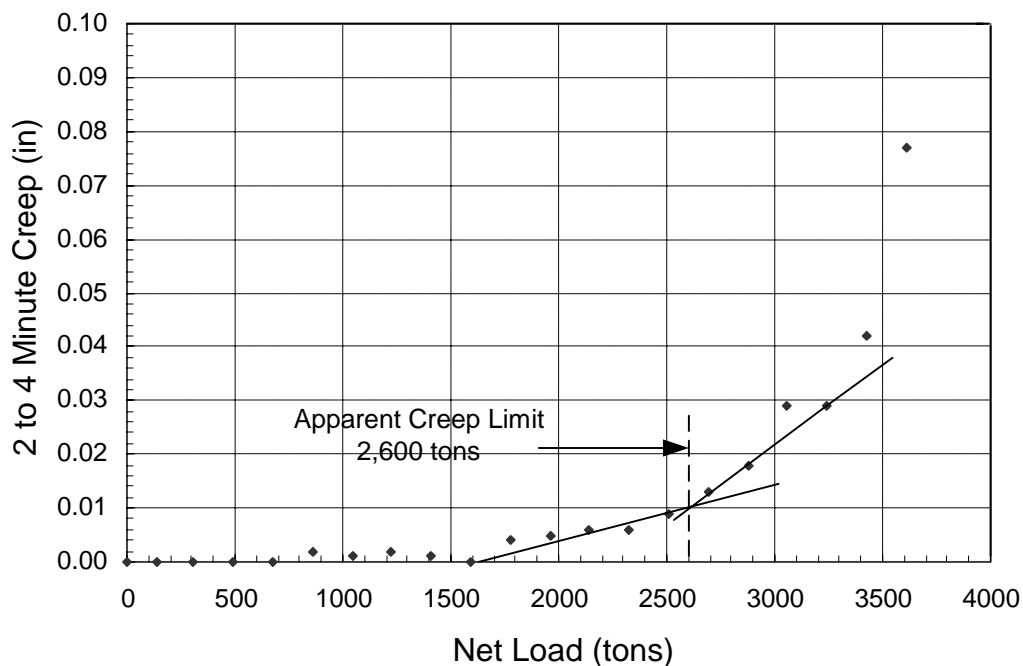


Figure 5.24- Creep displacement for the upper portion of Grandview Triangle test shaft.

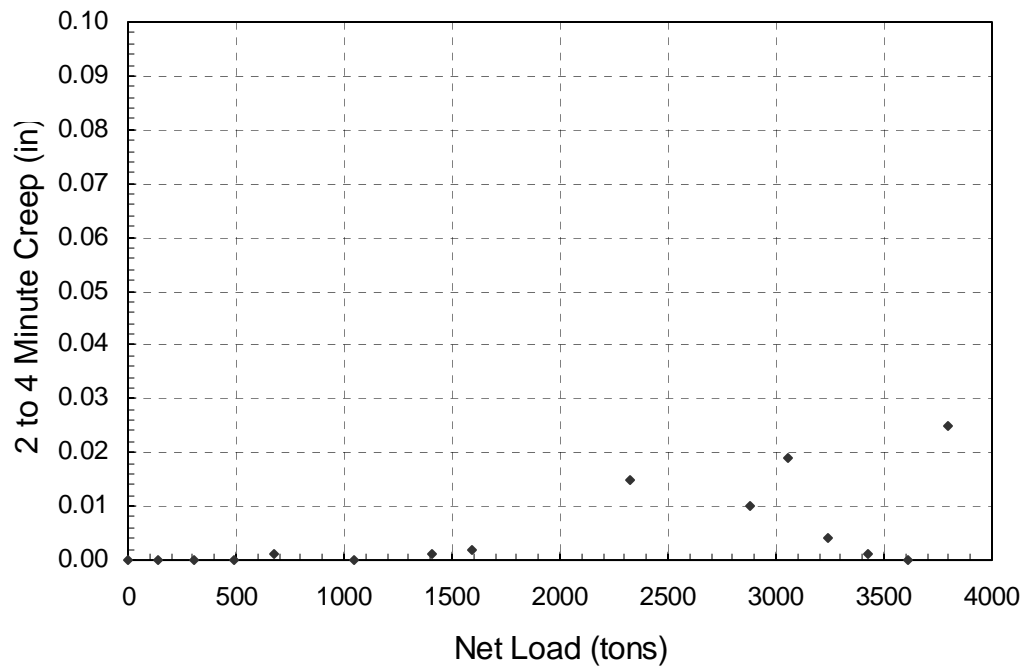


Figure 5.25- Creep displacement for the lower portion of Grandview Triangle test shaft.

5.8 Practical Applications

Data from the Osterberg cell load test would allow the 7.5 feet (2.3 m) diameter rock sockets at bridge A6252 to be shortened a total of 214 feet (65.2 m) for a cost savings of \$214,000. The cost of the test shaft excavation and the Osterberg cell load test was \$195,000 for a net savings of \$19,000. Additional cost savings of \$50,000 dollars were anticipated for Pier 11 of bridge A6254 but the footing was subsequently designed as a spread footing. Although the net cost savings of \$19,000 was not significant, it indicates the magnitude of cost savings that could be realized in applying Osterberg cell load test information to future projects in this area.

5.9 Discussion

Several points regarding the interpretation of results from the O-cell load tests warrant discussion. Although the upper segment of the rock socket mobilized the full side shear capacity, the ultimate unit side shear for the Cement City Limestone and the Quivira Shale could not be determined individually since the strain gages at the Cement City-Quivira contact did not function properly. The level 3 strain gages were too close to the O-CellTM and did not produce reliable data. Because the steel plates above and below the O-cellTM are not infinitely stiff, a cone of compression develops above and below the O-cellTM that distributes the applied load out to the sides of the socket. This is shown graphically for the zone above the O-cellTM in Figure 5.26. The level 3 strain gages were located near the sides of the rock socket, in a transition zone where material at the sides of the socket is in tension. A possible solution would be to position the strain gages towards the center of the rock socket. This, however, would position the strain gages in a cone of influence of an unknown diameter. This may also be a point of error for the Osterberg test in general.

Since the level 3 strain gages did not function properly the unit side shear values could not be determined directly from the strain gage data for either the Cement City Limestone or Quivira Shale. A value of unit side shear of 4.8 tsf (460 kPa) was assumed for the Quivira Shale in order to calculate the unit side shear capacity of the Cement City Limestone. The revised distribution of axial force is shown in Figure 5.27. The assumed unit side shear value was determined by a comparison of calculated unit shear values and unconfined compressive strength data for the shale formations. The adjusted axial load curve indicates that only about 729.1 tons (6.5 MN) of the axial load is shed in the

Quivira Shale with most of the axial load 1,896.9 tons (16.9 MN) is carried by the Cement City Limestone even though the Cement City Limestone is a thinner layer.

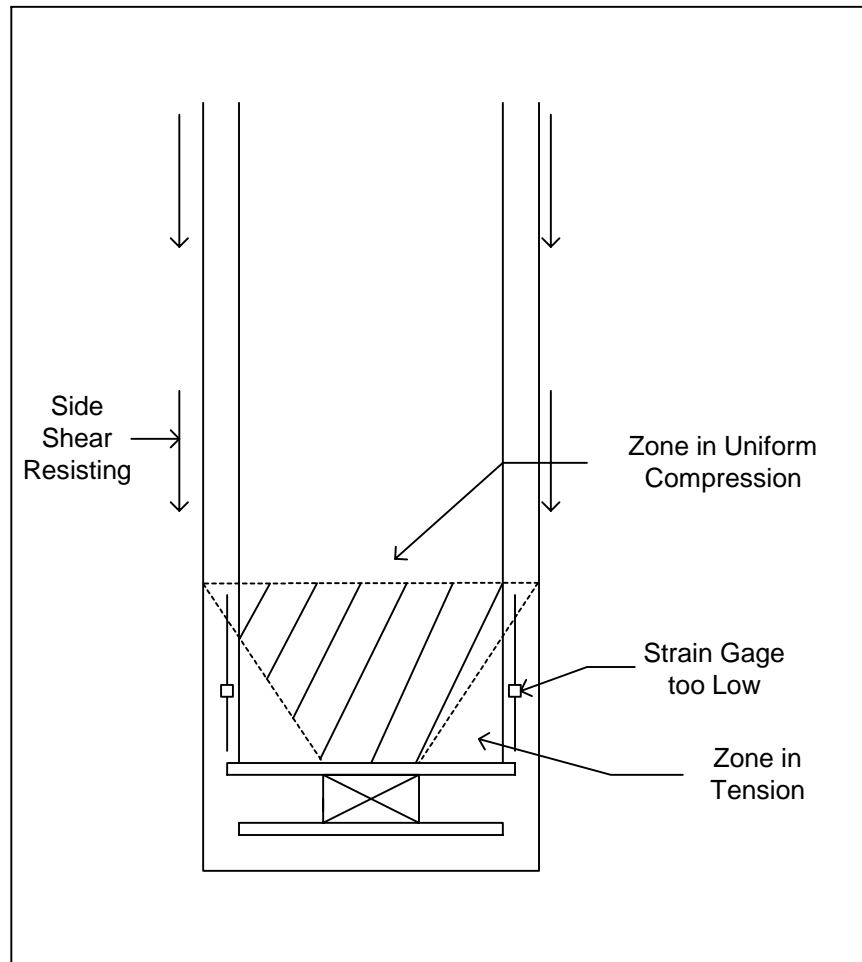


Figure 5.26- Influence of strain gage positioning (after Hayes and Simmonds 2002).

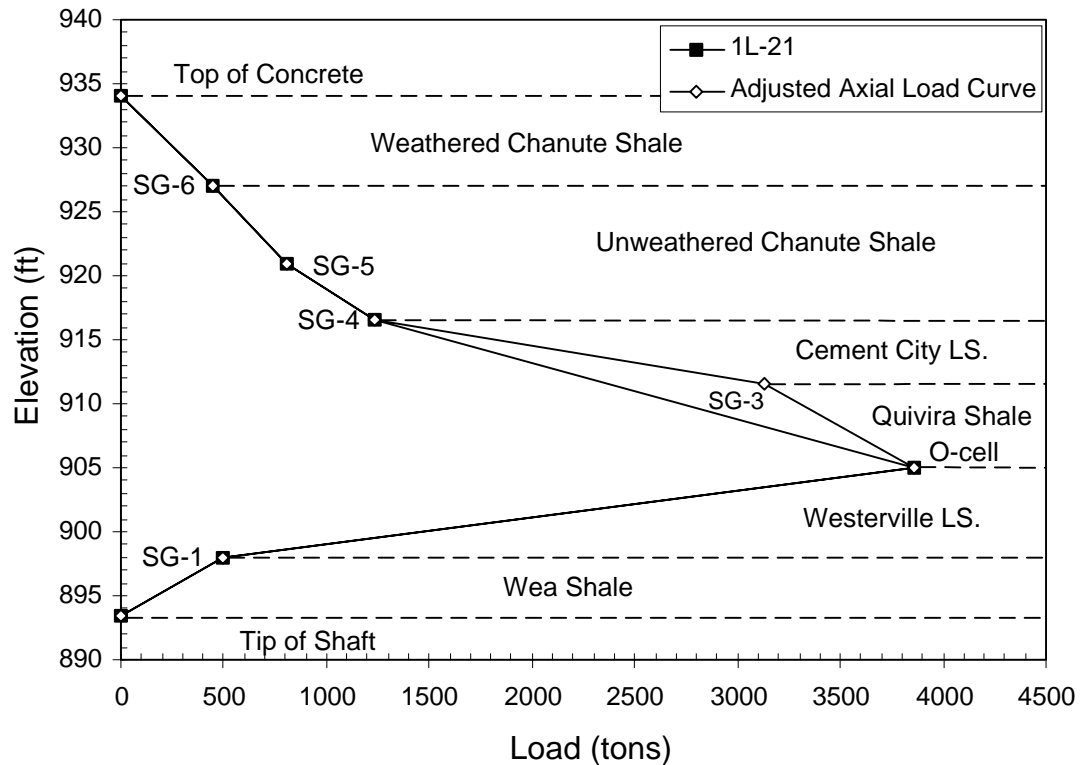


Figure 5.27- Adjusted axial load curve based on assumed unit side shear value for Quivira Shale.

Another issue with interpretation of Osterberg cell load tests involves when to subtract the buoyant weight of the shaft from the gross load to calculate the net load. Theoretically, the O-CellTM does not impose an additional upward load until the O-cellTM force exceeds the buoyant weight of the shaft above the cell. Loadtest (2002) therefore uses the net load, defined as the gross O-CellTM load minus the buoyant weight of the shaft above the cell, to determine side shear above the cell. The difference in the Grandview Triangle load test and the test at the Lexington site is that the buoyant weight of the shaft was not subtracted from the gross O-CellTM load to calculate the lower side shear and end-bearing for the Grandview Triangle test shaft. However, Loadtest (2002) reports that the top-down load-displacement curve determined for the Grandview Triangle test shaft is still the same as the top-down load-displacement curves determined

for Lexington test shafts because they added the net upward load and gross downward load and then subtracted the buoyant weight of the shaft.

5.10 Summary and Conclusions

The Missouri Department of Transportation (MoDOT) is currently reconstructing and updating an intersection in the Kansas City metropolitan area known as the Grandview Triangle. Three major interstate routes and 7 local routes intersect at this location. All the bridges, ramps, and pavement will be replaced with 25 new bridges and more than 40 retaining walls.

A twelve span structure (A6252) and a thirteen span structure (A6254) will cross route US 71 and will require the construction of footings in the median of US 71. The use of conventional spread footings or pile caps would require a detour to allow room for the footing excavation. Drilled shafts socketed into bedrock would not require a detour and were investigated as the preferred foundation type. Since the closest limestone layer thick enough to support the axial loads in end bearing only is about 80 feet (24.4 m) below the top of the shaft, an Osterberg cell load test was performed to investigate the unit side shear characteristics of the bedrock.

A 34 inch (870 mm) diameter O-CellTM, with its base located 11.6 feet (3.54 m) above the tip of the rock socket was pressurized to assess the combined end bearing and side shear below the O-CellTM and side shear above the cell. Initial assessments of the side shear capacities based on FHWA guide lines indicated that the segment of shaft below the O-CellTM would fail in side shear first. After determination of the side shear in the lower segment of the shaft, continued loading would compress the end-bearing device mobilizing the end-bearing. The combined end-bearing and side shear below the O-

CellTM would then be used as a reaction to assess the side shear above the O-CellTM.

However, the combined side shear capacity of the Westerville Limestone and Wea Shale below the O-CellTM was greater than anticipated and the ultimate side shear capacity of the segment of the shaft below the O-cellTM could not be determined. Although the side shear in the socket segment below the O-cellTM was not fully mobilized, values achieved were greater than anticipated.

CHAPTER SIX

WAVERLY, MO. TEST SITE

A new bridge is proposed across the Missouri River in central Missouri on Route 65 in Waverly, Missouri. The bridge site is located about 18 miles downstream of the Lexington site. Foundation elements chosen for the piers in the river are to be drilled shafts socketed into bedrock. The bedrock at the bridge site is similar to the Lexington site and consists of older Pennsylvanian Age shales, siltstones, sandstones, limestones, and scattered coal beds. Present design methods used by MoDOT would dictate that as a result, rock sockets with a diameter of 6.5 ft. (1.98 m) would need to be as long as 63 feet (19.2 meters) in order to carry the anticipated axial load of 1525 tons (13.6 MN). The bridge design consultant, Harrington and Cortelyou, Inc. wanted to use both side shear and end bearing for the design of shafts at Pier 11. Due to the questionable nature of the bedrock at Pier 11 and the desire to use some end bearing, it was decided to test a rock socketed drilled shaft using an Osterberg load cell. Since time did not allow a load test to be conducted during the design phase of this project, the load test was conducted on a “production” drilled shaft at Pier 11. A 26 inch (660 mm) Osterberg load cell with a capacity of 1800 tons (16MN) in each direction was chosen to test the production shaft to twice the design load. The “production” test shaft was constructed by Jensen Construction Co. and the Osterberg cell load test was performed by Loadtest Inc. on September 30, 2002. The test indicated that the bedrock would be adequate to support design loads at Pier 11 using side shear and end bearing.

A general geologic description of the Waverly test site is presented in this chapter followed by a summary of the engineering characteristics of the most pertinent strata.

The construction and testing procedures for the test shaft are then described, followed by presentation of the results from the load test.

6.1 Site Description

The Missouri Department of Transportation (MoDOT) is planning a realignment of Route 65 at Waverly, Missouri. The realignment includes a new bridge across the Missouri River downstream of the present structure, which was opened to traffic in the 1920's.

The project is situated in the Missouri River alluvial plain in the central part of the state of Missouri as shown in Figures 6.1 and 6.2. The project was designed and constructed using English units; English units are therefore used in this chapter. The alluvial plain is mostly flat with some earthen levees constructed to protect row crop production. Currently the river channel is located adjacent to the rolling hills on the southern limit of the plain. The Missouri River alluvial plain is about 3600 feet (1.1 kilometers) wide in the project area and alluvial materials consist of 9 to 12 feet (2.7 to 3.7 meters) of cohesive soil overlying sand with scattered gravel layers. The thickness of the alluvial materials in the flood plain north of the river varies from 50 to 67 feet (15.2 to 20.4 meters). Two possible shipwrecks are thought to be in this area: the Tropic sunk in 1857 and the Grace Houston sunk in 1881. Within the river, the alluvial sand and gravel layers range in thickness from 25.7 to 45.8 feet (7.8 to 14 meters). Three further shipwrecks were noted in the channel of the Missouri River, but due to present dredging of the river for sand, it is highly unlikely that any remains will be found. The depth of wind blown loess on the rolling hills south of the river varies in thickness from 15 to 26 feet (4.6 to 7.9 meters). The former weigh station for the Steamboat Coal and Mining

Company is located in the vicinity of Pier 13. A 1912 Bureau of Mines report, stated that the Steamboat Coal and Mining Company operated a mine about 0.25 miles (0.4 kilometers) east of Waverly and the mine was 102 feet (31m) deep. In the vicinity of the mine, the Waverly coal is 3 to 4 feet (0.9 to 1.2 m) thick. Borings at Piers 12 and 14 were advanced to an elevation sufficient to intercept the Waverly coal bed. No voids were encountered at either pier and the mine is probably located farther to the east and does not appear to be a concern for the proposed bridge.

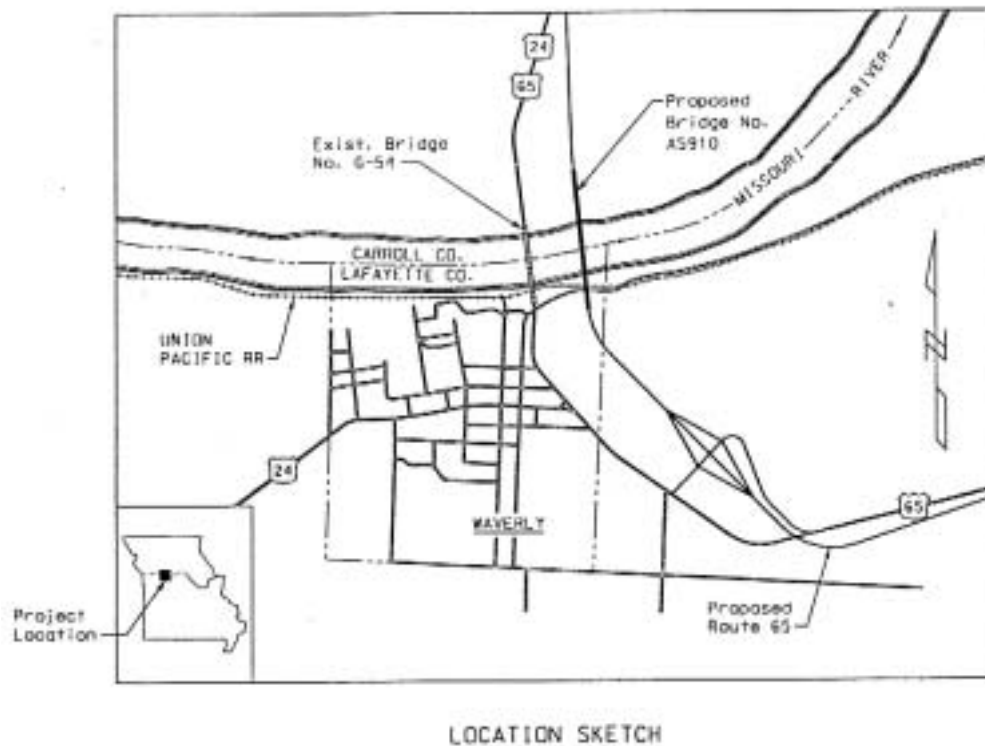
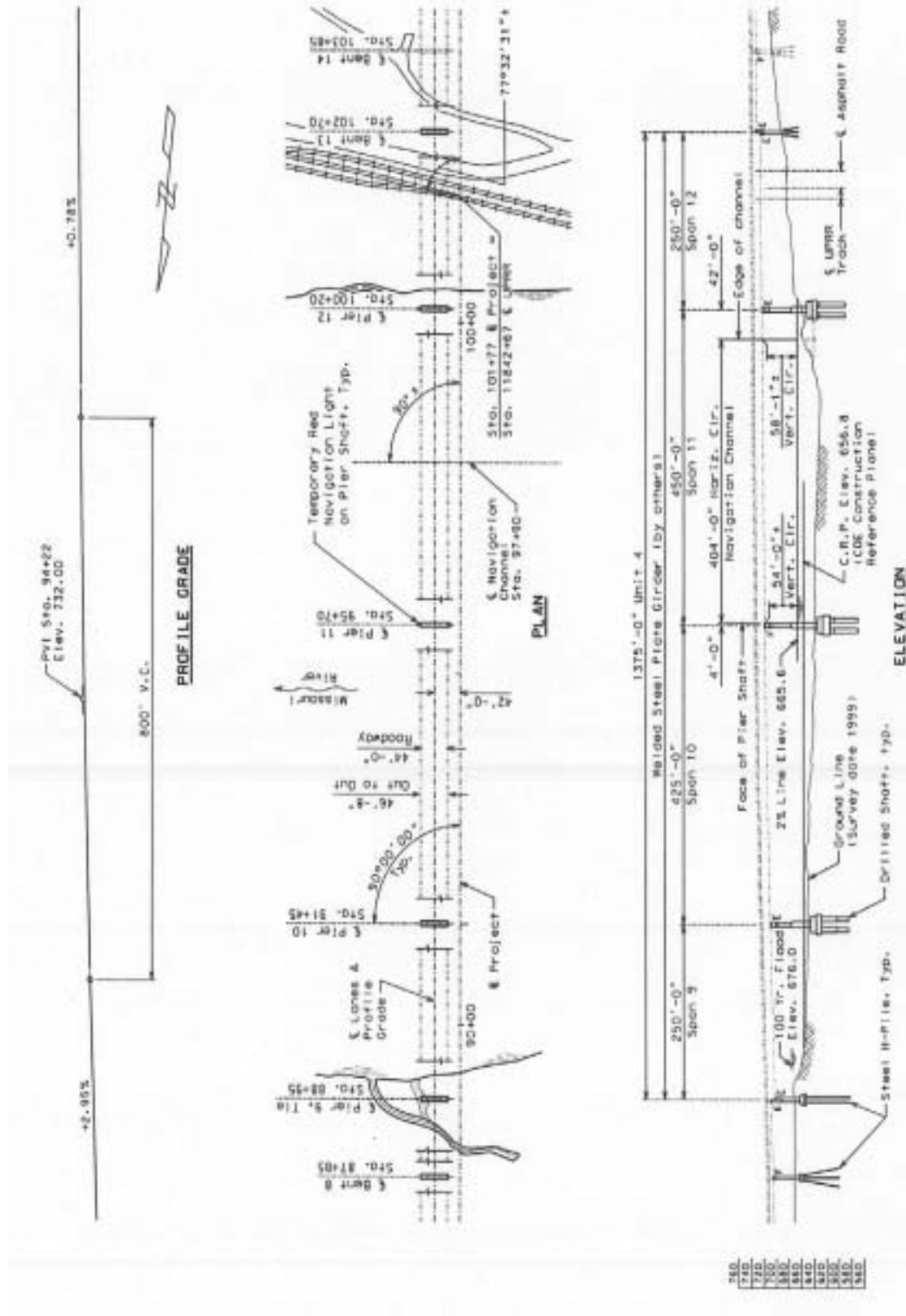


Figure 6.1- Location sketch of Waverly bridge site.

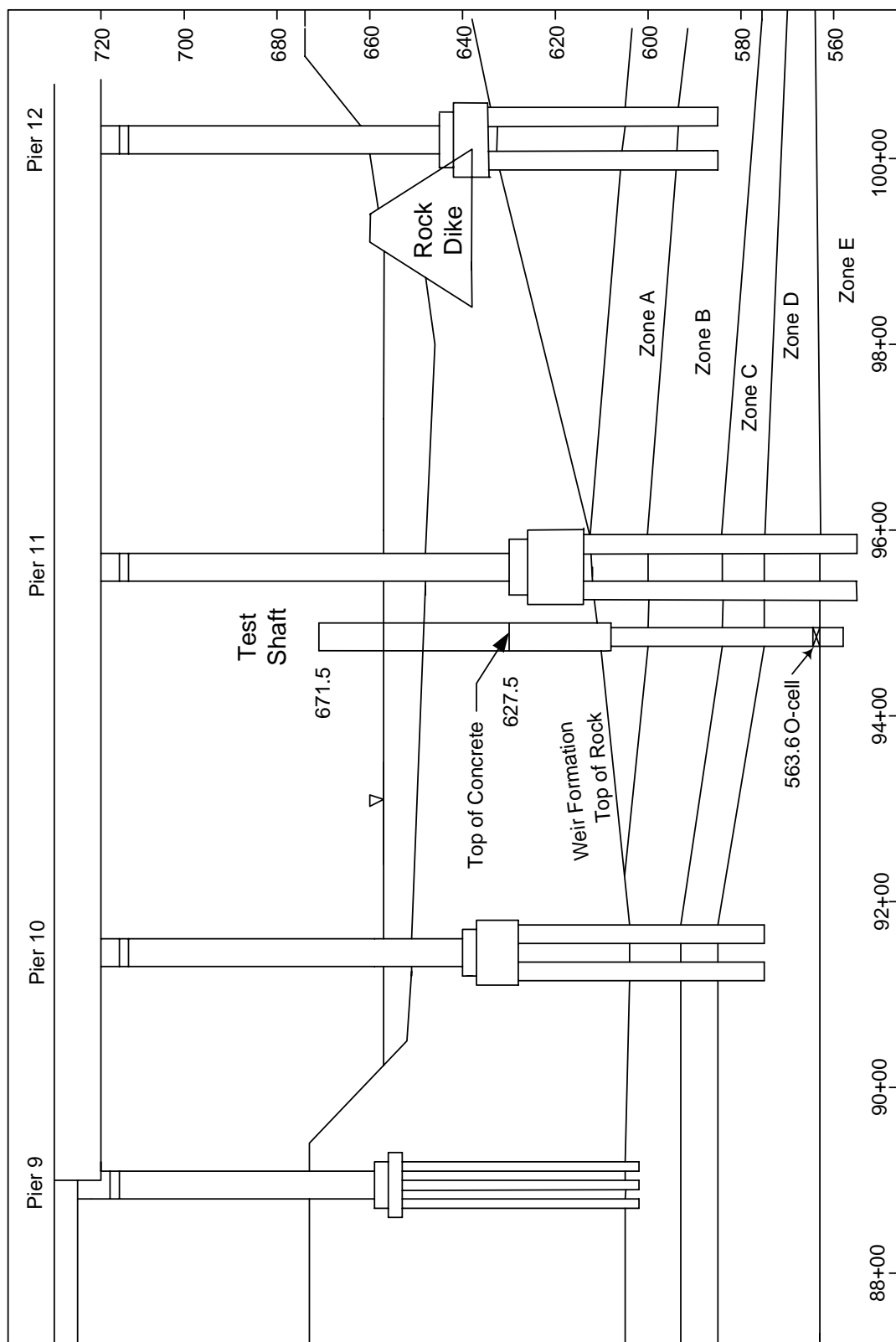


The bridge will extend from the north abutment located in the flood plain south across the flood plain and river to the south abutment located on the rolling hills on the south side of the river. The total length of the bridge is to be 2673 feet (814.7 meters) with 15 spans of various lengths. The two main river spans will be 450 and 425 feet (137.2 and 129.5 m) as shown in Figure 6.2.

Foundation elements for piers 1 through 9 and 13 through 16 were anticipated to be H-piles driven to bedrock. Drilled shafts socketed into the shale bedrock were anticipated for the three piers in the river (Piers 10, 11 and 12). An elevation view of piers 9 through 12 is shown in Figure 6.3 and the anticipated rock socket lengths and bearing values are presented in Table 6.1. Rock sockets for Piers 10, 11, and 12 will encounter the Weir Formation.

Table 6.1- Drilled shaft parameters for Piers 10, 11, and 12.

Pier	No. of Drilled Shafts	Rock Socket Length ft(m)	Rock Socket Dia. ft(m)	Design Bearing tons (MN)	Elev From-to (ft)	Allowable Unit Side Shear tsf (kPa)	Allowable Unit End Bearing tsf (kPa)
10	6	29(8.8)	6.5(2)	1000 (8.9)	602 - 594 594 - 586 586 - 570 570 - 560 560 - 550	0.6 (57) 2.0 (191.5) 2.6 (249) 1.6 (153.2) 2.0 (191.5)	0 0 25(2,394) 25(2,394) 25(2,394)
11	6	54(16.5)	6.5(2)	1524 (13.6)	608 - 585 585 - 564 564 - 555	0.6 (57) 1.4 (134.1) 2.0 (191.5)	0 0 25(2,394)
12	6	46(14)	6.5(2)	1,100 (9.8)	631 - 602 602 - 585 585 - 570	0.9 (86.2) 2.0 (191.5) 2.0 (191.5)	0 0 25(2,394)



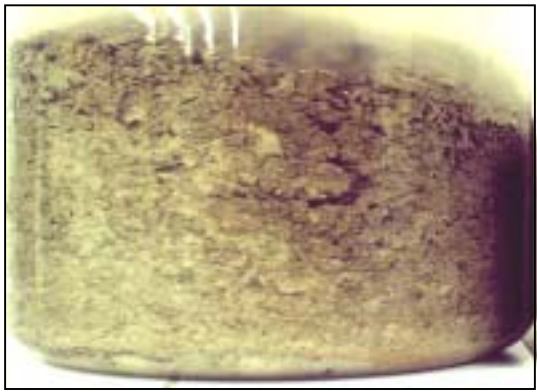
6.2 Geology of the Area

The underlying bedrock is of lower Pennsylvanian Age, Desmoinesian Series, Cherokee Group. The Cherokee Group contains most of the mineable coal beds in Missouri. The group is divided into the Krebs and Cabaniss Subgroups and the rock sockets for the drilled shafts are planned in the Cabaniss Subgroup.

The Cabaniss Subgroup consists of sandstone, siltstone, underclay, limestone, and coal beds. The subsurface investigation for the river piers encountered only the Weir Formation of the Cabaniss Subgroup. The subsurface investigation for the piers on the South river bank encountered (from the base upwards): the Weir Formation, the Tebo Formation, the Scammon Formation, and the Mineral Formation. The Weir Formation is described in the following paragraphs and the location of the rock socket for the test shaft at Pier 11 with respect to the formations is shown in Figure 6.3.

The Weir Formation is composed of (from the base upward) of shale, coarse grained sandstone, irregular bedded limestone, black carbonaceous shale, the Waverly Coal Bed, black carbonaceous shale, coal, micaceous siltshale, underclay, one to two coal beds, shale, limestone about 1 foot (0.3 m) thick, micaceous siltshale, underclay, and the Weir Pittsburg Coal bed. The top of the Weir Formation varied from elevation 625.0 to 629.4. The Weir Formation was encountered from about elevation 555 to 610 ft at Pier 11 and averages about 55 feet (16.8 m) in thickness at this location. The bedrock profile at Pier 11 was divided into 5 zones based on trends in material strength and properties.

Weir Zone A: Zone A was encountered from elevation 600 to 609 ft and consisted of gray to purple claystone and greenish-gray clay shale. Numerous slickensides were observed in the NX core. The slickensides may be attributed to natural faulting or faulting caused by the collapse of a mine. SPT blow counts in Zone A averaged 100 blows in 8 inches (20.3 cm). Liquid limits (LL) varied from 36 to 40 and the plasticity index (PI) varied from 15 to 20. Jar slake tests performed on this material produced a jar slake index of 2 as shown in Figure 6.4. Results of jar slake tests performed on various zones of the Weir Formation are summarized in Table 6.2.



a. Slake Index (2)



b. Slake Index (2)

Figure 6.4- Range of jar slake index test results for Zone A Weir Formation: (a) elevation 606.1 ft., slake index (2), (b) elevation 602.6 ft., slake index (2).

Table 6.2-Summary of jar slake index test results for Weir Formation at Waverly site.

Formation	Zone	Elevation (ft)	1440 (min)
Weir	A	606.1	2
Weir	A	602.6	2
Weir	B	597.1	1
Weir	B	590.6	3
Weir	B	587.5	3
Weir	C	581.9	5
Weir	C	578.5	6
Weir	D	571.5	5
Weir	D	565.2	3

Weir Zone B: Zone B was encountered from elevation 584.7 to 600 ft and consisted of (from the base upwards): gray clay shale, gray micaceous siltshale, a gray claystone (underclay), and two separate coal layers. SPT blow counts in Zone B averaged 100 blows in 5.75 inches (14.6 cm). Atterberg limits varied from a LL of 31 with a PI of 12 in the siltshale to a liquid limit of 48 and a PI of 21 in the underclay. Jar slake indices for this material varied from a jar slake index of 1 in the underclay to a jar slake index of 3 in the siltshale as shown in Figure 6.5.



a. Slake Index (1)



b. Slake Index (3)

Figure 6.5- Range of jar slake index test results for Zone B Weir Formation: (a) elevation 597.1 ft., slake index (1), (b) elevation 590.6 ft., slake index (3).

Weir Zone C: Zone C was encountered from elevation 574 to 584.7 ft and consisted of black shale and the Waverly Coal Bed. The Waverly coal was mined in the early part of the twenty century. SPT blow counts in Zone C averaged 100 blows in 4 inches (10.2 cm). Liquid limits varied from 29 to 30 and the PI varied from 4 to 9. Jar slake indices for the black shale varied from a jar slake index of 5 to 6 as shown in Figure 6.6.



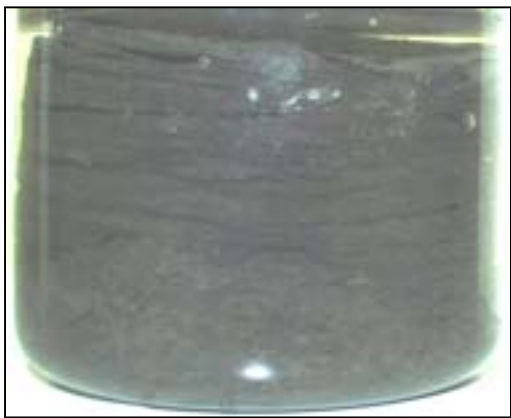
a. Slake Index (5)



b. Slake Index (6)

Figure 6.6- Range of jar slake index test results for Zone C, Weir Formation: (a) elevation 581.9 ft., slake index (5), (b) elevation 578.5 ft., slake index (6).

Weir Zone D: Zone D was encountered from elevation 564 to 574 ft and consisted of black carbonaceous shale. SPT blow counts in Zone D averaged 100 blows in 3 inches (7.6 cm). Liquid limits varied from 30 to 34 and the PI varied from 12 to 15. Jar slake test results for the black shale varied from a jar slake index of 3 to 5 as shown in Figure 6.7.



a. Slake Index (3)



b. Slake Index (5)

Figure 6.7- Range of jar slake index test results for Zone D, Weir Formation: (a) elevation 565.2 ft., slake index (3), (b) elevation 571.5 ft., slake index (5).

Weir Zone E: Zone E was encountered from elevation 555 to 564 ft and consisted of a coarse grained sandstone and fossiliferous limestone. At Pier 11, an unconfined compressive strength of 5,429 kPa (56.7 tsf) was reported for Zone E. RQD values for this stratum varied from 72 to 100 percent.

6.3 Unconfined Compressive Strength of Bedrock at Pier 11

Bedrock samples were taken with a standard split spoon and a NX sized double core barrel. The core was logged with the amount of core recovered and the RQD being noted in the limestone and sandstone layers. The core was returned to Jefferson City to be photographed and for further testing. Unconfined compressive strengths of the rock cores for Pier 11 varied from 1.6 to 120.2 tsf (153.2 to 11,510 kPa) as shown in Table 6.3. Since the unconfined compressive strength data was limited for Zone E, additional data from Pier 10 was used to calculate the average q_u and the standard deviation. Zones A and B had the lowest unconfined compressive strengths of all the shale strata while Zone C had the highest unconfined compressive strengths for the shales. Zone D had intermediate unconfined strengths that were approximately double that of Zones A and B. Zone E, which is composed of sandstone and limestone had the highest overall strengths, far exceeding the strength of the shale strata.

Table 6.3- Unconfined compressive strengths for Pier 11.

Strata	Elev.	Avg q_u		Range	Std. Dev.
Zone	ft.	MPa	tsf	tsf (MPa)	tsf (MPa)
A	600 – 609	0.43	4.5	1.6 (0.15)-7.2 (0.69)	1.5 (0.14)
B	584.7 – 600	0.47	4.9	2.1 (0.20) - 10.2 (0.98)	2.5 (0.26)
C	574 - 584.7	2.36	24.6	9.2 (0.88) – 38.1 (3.65)	15.2 (1.46)
D	564 – 574	0.89	9.3	2.1 (0.20) – 18.8 (1.80)	4.7 (0.45)
E	555 - 564	6.56	68.5	17.7 (1.69) – 120.2 (11.51)	33.4 (3.20)

6.4 Foundation Design

Drilled shafts socketed into bedrock were chosen for the foundations of the piers in the river. Drilled shafts were chosen due to the thickness of the alluvium and the high potential depth of scour. Due to the alternating layers of shale, sandstone, siltstone, coal, and underclay the rock socket design was originally based on side resistance and ignored end bearing. The design load for the shafts at Pier 11 was estimated to be about 1,525 tons (13.6 MN). The allowable side friction, for 6.5 foot (1.98 m) diameter rock sockets was determined following procedures by Horvath and Kenney (1979). Based on these calculations the required socket lengths would be 63 feet (19.2 meters) and would be very costly. It was therefore decided to allow the design consultant to use some end bearing at Pier 11 in addition to side shear.

Due to the questionable nature of the shale bedrock, the importance of the mid-river pier (Pier 11), and the large design load, MoDOT recommended an Osterberg cell load test be performed. Since the cost and time required to complete the Osterberg cell load test during the design stage was prohibitive, it was decided to conduct the test on a production shaft. The test shaft location and Pier 11 are shown in Figure 6.3.

6.5 Construction of Test Shaft

The Osterberg cell load test was to be performed on one of the 6 “production” shafts at Pier 11 in the middle of the river as shown in Figure 6.8. A 26 inch (660 mm) Osterberg cell with a capacity of 1800 tons (16 MN) in each direction was chosen to test the production shaft to twice the design load. The Osterberg cell would be located about 5.6 feet (1.7 m) above the base of the rock socket at the interface between Zones D and E as shown in Figure 6.9.



Figure 6.8- Pier 11 at Waverly site.

The test shaft was constructed by Jensen Construction Co. using a 9270 Series American crane with a Hain twin drill assembly as shown in Figure 6.10. Jensen mobilized and installed a 9 feet (2.74 m) diameter temporary casing almost to the top of rock using a vibratory hammer and casing clamp on September 9, 2002. The contractor began excavating the overburden material on September 11, 2002. After the overburden was removed, 84 inch (2134 mm) permanent casing was seated into the shale bedrock as shown in Figure 6.11. A 48 inch (1220 mm) diameter pilot hole was then excavated to about 10 feet (3m) above the planned tip elevation of the rock socket (elevation 555 ft). A NX size core was drilled at the bottom of the pilot hole in order to evaluate the material below the rock socket. MoDOT requires a NX size foundation test hole to be drilled after excavation of the rock socket for shafts that derive axial capacity in end bearing. Since the contractor drilled a pilot hole, the NX size foundation test hole was allowed to be

completed before the rock socket was completely excavated. The purpose of the pilot holes was to limit the time the side walls of the rock socket were exposed to drilling slurry.

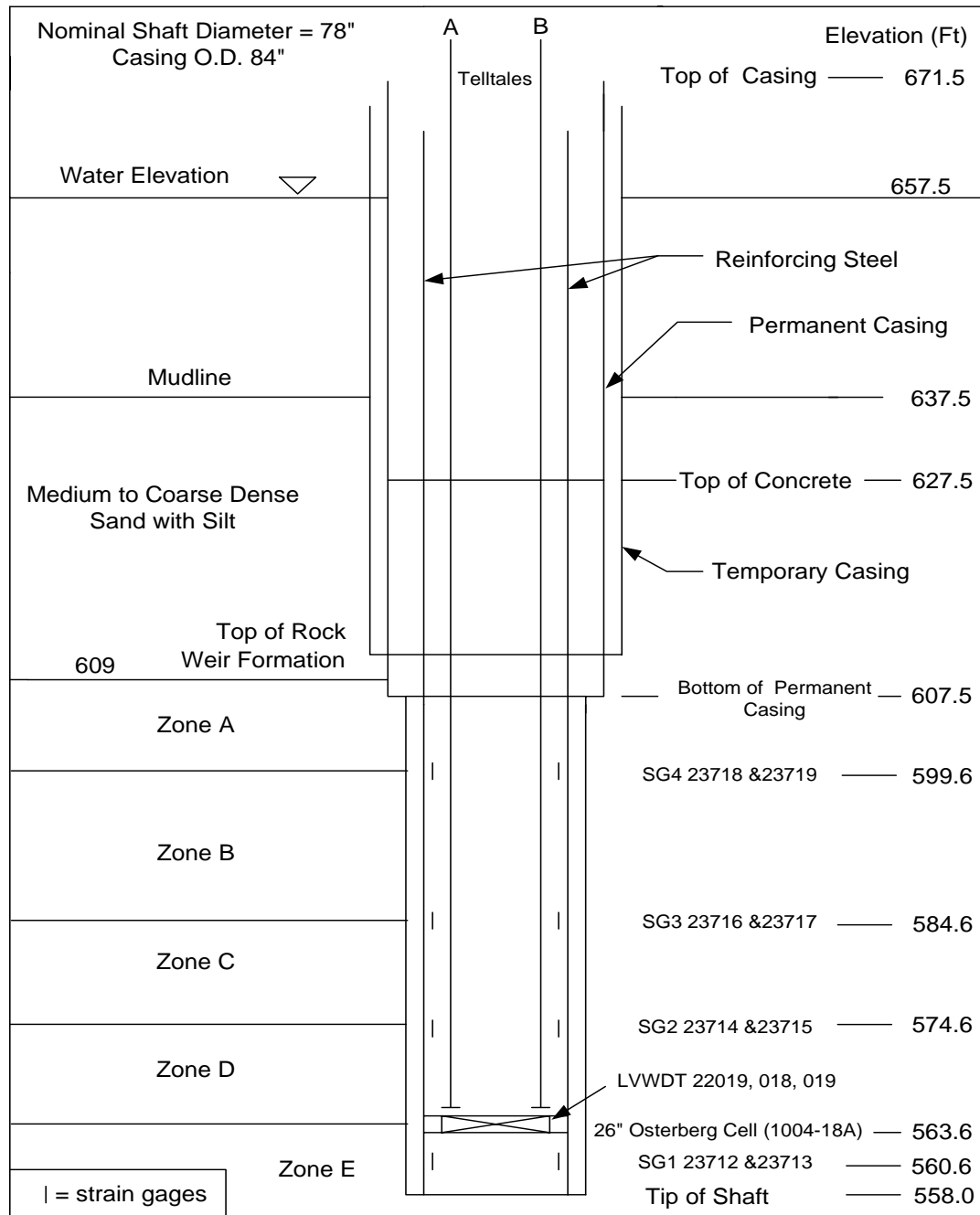


Figure 6.9- Schematic of the test shaft at Pier 11.



Figure 6.10- American 9270 Series crane with a Hain twin drill, drilling rock socket at Pier 12, existing bridge in background.



Figure 6.11- Temporary outer casing, inner permanent casing, and casing clamp at Pier 12 (Pier 11 is in the background).

Prior to drilling the rock socket to full diameter, a polymer slurry was introduced into the hole to help keep the shale from degrading. The polymer slurry, known as Super Mud, was supplied by the Polymer Drilling Systems Company. The rock socket was drilled using a bullet tooth rock auger and a 78 inch (1980 mm) core barrel as shown in Figures 6.12 and 6.13. Excavation of the rock socket began on September 19, 2002 with a 78 inch (1980 mm) bullet tooth rock auger. The excavation advanced to elevation 558 ft., where a hard layer of limestone was encountered. Although the rock socket was about 3 feet (0.9 m) above the planned tip elevation, MoDOT approved the socket. The socket was cleaned with a cleanout bucket and the cleanliness of the rock socket bottom was inspected with an underwater video inspection system shown in Figure 6.14.



Figure 6.12- Bullet tooth rock auger used to excavate rock socket at Waverly test site.



Figure 6.13- Core Barrel used to excavate rock socket at Waverly test site.



Figure 6.14- Miniature shaft inspection device (Mini-SID) used to inspect bottom of rock sockets at Waverly bridge site.

The rebar cage with the Osterberg load cell shown in Figure 6.15 was placed in the socket and an attempt was made to place the concrete in the socket on the September 20, 2002. Due to clogging of the 8 inch (203mm) tremie the concrete pour could not be completed. The rebar cage and about 20 cubic yards (15 cubic meters) of fluid concrete was removed, and the socket was cleaned. Holes in the top and bottom plate adjacent to the O-cell™ were enlarged to allow a larger 12 inch (305 mm) tremie to be used with the approval of Loadtest. The shaft was then completed on the September 21, 2002 still within the required 72-hour time limit.



Figure 6.15- Rebar cage with Osterberg load cell.

The slump of the concrete was about 1 inch (25 mm) when it arrived on the job. Plastizer “Super P” was added to the concrete and the slump was about 7.5 to 8 inches (195 mm) when it was poured into the shaft. Test cylinders made of the shaft concrete were tested to a compressive strength of 7520 psi (51.8 MPa) on the day of the Osterberg cell load test. Loadtest personnel arrived on the site and completed the load test on September 30, 2002.

6.6 Load Test Setup and Procedures

The load test for the production shaft was performed by Loadtest Inc. on September 30, 2002. A schematic of the test shaft with associated instruments is shown in Figure 6.16; a summary of shaft dimensions is given in Table C.1 in Appendix C. The 26 inch (660 mm) diameter O-CellTM, with its base located 5.6 feet (1.7 m) above the tip of the rock socket, was pressurized to assess the combined end bearing and side shear below the O-CellTM and side shear above the cell. The O-CellTM was pressurized in 23 even increments of 600 psi (4,137 kPa) to a maximum O-CellTM pressure of 13,800 psi (95,147 MPa), which corresponds to a load of 2525 tons (22.5 MN) in each direction. At this load, the capacity of the Osterberg cell had been exceeded by more than 40 percent and more than twice the design load had been achieved. The O-CellTM was then unloaded in 4 equal increments and the test was concluded. The applied load increments followed procedures in ASTM D1143- Standard Test Method for Piles Under Static Axial Compressive Load.

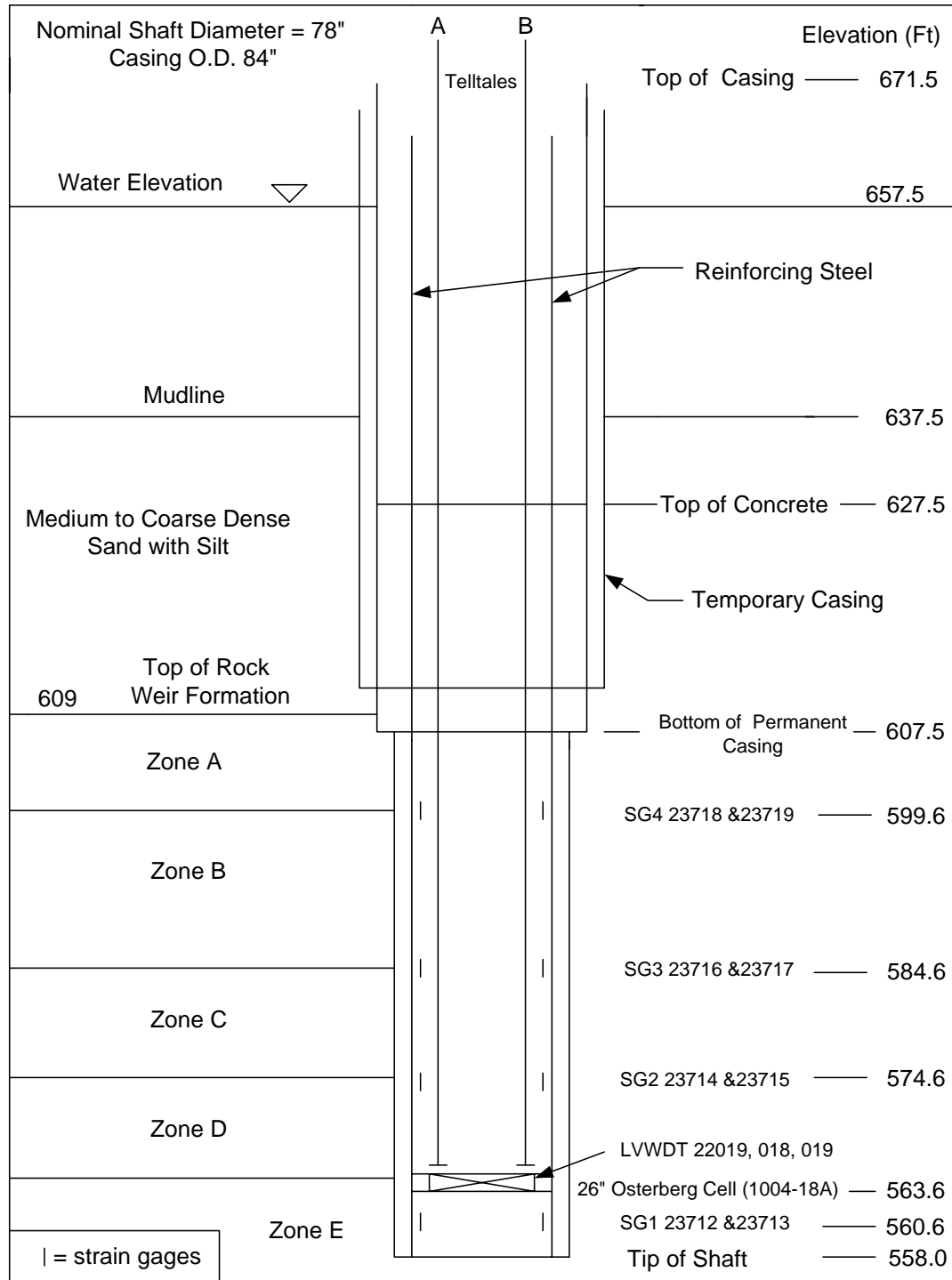


Figure 6.16- Schematic of test shaft showing location of instrumentation.

Expansion of the O-CellTM was measured by three LVWDTs (Geokon Model 4450 Series) positioned between the lower and upper plates of the O-CellTM. Telltales were inserted in pre-installed steel pipes from the upper plate of the O-CellTM to the top of shaft. Two LVWDTs (Geokon 4450 Series) attached to the telltales were used to measure compression of the shaft between the O-CellTM and the top of the shaft. Two additional LVWDTs (Geokon 4450 Series) were attached to the reference beam to measure top of shaft movement.

Strain gages were used to assess load transfer in the shaft above and below the O-CellTM. Four levels of sister bar vibrating wire strain gages, with two sister bars at each level, were installed in the shaft at the location of changes in strata as shown in Figure 6.16.

6.7 General Test Results

The results of the Osterberg cell load test at the Waverly site are presented in this section. Detailed load test data is provided in Appendix C. The measured load-displacement response for the load test on the test shaft is shown in Figure 6.17. The maximum gross load applied to the base of the shaft was equal to 2525 tons (22.5 MN) and occurred at load interval 1L-23. At this point, the O-CellTM had expanded 0.122 inches (3.10 mm) with 0.043 inches (1.10 mm) of upward movement and 0.078 inches (1.99 mm) of downward movement. The maximum net load applied to the upper portion of the shaft was equal to 2525 tons (22.5 MN) minus the buoyant weight of the shaft 115.3 tons (1.03 MN), for a net applied load of 2410 tons (21.4 MN).

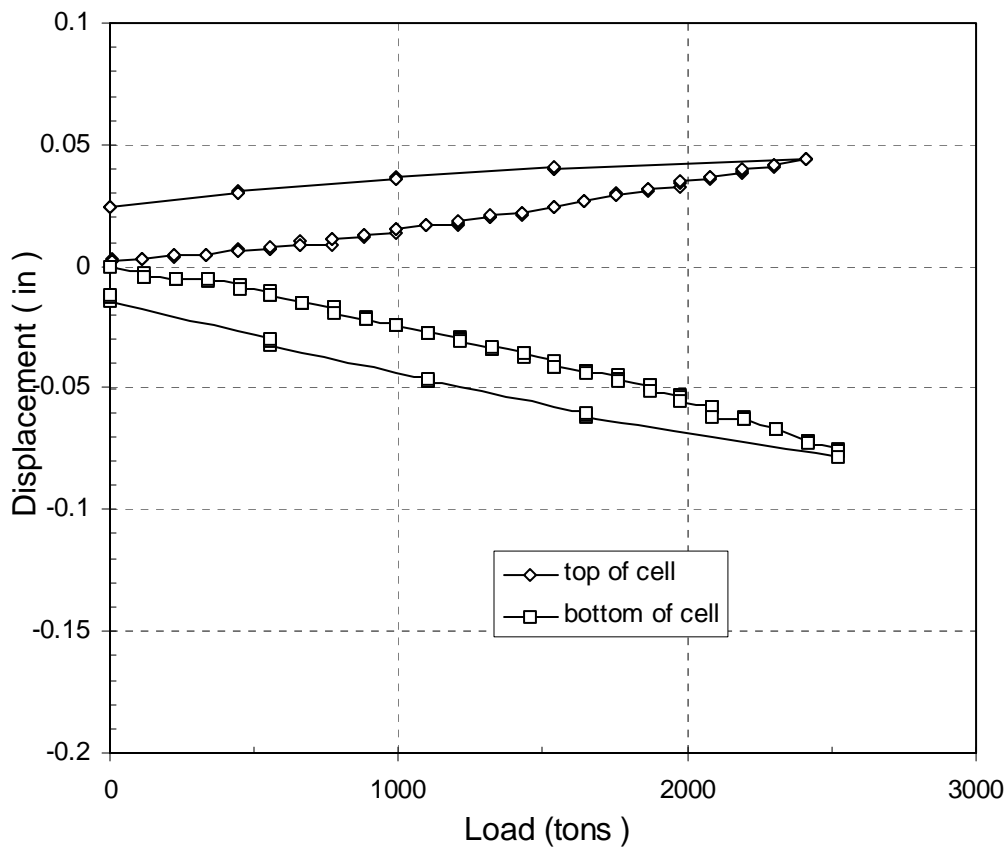


Figure 6.17- Measured load-displacement curves for test shaft at Waverly site.

Equivalent top-down load-displacement curves for the Waverly test shaft are shown in Figure 6.18. The “measured” equivalent top-down load-displacement curve indicates a settlement of approximately 0.078 inches (1.99 mm) at the maximum load of 4935 tons (43.9 MN). When adjusted for additional elastic compression that would occur in a top-down load test, a shaft loaded from the top with a load of 4,935 tons (43.9 MN) would settle about 0.26 inches (6.6 mm) of which 0.18 inches (4.6 mm) is estimated elastic compression. The equivalent top-down load-displacement curves are essentially linear over the range of loads shown, which indicates that the shaft had additional capacity beyond the load applied in the load test.

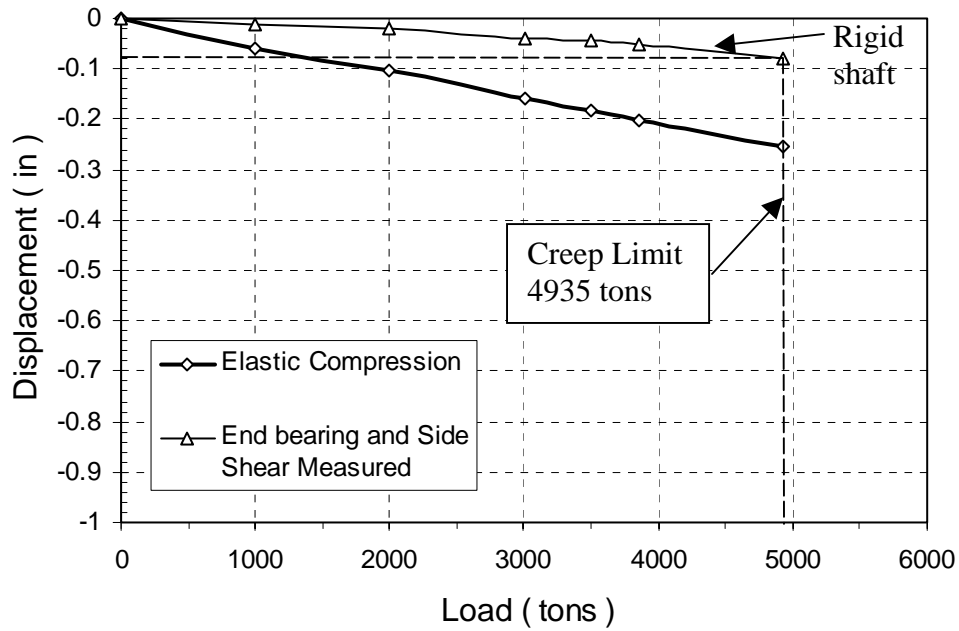


Figure 6.18- Equivalent top-down load-displacement curves for Waverly test shaft.

The distribution of axial force with elevation at various load increments was generated from strain gage data, the equivalent modulus of the shaft, and the cross-sectional area of the shaft as described in Chapter 3 (Eq. 3.7). The distribution of axial force determined for several load increments is shown in Figure 6.19. The strain gage data used to compute the distribution of axial force is provided in Appendix C. On the day of the test, the concrete compressive strength was 7520 psi (51.8 MPa). This, combined with the area of the reinforcing steel and nominal shaft diameters of 84 inches (2134 mm) above the bottom of the permanent casing and 78 inches (1981 mm) below, was used to determine an average shaft stiffness (AE) of 31,800,000 kips (141,500 MN) above the bottom of the casing and 24,900,000 kips (110,700 MN) below. The shaft stiffness along with strain gage data was used to calculate the axial force at various

elevations. The point of zero shear in Zone A (Elevation 606.5 ft) was estimated by projecting the unit side shear transferred in Zone B to that transferred in the shaft along Zone A.

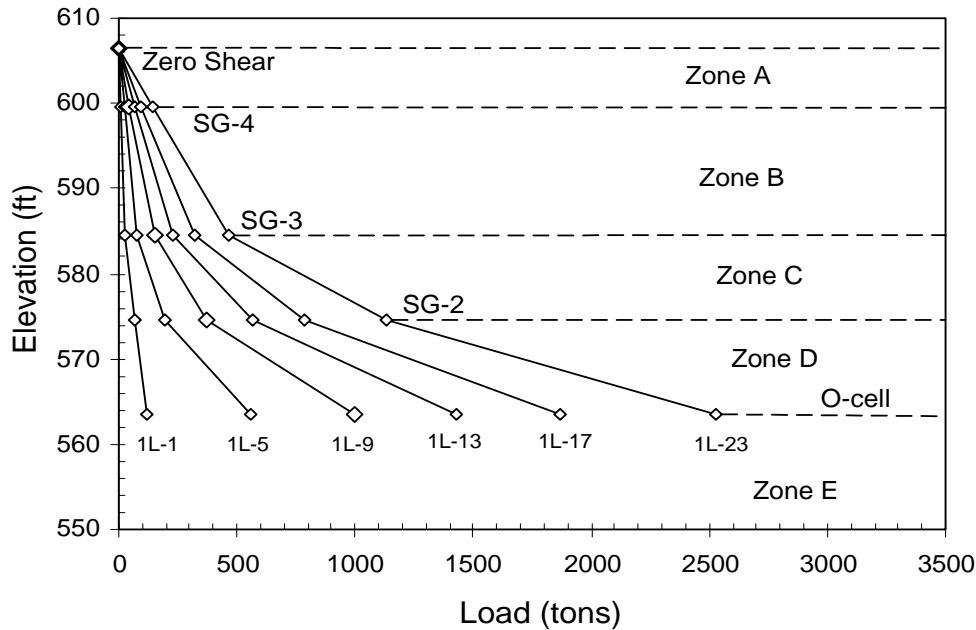


Figure 6.19- Distribution of axial force for the Waverly test shaft.

The mobilized unit side shear for each load increment is plotted versus O-cellTM displacement in Figure 6.20. The unit side shear curves indicate that side shear had not been fully mobilized in any of the shaft segments above the O-cellTM. The unit side shear below the O-cellTM in Zone E could not be determined due to problems with the level-1 strain gages.

Values of the average mobilized unit side shear determined for various segments of the shaft are shown in Table 6.4 and plotted in Figure 6.21. These values were calculated for the peak load, which occurred at load interval 1L-23. The unit side shear mobilized in Zones C and D was significantly greater than that mobilized in Zones A and B.

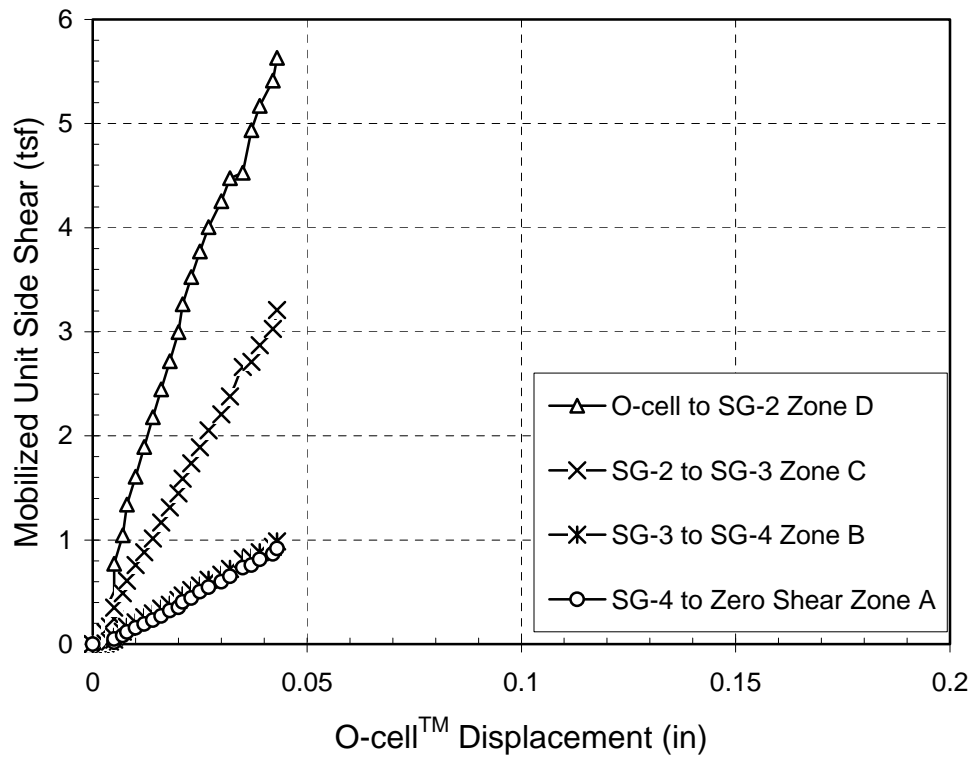


Figure 6.20- Mobilized unit side shear versus O-cell™ displacement for Waverly test shaft.

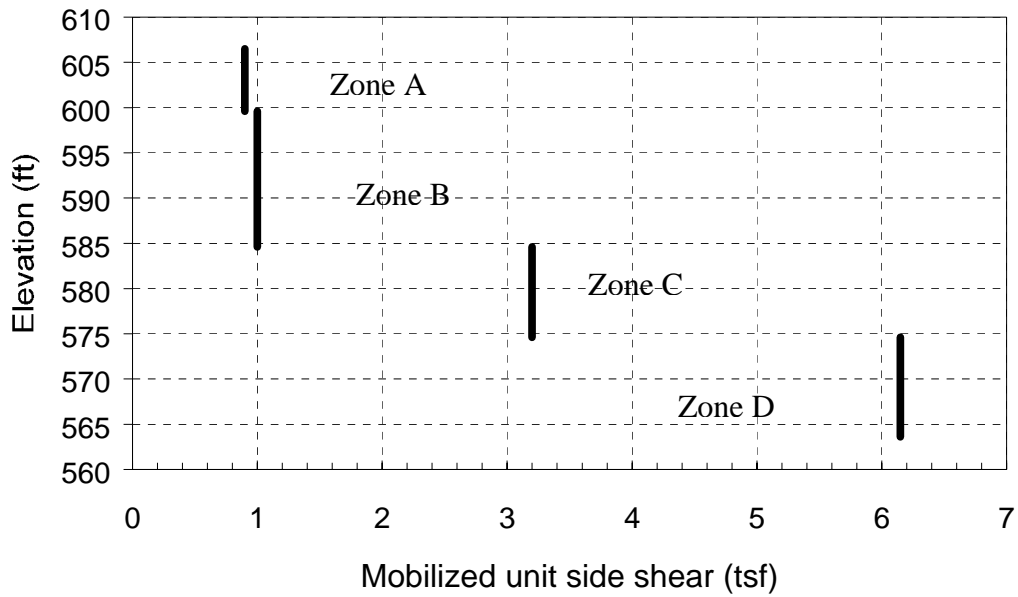


Figure 6.21- Mobilized unit side shear values calculated from strain gage data for the Waverly test shaft.

Table 6.4- Mobilized unit side values calculated from strain gage data for the Waverly test shaft.

Load Transfer Zone	Zone	Elevation (ft)	Unit Side Shear	
			kPa	tsf
0 shear to SG-4	A	606.5 - 599.6	88	0.9
SG-4 to SG-3	B	599.6 - 584.6	94	1.0
SG-3 to SG-2	C	584.6 - 574.6	306	3.2
SG-2 to O-Cell TM	D	574.6 - 563.6	587	6.15

Level-1 strain gages did not produce reliable data.

Figures 6.22 and 6.23 show creep displacements that occurred over the time interval 2 to 4 minutes after application of the load while the load was maintained constant. As shown in the figures, no creep limit was reached for either the upper or lower portions of the shaft. These data indicate that significant creep would not occur for a top loaded shaft until a load greater than 43.9 MN (4935 tons) is exceeded by some unknown amount.

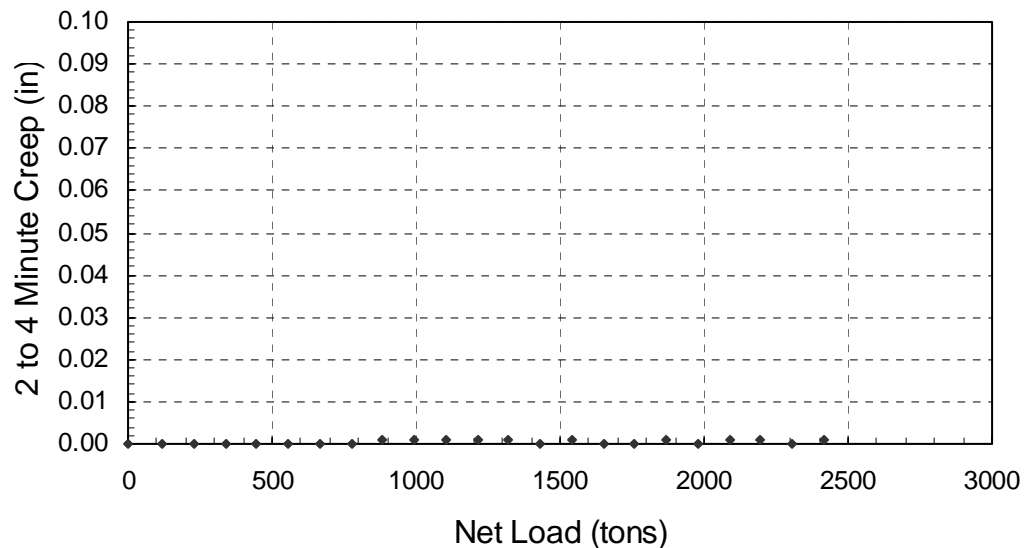


Figure 6.22- Creep displacements for the upper portion of the Waverly test shaft.

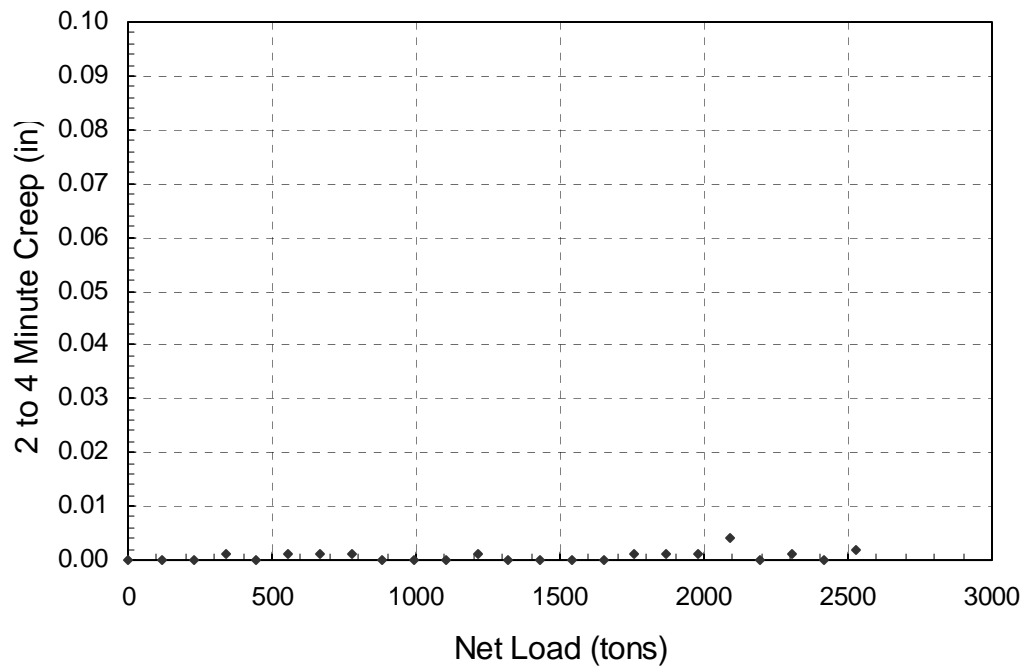


Figure 6.23- Creep displacements for the lower portion of the Waverly test shaft.

6.8 Practical Applications

Some thought was given to specifying a 34 inch (870mm) Osterberg load cell with a capacity of 3,000 tons (27 MN) and trying to achieve twice the design load (1524 tons (13.6 MN) above the Osterberg load cell. This would allow 10 feet (3.3 m) of rock socket on the remaining 5 shafts at Pier 11 to be eliminated. This would save about \$80,000 in drilled shaft cost. This was offset by the additional cost of a 34 inch (870mm) cell (\$40,000) and possible additional contract costs. As it was about 3 feet (0.9 m) of socket was eliminated on all 6 shafts and \$29,700 was saved to offset the \$70,000 cost for the original Osterberg cell load testing. The cost for the Osterberg cell load test at the Waverly site was significantly lower than the costs at either the Lexington site or the Grandview site. This is because the test was performed during the construction phase on

a production shaft. There were therefore no costs for construction of the shaft or mobilization. However, very little cost benefit can be realized during the construction phase.

6.9 Summary and Conclusions

The Missouri DOT proposed to build a new bridge across the Missouri River in the vicinity of Waverly Missouri. The foundation design for the piers in the vicinity of the river would consist of drilled shafts socketed into bedrock. The bedrock at this location consisted of alternating layers of clay shale, siltstone, coal, and underclay with scattered layers of limestone and sandstone. Since the shales could not support large axial loads in end bearing, it was decided to design the rock sockets based on side shear only. Current design methods used by MoDOT would require exceedingly long rock sockets that would be very expensive. Due to the questionable nature of the bedrock at Pier 11 and the desire to use some end bearing it was decided to test a rock socketed drilled shaft using an Osterberg cell load test. The Osterberg cell load test was performed on a production shaft for Pier 11 in September 2002. The shaft was constructed following lessons learned at the Lexington test site: the rock socket was excavated and concrete placed within 72 hours and polymer slurry was used to reduce the degradation or softening of the rock socket walls.

A general geologic description of the Waverly test site was presented in this chapter followed by a summary of the engineering characteristics of the most pertinent strata. The construction and testing procedures for the shaft were described, followed by presentation of the results from the load test.

The Osterberg cell load test was successful in testing the shaft to twice the design load and assuring the foundation engineers that the main pier in the river would be safe. However, the test did not fully indicate the capacity of the rock socket in either side shear or end bearing.

CHAPTER SEVEN EVALUATION OF DESIGN METHODS

7.1 Introduction

The current procedures used by the Missouri Department of Transportation (MoDOT) to estimate the ultimate unit side shear in shales roughly predict the ultimate unit side shear to be equal to 0.15 times the average unconfined compressive strength (q_u) of the shale. In order to achieve more economical designs and to take some of the uncertainty out of the prediction of the ultimate unit side shear, MoDOT has conducted four Osterberg cell load tests at three bridge sites. Details of the load test(s) at each site were described in Chapters 4, 5, and 6. In this chapter, the results of analyses performed to evaluate the suitability of several methods for predicting the ultimate unit side shear based on these tests are presented.

Because the load tests were originally performed and analyzed using different units, all results are presented in English units in this chapter. Rather than simultaneously presenting results in dual units, the tables and figures presented in this chapter are provided in Appendix D using SI units.

7.2 Summary of Test Results

A summary of the average unconfined compressive strengths for all strata at the three sites is presented in Table 7.1 along with the maximum measured unit side shear values determined for each strata from the load tests. Measured unit side shear values for all three sites ranged from 0.9 to 17.3 tsf (88 to 1653 kPa) for the shale strata. Measured unit side shear values reported for several of these strata do not represent ultimate values since side shear was not fully mobilized in some portions of the shafts. These values

therefore represent lower-bounds of the ultimate unit side shear that can be achieved in these strata as indicated in the table. In strata where the ultimate side shear was fully mobilized, unit side shear values ranged from 3.1 to 10.7 tsf (295 to 1020 kPa).

Table 7.1- Summary of measured unit side shear values and average unconfined compressive strength (q_u) values of shale at test sites.

Formation	Elevation of Strata	Shaft Section used to calc unit side shear	Elevation of Shaft Segment	q_u		Measured Unit side shear, $f_s^{(1)}$
				Avg.	Std. Dev.	
	(ft)		(ft)	(tsf)	(tsf)	(tsf)
		Lexington				
Bevier (C1)	591.9–613.5	TS-2 upper cell to TOS	591.1 - 605	39.8	23.1	10.7
Bevier (C1)	591.9–613.5	TS-2 SG-3 to SG-4	596.1–599.3	39.8	23.1	>7.3 ⁽²⁾
Bevier (C1)	591.9–613.5	TS-2 upper cell to SG-3	591.1–596.1	39.8	23.1	>17.3
Bevier (C2)	578.8–591.9	TS-2, stage 1, lower cell to SG-2	578 – 586.2	31.3	26.8	9.2
Verdigris (D)	569.3–578.8	TS-1A, SG-4 to TOS	572.5–577.2	12.7	13.0	>4.1
Verdigris (D)	569.3–578.8	TS-1A, SG-3 to SG-4	567.6–572.5	12.7	13.0	>10.1
Croweburg (E)	554.5–569.3	TS-1A, O-cell to SG-2	559.4–564.4	17.9	16.2	7.6
Croweburg (E)	554.5–569.3	TS-1A, SG-1 to O-cell	556.5–559.4	17.9	16.2	10.1
		Grandview				
W. Chanute	927.2- 934	SG-6 to TOS	927 – 934	9.8	2.3	>3.1
Chanute	916.5–927.2	SG-5 to SG-6	921 - 927	7.2	3.5	3.1
Chanute	916.5–927.2	SG-4 to SG-5	916.5 – 921	7.2	3.5	4.8
Cement City	911.3– 916.5	SG-3 to SG-4	911.5–916.5	386.6	179.8	>17.2
Quivira	904.8– 911.3	O-cell to SG-3	905 – 911.5	14.9	3.0	4.8 ⁽³⁾
Westerville	898.1– 904.8	SG-1 to O-cell	898 - 905	657.1	311.9	>24.0
Wea	< 898.1	Tip to SG-1	893.4 – 898	24.1	8.7	5.9
		Waverly				
Weir (A)	600 – 609	SG-4 to O shear	599.6–606.5	4.5	1.5	>0.9
Weir (B)	584.7 – 600	SG-3 to SG-4	584.6–599.6	4.9	2.5	>1.0
Weir (C)	574 – 584.7	SG-2 to SG-3	574.6–584.6	24.6	15.2	>3.2
Weir (D)	564 – 574	O-cell to SG-2	563.6–574.6	9.3	4.7	>6.15
Weir (E)	555 - 564			68.5	33.4	

(1) Values reported are ultimate values unless otherwise indicated.

(2) The symbol ">" indicates that the ultimate unit side shear was not reached during test, value reported is maximum value during test.

(3) Assumed ultimate unit side shear.

Figure 7.1 shows the measured unit side shear values plotted as a function of the average unconfined compressive strength for the respective strata. In the figure, closed symbols are used to represent data where the ultimate unit side shear was fully mobilized while open symbols are used to represent data where the ultimate unit side shear was not fully mobilized. Also shown are lines representing unit side shear values equal to $0.15 q_u$ (roughly equivalent to MoDOT's current design procedure) and $0.30 q_u$. As shown in the figure, the line for $f_s = 0.15 q_u$ is well below the ultimate unit side shear values determined from all of the load tests. The line representing $f_s = 0.30$ is a better fit but tends to under predict f_s for values of q_u less than 20 tsf and slightly over predict f_s for values of q_u greater than 20 tsf.

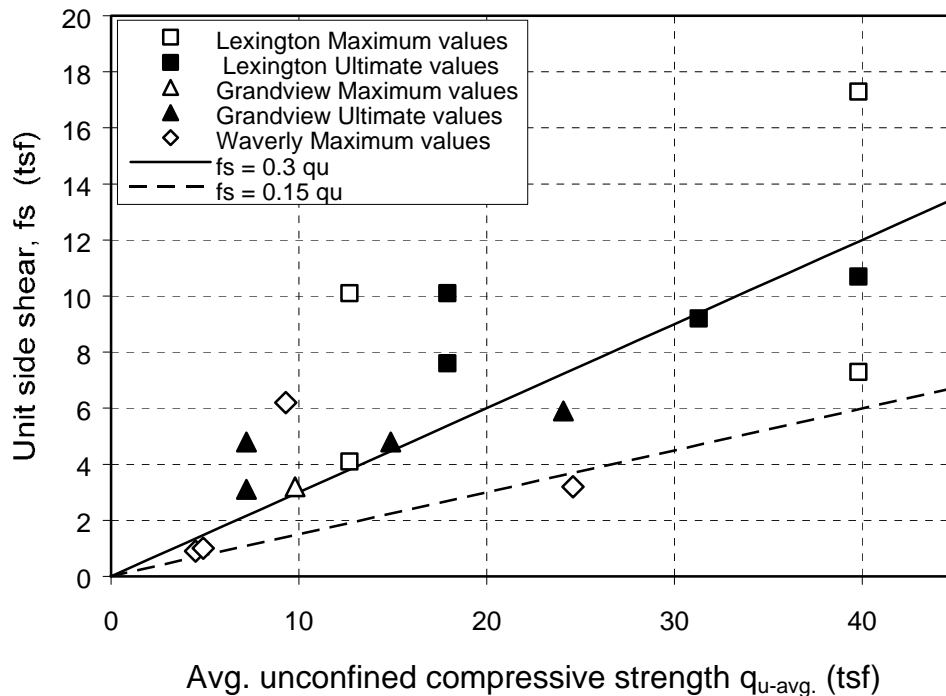


Figure 7.1- Unit side shear versus average q_u .

7.3 Interpreted Alpha Factors

The simplest method for interpreting and designing for side shear in drilled shafts is to represent the capacity as

$$f_s = \alpha \cdot q_u \quad (7.1)$$

where α is an empirical proportionality factor to account for load transfer in the shaft. It is important to note that α , as used in Equation 7.1, is defined with respect to the unconfined compressive strength, q_u . This is a source of some confusion given that α is also frequently used as the proportionality factor relating unit side shear to the undrained shear strength ($q_u/2$) in clay soils. The two values are not the same. However, previous investigators (e.g. O'Neill et al. 1996) have used α for weak rock (“intermediate geomaterials”) in a similar manner so this convention has also been used here.

Rearranging Equation 7.1, back-calculated α values can be computed by dividing the measured values of unit side shear by the unconfined compressive strength of the stratum. Alpha (α) values computed in this manner using average values of q_u for each stratum are summarized in Table 7.2 and plotted versus average values of q_u in Figure 7.2. In the figure, back-calculated α values for the shale ranged from 0.13 to 0.80 for all the sites.

For sites where the ultimate unit side shear was mobilized in the shale, α ranged from 0.24 to 0.67. Osterberg (1992) has reported that previous O-cellTM tests in weak rock have produced values of unit side shear as high as 0.3 to 0.5 times q_u . Data from

Williams et al. (1980) show values of α as high as 1.0 or larger (Figure 2.2). Alpha (α)

values greater than 0.5 indicate that the unit side shear is greater than the undrained shear strength of the shale ($q_u/2$). The values reported for α greater than 0.5 are believed to be primarily due to variability in the unconfined compressive strength as considered in more detail below. The high α values may also be attributed to the roughness of the sockets resulting from the use of a rock auger to excavate shafts in shale. In rough sockets, the interface between the shaft and concrete may tend to dilate when loaded, thereby increasing the available shear resistance above the undrained shear strength in soil or rock with $\phi > 0$.

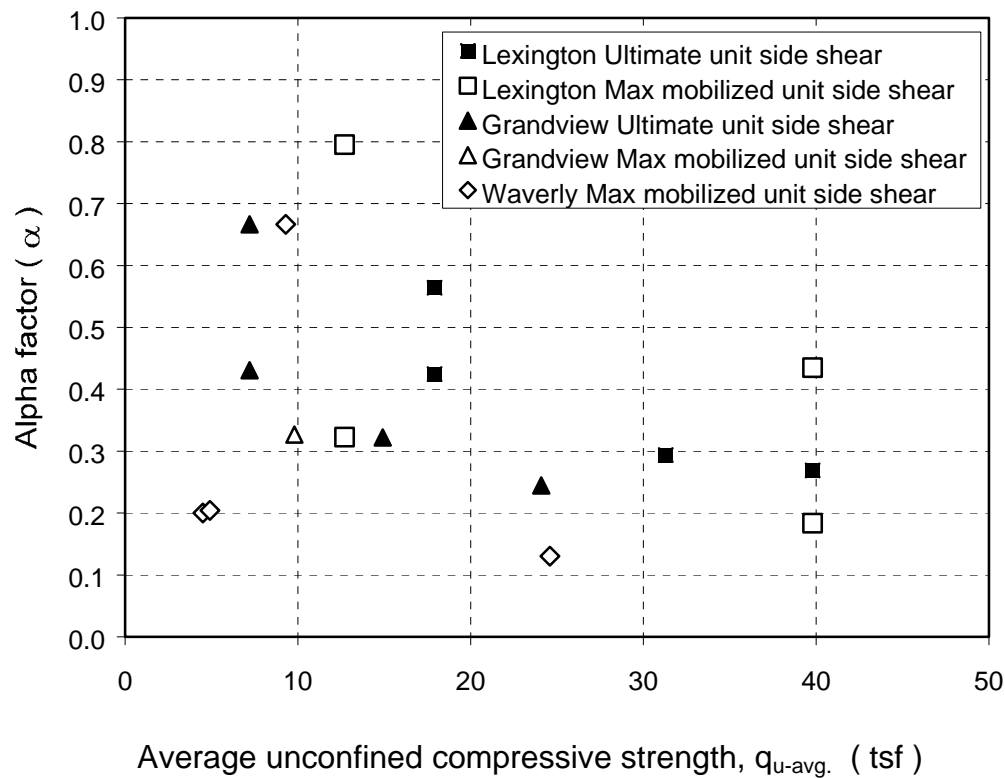


Figure 7.2- Back-calculated alpha factor (α) versus average q_u for test sites in shale.

Table 7.2- Summary of back-calculated alpha values for shale at Missouri test sites.

Formation	Shaft Section used to calc unit side shear	Elevation of shaft Segment	Qu,		Meas unit side shear, $f_s^{(1)}$	α		
			Avg.	Std. Dev.		Avg.	+ 1 Std. Dev.	- 1 Std. Dev.
		(ft)	(tsf)	(tsf)	(tsf)			
	Lexington							
Bevier (C1)	TS-2 upper cell to TOS	591.1-605	39.8	23.1	10.7	0.27	0.17	0.64
Bevier (C1)	TS-2 SG-3 to SG-4	596.1-599.3	39.8	23.1	>7.3 ⁽²⁾	0.18	0.12	0.44
Bevier (C1)	TS-2 upper cell to SG-3	591.1-596.1	39.8	23.1	>17.3	0.43	0.28	1.04
Bevier (C2)	TS-2, stage 1, lower cell to SG-2	578 – 586.2	31.3	26.8	9.2	0.29	0.16	2.04
Verdigris (D)	TS-1A, SG-4 to TOS	572.5- 77.2	12.7	13.0	>4.1	0.32	0.16	-13.7
Verdigris (D)	TS-1A, SG-3 to SG-4	567.6-572.5	12.7	13.0	>10.1	0.80	0.39	-33.7
Croweburg (E)	TS-1A, O-cell to SG-2	559.4-564.4	17.9	16.2	7.6	0.42	0.22	4.47
Croweburg (E)	TS-1A, SG-1 to O-cell	556.5-559.4	17.9	16.2	10.1	0.56	0.30	5.94
	Grandview							
W. Chanute	SG-6 to TOS	927 – 934	9.8	2.3	>3.2	0.33	0.26	0.43
Chanute	SG-5 to SG-6	921 - 927	7.2	3.5	3.1	0.43	0.29	0.84
Chanute	SG-4 to SG-5	916.5 – 921	7.2	3.5	4.8	0.67	0.45	1.30
Cement City	SG-3 to SG-4	911.5-916.5	386.6	179.8	>17.2			
Quivira	O-cell to SG-3	905 – 911.5	14.9	3.0	4.8 ⁽³⁾	0.32	0.27	0.40
Westerville	SG-1 to O-cell	898 – 905	657.1	311.9	>24.0			
Wea	Tip to SG-1	893.4 – 898	24.1	8.7	5.9	0.24	0.18	0.38
	Waverly							
Weir (A)	SG-4 to O shear	599.6-606.5	4.5	1.5	>0.9	0.20	0.15	0.30
Weir (B)	SG-3 to SG-4	584.6-599.6	4.9	2.5	>1.0	0.20	0.14	0.42
Weir (C)	SG-2 to SG-3	574.6-584.6	24.6	15.2	>3.2	0.13	0.08	0.34
Weir (D)	O-cell to SG-2	563.6-574.6	9.3	4.7	>6.15	0.67	0.44	1.35
Weir (E)			68.5	33.4				

(1) Values reported are ultimate values unless otherwise indicated.

(2) The symbol “>” indicates that the ultimate unit side shear was not reached during test, value reported is maximum value during test.

(3) Assumed ultimate unit side shear.

Because there is variability in the value of q_u for each stratum, α -values were also calculated for q_u equal to the mean value of q_u plus one standard deviation and the mean value minus one standard deviation. Alpha values, calculated for the higher and lower q_u -values are plotted in Figure 7.3. Back calculated α values from the higher q_u -values ranged from 0.08 to 0.45 for all the sites. For sites where the ultimate unit side shear was mobilized, back calculated α ranged from 0.16 to 0.45. Back calculated α - values for the lower q_u -values ranged from 0.30 to as high as 5.94 for the Croweburg Formation at the Lexington site. Negative values were also noted for the Verdigris Formation. The high α values in the Croweburg Formation and the negative values in the Verdigris Formation may be attributed to very large standard deviations for the unconfined compressive strength of these strata, which are caused by the large ranges in unconfined compressive strengths. For the Croweburg Formation, the unconfined compressive strength ranged from 2.6 to 58.4 tsf (253 to 5,590 kPa) and for the Verdigris Formation q_u ranged from 2.3 to 46.8 tsf (218 to 4,482 kPa).

7.4 Evaluation of Design Methods

As shown in Figure 7.1, the relationship between the unit side shear and the unconfined compressive strength is nearer to a power function than a linear relationship. Measured values of unit side shear were compared to predicted unit side shear values using several common design methods. The predicted unit side shear values were calculated using the following methods:

- Horvath and Kenney, 1979 (Eq. 2.5)
- Rowe and Armitage, 1987 (Eq. 2.9)
- Reese and O'Neill, 1988 (Eq. 2.5, 2.11, and 2.12)
- Kulhawy and Phoon, 1993 (Eq. 2.13)
- O'Neill and Reese, 1999 (Eq. 2.17 and 2.18)

where $\alpha = 0.25$ was used in the prediction of unit side shear for the method developed

by Horvath and Kenney and $\alpha = 0.45$ was used with Rowe and the Armitage method.

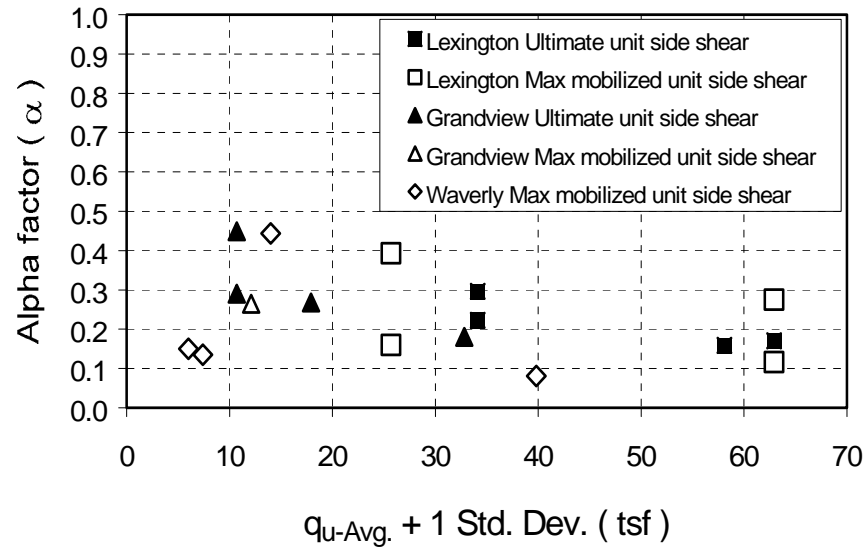
The unit side shear for the method proposed by Reese and O'Neill (1988) was calculated using $\alpha = 0.21$. A mean value of $\psi = 2$ was used with the Kulhawy and Phoon method.

For each method, the ultimate unit side shear was calculated using SI units and converted to English units. Comparisons of predicted versus measured unit side shear values are presented in Table 7.3 and Figure 7.4 for each of these methods.

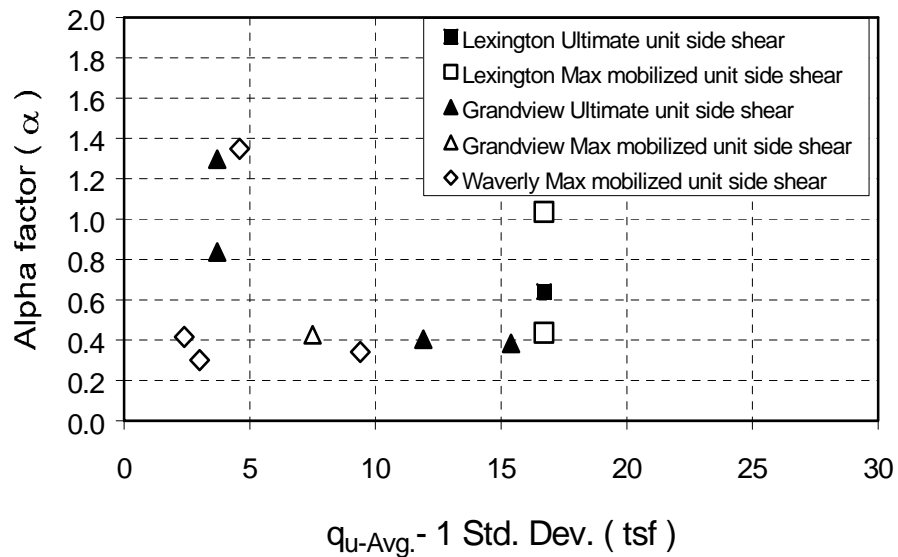
As shown in Figure 7.4, Rowe and Armitage (1987) and Kulhawy and Phoon (1993) produced almost identical results and best fit the measured data where the unit side shear was fully mobilized. Horvath and Kenney (1979) and Reese and O'Neill (1988) produced similar predictions, but both methods significantly underestimated the measured unit side shear observed in the load tests. O'Neill and Reese (1999) tended to be even more conservative than either Horvath and Kenney or Reese and O'Neill (1988) when the simplified method for smooth sockets was used. However, the method proposed by O'Neill and Reese (1999) is not intended for use when the slump of the concrete is less than 7 inches (175 mm) as was the case for the Lexington test shaft. Predicted values obtained for the Lexington test shafts where the slump of the concrete was about 4 inches (102 mm) were extrapolated using Equation 7.2 and Figure 7.5:

$$\sigma_n = M \gamma_c Z_i \quad (7.2)$$

where M is a factor to account for the slump of the concrete, γ_c is the unit weight of concrete in kN/m^3 , and Z_i is the depth to middle of layer in meters with a maximum depth of 40 feet (12 m).



a. $q_{u-avg.}$ plus one standard deviation.



b. $q_{u-avg.}$ minus one standard deviation.

Figure 7.3- Back-calculated alpha (α) versus q_u : (a) $q_{u-avg.}$ plus one standard deviation, (b) $q_{u-avg.}$ minus one standard deviation.

Table 7.3- Comparison of measured and predicted unit side shear determined by various methods.

Formation	Shaft Segment	Elevation of Shaft Segment	q_u Avg.	Meas. unit side shear, $f_s^{(1)}$	Predicted ultimate unit side shear				
					Horvath & Kenney (1979) $\alpha = 0.25$	Rowe & Armitage (1987) $\alpha = 0.45$	Reese & O'Neill (1988) $\alpha = 0.21$	Kulhawy & Phoon (1993) $\psi = 2$	O'Neill & Reese (1999) (4)
		(ft)	(tsf)	(tsf)	(tsf)	(tsf)	(tsf)	(tsf)	(tsf)
	Lexington								
Bevier C1	TS-2, upper cell to TOS	591.1 - 605	39.8	10.7	5.1	9.2	4.3	9.2	2.0
Bevier C1	TS-2, SG-3 to SG-4	596.1 - 599.3	39.8	>7.3 ⁽²⁾	5.1	9.2	4.3	9.2	2.4
Bevier C1	TS-2, upper cell to SG-3	591.1 - 596.1	39.8	>17.3	5.1	9.2	4.3	9.2	2.4
Bevier C2	TS-2, stage 1, lower cell to SG-2	578 - 586.2	31.3	9.2	4.5	8.1	3.8	8.1	2.8
Verdigris (D)	TS-1A SG-4 to TOS	572.5 - 577.1	12.7	>4.1	2.9	5.2	3.5	5.2	1.8
Verdigris (D)	TS-1A SG-3 to SG-4	567.6 - 572.5	12.7	>10.1	2.9	5.2	3.5	5.2	1.8
Crowebug (E)	TS-1A O-cell to SG-2	559.4 - 564.4	17.9	7.6	3.4	6.2	4.9	6.1	2.5
Crowebug (E)	TS-1A SG-1 to O-cell	556.5 - 559.4	17.9	10.1	3.4	6.2	4.9	6.1	2.5
	Grandview								
W. Chanute	SG-6 to TOS	927 - 934	9.8	>3.2	2.5	4.6	2.7	4.6	0.6
Chanute	SG-5 to SG-6	921 - 927	7.2	3.1	2.5	3.9	2.0	3.9	0.6
Chanute	SG-4 to SG-5	916.5 - 921	7.2	4.8	2.2	3.9	2.0	3.9	0.7
Cement City	SG-3 to SG-4	911.5 - 916.5	386.6						
Quivira	O-cell to SG-3	905 - 911.5	14.9	4.8 ⁽³⁾	3.1	5.6	4.0	5.6	2.0
Westerville	SG-1 to O-cell	898 - 905	657.1						
Wea	Tip to SG-1	893.4 - 898	24.1	5.9	4.0	7.1	3.3	7.1	3.4
	Waverly								
Weir (A)	SG-4 to O shear	599.6 - 606.5	4.5	>0.9	1.8	3.2	1.3	3.2	1.2
Weir (B)	SG-3 to SG-4	584.6 - 599.6	4.9	>1.0	1.8	3.2	1.3	3.2	1.5
Weir (C)	SG-2 to SG3	574.6 - 584.6	24.6	>3.2	4.0	7.2	3.4	7.2	3.4
Weir (D)	O-cell to SG-2	563.6 - 574.6	9.3	>6.2	2.5	4.4	1.4	4.4	2.0
Weir (E)			68.5						

(1) Values reported are ultimate (2) The symbol ">" indicates that the ultimate unit side shear was not reached during test, value reported is maximum value during test. (3) Assumed unit side shear slump less than 175 mm (7 in) values unless otherwise indicated. (4) Method not intended for

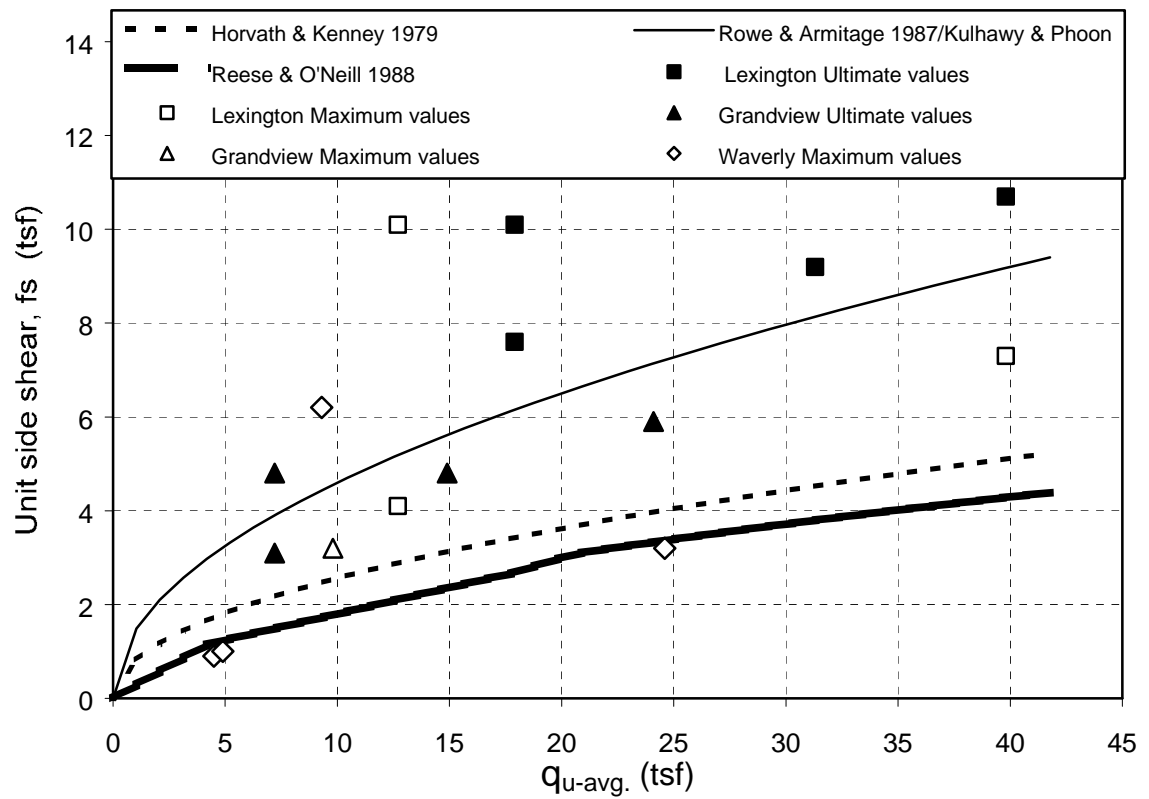


Figure 7.4- Comparison of measured unit side shear data to predicted unit side shear by several methods.

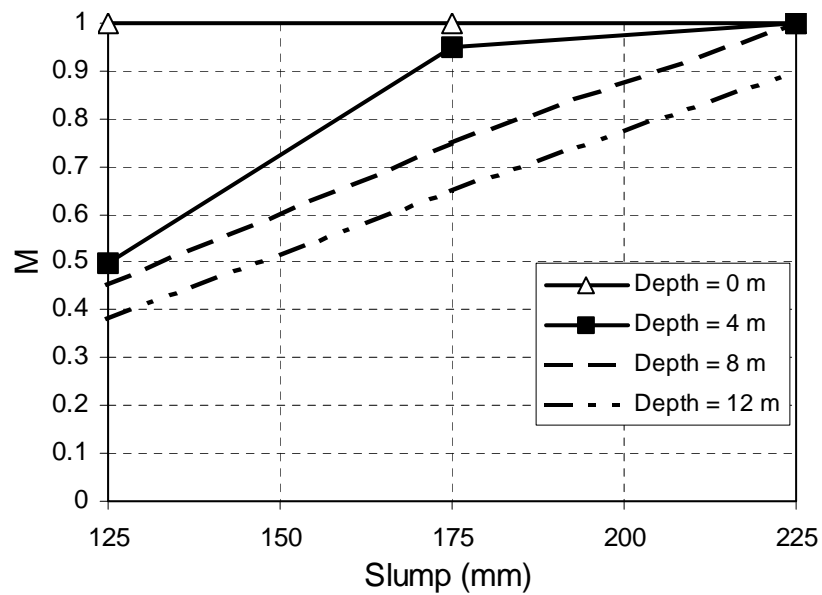


Figure 7.5- Factor M versus concrete slump (after O'Neill et al. 1996).

Because the Rowe and Armitage method slightly over predicts values of f_s determined from load tests, a slight modification to the method is proposed for use in predicting f_s for large drilled shafts in Missouri Pennsylvanian Age shales. As shown in Figure 7.6, this adjustment produces slightly more conservative values and tends to better fit the lower bound of the measured ultimate unit side shear values determined at the three Missouri test sites. The modified Rowe and Armitage method is recommended for design of large drilled shafts in Missouri Pennsylvanian Age shales drilled with a rock auger.

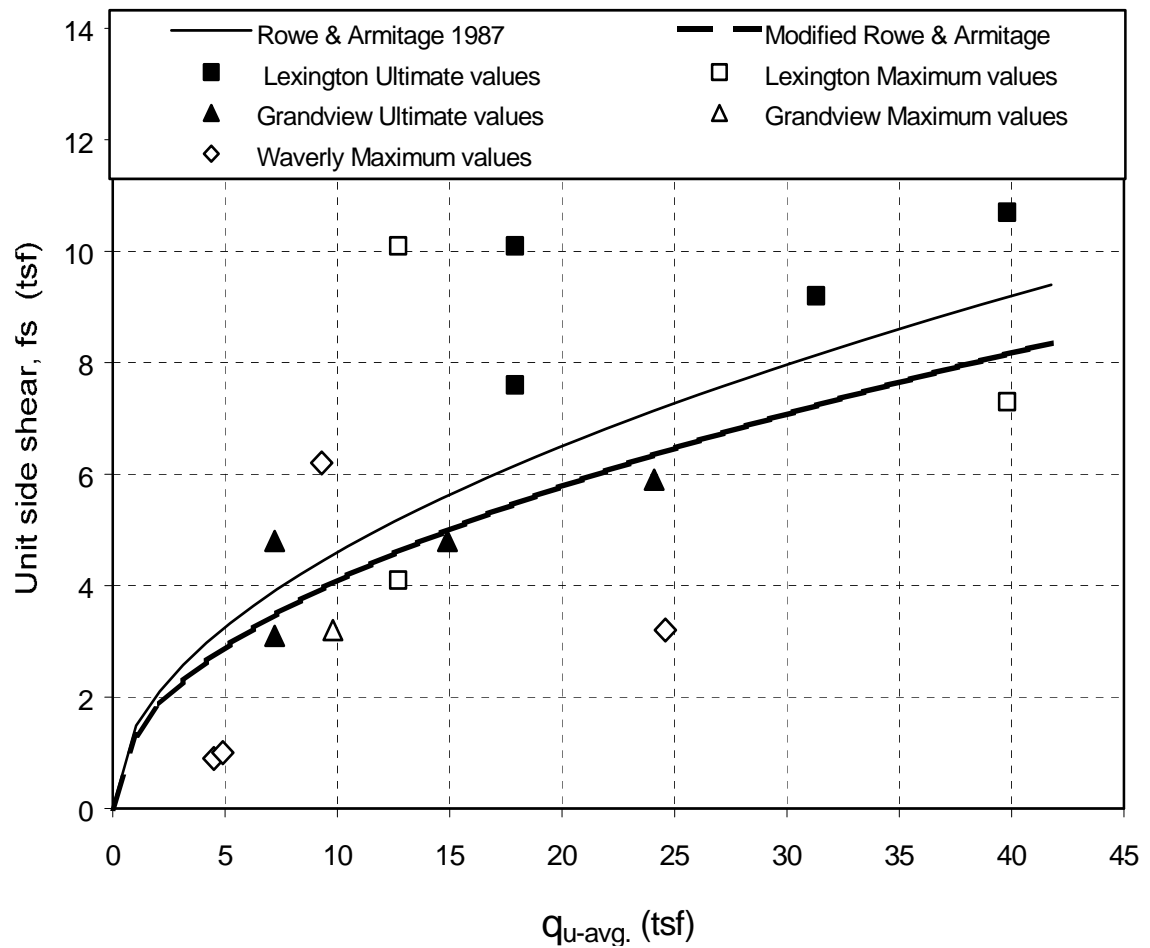


Figure 7.6-Modified Rowe and Armitage method.

Direct comparisons of predicted and measured unit side shear values are presented in Figures 7.7, 7.8, and 7.9 for the Horvath and Kenney, Rowe and Armitage, and the modified Rowe and Armitage methods, respectively. Also shown in the figures is a line that represents a factor of safety of one (a perfect prediction), and lines that represent factors of safety of 0.5 and 2.0, respectively. Points above the $FS = 1$ line indicate conservative predictions while points falling below this line represent unconservative predictions. As can be seen in Figure 7.7, the method proposed by Horvath and Kenney (1979) is generally conservative by a factor of approximately 2. Figure 7.8 indicates that the method proposed by Rowe and Armitage is slightly unconservative for shales with relatively low shear strength however; most of the data fell well above the line representing a factor of safety of 0.5, which suggests that the method would be acceptable if a factor of safety greater than 2.0 is used. The modified Rowe and Armitage method proposed here is slightly more conservative as shown in Figure 7.9, particularly for shales with low unconfined compressive strengths.

7.5 Summary

In this chapter, a summary and discussion of the results of four full-scale Osterberg cell load tests performed at three sites for the Missouri Department of Transportation were presented. Predicted values of f_s from several different methods were compared to the measured ultimate unit side shear values determined from the load tests. These analyses indicate that the method proposed by Rowe and Armitage (1987) most closely predicts the measured values for unit side shear. However, the method slightly over predicts f_s for relatively weak shales. A modification to the Rowe and

Armitage method was therefore proposed to predict slightly more conservative values of f_s for weak shales.

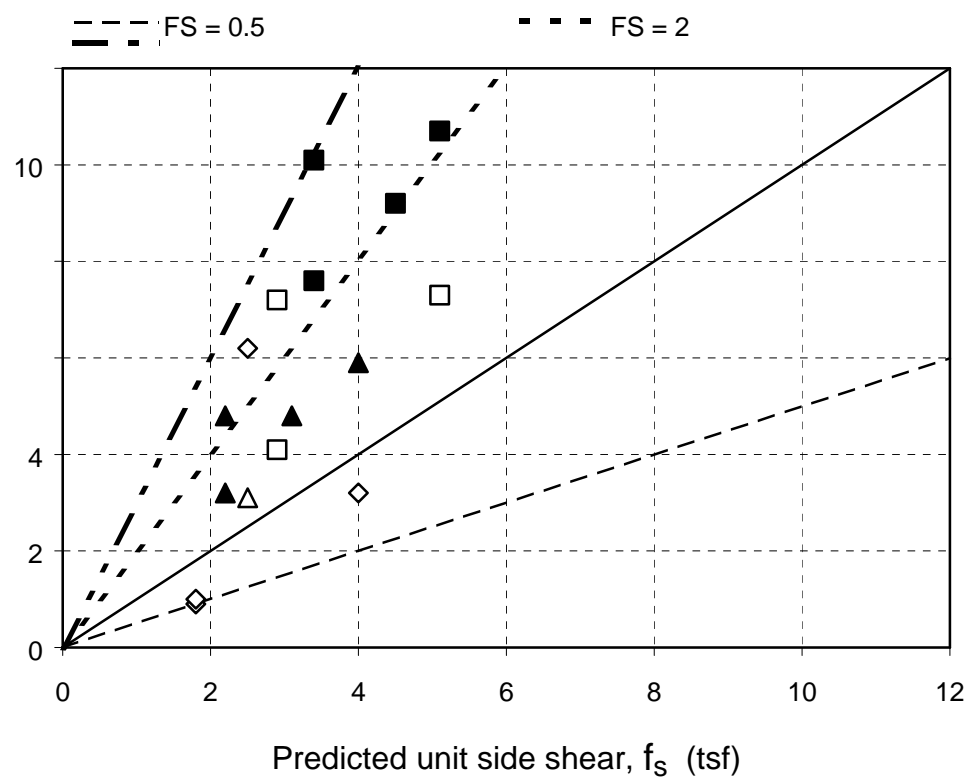


Figure 7.7- Comparison of measured and predicted unit side shear value using the Horvath and Kenney (1979) method.

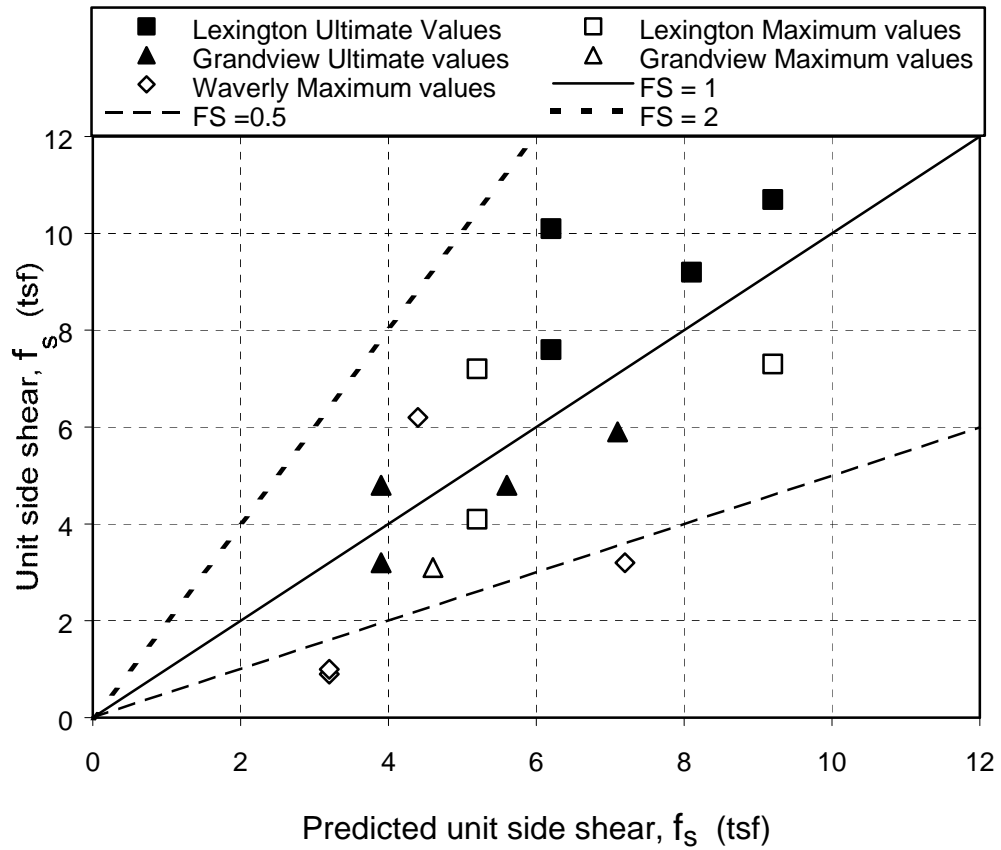


Figure 7.8- Comparison of measured and predicted unit side shear value using the Rowe and Armitage (1987) method.

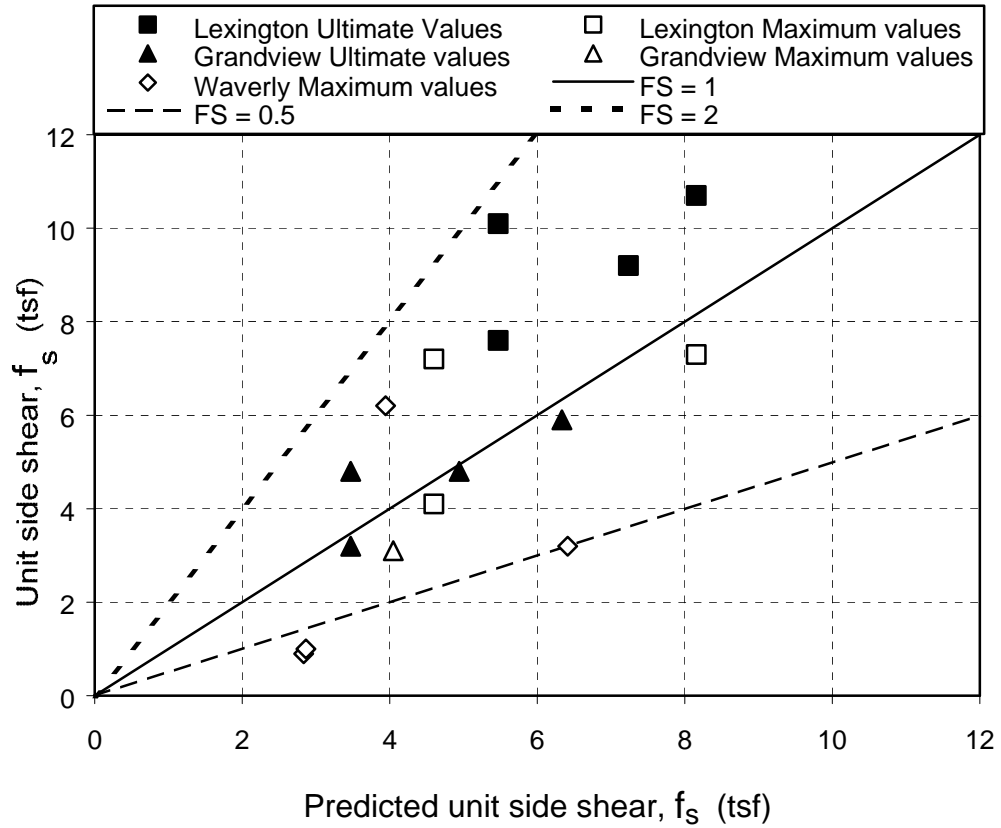


Figure 7.9- Comparison of measured and predicted unit side shear value using the modified Rowe and Armitage (1987) method.

CHAPTER EIGHT

SUMMARY, CONCLUSIONS, AND RECOMMENDATIONS

8.1 Summary

The focus of this research study has been to evaluate several design methods for predicting the ultimate unit side shear of drilled shafts socketed into weak Pennsylvanian shales. Load tests were performed on four full-scale, instrumented drilled shafts at three sites using the Osterberg load cell.

A literature survey was undertaken to identify a number of available design methods. Empirical and analytical methods for predicting the ultimate side shear capacity of drilled shafts socketed into weak rock were presented in Chapter 2. Empirical methods are generally based on results of full-scale load tests while analytical methods attempt to model the soft rock-drilled shaft interface numerically, often using finite-element solutions.

In Chapter 3, a new test method for full-scale load testing of drilled shafts using the Osterberg cell (O-cellTM) was described. The Osterberg load cell, along with instrumentation such as strain gages and telltales, may be used to determine end bearing and side shear capacities of drilled shafts and piles.

Load testing of two 1.2 meter (4 ft) diameter drilled shafts located in the Missouri River at Lexington, Missouri was presented in Chapter 4. The drilled shafts were socketed 12.3 and 20.3 meters (40 to 66.6 ft) into bedrock at the bridge site, which consists of Pennsylvanian Age shales, siltstones, sandstones, limestones, and scattered coal beds. Due to difficulty with access to the sites by land and to avoid hindering river traffic, the two Osterberg cell load test shafts were located in the river but near the river

banks. Both test shafts were impacted by high river levels and scheduling conflicts. The drilled shafts were tested to maximum loads of 13.3 MN (1,495 tons) and 17.5 MN (1,968 tons) by Loadtest Inc. in May and June of 1999. Test shaft TS-1A included one 660mm (26 in) Osterberg load cell while test shaft TS-2 included two 660 mm (26 in) Osterberg load cells. The Osterberg cell load tests were successful in allowing MoDOT to develop a more economical design for the drilled shafts for the proposed bridge alignment. Data from the Osterberg cell load test allowed 1.68 m (5.5 ft) diameter rock sockets at bridge A5664 to be shortened a total of 704.5 m (2311.5 ft) for a net savings of \$1.8 million.

In Chapter 5, the results of an Osterberg cell load test performed on a 1.8 meter (6 ft) diameter drilled shaft as part of the reconstruction of an intersection in the Kansas City metropolitan area was presented. The drilled shaft was socketed 13 meters (42.7 ft) into bedrock, which consisted of horizontally bedded layers of limestones and shales known as the Kansas City Group. The 870 mm (34 in) Osterberg load cell was successfully loaded to 33.78 MN (3789 tons) on June 4, 2002. Data from the Osterberg load test would allow 2.3 m (7.5 ft) diameter rock sockets at bridge A6252 to be shortened a total of 65.2 m (214 ft) for a net savings of \$19 thousand.

Load testing of a “production” drilled shaft with a 660 mm (26 in) Osterberg load cell is presented in Chapter 6 for a proposed bridge across the Missouri River at Waverly, Missouri. The production shaft was one of 6 shafts used to construct the footing of Pier 11 in the middle of the Missouri River. The two-meter (6.5 ft) diameter shaft was socketed 15.1 meters (49.5 ft) into bedrock consisting of Pennsylvanian Age shales, siltstones, sandstones, limestones, and scattered coal beds. The production shaft was

tested to a maximum load of 22.5 MN (2,525 tons) on September 30, 2002. The Osterberg cell load test was successful in testing the shaft to twice the design load and assuring the foundation engineers that the main pier in the river would be safe.

Finally, measured values of unit side shear determined for various strata involved in the load tests were collectively analyzed to evaluate the suitability of several design methods. The results of these analyses are presented in Chapter 7, where the measured values of unit side shear are compared to values predicted by several design methods. In addition, conclusions are drawn on the appropriateness of the respective design methods for use with Missouri shales and a modified design method is proposed. This chapter provides a summary of this thesis, conclusions reached, lessons learned from the work, and several recommendations for future work.

8.2 Conclusions

A number of conclusions can be drawn from the results of the four load tests and subsequent analysis of the test results. Analysis of the load test data indicated that the ultimate unit side shear may be conservatively estimated as 0.3 times the unconfined compressive strength of the shale. This more than doubles the values predicted by the method currently used by MoDOT.

The results of a series of four load tests in Missouri Pennsylvanian Age shales indicate that design methods by Rowe and Armitage (1987) and Kulhawy and Phoon (1993) produced almost identical results and most closely predicted the measured ultimate unit side shear in these materials.

Because the Rowe and Armitage (1987) method slightly over-estimates the ultimate unit side shear for shale with low compressive strengths, a minor modification of

the method is proposed to produce slightly more conservative values. In the proposed modification, the ultimate unit side shear is predicted as 0.4 times the square root of q_u rather than 0.45 as recommended by Rowe and Armitage. This would lead to about a 60 per cent increase in the predicted ultimate unit side shear over current methods followed by MoDOT.

Methods by Horvath and Kenney (1979) and Reese and O'Neill (1988) produced similar results. However, both methods significantly under-predicted measured values observed in the load tests by as much as a factor of 2.

O'Neill and Reese (1999) tended to be more conservative than either Horvath and Kenney or Reese and O'Neill (1988) when the simplified method for smooth sockets was used. However, the method proposed by O'Neill and Reese (1999) is not intended for use when the slump of the concrete is less than 175 mm (7in) as was the case for load tests at the Lexington site.

The use of the Osterberg cell load test method has lead to significant cost savings in the design of foundations for bridges, increased the confidence level in design methods used, and has the potential to improve future designs over time. The testing of two full-scale shafts in the River at Lexington, Missouri cost approximately \$0.5 million and generated a net cost saving of about \$1.8 million. At the Grandview site, data from the Osterberg cell load test would allow the 7.5 feet (2.3 m) diameter rock sockets at bridge A6252 to be shortened a total of 214 feet (65.2 m) for a cost savings of \$214 thousand. The cost of the shaft excavation and the Osterberg cell load test was \$195 thousand for a net savings of \$19 thousand. At the Waverly site, a production shaft was tested during

the construction phase of the project. Although it is difficult to obtain cost savings during construction, with most construction testing being “proof” testing (testing to twice the design load), about 3 feet (0.9 m) of socket was eliminated on all 6 shafts at Pier 11. The shortening of the sockets saved \$29 thousand to offset the \$70 thousand cost for the Osterberg cell load test. The cost savings at the three test sites indicate the magnitude of cost savings that could be realized in using Osterberg cell load tests on future projects.

8.3 Lessons Learned

A number of lessons were learned in performing and evaluating these load tests. The collapse of test shaft TS-1 at the Lexington site has led to specification changes that require rock sockets to be excavated and the shaft concrete to be placed within 3 days for shafts constructed in shales. Further specification changes require the use of polymer slurry in drilled shafts constructed in shale that cannot be constructed in the dry.

The Osterberg cell load test at test shaft TS-1A at the Lexington site did not occur as planned. No failure was achieved in TS-1A even though the capacity of the Osterberg load cell was not reached. The test was stopped because the applied pressure to the cell exceeded the capacity of the pressure gage and a higher capacity gage was not available on site. Care should be taken in future load tests using the O-cellTM to ensure that adequate pressure gages are available.

Strain gages placed near the O-cellsTM did not function correctly at all three sites due to the zone of influence caused by the non-rigid bearing plates. In future tests using the Osterberg load cell, strain gages should be located no closer than one diameter, and preferably two diameters from the O-cellTM.

Problems were also experienced with clogging of the concrete tremie pipes for pipes with diameters less than 30 cm (12 in) at two of the sites. In the future, significant effort should be made to maintain a minimum concrete slump of 203mm (8 in) at the time of concrete placement. The holes in the O-cellTM bearing plates should also be enlarged to allow the use of 30 cm (12 in) tremie pipe, particularly for deep shafts.

8.4 Recommendations for Future Work

Several recommendations can be made based on experiences resulting from this research. Due to the limited amount of data for the ultimate side shear capacities of drilled shafts in Missouri shales, further load testing is recommended to expand the database of measured unit side shear values. For additional tests, every effort should be made to load shafts so that side shear is fully mobilized to allow direct evaluation of current design methods.

Due to the difficulty present in accurately testing shales with low strength, the unconfined compression strength, q_u should be replaced by strengths determined from confined triaxial tests (i.e. Q or R tests). In addition, extreme care should be taken in evaluating laboratory strength parameters for all load test sites.

Other methods for predicting the ultimate unit side shear should be evaluated that account for the roughness of the socket and other parameters that may affect the capacity of drilled shafts. One such example is the computer program (ROCKET 95) developed by Seidel and Haberfield (1995). Another method is using borehole shear testing to determine the ultimate unit side shear. Particular attention should also be paid to emerging methods for accurately providing a caliper log of the excavated shaft.

An evaluation of side shear load capacities for different diameter shafts should be performed and an adjustment developed to account for the diameter of the shaft. Very little testing has been done in this area although expanding cavity theory suggests that there is an effect of diameter on load transfer (Hassan and O'Neill 1997). Baycan (1996) used a computer program (ROCKET 95) developed by Seidel and Haberfield (1995) and found diameter has a significant effect on unit side shear. Having direct knowledge of the relation between capacity and diameter would allow for the testing of smaller diameter shafts, which would lead to substantial cost savings by reducing the costs of constructing the test shafts in addition to reducing the costs of the O-cell tests because smaller cells could be used. This in turn, may lead to more tests being performed because of the reduced costs of each test.

The relation between conventional top-down load testing and Osterberg cell load tests should be investigated. Although many investigators believe that there is little difference in side shear capacities attributed to loading direction, very little full-scale testing exists. Finite element analyses performed by Shi (2002) indicate that, as the modulus of the rock increased, the difference in side shear capacities for top-down and O-cell loading increased with the Osterberg cell load test method becoming more conservative.

Finally, current design methods should be periodically re-evaluated to determine if the predicted ultimate unit side shear can be improved based on new data from additional load tests.

APPENDIX A
DETAILED DATA FOR LOAD TESTS AND UNCONFINED COMPRESSIVE
STRENGTH OF NX CORES AT LEXINGTON SITE

Table A.1
Summary of dimensions, elevations, and shaft properties (TS-1A)

Shaft:

Average Shaft Diameter (EL 175.93 m to 167.27 m)	=	1111 mm	43.75 in
O-Cell TM : 8037-11	=	660 mm	26 in
Length of side shear above break at base of O-cell TM	=	5.42 m	17.8 ft
Length of side shear below break at base of O-cell TM	=	3.24 m	10.6 ft
Shaft side shear area above O-cell TM base	=	19.9 m ²	214.4 ft ²
Shaft side shear area below break at base of O-cell TM	=	11.9 m ²	128.2 ft ²
Shaft base area	=	1.08 m ²	11.6 ft ²
Bouyant weight of shaft above base of O-cell TM	=	0.11 MN	25 kips
Estimated shaft stiffness (EL 175.93 m to 170.51 m)	=	25,506 MN	5,734,159 kips
Estimated shaft stiffness (EL 170.51 m to 167.27 m)	=	25,506 MN	5,734,159 kips
Elevation of Water Table	=	208.24 m	683.2 ft
Elevation of Mud line	=	207.63 m	681.2 ft
Elevation top of shaft concrete	=	175.93 m	577.2 ft
Elevation of base of O-cell TM	=	170.51 m	559.4 ft
Elevation of shaft tip	=	167.27 m	548.8 ft

Casing:

Elevation of top of permanent casing (1220 mm O.D.)	=	210.68 m	691.2 ft
Elevation of bottom of permanent casing	=	179.59 m	589.2 ft

Compression Sections:

EL. of top of telltale used for shaft compression above cell	175.07 m	574.4 ft
EL. of bottom of telltale used for shaft compression above cell	170.87 m	560.6 ft

Strain Gages:

Elevation of strain gage level 4	=	174.51 m	572.5 ft
Elevation of strain gage level 3	=	173.01 m	567.6 ft
Elevation of strain gage level 2	=	172.01 m	564.3 ft
Elevation of strain gage level 1	=	169.56 m	556.3 ft

Miscellaneous:

Top Plate Diameter	=	815 mm	32.1 in
Bottom Plate Diameter	=	915 mm	36.0 in
Carrying frame cross sectional area (2 No. C4 x 7.25)	=	2748 mm ²	4.26 in ²
Unconfined compressive concrete strength	=	28.1 MPa	4075 psi
O-Cell TM LVWDTs @ 0 ⁰ , 90 ⁰ , and 180 ⁰ with radius	=	432 mm	17 in

Table A.2- Osterberg O-cell™ versus top and bottom plate movement for load increments 1L-0 to 1U-7 (TS-1A).

Load Test Incre.	O-cell Loads		Upwrd Mvment		Creep	Bottom of Cell		Creep	Dnwrdr Mvment
	Gross (MN)	Net (MN)	2 min (mm)	4 min (mm)	2-4 Min (mm)	2 min (mm)	4 min (mm)	2-4 Min (mm)	
1L-0	0	0	0	0	0	0	0	0	0
1L-1	0.62	0.51	0	0.01	0.01	0.04	0.03	-0.01	-0.03
1L-2	1.11	1	0.02	0.02	0	0.04	0.04	0	-0.04
1L-3	1.58	1.47	0.03	0.02	-0.01	0.07	0.08	0.01	-0.08
1L-4	2.08	1.97	0.1	0.1	0	0.59	0.61	0.02	-0.61
1L-5	2.56	2.45	0.22	0.25	0.03	1.04	1.02	-0.02	-1.02
1L-6	3.04	2.93	0.35	0.36	0.01	1.25	1.25	0	-1.25
1L-7	3.53	3.42	0.44	0.46	0.02	1.42	1.5	0.08	-1.5
1L-8	4.03	3.92	0.53	0.55	0.02	1.67	1.68	0.01	-1.68
1L-9	4.5	4.39	0.62	0.64	0.02	1.88	1.88	0	-1.88
1L-10	4.98	4.87	0.72	0.73	0.01	2.11	2.09	-0.02	-2.09
1L-11	5.46	5.35	0.81	0.83	0.02	2.31	2.34	0.03	-2.34
1L-12	5.93	5.82	0.9	0.95	0.05	2.47	2.54	0.07	-2.54
1L-13	6.43	6.32	1.07	1.11	0.04	2.64	2.66	0.02	-2.66
1L-14	6.9	6.79	1.22	1.24	0.02	2.84	2.85	0.01	-2.85
1L-15	7.38	7.27	1.32	1.34	0.02	3.18	3.27	0.09	-3.27
1L-16	7.85	7.74	1.43	1.45	0.02	3.4	3.43	0.03	-3.43
1L-17	8.35	8.24	1.55	1.57	0.02	3.65	3.72	0.07	-3.72
1L-18	8.82	8.71	1.67	1.69	0.02	3.89	3.93	0.04	-3.93
1L-19	9.28	9.17	1.78	1.79	0.01	4.25	4.27	0.02	-4.27
1L-20	9.74	9.63	1.91	1.91	0	4.58	4.61	0.03	-4.61
1L-21	10.26	10.15	2.02	2.04	0.02	4.92	5.02	0.1	-5.02
1L-22	10.73	10.62	2.15	2.18	0.03	5.26	5.33	0.07	-5.33
1L-23	11.18	11.07	2.3	2.33	0.03	5.59	5.69	0.1	-5.69
1L-24	11.7	11.59	2.45	2.47	0.02	5.91	6.07	0.16	-6.07
1L-25	12.17	12.06	2.6	2.62	0.02	6.39	6.51	0.12	-6.51
1L-26	12.67	12.56	2.75	2.77	0.02	6.73	6.92	0.19	-6.92
1L-27	13.17	13.06	2.94	2.98	0.04	7.32	7.44	0.12	-7.44
1L-28	13.57	13.46	3.1	3.14	0.04	7.7	7.7	0	-7.7
1L-29	14.09	13.98	3.3	3.35	0.05	8.19	8.33	0.14	-8.33
1L-30	14.58	14.47	3.5	3.53	0.03	8.69	8.78	0.09	-8.78
1L-31	15.09	14.98	3.7	3.74	0.04	9.34	9.49	0.15	-9.49
1L-32	15.57	15.46	3.9	3.94	0.04	10.02	10.31	0.29	-10.31
1L-33	16.04	15.93	4.16	4.23	0.07	10.69	10.78	0.09	-10.78
1L-34	16.59	16.48	4.58	4.66	0.08	11.58	11.66	0.08	-11.66
1L-35	17.05	16.94	4.94	5.06	0.12	12.48	12.63	0.15	-12.63
1L-36	17.5	17.39	5.35	5.47	0.12	13.35	13.6	0.25	-13.6
1U-1	16.03	15.92		5.74			13.99		-13.99
1U-2	13.4	13.29		5.57			14.08		-14.08
1U-3	9.93	9.82		5.19			14.14		-14.14
1U-4	6.85	6.74		4.61			13.77		-13.77
1U-5	3.45	3.34		3.77			13.23		-13.23
1U-6	1.81	1.7		3.06			11.47		-11.47
1U-7	0.06	0		2.45			10.74		-10.74

Table A.3- Strain gage data, Lexington, Missouri test site (TS-1A).

Load Test Incre.	O-cell Loads		Top of Conc Avg. Load (MN)	Level 4 Avg. Load (MN)	Level 3 Avg. Load (MN)	Level 2 Avg. Load (MN)	O-cell Net (MN)	Level 1 Avg. Load (MN)
	Gross (MN)	Net (MN)						
Elev (m)			175.93	174.51	173	172	170.5	169.6
1L-0	0	0	0	0	0	0	0	0
1L-1	0.62	0.51	0	0	0.02	0.05	0.51	0.06
1L-2	1.11	1	0	0.01	0.06	0.11	1	0.14
1L-3	1.58	1.47	0	0.03	0.1	0.2	1.47	0.25
1L-4	2.08	1.97	0	0.12	0.36	0.75	1.97	0.76
1L-5	2.56	2.45	0	0.21	0.61	1.24	2.45	1.31
1L-6	3.04	2.93	0	0.3	0.82	1.64	2.93	1.75
1L-7	3.53	3.42	0	0.35	1.05	2.03	3.42	2.2
1L-8	4.03	3.92	0	0.43	1.24	2.37	3.92	2.56
1L-9	4.5	4.39	0	0.49	1.42	2.7	4.39	2.9
1L-10	4.98	4.87	0	0.58	1.61	3.05	4.87	3.26
1L-11	5.46	5.35	0	0.63	1.82	3.43	5.35	3.65
1L-12	5.93	5.82	0	0.69	2	3.76	5.82	4
1L-13	6.43	6.32	0	0.75	2.2	4.14	6.32	4.39
1L-14	6.9	6.79	0	0.8	2.39	4.51	6.79	4.76
1L-15	7.38	7.27	0	0.86	2.59	4.88	7.27	5.14
1L-16	7.85	7.74	0	0.91	2.78	5.24	7.74	5.52
1L-17	8.35	8.24	0	0.96	2.98	5.61	8.24	5.91
1L-18	8.82	8.71	0	1	3.17	5.98	8.71	6.29
1L-19	9.28	9.17	0	1.07	3.35	6.31	9.17	6.62
1L-20	9.74	9.63	0	0.79	3.54	6.71	9.63	7.03
1L-21	10.26	10.15	0	1.16	3.75	7.1	10.15	7.48
1L-22	10.73	10.62	0	1.22	3.95	7.48	10.62	7.89
1L-23	11.18	11.07	0	1.22	4.15	7.87	11.07	8.3
1L-24	11.7	11.59	0	1.32	4.35	8.29	11.59	8.74
1L-25	12.17	12.06	0	1.37	4.57	8.71	12.06	9.19
1L-26	12.67	12.56	0	1.43	4.78	9.13	12.56	9.62
1L-27	13.17	13.06	0	1.47	5	9.52	13.06	10.07
1L-28	13.57	13.46	0	1.52	5.18	9.91	13.46	10.47
1L-29	14.09	13.98	0	1.56	5.39	10.34	13.98	10.97
1L-30	14.58	14.47	0	1.61	5.59	10.76	14.47	11.45
1L-31	15.09	14.98	0	1.66	5.81	11.24	14.98	12.03
1L-32	15.57	15.46	0	1.7	6.01	11.69	15.46	12.55
1L-33	16.04	15.93	0	1.76	6.22	12.15	15.93	13.13
1L-34	16.59	16.48	0	1.81	6.48	12.79	16.48	13.9
1L-35	17.05	16.94	0	1.87	6.75	13.37	16.94	14.63
1L-36	17.5	17.39	0	1.91	6.97	13.88	17.39	15.33
1U-1	16.03	15.92	0	1.94	7.13	14.25	15.92	15.98
1U-2	13.4	13.29	0	21.74	6.74	13.54	13.29	15.17
1U-3	9.93	9.82	0	21.56	6.07	12.18	9.82	13.55
1U-4	6.85	6.74	0	21.32	5.12	10.22	6.74	11.22
1U-5	3.45	3.34	0	21.1	4.04	8.06	3.34	8.65
1U-6	1.81	1.7	0	20.75	2.4	4.77	1.7	5.01
1U-7	0.06	0	0	20.72	1.88	3.7	-0.05	3.67

Table A.4- Unit side shear data, Lexington, Missouri test site (TS-1A).

Load Test Incre	O-cell Loads		Upwrd	Bottom	Level 1	SG-1	Level 2	O-cell	Level 3	SG-2	Level 4	SG-3	SG-4
			Mvmnt	of Cell	Avg.	to	Avg.	to	Avg.	to	Avg.	to	To
	Gross (MN)	Net (MN)	4 min (mm)	4 min (mm)	Load (MN)	O-cell (kPa)	Load (MN)	SG-2 (kPa)	Load (MN)	SG-3 (kPa)	Load (MN)	SG-4 (kPa)	TOS (kPa)
Elev (m)						170.5- 169.6		170.5- 172		172.0- 173		173- 174.5	174.5- 175.9
1L-0	0	0	0	0	0		0		0		0		
1L-1	0.62	0.51	0.01	0.03	0.06	143	0.05	88	0.02	9	0.00	4	0
1L-2	1.11	1	0.02	0.04	0.14	274	0.11	170	0.06	14	0.01	10	2
1L-3	1.58	1.47	0.02	0.08	0.25	389	0.2	243	0.10	29	0.03	13	6
1L-4	2.08	1.97	0.1	0.61	0.76	386	0.75	233	0.36	112	0.12	46	25
1L-5	2.56	2.45	0.25	1.02	1.31	363	1.24	231	0.61	181	0.21	77	43
1L-6	3.04	2.93	0.36	1.25	1.75	376	1.64	247	0.82	235	0.30	99	61
1L-7	3.53	3.42	0.46	1.5	2.2	389	2.03	266	1.05	281	0.35	134	72
1L-8	4.03	3.92	0.55	1.68	2.56	434	2.37	296	1.24	324	0.43	155	88
1L-9	4.5	4.39	0.64	1.88	2.9	475	2.7	323	1.42	367	0.49	178	100
1L-10	4.98	4.87	0.73	2.09	3.26	513	3.05	348	1.61	413	0.58	197	119
1L-11	5.46	5.35	0.83	2.34	3.65	542	3.43	367	1.82	462	0.63	228	129
1L-12	5.93	5.82	0.95	2.54	4	580	3.76	394	2.00	505	0.69	251	141
1L-13	6.43	6.32	1.11	2.66	4.39	615	4.14	417	2.20	557	0.75	277	154
1L-14	6.9	6.79	1.24	2.85	4.76	647	4.51	436	2.39	608	0.80	304	164
1L-15	7.38	7.27	1.34	3.27	5.14	679	4.88	457	2.59	657	0.86	331	176
1L-16	7.85	7.74	1.45	3.43	5.52	708	5.24	478	2.78	706	0.91	358	186
1L-17	8.35	8.24	1.57	3.72	5.91	743	5.61	503	2.98	755	0.96	386	197
1L-18	8.82	8.71	1.69	3.93	6.29	771	5.98	522	3.17	806	1.00	415	205
1L-19	9.28	9.17	1.79	4.27	6.62	813	6.31	547	3.35	849	1.07	436	219
1L-20	9.74	9.63	1.91	4.61	7.03	829	6.71	559	3.54	910	1.12	463	230
1L-21	10.26	10.15	2.04	5.02	7.48	851	7.1	583	3.75	961	1.16	495	238
1L-22	10.73	10.62	2.18	5.33	7.89	870	7.48	601	3.95	1013	1.22	522	250
1L-23	11.18	11.07	2.33	5.69	8.3	883	7.87	612	4.15	1067	1.22	560	250
1L-24	11.7	11.59	2.47	6.07	8.74	909	8.29	631	4.35	1130	1.32	580	271
1L-25	12.17	12.06	2.62	6.51	9.19	915	8.71	641	4.57	1188	1.37	612	281
1L-26	12.67	12.56	2.77	6.92	9.62	937	9.13	656	4.78	1248	1.43	641	293
1L-27	13.17	13.06	2.98	7.44	10.07	953	9.52	677	5.00	1297	1.47	675	301
1L-28	13.57	13.46	3.14	7.7	10.47	953	9.91	679	5.18	1357	1.52	700	312
1L-29	14.09	13.98	3.35	8.33	10.97	960	10.34	696	5.39	1420	1.56	733	320
1L-30	14.58	14.47	3.53	8.78	11.45	963	10.76	710	5.59	1483	1.61	761	330
1L-31	15.09	14.98	3.74	9.49	12.03	940	11.24	715	5.81	1558	1.66	794	340
1L-32	15.57	15.46	3.94	10.31	12.55	928	11.69	721	6.01	1630	1.70	824	348
1L-33	16.04	15.93	4.23	10.78	13.13	893	12.15	723	6.22	1701	1.76	853	361
1L-34	16.59	16.48	4.66	11.66	13.9	822	12.79	706	6.48	1810	1.81	893	371
1L-35	17.05	16.94	5.06	12.63	14.63	736	13.37	683	6.75	1899	1.87	933	383
1L-36	17.5	17.39	5.47	13.6	15.33	657	13.88	671	6.97	1983	1.91	968	391

Table A.5
Summary of dimensions, elevations, and shaft properties (TS-2)

Shaft:

Average Shaft Diameter (EL 184.4 m to 180.17 m)	=	1182 mm	46.5 in
Average Shaft Diameter (EL 180.17 m to 176.17 m)	=	1167 mm	46.0 in
Average Shaft Diameter (EL 176.17 m to 174.65 m)	=	1107 mm	43.6 in
Upper cell: 8037-13	=	660 mm	26 in
Bottom cell: 8037-12	=	660 mm	26 in
Length of side shear above break at base of upper cell	=	4.23 m	13.9 ft
Length of side shear between Bottom cell and upper cell	=	4.00 m	13.1 ft
Length of side shear below break at base of Bottom-cell	=	1.52 m	5.0 ft
Shaft side shear area above upper cell base	=	15.70 m ²	169 ft ²
Shaft side shear area between bottom cell and upper cell	=	14.67 m ²	157.9 ft ²
Shaft side shear area below break at base of Bottom-cell	=	5.30 m ²	57.1 ft ²
Shaft base area	=	0.96 m ²	10.4 ft ²
Bouyant weight of shaft above base of upper cell	=	0.07 MN	15.6 kips
Bouyant weight of shaft above base of bottom cell	=	0.13 MN	29.0 kips
Estimated shaft modulus (EL 184.4 m to 180.17 m)	=	28.0 GPa	4057 ksi
Estimated shaft modulus (EL 180.17 m to 176.17 m)	=	28.8 GPa	4173 ksi
Estimated shaft modulus (EL 176.17 m to 174.65 m)	=	26.9 GPa	3904 ksi
Elevation of Water Table	=	Variable	Variable
Elevation of Mud line	=	204.52 m	671.0 ft
Elevation top of shaft concrete	=	184.40 m	605.0 ft
Elevation of base of upper cell	=	180.17 m	591.1 ft
Elevation base of bottom cell	=	176.17 m	578.0 ft
Elevation of shaft tip	=	174.65 m	573.0 ft

Casing:

Elevation of top of inner permanent casing(1090 mm O.D.)	=	210.92 m	692.0 ft
Elevation of bottom of inner permanent casing	=	193.85 m	636.0 ft

Compression Sections:

Elevation of top of level 2 telltale	=	183.89 m	603.3 ft
Elevation of bottom of level 2 telltale	=	180.54 m	592.3 ft
Elevation of top of level 1 telltale	=	179.92 m	590.3 ft
Elevation of bottom of level 1 telltale	=	176.57 m	579.3 ft

Strain Gages:

Elevation of strain gage level 4	=	182.67 m	599.3 ft
Elevation of strain gage level 3	=	181.67 m	596.0 ft
Elevation of strain gage level 2	=	178.67 m	586.2 ft
Elevation of strain gage level 1	=	177.67 m	582.9 ft

Miscellaneous:

Carrying frame cross sectional area (C4 x 7.25)	=	8129 mm ²	12.6 in ²
Unconfined compressive concrete str. (EL. 184.4 to 178.46 m)	=	28.1 MPa	4070 psi
Unconfined compressive concrete str. (EL. 178.46 to 174.65 m)	=	33.7 MPa	4885 psi

Table A.6- Osterberg O-cells™ versus top and bottom plate movement for load increments 1L-0 to 1U-5 (TS-2, stage 1).

Load Test Incre.	O-cell Loads		Avg.	Avg.	Avg.	Shaft	Upward	Avg.	Dwnwrđ	
	Lower cell		Top of Shaft	Comp.	Comp.	Expnsn	Comp.	Mvment	Expnsn	Mvment
				ECT LEVEL 1	ECT LEVEL 2			Top	LVWDT 14985	
				Between cells	Above Upper cell	Upper cell		of Lower Cell	LVWDT 14986 LVWDT 14987 Lower cell	
	Gross (MN)	Net (MN)	4 min (mm)	4 min (mm)	4 min (mm)	4 min (mm)	4 min (mm)	4 min (mm)	4 min (mm)	4 min (mm)
1	2	3	5	6	7	8	9	10	11	12
							6+7-8	5+9		10 - 11
1L-0	0	0	0	0	0	0	0	0	0	0
1L-1	0.87	0.74	-0.1	0.02	0	0	0.02	-0.08	0.12	-0.2
1L-2	1.68	1.55	-0.1	0.07	0	0	0.07	-0.03	0.27	-0.3
1L-3	2.49	2.36	-0.14	0.12	0	-0.01	0.13	-0.01	0.51	-0.52
1L-4	3.3	3.17	-0.1	0.2	0	-0.01	0.21	0.11	1.06	-0.95
1L-5	4.11	3.98	-0.24	0.6	0.01	-0.02	0.63	0.39	3.22	-2.83
1L-6	4.92	4.79	-0.14	0.9	0.01	-0.03	0.94	0.8	5.49	-4.69
1L-7	5.73	5.6	-0.03	1.26	0.02	-0.03	1.31	1.28	8.74	-7.46
1L-8	6.54	6.41	0	1.71	0.02	-0.04	1.77	1.77	12.63	-10.86
1L-9	7.35	7.22	0.03	2.23	0.03	-0.05	2.31	2.34	17.83	-15.49
1L-10	8.16	8.03	-0.07	2.92	0.04	-0.06	3.02	2.95	23.41	-20.46
1L-11	8.97	8.84	-0.14	3.98	0.04	-0.06	4.08	3.94	30.18	-26.24
1L-12	9.78	9.65	-0.27	5.39	0.05	-0.07	5.51	5.24	45.27	-40.03
1L-13	10.59	10.46	-0.41	7.23	0.03	-0.09	7.35	6.94	67.62	-60.68
1U-1	6.54	6.41	-0.44	7.36	0.02	-0.06	7.44	7	68.67	-61.67
1U-2	3.3	3.17	-0.55	7.27	0.02	-0.04	7.33	6.78	67.01	-60.23
1U-3	1.68	1.55	-0.48	7.08	0.02	-0.05	7.15	6.67	65.81	-59.14
1U-4	0.87	0.74	-0.41	6.99	0.01	-0.05	7.05	6.64	64.91	-58.27
1U-5	0.06	-0.07	-0.44	6.82	0.01	-0.04	6.87	6.43	63.41	-56.98

Table A.7-Creep data, Lexington, Missouri test site (TS-2, stage 1).

Load Test Incre.	Q-cell Load	Upward Mvment	Upward Mvment	Creep	Dwnwrđ Mvment	Dwnwrđ Mvment	Creep
	Lower Cell Net (MN)	Top of Lower Cell 2 min (mm)	Top of Lower Cell 4 min (mm)	2 to 4 min (mm)	Bott of Lower Cell 2 min (mm)	Lower Cell 4 min (mm)	2 to 4 min (mm)
1L-0	0	0	0	0	0	0	0
1L-1	0.74	0	-0.08	-0.08	0	0.2	0.2
1L-2	1.55	0.06	-0.03	-0.09	0.21	0.3	0.09
1L-3	2.36	0.07	-0.01	-0.08	0.41	0.52	0.11
1L-4	3.17	0.14	0.11	-0.03	0.87	0.95	0.08
1L-5	3.98	0.46	0.39	-0.07	2.5	2.83	0.33
1L-6	4.79	0.82	0.8	-0.02	4.15	4.69	0.54
1L-7	5.6	1.13	1.28	0.15	6.67	7.46	0.79
1L-8	6.41	1.63	1.77	0.14	9.71	10.86	1.15
1L-9	7.22	2.24	2.34	0.1	14.11	15.49	1.38
1L-10	8.03	2.69	2.95	0.26	19.05	20.46	1.41
1L-11	8.84	3.66	3.94	0.28	24.34	26.24	1.9
1L-12	9.65	4.62	5.24	0.62	33.69	40.03	6.34
1L-13	10.46	6.68	6.94	0.26	57.34	60.68	3.34
1U-1	6.41	7.03	7			61.67	
1U-2	3.17	6.78	6.78			60.23	
1U-3	1.55	6.63	6.67			59.14	
1U-4	0.74	6.5	6.64			58.27	
1U-5	-0.07	6.48	6.43			56.98	

Table A.8-Load distribution data, Lexington, Missouri test site (TS-2, stage 1).

Load Test Incr.	Bottom O-cell Loads		Top of Conc Avg. Load (MN)	Level 4 Avg. Load (MN)	Level 3 Avg. Load (MN)	Level 2 Avg. Load (MN)	O-cell Net (MN)
	Gross (MN)	Net (MN)					
Elev (m)			184.4	182.67	181.67	178.67	176.17
1L-0	0	0	0	0	0	0	0
1L-1	0.87	0.74	0	0	0	0.18	0.74
1L-2	1.68	1.55	0	0.01	0.02	0.28	1.55
1L-3	2.49	2.36	0	0.01	0.03	0.42	2.36
1L-4	3.3	3.17	0	0.03	0.04	0.52	3.17
1L-5	4.11	3.98	0	0.05	0.11	0.66	3.98
1L-6	4.92	4.79	0	0.07	0.16	0.73	4.79
1L-7	5.73	5.6	0	0.1	0.19	0.94	5.6
1L-8	6.54	6.41	0	0.12	0.24	1.16	6.41
1L-9	7.35	7.22	0	0.15	0.31	1.17	7.22
1L-10	8.16	8.03	0	0.17	0.37	1.24	8.03
1L-11	8.97	8.84	0	0.19	0.41	1.54	8.84
1L-12	9.78	9.65	0	0.23	0.49	1.54	9.65
1L-13	10.59	10.46	0	0.22	0.51	3.95	10.46

Table A.9-Unit side shear data, Lexington, Missouri test site (TS-2, stage 1).

Load	Upward	Downward	O-cell	Level 1	O-cell	Level 2
Test	Movement	Movement	Net	Avg.	to	Avg.
Incre			Lower	Load	SG-1	Load
	4 min	4 min	Cell		176.17	
	(mm)	(mm)	(MN)	(MN)	to	
					177.67	
					(kPa)	(MN)
1L-0	0	0	0	0	0.00	0
1L-1	-0.08	0.2	0.74	0.08	120.07	0.18
1L-2	-0.03	0.3	1.55	0.17	251.07	0.28
1L-3	-0.01	0.52	2.36	0.27	380.24	0.42
1L-4	0.11	0.95	3.17	0.43	498.49	0.52
1L-5	0.39	2.83	3.98	0.67	602.19	0.66
1L-6	0.8	4.69	4.79	0.78	729.55	0.73
1L-7	1.28	7.46	5.6	0.89	856.90	0.94
1L-8	1.77	10.86	6.41	0.98	987.89	1.16
1L-9	2.34	15.49	7.22	0.96	1138.89	1.17
1L-10	2.95	20.46	8.03	0.82	1311.73	1.24
1L-11	3.94	26.24	8.84	0.52	1513.67	1.54
1L-12	5.24	40.03	9.65	1.6	1464.55	1.54
1L-13	6.94	60.68	10.46	2.35	1475.47	3.95

Load	SG-1	Level 3	SG-2	Level 4	SG-3	SG-4
Test	to	Avg.	to	Avg.	to	to
Incre	SG-2	Load	SG-3	Load	SG-4	TOS
	177.67		178.67		181.67	182.67
	to		to		to	to
	178.67		181.67		182.67	184.4
	(kPa)	(MN)	(kPa)	(MN)	(kPa)	(kPa)
1L-0	0.00	0.00	0.00	0.00	0.00	0.00
1L-1	-27.29	0.00	16.26	0.00	0.00	0.00
1L-2	-30.02	0.02	23.49	0.01	2.69	1.56
1L-3	-40.93	0.03	35.24	0.01	5.39	1.56
1L-4	-24.56	0.04	43.37	0.03	2.69	4.67
1L-5	2.73	0.11	49.69	0.05	16.17	7.79
1L-6	13.64	0.16	51.50	0.07	24.25	10.90
1L-7	-13.64	0.19	67.76	0.10	24.25	15.57
1L-8	-49.12	0.24	83.12	0.12	32.33	18.69
1L-9	-57.31	0.31	77.70	0.15	43.11	23.36
1L-10	-114.62	0.37	78.60	0.17	53.89	26.48
1L-11	-278.36	0.41	102.09	0.19	59.28	29.59
1L-12	16.37	0.49	94.86	0.23	70.05	35.82
1L-13	-436.64	0.51	310.79	0.22	78.14	34.26

Table A.10- Osterberg O-cells™ versus top and bottom plate movement for load increments 2L-0 to 2U-2 (TS-2, stage 2 & 3).

Load Test Incre.	O-cell Loads					Avg. Top of Shaft	Avg. Comp. ECT LEVEL 1 Between cells	Avg. Comp. ECT LEVEL 2 Above upper Cell	Avg. Expansion Upper Cell LVWDT 14991 14992	Shaft Comp.	Upward Mvment Top of Lower Cell	Avg. Expnsion Lower Cell LVWDT 14985 14986	Dwnwrld Mvment
	Upper Cell												
	Lower Cell												
	Gross (MN)	Net* (MN)	Gross (MN)	Up (MN)	Down (MN)	4 min (mm)	4 min (mm)	4 min (mm)	4 min (mm)	4 min (mm)	4 min (mm)	4 min (mm)	4 min (mm)
1	2	3			4	5	6	7	8	9	10	11	12
										6+7-8	5+9		10 - 11
2L-0	0.06	0.00	0.00	0.00	0.00	0.00	6.82	0.00	0.00	6.82	6.82		6.82
2L-1	0.06	0.00	0.85	0.78	0.91	-0.44	6.79	0.01	0.09	6.71	6.27	63.11	-56.84
2L-2	0.06	0.00	1.66	1.59	1.72	-0.48	6.80	0.02	0.17	6.65	6.17	63.02	-56.85
2L-3	0.06	0.00	2.48	2.41	2.54	-0.48	6.80	0.03	0.29	6.54	6.06	62.95	-56.89
2L-4	0.06	0.00	3.29	3.22	3.35	-0.41	6.81	0.11	0.56	6.36	5.95	62.86	-56.91
2L-5	0.06	0.00	4.10	4.03	4.16	-0.44	6.85	0.30	1.19	5.96	5.52	62.74	-57.22
2L-6	0.06	0.00	4.91	4.84	4.97	-0.48	6.88	0.44	1.76	5.56	5.08	62.57	-57.49
2L-7	0.06	0.00	5.72	5.65	5.78	-0.27	6.93	0.57	2.35	5.15	4.88	62.37	-57.49
2L-8	0.06	0.00	6.53	6.46	6.59	-0.27	6.99	0.70	2.96	4.73	4.46	62.13	-57.67
2L-9	0.06	0.00	7.34	7.27	7.40	-0.10	7.06	0.84	3.67	4.23	4.13	61.82	-57.69
2L-10	0.06	0.00	8.16	8.09	8.22	0.10	7.16	0.98	4.64	3.50	3.60	61.46	-57.86
2L-11	0.06	0.00	8.97	8.90	9.03	0.31	7.37	1.14	6.57	1.94	2.25	61.03	-58.78
2L-12	0.06	0.00	9.78	9.71	9.84	0.96	7.78	1.33	9.93	-0.82	0.14	60.58	-60.44
2L-13	0.06	0.00	10.59	10.52	10.65	1.47	8.62	1.56	15.91	-5.73	-4.26	60.00	-64.26
2L-14	1.89	1.76	11.40	11.33	11.33	2.32	12.10	2.08	47.21	-33.03	-30.71	57.37	-88.08
2L-15	3.31	3.18	12.21	12.14	12.14	2.56	13.61	2.75	67.71	-51.35	-48.79	56.75	-105.54
2L-16	4.61	4.48	13.03	12.96	12.96	3.31	15.99	3.22	130.92	111.71	-108.40	56.25	-164.65
2L-17	5.23	5.10	13.35	13.28	13.28	3.72	16.51	3.56	148.15	128.08	-124.36	56.05	-180.41
2U-1	3.53	3.40	0.00	0.00	0.00	2.79	15.97	3.17			2.79		2.79
2U-2	3.22	3.09	0.00	0.00	0.00	2.44	15.93	3.14			2.44		2.44

* Net load calculated as Lower O-cell™ load minus weight of shaft above Lower O-cell™ = 0.13 MN.

** Net load calculated as Upper O-cell™ load minus weight of shaft above Upper O-cell™ = 0.07 MN.

*** Net load calculated as Upper O-cell™ load plus weight of shaft between the O-cells™ = 0.06 MN (2L-1 to 2L-13).

*** Net load calculated as Upper O-cell™ load minus weight of shaft above the upper O-cells™ = 0.07 MN (2L-14 to 2L-17).

Table A.11-Creep data, Lexington, Missouri test site (TS-2, stage 2 & 3).

Load Test Incr.	O-cell Load Upper cell Net (MN)	Upward Mvment Top of Upper Cell 2 min (mm)	Upward Mvment Top of Upper Cell 4 min (mm)	Creep 2 to 4 min Stages 2&3 (mm)	Dwnwrđ Mvment Bott of Upper Cell 2 min (mm)	Dwnwrđ Mvment Bott of Upper Cell 4 min (mm)	Creep 2 to 4 min Stage 2 (mm)
2L-0	0	0	0	0.00	0	0	0
2L-1	0.79	-0.03	0.04	0.07	0.11	0.05	-0.06
2L-2	1.6	-0.1	0.01	0.11	0.27	0.17	-0.1
2L-3	2.42	0.03	0.02	-0.01	0.25	0.26	0.01
2L-4	3.23	0.07	0.17	0.10	0.48	0.4	-0.08
2L-5	4.04	0.37	0.32	-0.05	0.78	0.87	0.09
2L-6	4.85	0.52	0.43	-0.09	1.16	1.33	0.17
2L-7	5.66	0.68	0.76	0.08	1.61	1.59	-0.02
2L-8	6.47	0.89	0.9	0.01	2	2.06	0.06
2L-9	7.29	1.16	1.21	0.05	2.39	2.46	0.07
2L-10	8.1	1.53	1.55	0.02	2.9	3.09	0.19
2L-11	8.91	1.94	1.91	-0.03	4.16	4.66	0.5
2L-12	9.72	2.56	2.75	0.19	6.52	7.18	0.66
2L-13	10.53	3.4	3.49	0.09	10.39	12.42	2.03
2L-14	11.34	4.65	4.87	0.22	38.43	42.34	
2L-15	12.15	5.68	5.78	0.10	57.94	61.93	
2L-16	12.97	6.93	7	0.07	118.21	123.93	
2L-17	13.29	7.51	7.75	0.24	134.69	140.4	

Table A.12-Load distribution data, Lexington, Missouri test site (TS-2, stage 2 & 3).

Load Test Incr.	Top of Conc Avg. Load (MN)	Level 4 Avg. Load (MN)	Level 3 Avg. Load (MN)	Upper-Cell Net Load (MN)	Lower Cell Net Load (MN)
Elevation	184.4	182.67	181.67	180.17	176.17
2L-0	0	0.04	0.13	0	0.06
2L-1	0	0.03	0.16	0.78	0.06
2L-2	0	0.05	0.2	1.59	0.06
2L-3	0	0.08	0.24	2.41	0.06
2L-4	0	0.14	0.42	3.22	0.06
2L-5	0	0.32	0.9	4.03	0.06
2L-6	0	0.45	1.24	4.84	0.06
2L-7	0	0.57	1.57	5.65	0.06
2L-8	0	0.69	1.9	6.46	0.06
2L-9	0	0.79	2.22	7.27	0.06
2L-10	0	0.88	2.51	9.09	0.06
2L-11	0	0.97	2.78	8.9	0.06
2L-12	0	1.06	2.95	9.71	0.06
2L-13	0	1.16	3.19	10.52	0.06
2L-14	0	1.24	3.45	11.33	1.89
2L-15	0	1.36	3.72	12.14	3.3
2L-16	0	1.42	3.92	12.96	4.61
2L-17	0	1.52	4.09	13.28	5.23

Table A.13-Unit side shear data, Lexington, Missouri test site (TS-2, stage 2 & 3).

Load Test Icre.	Upper Cell		Bottom of Cell	O-cell to Upper cell	Upper Cell Net Load	Upper cell to SG-3	Level 3 Avg. Load	SG-3 to SG-4	Level 4 Avg. Load	SG-4 to TOS	Upper Cell to TOS
	Upward	Dwnwrđ									
	Mvment Top of Cell	Mvment									
			Net Load	176.17 to 180.17		180.17 to 181.67		181.67 to 182.67		182.67 to 184.4	180.17 to 184.4
	4 min (mm)	4 min (mm)	176.17 (MN)	(kPa)	180.17 (MN)	(kPa)	181.67 (MN)	(kPa)	182.67 (MN)	184.4 (kPa)	(kPa)
2L-0	0.00	0	0.06	0.00	0	0.00	0.13	24.25	0.04	6.23	0.00
2L-1	0.04	0.05	0.06	49.12	0.78	111.37	0.16	35.03	0.03	4.67	49.68
2L-2	0.01	0.16	0.06	104.38	1.59	249.68	0.2	40.42	0.05	7.79	101.28
2L-3	0.02	0.27	0.06	160.33	2.41	389.78	0.24	43.11	0.08	12.46	153.51
2L-4	0.17	0.39	0.06	215.59	3.22	502.94	0.42	75.44	0.14	21.80	205.10
2L-5	0.33	0.86	0.06	270.85	4.03	562.22	0.9	156.27	0.32	49.84	256.70
2L-6	0.43	1.33	0.06	326.11	4.84	646.64	1.24	212.85	0.45	70.08	308.29
2L-7	0.77	1.58	0.06	381.37	5.65	732.86	1.57	269.43	0.57	88.77	359.88
2L-8	0.90	2.06	0.06	436.64	6.46	819.08	1.9	326.02	0.69	107.46	411.48
2L-9	1.21	2.46	0.06	491.90	7.27	907.10	2.22	385.29	0.79	123.04	463.07
2L-10	1.55	3.09	0.06	548.52	8.1	1004.09	2.51	439.18	0.88	137.05	515.94
2L-11	1.92	4.65	0.06	603.10	8.9	1099.29	2.78	487.68	0.97	151.07	566.89
2L-12	2.76	7.17	0.06	658.37	9.71	1214.25	2.95	509.23	1.06	165.09	618.49
2L-13	3.50	12.41	0.06	713.63	10.52	1316.64	3.19	546.95	1.16	180.66	670.08
2L-14	4.87	42.34	1.89	644.04	11.33	1415.43	3.45	595.45	1.24	193.12	721.68
2L-15	5.78	61.93	3.3	603.10	12.14	1512.42	3.72	635.86	1.36	211.81	773.27
2L-16	7.00	123.92	4.61	569.67	12.96	1623.79	3.92	673.59	1.42	221.15	825.50
2L-17	7.75	140.4	5.23	549.21	13.28	1650.73	4.09	692.45	1.52	236.73	845.88

Table A.14- Unconfined compressive strength of NX rock cores

	Mulky	Lagonda	Bevier C1	Bevier C2	Verdigris	Croweburg	Fleming
	(kPa)	(kPa)	(kPa)	(kPa)	(kPa)	(kPa)	(kPa)
	340	680	5759	1948	386	1540	150
	140	140	5465	2060	724	443	333
	110	720	1320	3005	423	1695	620
	310	4807	2473	1646	1280	600	360
		7520	3412	2330	2440	568	195
		510	1648	7130	477	253	1241
		1381	8105	1579	4482	2760	908
		2060	2097	4108	2290	340	
		720	3282	2213	660	3844	
		1907	2140	1600	1727	1760	
		2440	2101	2870	310	452	
		1141	1020	1996	339	1562	
		780	7006	3168	218	5590	
		949	5788	11550		2620	
		914	7806	311			
		1120	5481	2332			
		860	4500	2855			
		637	1579	1320			
		535	2494				
			2578				
			3650				
			7870				
			2581				
			2662				
			2468				
Mean	225	1570	3811	3001	1212	1716	544
Std. Dev.	117	1775	2210	2565	1245	1552	404

Table A.15- Unconfined compressive strength and SPT data for Mulky and Lagonda Formations.

Boring	Elev.	Unconfined Compressive Strength and SPT Data					
		Pier 19	Pier 20	Pier 21	Pier 22	Pier 23	Pier 24
	(m)	(kPa)	(kPa)	(kPa)	(kPa)	(kPa)	(kPa)
		Mulky					
F-41	200.7						340
F-42	200.0						140
F-41	199.0						110
F-41	197.7						310
		Lagonda					
F-42	197.2						680
F-39	195.6					140	
F-40	195.4					720	
F-39	194.4					12,255*	
B-14	193.7				50 in 8 cm		
B-13	192.7				4807		
F-42	192.5						25,830*
B-15	192.3				50 in 6 cm		
F-39	191.9					7520	
F-40	191.7					510	
B-13	191.5				1381		
F-39	191.3					2060	
B-14	191.1				100 in 13 cm		
B-15	191.1				720		
B-14	190.3				1907		
B-13	190.1				50 in 8 cm		
F-39	189.8					2440	
B-15	189.7				1141		
F-40	189.4					780	
B-13	189.1				949		
B-15	188.9				50 in 11 cm		
B-14	188.9				914		
F-39	188.3					1120	
F-40	188.1					860	
B-13	187.9				637		
B-15	187.9				535		

* Values not used in calculation of mean

Table A.16- Unconfined compressive strength and SPT data for Bevier C1 Formation.

Boring	Elev.	Unconfined Compressive Strength and SPT Data					
		Pier 19	Pier 20	Pier 21	Pier 22	Pier 23	Pier 24
	(m)	(kPa)	(kPa)	(kPa)	(kPa)	(kPa)	(kPa)
		Bevier C1					
B-15	186.9				5759		
F-39	186.7					5465	
B-14	186.5				50 in 8 cm		
B-15	185.8				50 in 7 cm		
B-13	185.7				1320		
B-12	185.6			100 in 21 cm			
B-13	185.6				50 in 6 cm		
Pier 22	185.0	Scour	Depth				
B-13	185.0				2473		
B-14	185.0				3412		
B-15	184.8				1648		
B-11	184.1			50 in 4 cm			
TS-2	183.8				2140		
B-12	183.7			8105			
B-15	183.7				2097		
B-10	183.5			3282			
B-13	183.2				2101		
TS-2	183.1				1020		
B-11	183.0			7006			
B-15	182.8				50 in 5 cm		
B-12	182.7			5788			
B-14	182.6				7806		
Pier 21	182.1	Scour	Depth				
B-10	181.9			5481			
TS-2	181.9				4500		
B-14	181.9				50 in 6 cm		
B-3	181.4				100 in 8 cm		
B-13	181.3				2494		
B-9			50 in 6 cm				
B-13	181.0				50 in 6 cm		
B-13	180.7				2578		
TS-2	180.7				3650		
B-3	180.6		7870				
B-10	180.6			2581			
B-14	180.6				2662		

Table A.17- Unconfined compressive strength and SPT data for Bevier C2 Formation.

Boring	Elev.	Unconfined Compressive Strength and SPT Data					
		Pier 19	Pier 20	Pier 21	Pier 22	Pier 23	Pier 24
	(m)	(kPa)	(kPa)	(kPa)	(kPa)	(kPa)	(kPa)
		Bevier C2					
B-12	180.3			100 in 8cm			
B-15	180.3				2468		
B-14	179.9				1948		
B-8	179.8		2060				
B-12	179.8			3005			
B-3	179.6				100 in 13 cm		
B-11	179.5			50 in 6 cm			
F-36	179.3	100 in 10cm					
F-37	179.3	100 in 8 cm					
B-10	179.2			1646			
TS-2	179.2				2330		
B-3	179.0		7130				
B-15	179.0				1579		
B-11	178.5			4108			
B-13	178.4				2213		
B-8	178.2		1600				
B-9	177.9		100 in 9 cm				
F-37	177.9	2870					
B-10	177.9			1996			
B-9	177.7		3168				
B-3	177.6		11,550				
B-12	177.5			311			
B-15	177.5				2332		
B-14	177.4				50 in 10 cm		
B-14	177.1				2855		
B-8	176.9			1320			

Table A.18- Unconfined compressive strength and SPT data for Verdigris Formation.

Boring	Elev.	Unconfined Compressive Strength and SPT Data					
		Pier 19	Pier 20	Pier 21	Pier 22	Pier 23	Pier 24
	(m)	(kPa)	(kPa)	(kPa)	(kPa)	(kPa)	(kPa)
		Verdigris					
B-12	176.4			386			
B-3	176.3				100 in 6 cm		
F-36	176.2	100 in 11 cm					
B-10	176.1			724			
B-14	176.1				423		
B-11	175.8			1280			
B-3	175.4		2440				
B-9	175.3		477				
B-12	175.1			4482			
TS-2	175.1				2290		
F-37	174.9	100 in 18 cm					
B-9	174.8		50 in 8 cm				
B-3	174.7				100 in 11 cm		
B-10	174.4			1727			
TS-2	174.3				310		
B-12	174.2			100 in 14 cm			
B-9	173.9		339				
B-11	173.5			50 in 10 cm			
B-11	173.3			218			

Table A.19- Unconfined compressive strength and SPT data for Croweburg Formation and Fleming Formation.

Boring	Elev.	Unconfined Compressive Strength and SPT Data					
		Pier 19	Pier 20	Pier 21	Pier 22	Pier 23	Pier 24
	(m)	(kPa)	(kPa)	(kPa)	(kPa)	(kPa)	(kPa)
		Croweburg					
F-36	173.1	100 in 14 cm					
B-3	173.1				100 in 2 cm		
B-8	172.8		1540				
B-10	172.8			443			
B-3	172.6		16460*				
B-9	172.0		1695				
TS-2	171.9				600		
B-3	171.6				100 in 15 cm		
B-12	171.1			568			
B-10	171.0			253			
B-8	170.8		2760				
TS-2	170.7				340		
B-10	170.6			3844			
B-3	170.4		1760				
F-37	169.9	170*					
B-12	169.6			452			
B-12	169.5			100 in 1 cm			
B-11	169.4			1562			
B-8	169.1		5590				
B-3	168.9		2620				
		Fleming					
TS-2	168.7				150		
B-9	168.6		333				
B-3	168.3				100 in 6 cm		
TS-2	168.0				620		
B-8	167.9		360				
TS-2	167.2				195		
B-9	166.9		1241				
B-9	165.4		908				

* Values not used in calculation of mean

APPENDIX B
DETAILED DATA FOR LOAD TESTS AND UNCONFINED COMPRESSIVE
STRENGTH OF NX CORES AT GRANDVIEW SITE

Table B.1
Summary of Dimensions, Elevations, and Shaft Properties

Shaft:

Average Shaft Diameter (EL 934.0 ft to 905.0 ft)	=	1976 mm	77.8 in
Average Shaft Diameter (EL 905.0 ft to 893.4 ft)	=	1938 mm	76.3 in
O-cell TM : 2173-3	=	870 mm	34 in
Length of side shear above break at base of O-cell TM	=	8.64 m	29.0 ft
Length of side shear below break at base of O-cell TM	=	3.54 m	11.6 ft
Shaft side shear area above O-cell TM base	=	53.64 m ²	590.7 ft ²
Shaft side shear area below break at base of O-cell TM	=	21.55 m ²	231.7 ft ²
Shaft base area	=	2.95 m ²	31.8 ft ²
Bouyant weight of shaft above base of O-cell TM	=	0.53 MN	118 kips
Estimated shaft stiffness (EL 934.0 ft to 905.0 ft)	=	93,800 MN	21,100,000 kips
Estimated shaft stiffness (EL 905.0 ft to 893.4 ft)	=	90,300 MN	20,300,000 kips
Elevation of Water Table	=	279.61 m	917.4 ft
Elevation of Mud line	=	287.23 m	942.4 ft
Elevation top of shaft concrete	=	284.67 m	934.0 ft
Elevation of base of O-cell TM	=	275.84 m	905.0 ft
Elevation of shaft tip	=	272.29 m	893.4 ft

Casing:

Elevation of top of temporary casing (2134 mm O.D.)	=	287.53 m	943.4 ft
Elevation of bottom of temporary casing (84 in O.D.)	=	285.32 m	936.1 ft

Compression Sections:

EL. of top of telltale used for upper shaft compression	=	284.67 m	934.0 ft
EL. of bottom of telltale used upper shaft compression	=	276.23 m	906.3 ft
EL. of top of telltale used lower shaft compression	=	275.79 m	904.8 ft
EL. of bottom of telltale used lower shaft compression	=	272.36 m	893.6 ft

Strain Gages:

Elevation of strain gage level 6	=	282.54 m	927.0 ft
Elevation of strain gage level 5	=	280.71 m	921.0 ft
Elevation of strain gage level 4	=	279.34 m	916.5 ft
Elevation of strain gage level 3	=	277.81 m	911.5 ft
Elevation of strain gage level 2	=	274.62 m	901.0 ft
Elevation of strain gage level 1	=	273.70 m	898.0 ft

Miscellaneous:

Top Plate Diameter	=	1676 mm	66 in
Bottom Plate Diameter	=	1676 mm	66 in
Frame cross sectional area (2 No. C4x7.25)	=	2748 m ²	4.26 in ²
Rebar cage diameter	=	1676 mm	66 in
Spiral size (60 in spacing)	=	M 16	# 5
Unconfined compressive concrete strength	=	41.4 MPa	6000 psi
O-cell TM LVWDTs @ 0 ⁰ , 90 ⁰ , and 180 ⁰ with radius	=	500 mm	20 in

Table B.2- Osterberg O-cell™ versus top and bottom plate movement for load increments 1L-0 to 1L-21.

Load	Hold	O-cell Loads				Top of	Upper	Upward Mvemnt		O-cell		Dnwrđ Mvment	
Test Ince	Time Min	Gross (MN)	Gross (tons)	Net (MN)	Net (tons)	Shaft (in)	Compre (in)	Top Plate (mm) (in)		expansion (mm) (in)		(mm)	(in)
						A	B	A + B		C		A + B - C	
1L-0		0.00	0	0	0	0	0	0.00	0	0	0	0	0
1L-1	1	1.72	193.5	1.19	134.5	0.004	0.002	0.15	0.006	0.33	0.013	-0.18	-0.007
1L-1	2	1.63	183.5	1.10	124.5	0.004	0.002	0.15	0.006	0.33	0.013	-0.18	-0.007
1L-1	4	1.72	193.6	1.19	134.6	0.004	0.002	0.15	0.006	0.33	0.013	-0.18	-0.007
1L-2	1	3.26	367	2.73	308	0.005	0.002	0.18	0.007	0.36	0.014	-0.18	-0.007
1L-2	2	3.26	367	2.73	308	0.005	0.002	0.18	0.007	0.36	0.014	-0.18	-0.007
1L-2	4	3.26	367	2.73	308	0.005	0.002	0.18	0.007	0.36	0.014	-0.18	-0.007
1L-3	1	4.90	550.5	4.37	491.5	0.007	0.003	0.25	0.010	0.43	0.017	-0.18	-0.007
1L-3	2	4.90	550.5	4.37	491.5	0.007	0.003	0.25	0.010	0.43	0.017	-0.18	-0.007
1L-3	4	4.90	550.5	4.37	491.5	0.007	0.003	0.25	0.010	0.43	0.017	-0.18	-0.007
1L-4	1	6.53	734	6.00	675	0.007	0.004	0.28	0.011	0.46	0.018	-0.18	-0.007
1L-4	2	6.53	734	6.00	675	0.008	0.004	0.30	0.012	0.46	0.018	-0.15	-0.006
1L-4	4	6.53	734	6.00	675	0.008	0.004	0.30	0.012	0.48	0.019	-0.18	-0.007
1L-5	1	8.16	917.5	7.63	858.5	0.010	0.005	0.38	0.015	0.56	0.022	-0.18	-0.007
1L-5	2	8.16	917.5	7.63	858.5	0.010	0.006	0.41	0.016	0.53	0.021	-0.13	-0.005
1L-5	4	8.16	917.5	7.63	858.5	0.012	0.006	0.46	0.018	0.56	0.022	-0.10	-0.004
1L-6	1	9.79	1101	9.26	1042	0.014	0.007	0.53	0.021	0.69	0.027	-0.15	-0.006
1L-6	2	9.79	1101	9.26	1042	0.015	0.006	0.53	0.021	0.64	0.025	-0.10	-0.004
1L-6	4	9.79	1101	9.26	1042	0.015	0.007	0.56	0.022	0.66	0.026	-0.10	-0.004
1L-7	1	11.43	1284.5	10.90	1225.5	0.020	0.008	0.71	0.028	1.02	0.04	-0.30	-0.012
1L-7	2	11.43	1284.5	10.90	1225.5	0.019	0.008	0.69	0.027	1.07	0.042	-0.38	-0.015
1L-7	4	11.43	1284.5	10.90	1225.5	0.020	0.009	0.74	0.029	1.07	0.042	-0.33	-0.013
1L-8	1	13.06	1468	12.53	1409	0.024	0.010	0.86	0.034	1.17	0.046	-0.30	-0.012
1L-8	2	13.06	1468	12.53	1409	0.025	0.010	0.89	0.035	1.19	0.047	-0.30	-0.012
1L-8	4	13.06	1468	12.53	1409	0.026	0.010	0.91	0.036	1.24	0.049	-0.33	-0.013
1L-9	1	14.69	1651.5	14.16	1592.5	0.036	0.011	1.19	0.047	1.63	0.064	-0.43	-0.017
1L-9	2	14.69	1651.5	14.16	1592.5	0.036	0.012	1.22	0.048	1.68	0.066	-0.46	-0.018
1L-9	4	14.69	1651.5	14.16	1592.5	0.036	0.012	1.22	0.048	1.73	0.068	-0.51	-0.020
1L-10	1	16.32	1835	15.79	1776	0.044	0.013	1.45	0.057	1.91	0.075	-0.46	-0.018
1L-10	2	16.32	1835	15.79	1776	0.046	0.013	1.50	0.059	2.29	0.09	-0.79	-0.031
1L-10	4	16.32	1835	15.79	1776	0.050	0.013	1.60	0.063	2.34	0.092	-0.74	-0.029
1L-11	1	17.96	2018.5	17.43	1959.5	0.062	0.015	1.96	0.077	2.62	0.103	-0.66	-0.026
1L-11	2	17.96	2018.5	17.43	1959.5	0.066	0.015	2.06	0.081	3.07	0.121	-1.02	-0.040
1L-11	4	17.96	2018.5	17.43	1959.5	0.071	0.015	2.18	0.086	3.15	0.124	-0.97	-0.038
1L-12	1	19.59	2202	19.06	2143	0.085	0.017	2.59	0.102	3.71	0.146	-1.12	-0.044
1L-12	2	19.59	2202	19.06	2143	0.090	0.017	2.72	0.107	3.81	0.15	-1.09	-0.043
1L-12	4	19.59	2202	19.06	2143	0.096	0.017	2.87	0.113	3.94	0.155	-1.07	-0.042
1L-13	1	21.22	2385.5	20.69	2326.5	0.113	0.019	3.35	0.132	4.09	0.161	-0.74	-0.029
1L-13	2	21.22	2385.5	20.69	2326.5	0.121	0.019	3.56	0.140	4.72	0.186	-1.17	-0.046
1L-13	4	21.22	2385.5	20.69	2326.5	0.127	0.019	3.71	0.146	5.26	0.207	-1.55	-0.061

Table B.2- Continued

Load	Hold	O-cell Loads				Top of	Upper	Upward Mvemnt		O-cell		Dnwrđ Mvmnt	
Test Inre	Time Min	Gross (MN)	Gross (tons)	Net (MN)	Net (tons)	Shaft (in)	Compre (in)	Top Plate (mm) (in)		expansion (mm) (in)		(mm)	(in)
						A	B	A + B		C		A + B - C	
1L-14	1	22.85	2568.5	22.32	2509.5	0.157	0.021	4.52	0.178	6.17	0.243	-1.65	-0.065
1L-14	2	22.85	2568.5	22.32	2509.5	0.162	0.021	4.65	0.183	6.27	0.247	-1.63	-0.064
1L-14	4	22.86	2569.5	22.33	2510.5	0.171	0.021	4.88	0.192	6.43	0.253	-1.55	-0.061
1L-15	1	24.48	2752	23.95	2693	0.197	0.023	5.59	0.220	7.32	0.288	-1.73	-0.068
1L-15	2	24.48	2752	23.95	2693	0.207	0.023	5.84	0.230	7.87	0.31	-2.03	-0.080
1L-15	4	24.48	2752	23.95	2693	0.220	0.023	6.17	0.243	8.08	0.318	-1.91	-0.075
1L-16	1	26.11	2935.5	25.58	2876.5	0.250	0.025	6.99	0.275	9.12	0.359	-2.13	-0.084
1L-16	2	26.11	2935.5	25.58	2876.5	0.267	0.025	7.42	0.292	9.65	0.38	-2.24	-0.088
1L-16	4	26.11	2935.5	25.58	2876.5	0.285	0.025	7.87	0.310	10.36	0.408	-2.49	-0.098
1L-17	1	27.75	3119	27.22	3060	0.321	0.026	8.81	0.347	11.43	0.45	-2.62	-0.103
1L-17	2	27.75	3119	27.22	3060	0.329	0.026	9.02	0.355	11.56	0.455	-2.54	-0.100
1L-17	4	27.75	3119	27.22	3060	0.358	0.026	9.75	0.384	12.78	0.503	-3.02	-0.119
1L-18	1	29.38	3302.5	28.85	3243.5	0.432	0.027	11.66	0.459	14.81	0.583	-3.15	-0.124
1L-18	2	29.38	3302.5	28.85	3243.5	0.454	0.028	12.24	0.482	15.37	0.605	-3.12	-0.123
1L-18	4	29.38	3302.5	28.85	3243.5	0.483	0.028	12.98	0.511	16.21	0.638	-3.23	-0.127
1L-19	1	31.01	3486	30.48	3427	0.561	0.028	14.96	0.589	18.47	0.727	-3.51	-0.138
1L-19	2	31.01	3486	30.48	3427	0.581	0.028	15.47	0.609	19.28	0.759	-3.81	-0.150
1L-19	4	31.01	3486	30.48	3427	0.622	0.029	16.54	0.651	20.37	0.802	-3.84	-0.151
1L-20	1	32.64	3669.5	32.11	3610.5	0.746	0.030	19.71	0.776	23.85	0.939	-4.14	-0.163
1L-20	2	32.64	3669.5	32.11	3610.5	0.797	0.030	21.01	0.827	25.48	1.003	-4.47	-0.176
1L-20	4	32.64	3669.5	32.11	3610.5	0.874	0.030	22.96	0.904	27.43	1.08	-4.47	-0.176
1L-21	1	33.76	3795	33.23	3736	1.098	0.030	28.65	1.128	33.66	1.325	-5.00	-0.197
1L-21	2	33.87	3807	33.34	3748	1.191	0.030	31.01	1.221	36.07	1.42	-5.05	-0.199
1L-21	4	34.30	3856	33.77	3797	1.380	0.029	35.79	1.409	41.48	1.633	-5.69	-0.224
1L-21	7	33.76	3795	33.23	3736	1.683	0.028	43.46	1.711	48.82	1.922	-5.36	-0.211
1U-1	1	20.67	2324	20.14	2265	1.712	0.019	43.97	1.731	50.88	2.003	-6.91	-0.272
1U-1	2	20.67	2324	20.14	2265	1.711	0.019	43.94	1.730	50.77	1.999	-6.83	-0.269
1U-1	4	20.67	2324	20.14	2265	1.708	0.019	43.87	1.727	50.42	1.985	-6.55	-0.258
1U-2	1	15.23	1712.5	14.70	1653.5	1.642	0.014	42.06	1.656	48.06	1.892	-5.99	-0.236
1U-2	2	15.23	1712.5	14.70	1653.5	1.638	0.014	41.96	1.652	47.90	1.886	-5.94	-0.234
1U-2	4	15.23	1712.5	14.70	1653.5	1.634	0.014	41.86	1.648	47.88	1.885	-6.02	-0.237
1U-3	1	9.79	1101	9.26	1042	1.533	0.010	39.19	1.543	44.50	1.752	-5.31	-0.209
1U-3	2	9.79	1101	9.26	1042	1.519	0.010	38.84	1.529	43.99	1.732	-5.16	-0.203
1U-3	4	9.79	1101	9.26	1042	1.513	0.009	38.66	1.522	43.87	1.727	-5.21	-0.205
1U-4	1	4.35	489.5	3.82	430.5	1.313	0.005	33.48	1.318	37.52	1.477	-4.04	-0.159
1U-4	2	4.35	489.5	3.82	430.5	1.303	0.005	33.22	1.308	37.41	1.473	-4.19	-0.165
1U-4	4	4.35	489.5	3.82	430.5	1.298	0.006	33.12	1.304	37.11	1.461	-3.99	-0.157
1U-5	1	0.00	0	-0.53	-59	0.992	0.001	25.22	0.993	28.47	1.121	-3.25	-0.128
1U-5	2	0.00	0	-0.53	-59	0.979	0.001	24.89	0.980	28.27	1.113	-3.38	-0.133
1U-5	4	0.00	0	-0.53	-59	0.964	0.000	24.49	0.964	27.71	1.091	-3.23	-0.127

Table B.3-Creep Data, Grandview, Missouri Test Site (English version).

	O-cell Load	Upward Mvment Top of Cell	Upward Mvment Top of Cell	Creep 2 to 4 min	Downward Mvment Bott of Cell	Downward Mvment Bott of Cell	Creep 2 to 4 min
	Net (Tons)	2 min (in)	4 min (in)	(in)	2 min (in)	4 min (in)	(in)
1L-0	0.0	0.000	0.000	0.000	0.000	0.000	0.000
1L-1	134.6	0.006	0.006	0.000	0.007	0.007	0.000
1L-2	308.0	0.007	0.007	0.000	0.007	0.007	0.000
1L-3	491.5	0.010	0.010	0.000	0.007	0.007	0.000
1L-4	675.0	0.012	0.012	0.000	0.006	0.007	0.001
1L-5	858.5	0.016	0.018	0.002	0.005	0.004	-0.001
1L-6	1042.0	0.021	0.022	0.001	0.004	0.004	0.000
1L-7	1225.5	0.027	0.029	0.002	0.015	0.013	-0.002
1L-8	1409.0	0.035	0.036	0.001	0.012	0.013	0.001
1L-9	1592.5	0.048	0.048	0.000	0.018	0.020	0.002
1L-10	1776.0	0.059	0.063	0.004	0.031	0.029	-0.002
1L-11	1959.5	0.081	0.086	0.005	0.040	0.038	-0.002
1L-12	2143.0	0.107	0.113	0.006	0.043	0.042	-0.001
1L-13	2326.6	0.140	0.146	0.006	0.046	0.061	0.015
1L-14	2509.5	0.183	0.192	0.009	0.064	0.061	-0.003
1L-15	2693.0	0.230	0.243	0.013	0.080	0.075	-0.005
1L-16	2876.5	0.292	0.310	0.018	0.088	0.098	0.010
1L-17	3060.0	0.355	0.384	0.029	0.100	0.119	0.019
1L-18	3243.5	0.482	0.511	0.029	0.123	0.127	0.004
1L-19	3427.0	0.609	0.651	0.042	0.150	0.151	0.001
1L-20	3610.5	0.827	0.904	0.077	0.176	0.176	0.000
1L-21	3797.0	1.221	1.409	0.188	0.199	0.224	0.025

Table B.4-Creep Data, Grandview, Missouri Test Site (Metric version).

	O-cell Load	Upward Mvment Top of Cell	Upward Mvment Top of Cell	Creep 2 to 4 min	Downward Mvment Bott of Cell	Downward Mvment Bott of Cell	Creep 2 to 4 min
	Net (MN)	2 min (mm)	4 min (mm)	(mm)	2 min (mm)	4 min (mm)	(mm)
1L-0	0.0	0.000	0.000	0.000	0.000	0.000	0.000
1L-1	1.2	0.152	0.152	0.000	0.178	0.178	0.000
1L-2	2.7	0.178	0.178	0.000	0.178	0.178	0.000
1L-3	4.4	0.254	0.254	0.000	0.178	0.178	0.000
1L-4	6.0	0.305	0.305	0.000	0.152	0.178	0.025
1L-5	7.6	0.406	0.457	0.051	0.127	0.102	-0.025
1L-6	9.3	0.533	0.559	0.025	0.102	0.102	0.000
1L-7	10.9	0.686	0.737	0.051	0.381	0.330	-0.051
1L-8	12.5	0.889	0.914	0.025	0.305	0.330	0.025
1L-9	14.2	1.219	1.219	0.000	0.457	0.508	0.051
1L-10	15.8	1.499	1.600	0.102	0.787	0.737	-0.051
1L-11	17.4	2.057	2.184	0.127	1.016	0.965	-0.051
1L-12	19.1	2.718	2.870	0.152	1.092	1.067	-0.025
1L-13	20.7	3.556	3.708	0.152	1.168	1.549	0.381
1L-14	22.3	4.648	4.877	0.229	1.626	1.549	-0.076
1L-15	24.0	5.842	6.172	0.330	2.032	1.905	-0.127
1L-16	25.6	7.417	7.874	0.457	2.235	2.489	0.254
1L-17	27.2	9.017	9.754	0.737	2.540	3.023	0.483
1L-18	28.9	12.243	12.979	0.737	3.124	3.226	0.102
1L-19	30.5	15.469	16.535	1.067	3.810	3.835	0.025
1L-20	32.1	21.006	22.962	1.956	4.470	4.470	0.000
1L-21	33.8	31.013	35.789	4.775	5.055	5.690	0.635

Table B.5- Strain gage data, Grandview, Missouri test site (English Units).

Load Test Incre.	Top of Conc Avg. Net Load (tons)	Level 6 Avg. Net Load (tons)	Level 5 Avg. Net Load (tons)	Level 4 Avg. Net Load (tons)	O-Cell™ Gross Load (tons)	Level 1 Avg. Gross Load (tons)	Tip Avg. Load (tons)
EL (ft)	934	927	921	916.5	905	898	893.4
1L-0	0	0	0	0	0	0	0
1L-1	0	20.5	35.5	60	183.5	35	0
1L-3	0	40.0	72	126	550.5	73.5	0
1L-5	0	67	122	211	917.5	116.5	0
1L-7	0	110.5	202.5	338	1284.5	170.5	0
1L-9	0	167.5	312.5	510.5	1651.5	243	0
1L-11	0	227	440.5	722	2153.5	324	0
1L-13	0	274.5	563.5	940	2385.5	433	0
1L-15	0	310	683	1131	2752	514.5	0
1L-17	0	348.5	789.5	1263	3119	550	0
1L-19	0	407.5	890	1353.5	3486	501	0
1L-21	0	446.5	805.5	1230	3856	498	0
Level 2 & 3 strain gages yielded unusual/ unreliable data and are not included							

Table B.6- Strain gage data, Grandview, Missouri test site (Metric Units).

Load Test Incr.	Top of Conc Avg. Net Load (MN)	Level 6 Avg. Net Load (MN)	Level 5 Avg. Net Load (MN)	Level 4 Avg. Net Load (MN)	O-Cell™ Gross Load (MN)	Level 1 Avg. Gross Load (MN)	Tip Avg. Load (MN)
EL (m)	284.7	282.5	280.7	279.3	275.8	273.7	272.3
1L-0	0	0.00	0.00	0	0	0	0
1L-1	0	0.18	0.32	0.53	1.63	0.31	0
1L-3	0	0.36	0.64	1.12	4.90	0.65	0
1L-5	0	0.60	1.09	1.88	8.16	1.04	0
1L-7	0	0.98	1.80	3.01	11.40	1.52	0
1L-9	0	1.49	2.78	4.54	14.69	2.16	0
1L-11	0	2.02	3.92	6.42	19.16	2.88	0
1L-13	0	2.44	5.01	8.36	21.22	3.85	0
1L-15	0	2.76	6.08	10.06	24.48	4.58	0
1L-17	0	3.10	7.02	11.24	27.75	4.89	0
1L-19	0	3.63	7.92	12.04	31.01	4.46	0
1L-21	0	3.97	7.17	10.94	34.30	4.43	0
Level 2 & 3 strain gages yielded unusual/ unreliable data and are not included							

Table B.7- Unit strain gage data, Grandview, Missouri test site (English Units).

Load Test Incr.	O-cell Loads		Upwrd	Bottom	Tip to SG-1	Level 1	SG-1 to O-cell	Level 4
				of	Wea	Avg.	Westerville	Avg.
	Gross (tons)	Net (tons)	Mvment (in)	Cell (in)	893.4 to 898 (tsf)	Load (tons)	898 to 905 (tsf)	Load (tons)
1L-0	0	0	0	0	0	0	0	0
1L-1	184	125	0.006	0.007	0.2	35	1.1	60
1L-2	367	308	0.007	0.007	0.6	54.5	2.2	90.5
1L-3	551	492	0.010	0.007	0.9	73.5	3.4	126
1L-4	734	675	0.012	0.007	1.1	90.5	4.6	157
1L-5	918	859	0.018	0.004	1.4	116.5	5.7	211
1L-6	1101	1042	0.021	0.004	2.2	190	6.5	266.5
1L-7	1285	1226	0.028	0.014	2.0	170.5	8.0	338
1L-8	1468	1409	0.035	0.013	2.4	205	9.0	421.5
1L-9	1652	1593	0.048	0.019	2.8	243	10.1	510.5
1L-10	1835	1776	0.063	0.030	3.3	283	11.1	606
1L-11	2019	1960	0.086	0.038	3.8	324	12.1	722
1L-12	2202	2143	0.114	0.041	4.4	377	13.1	830.5
1L-13	2386	2327	0.147	0.060	5.0	433	14.0	940
1L-14	2569	2510	0.192	0.061	5.6	483	14.9	1049.5
1L-15	2752	2693	0.243	0.075	6.0	514.5	16.0	1131
1L-16	2936	2877	0.309	0.098	6.3	540	17.1	1205
1L-17	3119	3060	0.384	0.119	6.4	550	18.4	1263
1L-18	3303	3244	0.511	0.127	6.1	523.5	19.9	1313
1L-19	3486	3427	0.650	0.152	5.8	501	21.4	1353.5
1L-20	3670	3611	0.904	0.177	5.7	491	22.7	1382.5
1L-21	3856	3797	1.409	0.211	5.9	508	24.0	1299.5

Table B.8- Unit strain gage data, Grandview, Missouri test site (English Units)

Load Test Incre.	O-cell to SG-4 Quiv&Cem C 905 to 916.5 (tsf)	Level 5 Avg. Load (tons)	SG-4 to SG-5 Chanute 916.5 to 921 (tsf)	Level 6 Avg. Load (tons)	SG-5 to SG-6 Chanute 921 to 927 (tsf)	SG-6 to Top Chanute 927 to 934 (tsf)	SG-4 to Top Chanute 916.5 to 934 (tsf)
1L-0	0	0	0	0	0	0	0
1L-1	0.5	36	0.2	21	0.0	0.0	0.1
1L-2	1.1	52	0.3	30	0.1	0.1	0.2
1L-3	1.7	72	0.5	40	0.1	0.2	0.3
1L-4	2.4	90	0.6	50	0.2	0.2	0.4
1L-5	2.9	122	0.9	67	0.3	0.3	0.6
1L-6	3.5	157	1.1	86	0.5	0.5	0.7
1L-7	4.0	203	1.4	111	0.6	0.7	0.9
1L-8	4.4	255	1.7	140	0.8	0.9	1.2
1L-9	4.8	313	2.1	168	1.1	1.1	1.4
1L-10	5.2	373	2.4	196	1.3	1.3	1.7
1L-11	5.5	441	3.0	227	1.6	1.5	2.0
1L-12	5.8	504	3.5	254	1.9	1.7	2.3
1L-13	6.1	564	4.0	275	2.2	1.8	2.6
1L-14	6.4	626	4.5	295	2.6	1.9	2.9
1L-15	6.9	683	4.8	310	2.9	2.1	3.1
1L-16	7.3	739	5.0	327	3.2	2.2	3.4
1L-17	7.9	790	5.1	349	3.5	2.3	3.5
1L-18	8.4	845	5.0	375	3.7	2.5	3.7
1L-19	9.0	890	5.0	408	3.8	2.7	3.8
1L-20	9.7	917	5.0	443	3.8	3.0	3.9
1L-21	10.9	855	4.8	463	3.1	3.1	3.6

Table B.9- Unit strain gage data, Grandview, Missouri test site (Metric Units).

Load Test Incre.	O-cell Loads		Upwrd	Bottom	Tip to SG-1	Level 1	SG-1 to O-cell	Level 4
	Gross (MN)	Net (MN)	Mvment (mm)	of Cell (mm)	Wea 272.3-273.7 (kPa)	Avg. Load (MN)	Westerville 273.7-275.8 (kPa)	Avg. Load (MN)
1L-0	0	0	0	0	0	0.00	0	0
1L-1	1.63	1.11	0.2	0.2	14.5	0.31	101.8	0.53
1L-2	3.26	2.74	0.2	0.2	60.8	0.48	214.1	0.81
1L-3	4.90	4.37	0.3	0.2	82.0	0.65	326.9	1.12
1L-4	6.53	6.00	0.3	0.2	101.0	0.81	440.9	1.40
1L-5	8.16	7.64	0.5	0.1	130.0	1.04	548.9	1.88
1L-6	9.79	9.27	0.5	0.1	211.9	1.69	624.2	2.37
1L-7	11.43	10.90	0.7	0.4	190.2	1.52	763.3	3.01
1L-8	13.06	12.53	0.9	0.3	228.7	1.82	865.4	3.75
1L-9	14.69	14.17	1.2	0.5	271.1	2.16	965.1	4.54
1L-10	16.32	15.80	1.6	0.8	315.7	2.52	1063.5	5.39
1L-11	17.96	17.43	2.2	1.0	361.4	2.88	1161.1	6.42
1L-12	19.59	19.06	2.9	1.0	420.5	3.35	1250.5	7.39
1L-13	21.22	20.70	3.7	1.5	483.0	3.85	1337.9	8.36
1L-14	22.85	22.32	4.9	1.5	538.8	4.30	1429.0	9.34
1L-15	24.48	23.96	6.2	1.9	573.9	4.58	1533.2	10.06
1L-16	26.11	25.59	7.8	2.5	602.4	4.80	1641.5	10.72
1L-17	27.75	27.22	9.8	3.0	613.5	4.89	1760.4	11.24
1L-18	29.38	28.85	13.0	3.2	584.0	4.66	1904.3	11.68
1L-19	31.01	30.49	16.5	3.9	558.9	4.46	2045.4	12.04
1L-20	32.64	32.12	23.0	4.5	547.7	4.37	2178.0	12.30
1L-21	34.30	33.78	35.8	5.4	566.7	4.52	2294.1	11.56
For upward loaded shear, the bouyant weight of the shaft in each zone has been subtracted from the load shed in the respective zone above the O-cell™								

Table B.10- Unit strain gage data, Grandview, Missouri test site (Metric Units).

Load Test Incre.	O-cell to SG-4 Quiv&Cem C 275.8-279.3 (kPa)	Level 5 Avg. Load (MN)	SG-4 to SG-5 Chanute 279.3-280.7 (kPa)	Level 6 Avg. Load (MN)	SG-5 to SG-6 Chanute 280.7-282.5 (kPa)	SG-6 to Top Chanute 282.5-284.7 (kPa)	SG-4 to Top Chanute 282.5-284.7 (kPa)
1L-0	0	0.00	0	0.00	0	0	0
1L-1	43.7	0.32	13.7	0.18	0.1	2.1	13.5
1L-2	106.4	0.46	27.3	0.26	5.6	8.2	21.7
1L-3	166.9	0.64	41.4	0.36	13.5	15.2	31.2
1L-4	229.3	0.80	53.5	0.44	20.1	21.6	39.6
1L-5	282.3	1.09	74.1	0.60	31.5	33.4	54.1
1L-6	334.7	1.39	93.8	0.77	43.7	46.2	69.0
1L-7	380.5	1.80	117.7	0.98	60.5	62.6	88.3
1L-8	421.5	2.27	146.7	1.25	78.6	82.5	110.7
1L-9	460.1	2.78	176.2	1.49	102.1	101.0	134.6
1L-10	496.2	3.31	209.5	1.74	127.2	119.8	160.3
1L-11	523.8	3.92	254.4	2.02	155.8	141.0	191.5
1L-12	554.5	4.48	296.6	2.26	184.8	158.8	220.7
1L-13	584.8	5.01	343.4	2.44	215.0	172.9	250.2
1L-14	614.8	5.57	387.4	2.62	248.4	186.4	279.6
1L-15	656.6	6.08	410.4	2.76	280.9	196.8	301.5
1L-16	701.4	6.57	427.7	2.91	311.1	208.2	321.4
1L-17	752.8	7.02	434.3	3.10	334.3	222.7	337.0
1L-18	807.4	7.51	429.6	3.33	357.0	240.1	350.5
1L-19	865.9	7.92	424.9	3.63	366.8	262.3	361.4
1L-20	929.1	8.15	427.3	3.94	359.8	286.2	369.2
1L-21	1039.4	7.60	407.6	4.12	295.4	299.6	346.8

Table B.11- Unconfined compressive strength of NX rock cores

	Upper Chanute	Lower Chanute	Cement City	Quivira	Westerville	Wea
	(tsf)	(tsf)	(tsf)	(tsf)	(tsf)	(tsf)
	12.4	5.2	240.7	11.1	861.0	32.6
	8.5	4.6	571.4	14.3	725.8	19.4
	8.5	2.7	118.6	2.9*	164.8	13.8
		9.7	458.3	16.0	411.6	32.7
		10.1	410.2	18.2	884.2	18.9
		11.0	319.0		1104.4	27.6
			588.0		137.9	20.7
					707.3	25.9
					786.2	20.0
					800.9	33.1
					500.7	8.4
					800.9	29.9
						25.6
						24.9
						30.5
						17.5
						32.1
						20.1
						1.4*
Mean	9.8	7.2	386.6	14.9	657.1	24.1
Std. Dev.	2.3	3.5	179.8	3.0	311.9	8.7

Table B.12- Unconfined compressive strength and SPT data for Chanute Formation, Cement City , and Quivira.

Pier	Elev.	Unconfined Compressive Strength and SPT Data			
		A6251	A6252	Test Shaft	A6254
	(ft)	(tsf)	(tsf)	(tsf)	(tsf)
		Chanute			
TS	937.1			100 in 10.5"	
11	936.8				12.4
TS	932.1			100 in 7"	8.5
11	930.2				8.5
7	927.6	9.7			
TS	927.1			100 in 3"	
11	923.9				11
13	921.3	2.7			
TS	920.0			5.2	
7	919.5		10.1		
TS	918.3			4.6	
		Cement City			
8	916.1		571.4		
13	915.2	458.3			
5	915.0		240.7		
TS	914.8			118.6	
TS	913.1			319.0	
4	912.0		410.2		
TS	910.9			588.0	
		Quivira			
11	913.1				18.2
8	910.1		11.1		
TS	910.0			14.3	
6	906.9		16.0		
TS	906.1			2.9*	

* Values not used in calculation of mean

Table B.13- Unconfined compressive strength and SPT data for Westerville Limestone and Wea Shale Formation.

Pier	Elev.	Unconfined Compressive Strength and SPT Data			
		A6251	A6252	Test Shaft	A6254
	(ft)	(tsf)	(tsf)	(tsf)	(tsf)
		Westerville			
9	908.3				500.7
9	905.0				800.9
4	904.9		137.9		
8	904.1				1104.4
11	903.5	786.2			
TS	903.1			164.8	
8	901.1		725.8		
12	900.9	884.2			
4	900.7		707.3		
5	899.8		861.0		
TS	899.0			411.6	
		Wea			
8	896.7				20.1
5	896.6		17.5		
4	896.5		8.4		
TS	896.0			13.8	
6	896.0		20		
8	892.9		19.4		
TS	892.7			32.7	
6	891.4		33.1		
5	891.0		32.6		
TS	890.8			13.9	
8	890.1				32.1
TS	887.7			27.6	
4	886.6		29.9		
4	882.6		25.6		
TS	881.0			20.7	
10	877.4	50 in 6"			
4	876.4		24.9		
TS	874.3			25.9	
10	874.2	1.37*			
10	873.6		100 in 12"		
4	872.5		30.5		

* Values not used in calculation of mean

APPENDIX C
DETAILED DATA FOR LOAD TESTS AND UNCONFINED COMPRESSIVE
STRENGTH OF NX CORES AT WAVERLY SITE

Table C.1
Summary of Dimensions, Elevations, and Shaft Properties

Shaft:

Average Shaft Diameter (EL 937.5 ft to 607.6 ft)	=	2134 mm	84 in
Average Shaft Diameter (EL 607.6 ft to 558.0 ft)	=	1981 mm	78 in
O-cell TM : 1004-18A	=	660 mm	26 in
Length of side shear above break at base of O-cell TM	=	22.52 m	73.9 ft
Length of side shear below break at base of O-cell TM	=	1.7 m	5.6 ft
Shaft side shear area above O-cell TM base	=	144.5 m ²	1556.0 ft ²
Shaft side shear area below break at base of O-cell TM	=	10.59 m ²	113.97 ft ²
Shaft base area	=	3.08 m ²	33.2 ft ²
Bouyant weight of shaft above base of O-cell TM	=	1.03 MN	230.6 kips
Estimated shaft stiffness (EL 637.5 ft to 607.6 ft)	=	141.5 GN	31,800,000 kips
Estimated shaft stiffness (EL 607.6 ft to 558 ft)	=	110.7 GN	24,900,000 kips
Elevation of Water Table	=	200.4 m	657.5 ft
Elevation of Mud line	=	194.3 m	637.5 ft
Elevation top of shaft concrete	=	191.3 m	627.5 ft
Elevation of base of O-cell TM	=	171.8 m	563.6 ft
Elevation of shaft tip	=	170.1 m	558.0 ft

Casing:

Elevation of top of temporary casing (2134 mm O.D.)	=	202.8 m	665.5 ft
Elevation of bottom of temporary casing (84 in O.D.)	=	185.2 m	607.6 ft

Compression Sections:

EL. of top of telltale used for upper shaft compression	=	191.9 m	629.5 ft
EL. of bottom of telltale used upper shaft compression	=	172.2 m	565.0 ft

Strain Gages:

Elevation of strain gage level 4	=	182.8 m	599.6 ft
Elevation of strain gage level 3	=	178.2 m	584.6 ft
Elevation of strain gage level 2	=	175.1 m	574.6 ft
Elevation of strain gage level 1	=	170.9 m	560.6 ft

Miscellaneous:

Top Plate Diameter	=	1537 mm	60.5 in
Bottom Plate Diameter	=	1537 mm	60.5 in
Vertical Rebar size	=	M 45	#14
Number of vertical bars	=	22	
Hoop re-bar size	=	M 16	# 5
Unconfined compressive concrete strength	=	51.8 MPa	7529 psi

Table C.2- Osterberg O-cell™ versus top and bottom plate movement for load increments 1L-0 to 1U-4.

Load	Hold	O-cell Loads					Top of	Upper	Upward Movement		O-cell expansion		Dnwrld Mvment	
Test Incre	Time Min	Gross (MN)	Gross (kips)	Gross (tons)	Net (MN)	Net (tons)	Shaft (in)	Compre (in)	Top Plate (mm) (in)		(mm)	(in)	(mm)	(in)
							A	B	A + B		C		A + B - C	
1L-0		0.00	0	0	0	0	0	0	0.00	0	0	0	0	0
1L-1	1	1.06	239	119.5	0.03	4.2	0.002	0.001	0.08	0.003	0.15	0.006	-0.08	-0.003
1L-1	2	1.06	239	119.5	0.03	4.2	0.001	0.001	0.05	0.002	0.15	0.006	-0.10	-0.004
1L-1	4	1.06	239	119.5	0.03	4.2	0.001	0.001	0.05	0.002	0.15	0.006	-0.10	-0.004
1L-2	1	2.04	458	229	1.01	113.7	0.002	0.001	0.08	0.003	0.20	0.008	-0.13	-0.005
1L-2	2	2.04	458	229	1.01	113.7	0.002	0.001	0.08	0.003	0.20	0.008	-0.13	-0.005
1L-2	4	2.04	458	229	1.01	113.7	0.002	0.001	0.08	0.003	0.20	0.008	-0.13	-0.005
1L-3	1	3.01	677	338.5	1.98	223.2	0.003	0.002	0.13	0.005	0.25	0.01	-0.13	-0.005
1L-3	2	3.01	677	338.5	1.98	223.2	0.003	0.001	0.10	0.004	0.25	0.01	-0.15	-0.006
1L-3	4	3.01	677	338.5	1.98	223.2	0.003	0.002	0.13	0.005	0.25	0.01	-0.13	-0.005
1L-4	1	3.98	895	447.5	2.95	332.2	0.003	0.002	0.13	0.005	0.33	0.013	-0.20	-0.008
1L-4	2	3.98	895	447.5	2.95	332.2	0.003	0.002	0.13	0.005	0.33	0.013	-0.20	-0.008
1L-4	4	3.98	895	447.5	2.95	332.2	0.003	0.002	0.13	0.005	0.36	0.014	-0.23	-0.009
1L-5	1	4.96	1114	557	3.93	441.7	0.004	0.003	0.18	0.007	0.43	0.017	-0.25	-0.010
1L-5	2	4.96	1114	557	3.93	441.7	0.004	0.002	0.15	0.006	0.46	0.018	-0.30	-0.012
1L-5	4	4.96	1114	557	3.93	441.7	0.004	0.002	0.15	0.006	0.46	0.018	-0.30	-0.012
1L-6	1	5.93	1333	666.5	4.90	551.2	0.004	0.003	0.18	0.007	0.56	0.022	-0.38	-0.015
1L-6	2	5.93	1333	666.5	4.90	551.2	0.004	0.003	0.18	0.007	0.56	0.022	-0.38	-0.015
1L-6	4	5.93	1333	666.5	4.90	551.2	0.005	0.003	0.20	0.008	0.58	0.023	-0.38	-0.015
1L-7	1	6.90	1551	775.5	5.87	660.2	0.005	0.004	0.23	0.009	0.66	0.026	-0.43	-0.017
1L-7	2	6.90	1551	775.5	5.87	660.2	0.006	0.004	0.25	0.010	0.69	0.027	-0.43	-0.017
1L-7	4	6.90	1551	775.5	5.87	660.2	0.005	0.004	0.23	0.009	0.71	0.028	-0.48	-0.019
1L-8	1	7.87	1770	885	6.84	769.7	0.005	0.004	0.23	0.009	0.79	0.031	-0.56	-0.022
1L-8	2	7.87	1770	885	6.84	769.7	0.006	0.005	0.28	0.011	0.81	0.032	-0.53	-0.021
1L-8	4	7.87	1770	885	6.84	769.7	0.006	0.005	0.28	0.011	0.84	0.033	-0.56	-0.022
1L-9	1	8.84	1988	994	7.81	878.7	0.007	0.005	0.30	0.012	0.91	0.036	-0.61	-0.024
1L-9	2	8.84	1988	994	7.81	878.7	0.007	0.006	0.33	0.013	0.94	0.037	-0.61	-0.024
1L-9	4	8.84	1988	994	7.81	878.7	0.007	0.006	0.33	0.013	0.94	0.037	-0.61	-0.024
1L-10	1	9.82	2207	1103.5	8.79	988.2	0.008	0.006	0.36	0.014	1.04	0.041	-0.69	-0.027
1L-10	2	9.82	2207	1103.5	8.79	988.2	0.008	0.007	0.38	0.015	1.07	0.042	-0.69	-0.027
1L-10	4	9.82	2207	1103.5	8.79	988.2	0.008	0.007	0.38	0.015	1.07	0.042	-0.69	-0.027
1L-11	1	10.79	2426	1213	9.76	1097.7	0.009	0.008	0.43	0.017	1.17	0.046	-0.74	-0.029
1L-11	2	10.79	2426	1213	9.76	1097.7	0.009	0.008	0.43	0.017	1.19	0.047	-0.76	-0.030
1L-11	4	10.79	2426	1213	9.76	1097.7	0.009	0.008	0.43	0.017	1.22	0.048	-0.79	-0.031
1L-12	1	11.76	2644	1322	10.73	1206.7	0.009	0.008	0.43	0.017	1.30	0.051	-0.86	-0.034
1L-12	2	11.76	2644	1322	10.73	1206.7	0.009	0.009	0.46	0.018	1.32	0.052	-0.86	-0.034
1L-12	4	11.76	2644	1322	10.73	1206.7	0.010	0.009	0.48	0.019	1.32	0.052	-0.84	-0.033
1L-13	1	12.73	2863	1431.5	11.70	1316.2	0.010	0.010	0.51	0.020	1.42	0.056	-0.91	-0.036
1L-13	2	12.73	2863	1431.5	11.70	1316.2	0.010	0.010	0.51	0.020	1.45	0.057	-0.94	-0.037
1L-13	4	12.73	2863	1431.5	11.70	1316.2	0.011	0.010	0.53	0.021	1.45	0.057	-0.91	-0.036

Table C.2- Continued.

Load	Hold	O-cell Loads					Top of	Upper	Upward Movement		O-cell expansion		Dnwrld Mvment	
Test	Time	Gross	Gross	Gross	Net	Net	Shaft	Compr e	Top Plate					
Incre	Min	(MN)	(kips)	(tons)	(MN)	(tons)	(in)	(in)	(mm)	(in)	(mm)	(in)	(mm)	(in)
							A	B	A + B		C		A + B - C	
1L-14	1	13.71	3082	1541	12.68	1425.7	0.011	0.011	0.56	0.022	1.55	0.061	-0.99	-0.039
1L-14	2	13.71	3082	1541	12.68	1425.7	0.010	0.011	0.53	0.021	1.57	0.062	-1.04	-0.041
1L-14	4	13.71	3082	1541	12.68	1425.7	0.011	0.011	0.56	0.022	1.60	0.063	-1.04	-0.041
1L-15	1	14.68	3300	1650	13.65	1534.7	0.012	0.012	0.61	0.024	1.70	0.067	-1.09	-0.043
1L-15	2	14.68	3300	1650	13.65	1534.7	0.012	0.012	0.61	0.024	1.70	0.067	-1.09	-0.043
1L-15	4	14.68	3300	1650	13.65	1534.7	0.012	0.012	0.61	0.024	1.73	0.068	-1.12	-0.044
1L-16	1	15.65	3519	1759.5	14.62	1644.2	0.013	0.014	0.69	0.027	1.83	0.072	-1.14	-0.045
1L-16	2	15.65	3519	1759.5	14.62	1644.2	0.013	0.014	0.69	0.027	1.85	0.073	-1.17	-0.046
1L-16	4	15.65	3519	1759.5	14.62	1644.2	0.013	0.014	0.69	0.027	1.88	0.074	-1.19	-0.047
1L-17	1	16.63	3738	1869	15.60	1753.7	0.014	0.015	0.74	0.029	1.98	0.078	-1.24	-0.049
1L-17	2	16.63	3738	1869	15.60	1753.7	0.015	0.015	0.76	0.030	2.01	0.079	-1.24	-0.049
1L-17	4	16.63	3738	1869	15.60	1753.7	0.014	0.015	0.74	0.029	2.03	0.08	-1.30	-0.051
1L-18	1	17.60	3956	1978	16.57	1862.7	0.015	0.016	0.79	0.031	2.13	0.084	-1.35	-0.053
1L-18	2	17.60	3956	1978	16.57	1862.7	0.016	0.016	0.81	0.032	2.18	0.086	-1.37	-0.054
1L-18	4	17.60	3956	1978	16.57	1862.7	0.015	0.017	0.81	0.032	2.21	0.087	-1.40	-0.055
1L-19	1	18.57	4175	2087.5	17.54	1972.2	0.016	0.017	0.84	0.033	2.31	0.091	-1.47	-0.058
1L-19	2	18.57	4175	2087.5	17.54	1972.2	0.017	0.017	0.86	0.034	2.34	0.092	-1.47	-0.058
1L-19	4	18.57	4175	2087.5	17.54	1972.2	0.017	0.018	0.89	0.035	2.46	0.097	-1.57	-0.062
1L-20	1	19.54	4394	2197	18.51	2081.7	0.018	0.018	0.91	0.036	2.51	0.099	-1.60	-0.063
1L-20	2	19.54	4394	2197	18.51	2081.7	0.019	0.018	0.94	0.037	2.51	0.099	-1.57	-0.062
1L-20	4	19.54	4394	2197	18.51	2081.7	0.019	0.018	0.94	0.037	2.54	0.1	-1.60	-0.063
1L-21	1	20.51	4612	2306	19.48	2190.7	0.019	0.019	0.97	0.038	2.67	0.105	-1.70	-0.067
1L-21	2	20.51	4612	2306	19.48	2190.7	0.020	0.019	0.99	0.039	2.69	0.106	-1.70	-0.067
1L-21	4	20.51	4612	2306	19.48	2190.7	0.021	0.019	1.02	0.040	2.72	0.107	-1.70	-0.067
1L-22	1	21.49	4831	2415.5	20.46	2300.2	0.021	0.020	1.04	0.041	2.87	0.113	-1.83	-0.072
1L-22	2	21.49	4831	2415.5	20.46	2300.2	0.022	0.020	1.07	0.042	2.90	0.114	-1.83	-0.072
1L-22	4	21.49	4831	2415.5	20.46	2300.2	0.022	0.020	1.07	0.042	2.92	0.115	-1.85	-0.073
1L-23	1	22.46	5049	2524.5	21.43	2409.2	0.023	0.021	1.12	0.044	3.02	0.119	-1.91	-0.075
1L-23	2	22.46	5049	2524.5	21.43	2409.2	0.023	0.021	1.12	0.044	3.05	0.12	-1.93	-0.076
1L-23	3	22.46	5049	2524.5	21.43	2409.2	0.023	0.021	1.12	0.044	3.05	0.12	-1.93	-0.076
1L-23	4	22.46	5049	2524.5	21.43	2409.2	0.023	0.021	1.12	0.044	3.10	0.122	-1.98	-0.078
1U-1	1	14.68	3300	1650	13.65	1534.7	0.021	0.019	1.02	0.040	2.59	0.102	-1.57	-0.062
1U-1	2	14.68	3300	1650	13.65	1534.7	0.021	0.019	1.02	0.040	2.57	0.101	-1.55	-0.061
1U-1	4	14.68	3300	1650	13.65	1534.7	0.022	0.019	1.04	0.041	2.57	0.101	-1.52	-0.060
1U-2	1	9.82	2207	1103.5	8.79	988.2	0.020	0.017	0.94	0.037	2.13	0.084	-1.19	-0.047
1U-2	2	9.82	2207	1103.5	8.79	988.2	0.019	0.017	0.91	0.036	2.11	0.083	-1.19	-0.047
1U-2	4	9.82	2207	1103.5	8.79	988.2	0.019	0.017	0.91	0.036	2.08	0.082	-1.17	-0.046
1U-3	2	4.96	1114	557	3.93	441.7	0.017	0.013	0.76	0.030	1.55	0.061	-0.79	-0.031
1U-3	4	4.96	1114	557	3.93	441.7	0.017	0.013	0.76	0.030	1.52	0.06	-0.76	-0.030
1U-4	2	0.00	0	0	-1.03	0	0.014	0.010	0.61	0.024	0.94	0.037	-0.33	-0.013

1U-4	4	0.00	0	0	-1.03	0	0.014	0.010	0.61	0.024	0.91	0.036	-0.30	-0.012
------	---	------	---	---	-------	---	-------	-------	------	-------	------	-------	-------	--------

Table C.3-Creep data, Waverly, Missouri test site.

Load Ince.	O-cell Load	Upward Movement Top of Upper cell	Upward Movement Top of Upper cell	Creep 2 to 4 min	Downward Movement Bott of Upper cell	Downward Movement Bott of Upper cell	Creep 2 to 4 min
	Net (Tons)	2 min (in)	4 min (in)	(in)	2 min (in)	4 min (in)	(in)
1L-0	0.0	0.000	0.000	0.000	0.000	0.000	0.000
1L-1	119.5	0.003	0.003	0.000	0.004	0.004	0.000
1L-2	229.5	0.004	0.004	0.000	0.004	0.004	0.000
1L-3	338.5	0.005	0.005	0.000	0.005	0.006	0.001
1L-4	447.5	0.005	0.005	0.000	0.008	0.008	0.000
1L-5	556.5	0.007	0.007	0.000	0.011	0.012	0.001
1L-6	666.5	0.008	0.008	0.000	0.014	0.015	0.001
1L-7	775.5	0.010	0.010	0.000	0.017	0.018	0.001
1L-8	885.0	0.011	0.012	0.001	0.021	0.021	0.000
1L-9	994.0	0.013	0.014	0.001	0.024	0.024	0.000
1L-10	1103.5	0.015	0.016	0.001	0.026	0.026	0.000
1L-11	1213.0	0.017	0.018	0.001	0.029	0.030	0.001
1L-12	1322.0	0.019	0.020	0.001	0.033	0.033	0.000
1L-13	1431.5	0.021	0.021	0.000	0.036	0.036	0.000
1L-14	1541.0	0.022	0.023	0.001	0.040	0.040	0.000
1L-15	1650.0	0.025	0.025	0.000	0.043	0.043	0.000
1L-16	1759.5	0.027	0.027	0.000	0.046	0.047	0.001
1L-17	1869.0	0.029	0.030	0.001	0.049	0.050	0.001
1L-18	1978.0	0.032	0.032	0.000	0.054	0.055	0.001
1L-19	2087.5	0.034	0.035	0.001	0.058	0.062	0.004
1L-20	2197.0	0.036	0.037	0.001	0.063	0.063	0.000
1L-21	2306.0	0.039	0.039	0.000	0.067	0.068	0.001
1L-22	2415.5	0.041	0.042	0.001	0.072	0.072	0.000
1L-23	2524.5	0.044	0.043	-0.001	0.076	0.078	0.002

Table C.4- Strain gage data, Waverly, Missouri test site (English Units).

Load Test Incre.	0 Shear Avg. Net Load (tons)	Level 4 Avg. Net Load (tons)	Level 3 Avg. Net Load (tons)	Level 2 Avg. Net Load (tons)	O-Cell™ Gross Load (tons)	Level 1 Avg. Gross Load (tons)
EL (ft)	606.5	599.6	584.6	574.6	563.6	560.6
1L-0	0	0	0	0	0	0
1L-1	0	7.5	29	65.5	119.5	51.5
1L-3	0	13.5	47	110	338.5	62.5
1L-5	0	22.5	77	192.5	557	88
1L-7	0	33	116.5	284.5	775.5	107.5
1L-9	0	43.5	154	374.5	994	120
1L-11	0	56.5	192	473	1213	133
1L-13	0	68	231	568.5	1431.5	117
1L-15	0	82	274.5	673.5	1650	150.5
1L-17	0	95.5	320	784	1869	135
1L-19	0	114.5	384.5	941	2087.5	131
1L-21	0	125.5	415.5	1015	2306	35
1L-23	0	140.5	462.5	1130.5	2524.5	-238.5

Table C.5- Strain gage data, Waverly, Missouri test site (Metric Units).

Load Test Incr.	Mud Line Avg. Net Load (MN)	Level 4 Avg. Net Load (MN)	Level 3 Avg. Net Load (MN)	Level 2 Avg. Net Load (MN)	O-Cell™ Gross Load (MN)	Level 1 Avg. Gross Load (MN)
EL (m)	184.85	182.75	178.18	175.13	171.78	170.86
1L-0	0	0.00	0.00	0.00	0.0	0.0
1L-1	0	0.07	0.26	0.58	1.1	0.5
1L-3	0	0.12	0.42	0.98	3.0	0.6
1L-5	0	0.20	0.68	1.71	5.0	0.8
1L-7	0	0.29	1.04	2.53	6.9	1.0
1L-9	0	0.39	1.37	3.33	8.8	1.1
1L-11	0	0.50	1.71	4.21	10.8	1.2
1L-13	0	0.60	2.05	5.06	12.7	1.0
1L-15	0	0.73	2.44	5.99	14.7	1.3
1L-17	0	0.85	2.85	6.97	16.6	1.2
1L-19	0	1.02	3.42	8.37	18.6	1.2
1L-21	0	1.12	3.70	9.03	20.5	0.3
1L-23	0	1.25	4.11	10.06	22.5	-2.1

Table C.6- Unit strain gage data, Waverly, Missouri test site (English Units)

Load Test Incr.	O-cell Load		Upwrd	Bottom of	Level 2	O-cell to	Level 3	SG-2 to	Level 4	SG-3 to	SG-4 to
	Gross	Net	Mvment	Cell	Avg. Load	SG-2 563.6 to 574.6	Avg. Load	SG-3 574.6 to 584.6	Avg. Load	SG-4 584.6 to 599.6	0 Shear 599.6 to 606.5
	(tons)	(tons)	(in)	(in)	(tons)	(tsf)	(tons)	(tsf)	(tons)	(tsf)	(tsf)
1L-0	0	0	0	0	0	0	0	0	0	0	0
1L-1	120	4	0.003	0.004	65.5	-0.3	29	0.1	8	0.01	-0.02
1L-2	229	114	0.004	0.004	85.5	0.1	38	0.2	10	0.02	-0.01
1L-3	339	223	0.005	0.006	110	0.4	47	0.2	14	0.04	0.02
1L-4	448	332	0.005	0.008	144	0.8	60	0.3	18	0.07	0.05
1L-5	557	442	0.007	0.012	192.5	1.0	80	0.5	23	0.12	0.08
1L-6	667	551	0.008	0.015	235.5	1.3	98	0.6	28	0.17	0.12
1L-7	776	660	0.010	0.018	284.5	1.6	117	0.8	33	0.21	0.16
1L-8	885	770	0.012	0.021	330	1.9	137	0.9	38	0.26	0.19
1L-9	994	879	0.014	0.024	374.5	2.2	154	1.0	44	0.30	0.23
1L-10	1104	988	0.016	0.026	424.5	2.4	173	1.2	49	0.34	0.27
1L-11	1213	1098	0.018	0.030	473	2.7	192	1.3	57	0.38	0.32
1L-12	1322	1207	0.020	0.033	519	3.0	211	1.4	61	0.42	0.35
1L-13	1432	1316	0.021	0.036	568.5	3.3	231	1.6	68	0.47	0.41
1L-14	1541	1426	0.023	0.040	619.5	3.5	252	1.7	73	0.52	0.44
1L-15	1650	1535	0.025	0.043	673.5	3.8	275	1.9	82	0.56	0.51
1L-16	1760	1644	0.027	0.047	730	4.0	298	2.1	88	0.62	0.55
1L-17	1869	1754	0.030	0.050	784	4.3	320	2.2	96	0.67	0.60
1L-18	1978	1863	0.032	0.055	843	4.5	344	2.4	103	0.72	0.65
1L-19	2088	1972	0.035	0.062	941	4.5	385	2.7	115	0.82	0.74
1L-20	2197	2082	0.037	0.063	959	4.9	393	2.7	118	0.83	0.76
1L-21	2306	2191	0.039	0.068	1015	5.2	416	2.9	126	0.88	0.81
1L-22	2416	2300	0.042	0.072	1070.5	5.4	439	3.0	133	0.93	0.87
1L-23	2525	2409	0.043	0.078	1130.5	5.6	463	3.2	141	0.99	0.92

Table C.7- Unit strain gage data, Waverly, Missouri test site (Metric Units)

Load Test Incre.	O-cell Load		Upwrd	Bottom	Level 2	O-cell to	Level 3	SG-2 to	Level 4	SG-3 to	SG-4 to
	Gross	Net	Mvment	of Cell	Avg.	SC-2	Avg.	SC-3	Avg.	SG-4	0 Shear
	(MN)	(MN)	(mm)	(mm)	(MN)	171.8 to 175.1 (kPa)	Load (MN)	175.1 to 178.2 (kPa)	Load (MN)	178.2 to 182.7 (kPa)	182.7 to 184.9 (kPa)
1L-0	0	0	0	0	0	0	0.00	0	0.00	0	0
1L-1	1.06	0.04	0.1	0.1	0.58	-32.4	0.26	10.9	0.07	0.5	-2.3
1L-2	2.04	1.01	0.1	0.1	0.76	5.7	0.33	16.3	0.09	2.4	-0.6
1L-3	3.01	1.99	0.1	0.2	0.98	42.0	0.42	23.3	0.12	4.2	1.8
1L-4	3.98	2.96	0.1	0.2	1.28	74.0	0.53	33.4	0.16	6.7	4.8
1L-5	4.96	3.93	0.2	0.3	1.71	100.0	0.71	46.8	0.20	11.6	7.9
1L-6	5.93	4.90	0.2	0.4	2.10	128.4	0.87	58.3	0.24	15.8	11.3
1L-7	6.90	5.87	0.3	0.5	2.53	154.0	1.04	72.6	0.29	19.9	15.0
1L-8	7.87	6.85	0.3	0.5	2.94	181.3	1.21	84.6	0.34	24.6	18.4
1L-9	8.84	7.82	0.4	0.6	3.33	208.8	1.37	97.2	0.39	28.3	22.2
1L-10	9.82	8.79	0.4	0.7	3.78	234.2	1.54	111.8	0.44	32.6	25.9
1L-11	10.79	9.77	0.5	0.8	4.21	260.2	1.71	125.6	0.50	36.2	31.0
1L-12	11.76	10.73	0.5	0.8	4.62	287.0	1.87	138.5	0.54	40.7	33.7
1L-13	12.73	11.71	0.5	0.9	5.06	312.6	2.05	152.1	0.60	44.8	38.8
1L-14	13.71	12.68	0.6	1.0	5.51	337.6	2.24	166.2	0.65	49.8	42.2
1L-15	14.68	13.65	0.6	1.1	5.99	361.0	2.44	181.0	0.73	54.0	48.4
1L-16	15.65	14.63	0.7	1.2	6.49	383.6	2.65	196.7	0.78	59.3	52.4
1L-17	16.63	15.60	0.8	1.3	6.97	407.3	2.85	211.5	0.85	64.0	57.5
1L-18	17.60	16.57	0.8	1.4	7.50	428.6	3.06	227.9	0.91	69.3	62.3
1L-19	18.57	17.54	0.9	1.6	8.37	433.6	3.42	254.9	1.02	78.2	70.5
1L-20	19.54	18.52	0.9	1.6	8.53	472.6	3.49	259.6	1.05	79.6	72.8
1L-21	20.51	19.49	1.0	1.7	9.03	495.2	3.70	275.0	1.12	84.5	77.9
1L-22	21.49	20.46	1.1	1.8	9.52	518.2	3.91	290.1	1.18	89.5	83.0
1L-23	22.46	21.43	1.1	2.0	10.06	539.1	4.11	307.2	1.25	94.5	88.1

Table C.8- Unconfined compressive strength of rock cores Piers 9 and 10

Pier 9					
	Elevation (ft)				
	600-592	592-585	585-570	570-560	560-550
	(tsf)	(tsf)	(tsf)	(tsf)	(tsf)
	44.0	27	59.4	52	56.5
	20.9	63	101.9	14.4	27.5
	2.3		80.2	41.1	23.9
	6.7		35.3	55.4	24.8
	1.9		39.8	23.1	
	9.0		33.7	*117.4	
	2.4		89.5	*160.9	
	1.8		147.9		
	2.5		122		
			16.6		
			60.2		
			56.4		
			52.4		
			68		
Mean	10.2	45.0	68.8	37.2	33.2
Std. Dev	14.1	25.5	36.4	17.9	15.6
Pier 10					
	Elevation (ft)				
	602-594	594-586	586-570	570-560	560-550
	6.1	55.9	25.5	*128.8	78.8
	4.6	39.3	102.1	14.0	62.8
	2.9		137.6	26.0	17.7
	8.2		183.2	33.3	74.6
	3.6		262.7	35.7	120.2
			148.1	18.6	
			144.1	24.5	
			70.4		
			233		
			68.6		
			38.4		
Mean	5.1	47.6	128.5	25.4	70.8
Std. Dev	2.1	11.7	76.8	8.3	36.8

* Values not used in calculation of mean

Table C.9- Unconfined compressive strength of rock cores Piers 11 and 12

Pier 11					
	Elevation (ft)				
	Weir (A)	Weir (B)	Weir (C)	Weir (D)	Weir (E)
	609-600	600-584.7	584.7-574	574-564	564-555
	(tsf)	(tsf)	(tsf)	(tsf)	(tsf)
	1.6	3.1	9.2	2.1	56.7
	0.8*	2.1	13.9	7.2	78.8**
	4.1	0.7*	38.1	9.1	62.8**
	4.1	5.8	37.2	10.4	17.7**
	4.1	3.1		8.1	74.6**
	3.6	9.1		18.8	120.2**
	4.7	10.2		7.5	
	5.3	4.0		11.1	
	7.2	4.3			
	5.6	2.9			
		7.9			
		3.3			
		3.4			
Mean	4.5	4.9	24.6	9.3	68.5
Std. Dev	1.5	2.7	15.2	4.7	33.4
Pier 12					
	Elevation (ft)				
	631-602	631-602	602-574		
	2.2	2.2	101.9		
	10.9	2.1	86.7		
	72.7	12.0	77.8		
	7.3	13.7	194.0		
	13.3	4.5	35.4		
	12.1	25.2	2.2		
	2.7	13.7	7.8		
	11.2	3.7	170.9		
	9.2	12.2	7.0		
	19.8	4.6	20.2		
	7.6	3.0	136.1		
	10.4	8.2	66.5		
			31.1		
			36.2		
Mean		11.9	69.6		
Std. Dev		14.2	62.1		

* Values not used in calculation of mean

** Data from Pier 10

Table C.10- Unconfined compressive strength and SPT Data for Waverly, Mo.
(Elevation 633.0 to 606.4 ft.).

Station	Offset	Elev.	Unconfined Compressive Strength & SPT Data			
			Pier 9	Pier 10	Pier 11	Pier 12
	(ft)	(ft)	(tsf)	(tsf)	(tsf)	(tsf)
100+50	24' Lt.	632.9				9.2
100+20	42' Lt.	632.9				10.3
100+10	24" Lt.	631.3				10-30-38
100+50	24' Lt.	629.4				100 in 13"
100+22	60' Lt.	629.3				2.2
100+50	24' Lt.	628.2				10.9
100+10	24' Lt.	626.9				72.7
100+20	42' Lt.	626.0				7.3
100+10	60" Lt.	625.8				13.3
100+22	60' Lt.	624.2				12.1
100+50	24' Lt.	622.8				2.7
100+10	24' Lt.	622.3				11.2
100+10	60' Lt.	620.5				9.2
100+22	60' Lt.	618.2				19.8
100+20	42' Lt.	616.8				7.6
100+10	24' Lt.	616.3				10.4
100+50	24' Lt.	616.0				2.2
100+10	60' Lt.	614.9				2.1
100+50	24' Lt.	613.5				100 in 4"
100+10	24' Lt.	612.4				12
100+50	24' Lt.	612.1				13.7
100+20	42' Lt.	611.0				4.5
100+10	60' Lt.	610.9				25.2
100+22	60' Lt.	609.8				13.7
95+60.8	56.6' Lt.	609.8			12-28-42	
95+64	35.5' Lt.	609.2			100 in 11.5"	
					Weir (A)	
95+60.4	30.1' Lt.	608.4			1.6	
100+50	24' Lt.	607.6				3.7
95+77	28' Lt.	607.4			0.8	
95+78.5	55.3' Lt.	607.2			4.1	
100+20	42' Lt.	606.6				12.2
100+10	24' Lt.	606.4				4.6

* Values not used in calculation of mean

Table C.11- Unconfined compressive strength and SPT Data for Waverly, Mo.
(Elevation 604.3 to 598.2 ft.).

Station	Offset	Elev.	Unconfined Compressive Strength & SPT Data			
			Pier 9	Pier 10	Pier 11	Pier 12
	(ft)	(ft)	(tsf)	(tsf)	(tsf)	(tsf)
91+53.1	54.7' Lt.	604.3		100 in 8"		
100+10	60' Lt.	604.0				3
91+45.8	40.8' Lt.	604.0		100 in 10"		
95+64	35.5' Lt.	603.8			4.1	
95+60.8	56.6' Lt.	603.8			4.1	
100+22	60' Lt.	603.4				8.2
91+36.5	52.2' Lt.	603.2		8.9		
89+02	28' Lt.	602.9	100 in 9"			
88+95	42' Lt.	602.9	74 in 6"			
95+77	28' Lt.	602.8			3.6	
88+88	28' Lt.	602.5	100 in 11"			
95+78.5	53.3' Lt.	601.8			4.7	
95+60.4	30.1' Lt.	601.8			5.3	
100+50	24' Lt.	601.5				101.9
89+02	56' Lt.	601.5	5.5			
100+10	24' Lt.	601.3				86.7
91+53.1	54.7' Lt.	601.1		6.1		
100+20	42' Lt.	601.0				77.8
88+88	28' Lt.	600.9	9.5			
95+64	35.5' Lt.	600.8			7.2	
95+60.8	56.6' Lt.	600.8			5.6	
88+88	91' Lt.	600.4	100 in 6"			
100+22	60' Lt.	600.0				194.0
					Weir (B)	
95+78.5	55.3' Lt.	600.0			100 in 10"	
91+38	28' Lt.	599.7		4.6		
100+10	60' Lt.	599.5				35.4
91+50	32' Lt.	599.2		2.9		
88+95	42' Lt.	599.2	44.0			
95+77	28' Lt.	599.1			3.1	
91+38	28' Lt.	599.1		100 in 9"		
100+50	24' Lt.	598.2				100 in 5"
95+78.5	55.3' Lt.	598.2			2.1	

* Values not used in calculation of mean

Table C.12- Unconfined compressive strength and SPT Data for Waverly, Mo.
(Elevation 598.1 to 587.1 ft.).

Station	Offset	Elev.	Unconfined Compressive Strength & SPT Data			
			Pier 9	Pier 10	Pier 11	Pier 12
	(ft)	(ft)	(tsf)	(tsf)	(tsf)	(tsf)
89+02	28' Lt.	598.1	20.9			
95+60.4	30.1' Lt.	597.4			0.7	
89+02	56' Lt.	597.1	100 in 2"			
91+36.5	52.2' Lt.	596.9	2.3			
100+50	24' Lt.	596.6				2.2
91+45.8	40.8' Lt.	596.4		8.2		
88+88	91' Lt.	596.0	6.7			
91+38	28' Lt.	595.5		3.6		
89+02	56' Lt.	595.0	1.9			
100+50	24' Lt.	594.6				7.8
95+64	35.5' Lt.	594.2			5.8	
95+60.8	56.6' Lt.	594.2			3.1	
88+88	28' Lt.	594.2	9.0			
95+60.4	30.1' Lt.	594.0			9.1	
88+95	42' Lt.	593.3	2.4			
88+88	91' Lt.	593.2	1.8			
95+78.5	55.3' Lt.	592.8			10.2	
89+02	28' Lt.	592.8	2.5			
95+60.8	56.6' Lt.	592.2			4.0	
91+45.8	40.8' Lt.	591.9		55.9		
91+50	32' Lt.	591.7		39.3		
100+10	24' Lt.	591.4				170.9
95+64	35.5' Lt.	591.2			4.3	
95+77	28' Lt.	590.6			100 in 7.5"	
91+36.5	52.2' Lt.	590.2		100 in 4"		
95+60.4	30.1' Lt.	590.1			100 in 5.5"	
89+02	56' Lt.	589.3	27			
88+95	42' Lt.	589.2	63			
91+50	32' Lt.	588.4		100 in 2.5"		
95+60.8	56.6' Lt.	588.3			100 in 5"	
100+50	24' Lt.	588.0				7
91+45.8	40.8' Lt.	588.0		100 in 2"		
95+64	35.5' Lt.	587.7			100 in 5"	
95+48.5	53.3' Lt.	587.2			2.9	
88+95	42' Lt.	587.1	100 in 3"			

* Values not used in calculation of mean

Table C.13- Unconfined compressive strength and SPT data for Waverly, Mo.
(Elevation 586.8 to 576.4 ft.).

Station	Offset	Elev.	Unconfined Compressive Strength & SPT Data			
			Pier 9	Pier 10	Pier 11	Pier 12
	(ft.)	(ft)	(tsf)	(tsf)	(tsf)	(tsf)
89+02	28' Lt.	586.8	100 in 3"			
95+60.4	30.1' Lt.	586.7			7.9	
100+10	24' Lt.	586.5				20.2
88+88	28' Lt.	586.5	100 in 3"			
95+77	28" Lt.	585.9			3.3	
91+36.5	52.2' Lt.	585.8		25.5		
91+50	32' Lt.	585.7		102.1		
88+88	91' Lt.	584.9	100 in 4"			
91+38	28' Lt.	584.8		137.6		
95+64	35.5' Lt.	584.7			3.4	
89+02	28' Lt.	584.4	59.4		Weir (C)	
88+95	42' Lt.	583.9	101.9			
95+60.8	56.6' Lt.	583.8			9.2	
88+88	28' Lt.	583.6	80.2			
88+88	91' Lt.	583.2	35.3			
95+77	28' Lt.	582.9			13.9	
100+50	24' Lt.	582.8				100 in 2"
100+50	24' Lt.	582.6				136.1
100+10	60' Lt.	582.6				66.5
95+60.8	56.6' Lt.	582.2			38.1	
89+02	56' Lt.	581.9	100 in 3"			
91+50	32' Lt.	581.8		183.2		
88+88	28' Lt.	581.3	100 in 2"			
88+88	28' Lt.	580.9	39.8			
89+02	56' Lt.	579.7	33.7			
88+95	42' Lt.	579.5	89.5			
88+88	91' Lt.	579.3	147.9			
95+78.5	55.3' Lt.	579.2			100 in 4"	
91+38	28' Lt.	578.8		262.7		
100+50	24' Lt.	578.7				31.1
89+02	28' Lt.	578.6	122.0			
91+50	32' Lt.	578.5		148.1		
95+60.4	30.1' Lt.	578.0			37.2	
91+36.5	52.2' Lt.	576.7		144.1		
91+53.1	54.7' Lt.	576.4		70.4		

* Values not used in calculation of mean

Table C.14- Unconfined compressive strength and SPT data for Waverly, Mo.
(Elevation 575.0 to 563.1 ft.).

Station	Offset	Elev.	Unconfined Compressive Strength & SPT Data			
			Pier 9	Pier 10	Pier 11	Pier 12
	(ft)	(ft)	(tsf)	(tsf)	(tsf)	(tsf)
89+02	56' Lt.	575.0	16.6			
89+02	28' Lt.	575.0	60.2			
95+77	28' Lt.	574.9			100 in 4"	
100+50	24' Lt	574.5				36.2
91+38	28' Lt	573.8		233	Weir (D)	
95+60.8	56.6' Lt	573.4			2.1	
88+95	42' Lt.	572.8	56.4			
88+88	28' Lt.	572.7	52.4			
88+88	91' Lt.	572.6	68			
88+95	42' Lt	571.9	74 in 2"			
89+02	28' Lt	571.6	74 in 3"			
91+36.5	52.2' Lt	571.2		68.6		
95+60.8	56.6' Lt	571.2			7.2	
91+53.1	54.7' Lt	570.9		38.4		
95+78.5	53.3' Lt	570.2			9.1	
88+88	28' Lt	569.8	52			
89+02	28' Lt	569.7	14.4			
95+64	35.5' Lt	569.6			10.4	
91+38	28' Lt	569.3		128.8		
95+77	28' Lt	568.4			8.1	
95+60.8	56.6' Lt	568.3			100 in 3"	
88+88	91' Lt	567.8	41.1			
91+36.5	52.2' Lt	567.7		14		
100+50	24' Lt	567.6				100 in 5"
95+64	35.5' Lt	567.3			100 in 4"	
89+02	56' Lt	566.7	74 in 3"			
95+60.4	30.1' Lt	566.5			18.8	
91+38	28' Lt	565.3		26		
95+60.8	56.6' Lt	565.2			7.5	
95+64	35.5' Lt	565.1			11.1	
95+60.4	30.1' Lt	564.5			100 in 2"	
91+36.5	52.2' Lt	563.7		33.3	Weir (E)	
88+88	91' Lt	563.3	55.4			
100+50	24' Lt	563.2				33.2
91+45.8	40.8' Lt	563.1		35.7		

* Values not used in calculation of mean

Table C.15- Unconfined compressive strength and SPT Data for Waverly, Mo.
(Elevation 562.6 to 542.2 ft.).

Station	Offset	Elev.	Unconfined Compressive Strength & SPT Data			
			Pier 9	Pier 10	Pier 11	Pier 12
	(ft)	(ft)	(tsf)	(tsf)	(tsf)	(tsf)
89+02	56' Lt	562.6	23.1			
91+50	32' Lt	562.4		18.6		
91+38	28' Lt	562.3		24.5		
95+78.5	53.3' Lt	561.7			56.7	
88+88	28' Lt.	561.7	117.4*			
89+02	56' Lt	560.2	160.9*			
91+50	32' Lt	559.4		78.8		
88+88	91' Lt	558.4	56.5			
91+36.5	52.2' Lt	557.8		62.8		
88+88	28' Lt	557.1	27.5			
91+50	32' Lt	556.4		17.7		
91+38	28' Lt	555.8		74.6		
91+53.1	54.7'	555.6		120.2		
89+02	56'	552.7	100 in 3"			
88+88	91'	552.6	23.9			
100+50	24'	552.2				100 in 3"
88+88	28'	551.7	24.8			
89+02	28'	551.4	74 in 5"			
88+88	28'	551.2	100 in 4"			
100+50	24' Lt	542.2				100 in 2"

* Values not used in calculation of mean

APPENDIX D
SI UNITS FOR CHAPTER SEVEN TABLES AND FIGURES

Table D.1- Summary of measured unit side shear values and average unconfined compressive strength (q_u) values of shale at test sites.

Formation	Elevation of Strata	Shaft Section used to calc unit side shear	Elevation of Shaft Segment	q_u		Measured unit side shear, $f_s^{(1)}$
				Avg.	Std. Dev.	
	(m)		(m)	(kPa)	(kPa)	(kPa)
		Lexington				
Bevier (C1)	180.4 - 187	TS-2 upper cell to TOS	180.2 – 184.4	3811	2210	1020
Bevier (C1)	180.4 - 187	TS-2 SG-3 to SG-4	181.7 – 182.7	3811	2210	>694 ⁽²⁾
Bevier (C1)	180.4 - 187	TS-2 upper cell to SG-3	180.2 – 181.7	3811	2210	>1653
Bevier (C2)	176.4 – 180.4	TS-2, stage 1, lower cell to SG-2	176.2 – 178.7	3001	2565	885
Verdigris (D)	173.5 – 176.4	TS-1A, SG-4 to TOS	174.5 – 175.9	1212	1244	>391
Verdigris (D)	173.5 – 176.4	TS-1A, SG-3 to SG-4	173 – 174.5	1212	1244	>968
Croweburg (E)	169 – 173.5	TS-1A, O-cell to SG-2	170.5 -172	1716	1552	723
Croweburg (E)	169 – 173.5	TS-1A, SG-1 to O-cell	169.6 – 170.5	1716	1552	963
		Grandview				
W. Chanute	282.6 – 284.7	SG-6 to TOS	282.5 – 284.7	938	220	>301
Chanute	279.3 – 282.6	SG-5 to SG-6	280.7 - 282.5	690	335	295
Chanute	916.5 – 282.6	SG-4 to SG-5	279.3 – 280.7	690	335	453
Cement City	277.8 – 279.3	SG-3 to SG-4	277.8 – 279.3	37000	17217	>1651
Quivira	275.8 – 277.8	O-cell to SG-3	275.8 – 277.8	1427	287	460 ⁽³⁾
Westerville	273.7 – 275.8	SG-1 to O-cell	273.7 – 275.8	62900	29868	>2293
Wea	< 273.7	Tip to SG-1	272.3 – 273.7	2308	833	565
		Waverly				
Weir (A)	182.9 – 185.6	SG-4 to O shear	182.7 – 184.9	430	140	>88
Weir (B)	178.2 – 182.9	SG-3 to SG-4	178.2 – 182.7	470	260	>94
Weir (C)	174.9 – 178.2	SG-2 to SG-3	175.1 – 178.2	2360	1460	>306
Weir (D)	171.9 – 174.9	O-cell to SG-2	171.8 – 175.1	890	450	>587
Weir (E)	169.2 – 171.9			6560	3200	

(1) Values reported are ultimate values unless otherwise indicated.

(2) The symbol “>” indicates that the ultimate unit side shear was not reached during test, value reported is maximum value during test.

(3) Assumed ultimate unit side shear.

Table D.2- Summary of back-calculated alpha values of shale at Missouri test sites.

Formation	Shaft Section used to calc unit side shear	Elevation of shaft Segment	q_u		Meas. Unit side shear, $f_s^{(1)}$ (kPa)	α		
			Avg.	Std. Dev.		Avg..	+ 1 Std. Dev	- 1 Std. Dev.
		(m)	(kPa)	(kPa)	(kPa)			
	Lexington							
Bevier (C1)	TS-2 upper cell to TOS	180.2-184.4	3811	2210	1020	0.27	0.17	0.64
Bevier (C1)	TS-2 SG-3 to SG-4	181.7-182.7	3811	2210	>694 ⁽²⁾	0.18	0.12	0.44
Bevier (C1)	TS-2 upper cell to SG-3	180.2-181.7	3811	2210	>1653	0.43	0.28	1.04
Bevier (C2)	TS-2, stage 1, lower cell to SG-2	176.2-178.7	3001	2565	885	0.29	0.16	2.04
Verdigris (D)	TS-1A, SG-4 to TOS	174.5-175.9	1212	1244	>391	0.32	0.16	-13.7
Verdigris (D)	TS-1A, SG-3 to SG-4	173 – 174.5	1212	1244	>968	0.80	0.39	-33.7
Croweburg (E)	TS-1A, O-cell to SG-2	170.5 - 172	1716	1552	723	0.42	0.22	4.47
Croweburg (E)	TS-1A, SG-1 to O-cell	169.6–170.5	1716	1552	963	0.56	0.30	5.94
	Grandview							
W. Chanute	SG-6 to TOS	282.5-284.7	938	220	>301	0.33	0.26	0.43
Chanute	SG-5 to SG-6	280.7-282.5	690	335	295	0.43	0.29	0.84
Chanute	SG-4 to SG-5	279.3-280.7	690	335	453	0.67	0.45	1.30
Cement City	SG-3 to SG-4	277.8-279.3	37000	17217	>1651			
Quivira	O-cell to SG-3	275.8-277.8	1427	287	460 ⁽³⁾	0.32	0.27	0.40
Westerville	SG-1 to O-cell	273.7-275.8	62900	29868	>2293			
Wea	Tip to SG-1	272.3-273.7	2308	833	565	0.24	0.18	0.38
	Waverly							
Weir (A)	SG-4 to O shear	182.7-184.9	430	140	>88	0.20	0.15	0.30
Weir (B)	SG-3 to SG-4	178.2-182.7	470	260	>94	0.20	0.14	0.42
Weir (C)	SG-2 to SG-3	175.1-178.2	2360	1460	>306	0.13	0.08	0.34
Weir (D)	O-cell to SG-2	171.8-175.1	890	450	>587	0.67	0.44	1.35
Weir (E)			6560	3200				

(1) Values reported are ultimate values unless otherwise indicated.

(2) The symbol “>” indicates that the ultimate unit side shear was not reached during test, value reported is maximum value during test.

(3) Assumed ultimate unit side shear.

Table D.3- Comparison of measured and predicted unit side shear determined by various methods.

Formation	Shaft Segment	Elevation of Shaft Segment (m)	q_u Avg.	Meas. unit side shear, $f_s^{(1)}$	Predicted ultimate unit side shear				
					Horvath & Kenney (1979) $\alpha = 0.25$	Rowe & Armitage (1987) $\alpha = 0.45$	Reese & O'Neill (1988) $\alpha = 0.21$	Kulhawy & Phoon (1993) $\psi = 2$	O'Neill & Reese (1999) (4)
			(kPa)	(kPa)	(kPa)	(kPa)	(kPa)	(kPa)	(kPa)
	Lexington								
Bevier C1	TS-2, upper cell to TOS	180.2 - 184.4	3811	1020	488.0	878.5	410.0	877.4	190.6
Bevier C1	TS-2, SG-3 to SG-4	181.7 - 182.7	3811	>694 ⁽²⁾	488.0	878.5	410.0	877.4	228.7
Bevier C1	TS-2, upper cell to SG-3	180.2 - 181.7	3811	>1653	488.0	878.5	410.0	877.4	228.7
Bevier C2	TS-2, stage 1, lower cell to SG-2	176.2 - 178.7	3001	885	433.1	779.6	363.8	778.6	270.1
Verdigris (D)	TS-1A SG-4 to TOS	174.5 - 175.9	1212	>391	275.2	495.4	333.3	494.8	169.7
Verdigris (D)	TS-1A SG-3 to SG-4	173.0 - 174.5	1212	>968	275.2	495.4	333.3	494.8	169.7
Crowebug (E)	TS-1A O-cell to SG-2	170.5 - 172.0	1716	723	327.5	589.5	471.9	588.1	240.2
Crowebug (E)	TS-1A SG-1 to O-cell	169.6 - 170.5	1716	963	327.5	589.5	471.9	588.1	240.2
	Grandview								
W. Chanute	SG-6 to TOS	282.5 - 284.7	938	>301	242.4	436.3	258.5	435.8	56.4
Chanute	SG-5 to SG-6	280.7 - 282.5	690	295	207.7	373.8	189.8	373.3	55.2
Chanute	SG-4 to SG-5	279.3 - 280.7	690	453	207.7	373.8	189.8	373.3	69.0
Cement City	SG-3 to SG-4	277.8 - 279.3	37000						
Quivira	O-cell to SG-3	275.8 - 277.8	1427	460 ⁽³⁾	295.8	532.4	385.0	531.8	196.0
Westerville	SG-1 to O-cell	273.7 - 275.8	62900						
Wea	Tip to SG-1	272.3 - 273.7	2308	565	379.1	682.5	318.5	681.6	323.1
	Waverly								
Weir (A)	SG-4 to O shear	182.7 - 184.9	430	>88	169.5	305.1	126.4	304.7	119.5
Weir (B)	SG-3 to SG-4	178.2 - 182.7	470	>94	171.2	308.2	129.0	307.9	140.8
Weir (C)	SG-2 to SG3	175.1 - 178.2	2360	>306	383.7	690.7	322.3	689.8	329.8
Weir (D)	O-cell to SG-2	171.8 - 175.1	890	>587	235.9	424.7	133.6	424.1	195.9
Weir (E)			6560						

(1) Values reported are ultimate (2) The symbol ">" indicates that the ultimate unit side shear was not reached during test, value reported is maximum during test. (3) Assumed unit side shear (4) Method not intended for values unless otherwise indicated. slump less than 175 mm (7 in)

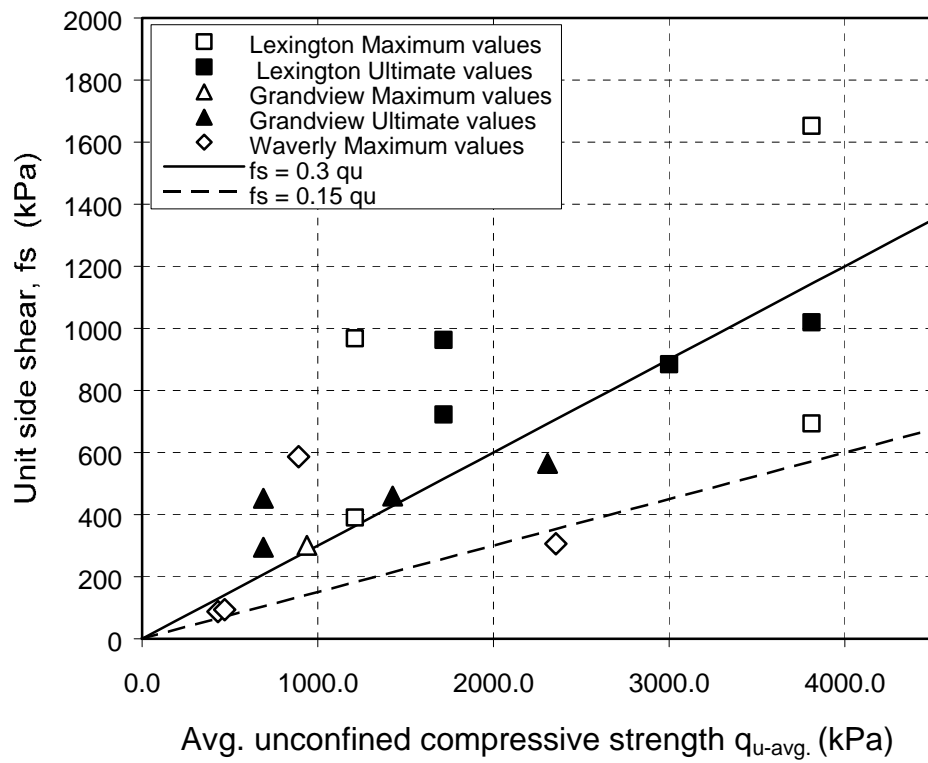


Figure D.1- Unit side shear versus average q_u .

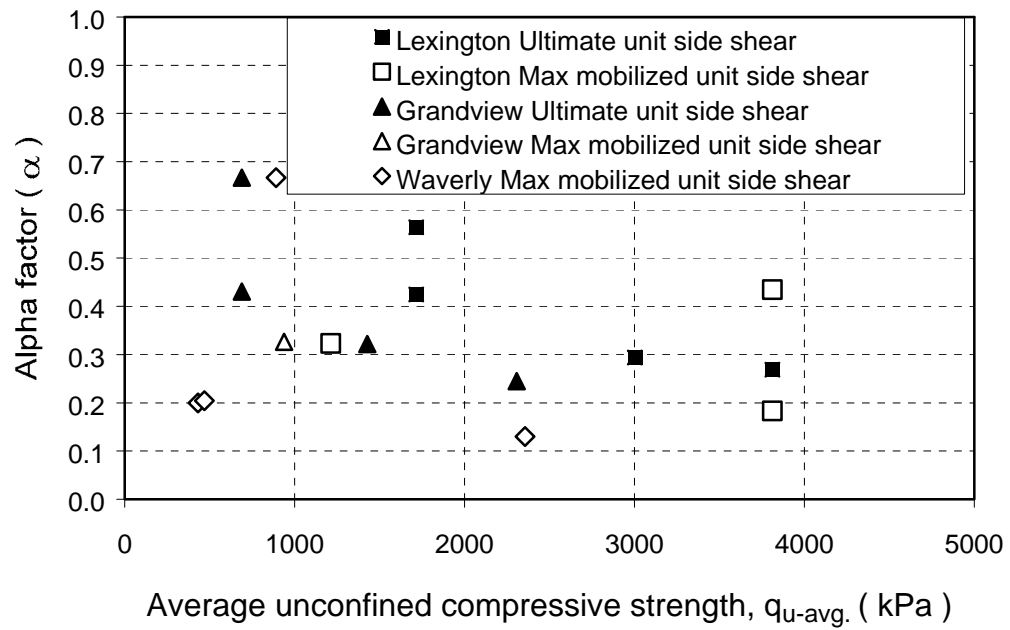
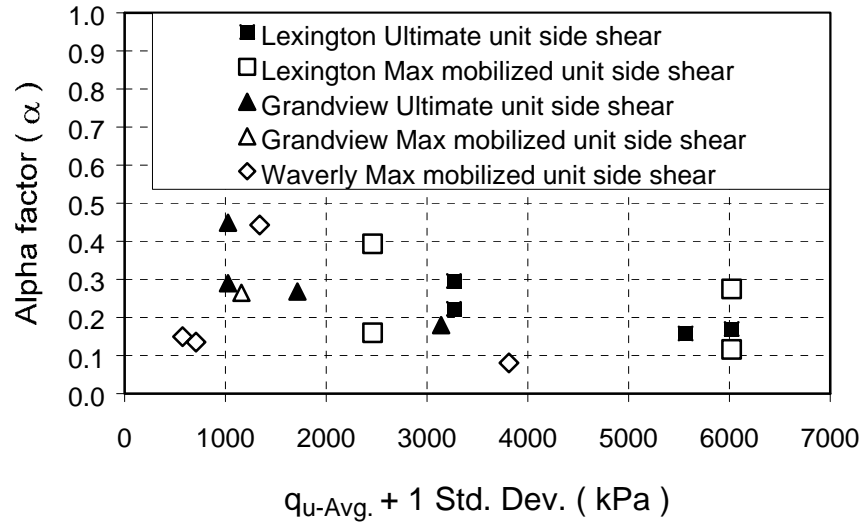
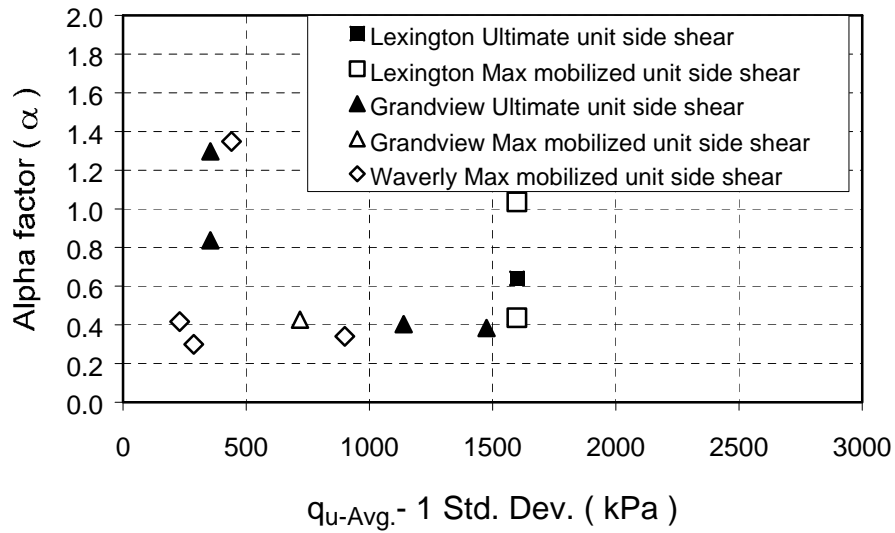


Figure D.2- Back-calculated alpha factor (α) versus average q_u for test sites in shale.



a. $q_{u-avg.}$ plus one standard deviation.



b. $q_{u-avg.}$ minus one standard deviation.

Figure D.3- Back-calculated alpha (α) versus q_u ; (a) $q_{u-avg.}$ plus one standard deviation, (b) $q_{u-avg.}$ minus one standard deviation.

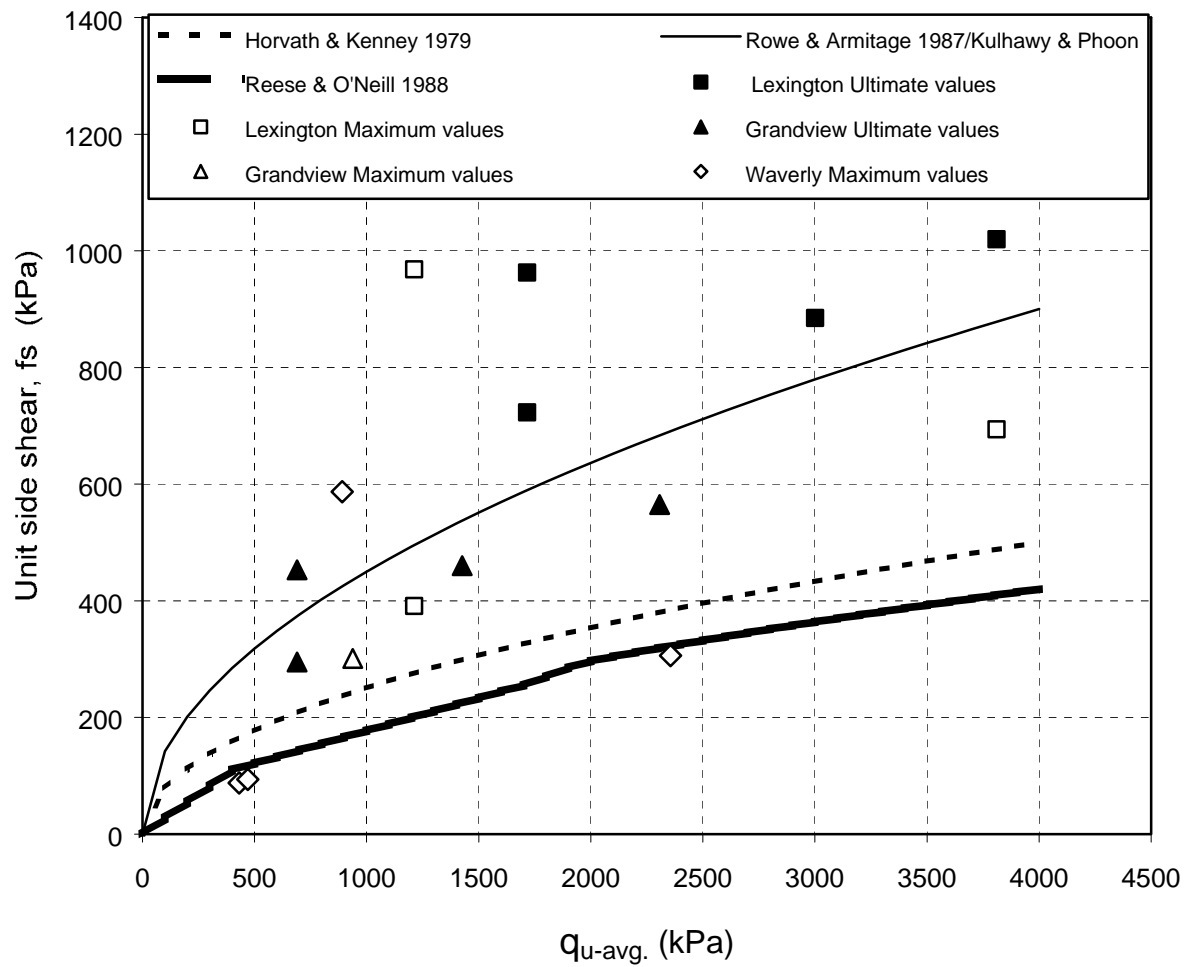


Figure D.4- Comparison of measured unit side shear data to predicted unit side shear by several methods.

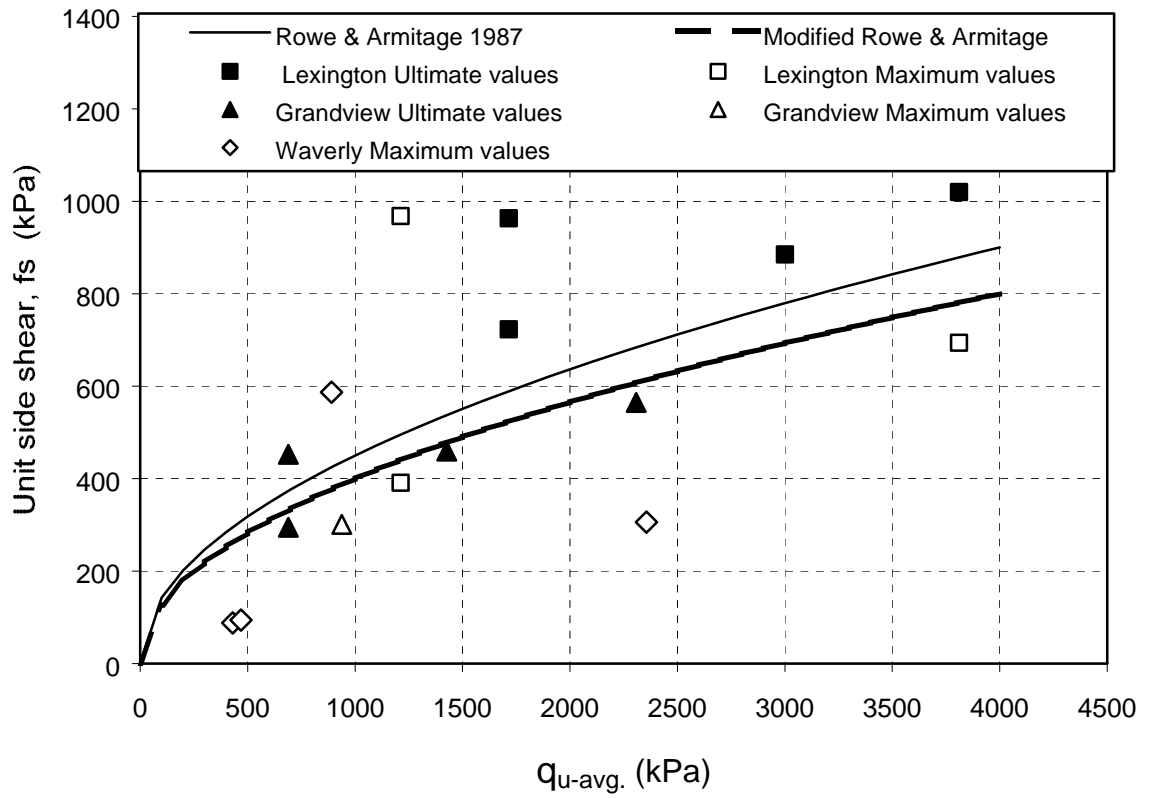


Figure D.6- Modified Rowe and Armitage method.

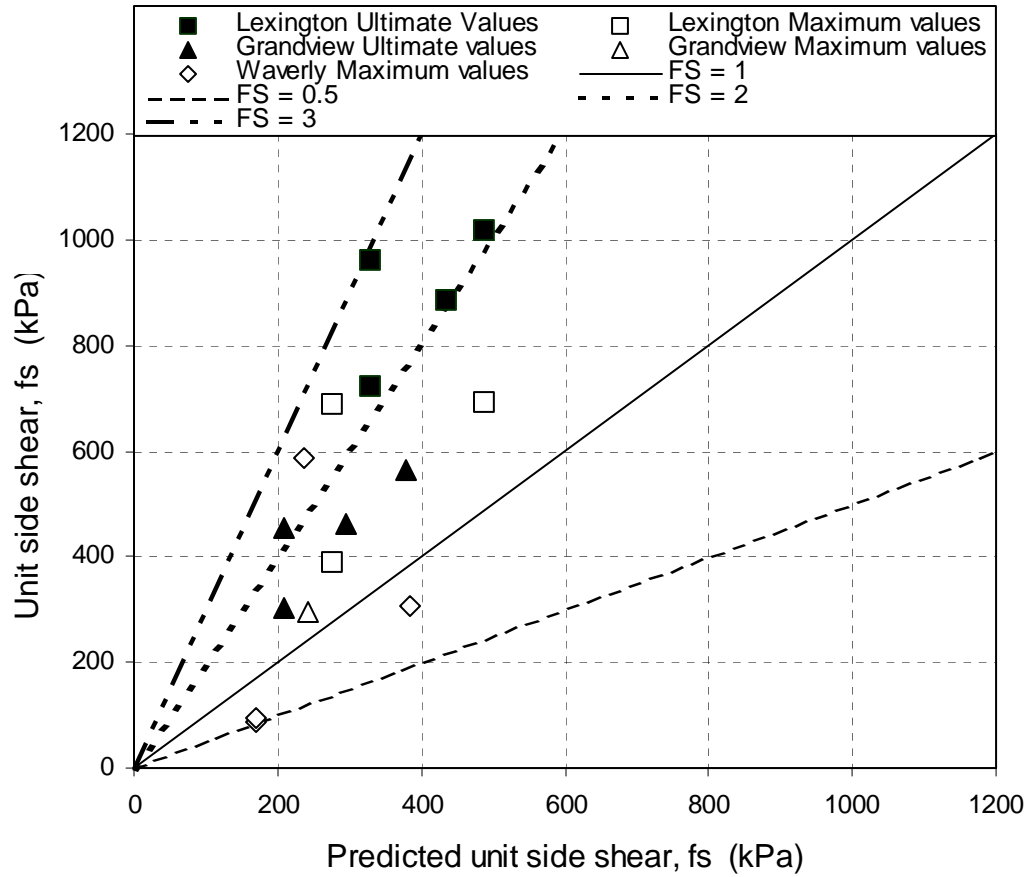


Figure D.7- Comparison of measured and predicted unit side shear value using the Horvath and Kenney (1979) method.

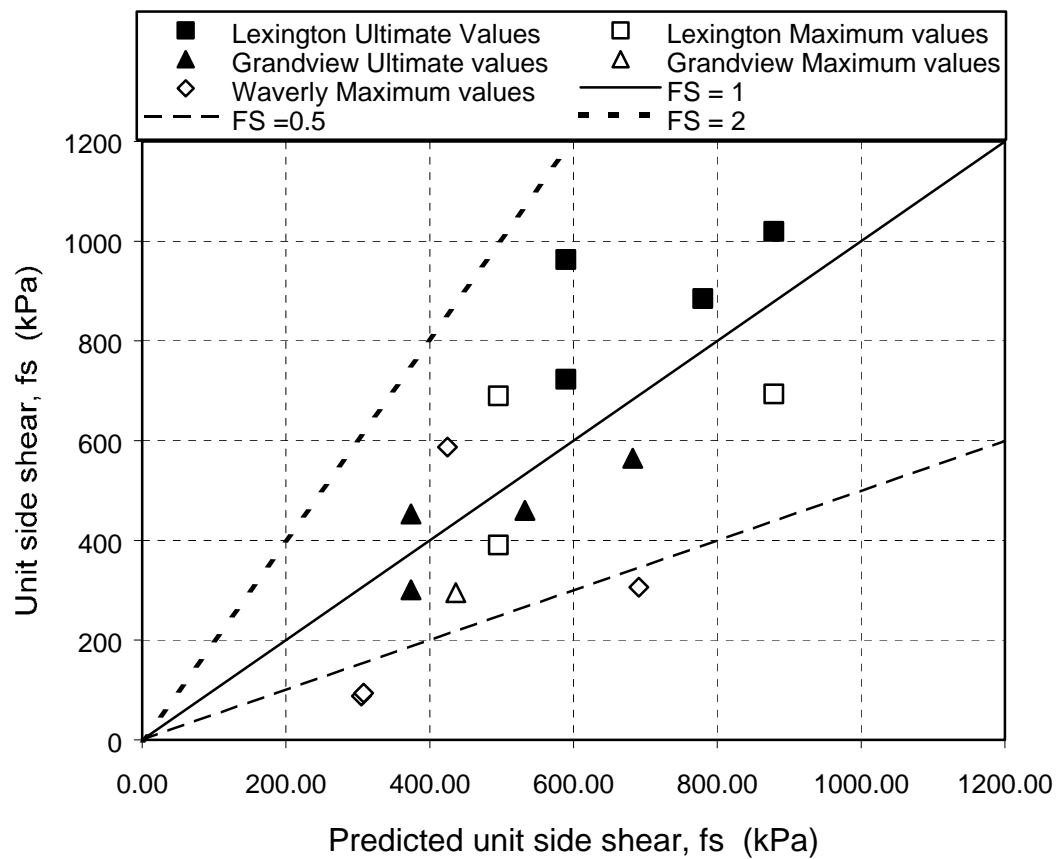


Figure D.8- Comparison of measured and predicted unit side shear using the Rowe and Armitage (1987) method.

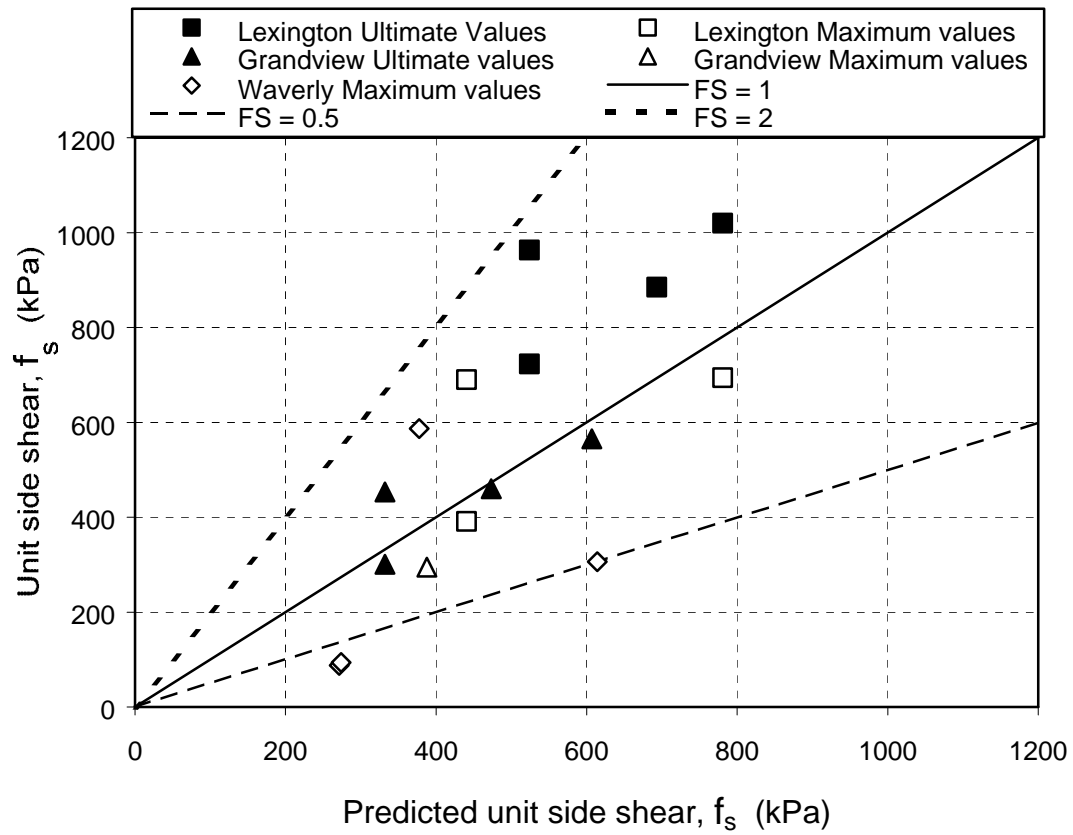


Figure D.9- Comparison of measured and predicted unit side shear using the modified Rowe and Armitage (1987) method.

APPENDIX E
CONSTRUCTION AND LOAD TEST PHOTOGRAPHS FOR LEXINGTON
TEST SITE (HNTB 1999)



E1- View of platform, temporary casing, and deflection wall sheeting



E2- Test shaft ts-1A in foreground. Test shaft TS-2 in background.



E3- Drilling bucket and Manitowoc 4100 Series with drill assembly



E4- Hardened steel cutting edge at bottom of permanent casing



E5- Replacing slurry with water after seating permanent casing.



E6- Bullet tooth rock auger.



E7- Using rock auger to drill rock socket



E8- Cleaning hole by airlift method.



E9- Bottom of airlift pipe.



E10- Assembling sister bars, strain gages, vibrating wire displacement transducers on carrying frame.



E11- Welding carrier frame to O-cell™



E12- Lifting O-cells and carrier frame



E13- Down hole rotating sonar "caliper" device



E14- Real-time sonar measurements and lowering of sonar.



E15- Airlift pipe and assembled load cells and carrier frames for TS-1A and TS-2



E16- Lowering O-cells and carrier frame into test shaft



E17- Lowering 125 mm tremie pipe to bottom of test shaft.



E18- Delivering concrete to test shaft by barge.



E19- Pumping concrete to tremie pipe.



E20- Dial gages for measuring displacement of top of carrying frame during load test.



E21- Water pump for pressurizing load cells.



E22- Recording readings from load test instruments.

MISSOURI DEPARTMENT OF TRANSPORTATION
Division of Materials

BORING DATA (CORE & SPT)

Sheet 12 of 18

Job No.	J4P1102					
County	Lafayette/Ray		Route	13	Design	A5664
Over	Missouri River				Skew	Right Angles
Logged by	Davis/Stevens				Operator	Lamberson/Wilde
Equipment	Failing 1500				Drillers Hole No.	A-96-55
Hole Stab. by	Casing				Date of Work	10/24/96

Bent		Station		Location		Barge Deck Elevation		LOG OF MATERIALS *	
22		0+112.7		10m LT.		209.39		0.0-1.54m	Barge.
B-13 Formerly		11+244		10m LT.		209.39		1.54-8.50m	Water.
TEST DATA								8.50-12.00m	Medium and fine grained sand, dense.
Depth, m		SPT Blows/15cm		Pocket Pen., kg/cm²		Est. Equiv. Qu, kPa		12.00-15.84m	Coarse sand and fine gravel, medium dense.
9.35		9-6-9		Sand				15.84-16.10m	Large cobble, hard.
12.50		3-4-4		Sand				16.10-17.15m	Fine to medium grained, medium to thick bedded, arkosic
15.50		5-13-12		Sand					and micaceous sandstone, hard, some cross bedding.
19.30		50 in 8cm		9.0+				17.15-22.20m	Gray thinly laminated clay shale, moderately hard.
23.80		50 in 6cm		Crumbled				22.20-22.30m	Black shale to coal.
28.36		50 in 6cm		7.50				22.30-28.56m	Gray thinly cross-laminated fine grained calcareous,
									micaceous silt shale, hard.
								28.56-31.42m	Gray, well cemented, thinly laminated clay shale,
									moderately hard.
CORING LOG (NX Double Tube Barrel)									
From	To	Run	Rec	Loss	% RQD	Notes			
16.30	17.80	1.50	1.46	0.04	0.00				
17.80	19.30	1.50	1.50	0.00	0.00				
19.38	20.88	1.50	1.30	0.20	0.00				
20.88	22.30	1.42	1.42	0.00	0.00				
22.30	23.80	1.50	1.50	0.00	0.00				
23.86	25.36	1.50	1.48	0.02	0.00				
25.36	26.86	1.50	1.50	0.00	0.00				
26.86	28.36	1.50	1.50	0.00	0.00				
28.42	29.92	1.50	1.41	0.09	0.00				
29.92	31.42	1.50	1.38	0.12	0.00				

Persons using this information are cautioned that the materials shown are determined by the equipment noted and accuracy of the "log of materials" is limited thereby and by judgment of the operator. THIS INFORMATION IS FOR DESIGN PURPOSES ONLY:

MISSOURI DEPARTMENT OF TRANSPORTATION
Division of Materials

BORING DATA (CORE & SPT)

Sheet 13 of 18

Job No.	J4P1102					
County	Lafayette/Ray		Route	13	Design	A5664
Over	Missouri River				Skew	Right Angles
Logged by	Davis/Stevens				Operator	Lamberson/Wilde
Equipment	Failing 1500				Drillers Hole No.	A-96-55
Hole Stab. by	Casing				Date of Work	10/24/96

<u>Bent</u>	<u>Boring</u>	<u>Station</u>	<u>Location</u>	<u>Barge Deck Elevation</u>
22	B-13	0+112.7	10m LT.	209.39
Formerly	B-13	11+244	10m LT.	209.39

SOIL CLASSIFICATION TEST DATA				UNCONFINED COMPRESSIVE DATA			
<u>Depth, m</u>	<u>LL</u>	<u>PI</u>	<u>ASTM Class</u>		<u>Depth, m</u>	<u>Qu, kPa</u>	<u>P.P., kg/cm²</u>
9.35		NP	SP		16.70	4807	9.0+
					17.90	1381	9.0+
					20.30	949	9.0+
					21.50	637	9.0+
					23.70	1320	9.0+
					24.40	2473	9.0+
					26.20	2101	9.0+
					28.10	2494	9.0+
					28.70	2578	9.0+
					31.0	2213	9.0+

SIEVE ANALYSIS (Percent Passing)
AASHTO T88

Depth, m

	9.35							
19mm	100.00							
9.5mm	99.00							
4.75mm	97.00							
2.00mm	95.00							
.850mm	91.00							
.425mm	64.00							
.300mm	32.00							
.150mm	23.00							
.075mm	4.00							

Persons using this information are cautioned that the materials shown are determined by the equipment noted and accuracy of the "log of materials" is limited thereby and by judgment of the operator. THIS INFORMATION IS FOR DESIGN PURPOSES ONLY:



MISSOURI DEPARTMENT OF TRANSPORTATION
Division of Materials

BORING DATA (CORE & SPT)

Sheet 16 of 18

Job No.	J4P1102					
County	Lafayette/Ray		Route	13	Design	A5664
Over	Missouri River				Skew	Right Angles
Logged by	Dietiker/Davis				Operator	Dodds/Lamberson
Equipment	Failing 1500				Drillers Hole No.	A-96-54
Hole Stab. by	Casing				Date of Work	10/24/96

Bent		Station		Location		Barge Deck Elevation		LOG OF MATERIALS *	
22		0+122.7		10m RT.		209.27		0.0-1.52m	Barge.
B-15 Formerly		11+254		10m RT.		209.27		1.52-7.52m	Water.
TEST DATA								7.52-12.20m	Gray fine to medium grained sand with scattered gravel,
Depth, m		SPT Blows/15cm		Pocket Pen., kg/cm²					medium dense.
11.00		5-6-6		Sand				12.20-15.16m	Gray medium grained sand with scattered coarse grained sand,
14.00		6-6-6		Sand					medium dense.
17.00		50 in 6cm		Sand				15.16-15.40m	Coarse gravel and scattered cobbles.
20.33		50 in 11cm		Sand				15.40-16.07m	Gray fine to medium grained sand, dense.
23.44		50 in 7cm		Sand				16.07-17.07m	Brown to gray coarse grained sandstone, very hard,
26.51		50 in 5cm		Sand					cut with rockbit.
								17.07-21.94m	Gray clay shale, thinly laminated, moderately hard.
								21.94-22.17m	Black coal seam.
								22.17-28.71m	Gray thin to medium laminated, calcareous, micaceous
									silt shale, moderately hard.
								28.71-32.01m	Gray thinly laminated clay shale, moderately hard.
								32.01-32.06m	Light brownish-gray, thin bedded, fine grained limestone,
									very hard.
								32.06-32.61m	Gray clay shale, moderately hard.
CORING LOG (NX Double Tube Barrel)									
From	To	Run	Rec	Loss	% RQD	Notes			
17.33	18.83	1.50	1.50	0.00	0.00	Shale			
18.83	20.33	1.50	1.18	0.32	0.00	Shale			
20.44	21.94	1.50	1.30	0.20	0.00	Shale			
21.94	23.44	1.50	1.50	0.00	0.00	Shale			
23.51	25.01	1.50	1.50	0.00	0.00	Shale			
25.01	26.51	1.50	1.50	0.00	0.00	Shale			
26.56	28.06	1.50	1.50	0.00	0.00	Shale			
28.06	29.56	1.50	1.34	0.16	0.00	Shale			
29.61	31.11	1.50	1.50	0.00	0.00	Shale			
31.11	32.61	1.50	1.50	0.00	0.00	Shale			

Persons using this information are cautioned that the materials shown are determined by the equipment noted and accuracy of the "log of materials" is limited thereby and by judgment of the operator. THIS INFORMATION IS FOR DESIGN PURPOSES ONLY:

MISSOURI DEPARTMENT OF TRANSPORTATION
Division of Materials

BORING DATA (CORE & SPT)

Sheet 17 of 18

Job No.	J4P1102					
County	Lafayette/Ray		Route	13	Design	A5664
Over	Missouri River				Skew	Right Angles
Logged by	Dietiker/Davis				Operator	Dodds/Lamberson
Equipment	Failing 1500				Drillers Hole No.	A-96-54
Hole Stab. by	Casing				Date of Work	10/24/96

<u>Bent</u>	<u>Boring</u>	<u>Station</u>	<u>Location</u>	<u>Barge Deck Elevation</u>
22	B-15	0+122.7	10m RT.	209.27
Formerly	B-15	11+254	10m RT.	209.27

					<u>UNCONFINED COMPRESSIVE DATA</u>		
					<u>Depth, m</u>	<u>Qu, kPa</u>	<u>P.P., kg/cm²</u>
					18.20	720	9.0+
					19.60	1141	9.0+
					21.40	535	9.0+
					22.40	5759	9.0+
					24.50	1648	9.0+
					25.60	2097	9.0+
					29.0	2468	9.0+
					30.30	1579	9.0+
					31.80	2332	9.0+

* Persons using this information are cautioned that the materials shown are determined by the equipment noted and accuracy of the "log of materials" is limited thereby and by judgment of the operator. THIS INFORMATION IS FOR DESIGN PURPOSES ONLY:



MISSOURI DEPARTMENT OF TRANSPORTATION
Division of Materials

BORING DATA (CORE & SPT)

Sheet 14 of 18

Job No.	J4P1102					
County	Lafayette/Ray		Route	13	Design	A5664
Over	Missouri River				Skew	Right Angles
Logged by	Davis/Stevens/Dietiker				Operator	Lamberson/Wilde/Dodds
Equipment	Failing 1500				Drillers Hole No.	A-96-53
Hole Stab. by	Casing				Date of Work	10/23/96

Bent		Station		Location		Barge Deck Elevation		LOG OF MATERIALS *	
22		0+117.7		C/L		209.16		0.0-1.55m	Barge.
B-14 Formerly		11+249		C/L		209.16		1.55-7.52m	Water.
TEST DATA								7.52-9.00m	Gray fine and medium grained coarse sand, dense to very dense.
Depth, m	SPT Blows/15cm	Pocket Pen., kg/cm²	Est. Equiv. Qu, kPa	9.00-13.20m	Gray fine to medium grained sand and fine gravel with some				
7.52	14-25-30				coarse grained sand, medium dense.				
9.50	5-3-6			13.20-14.30m	Coarse sand and cobbles.				
12.50	9-5-7			14.30-14.75m	Coarse sand, medium dense.				
15.50	50 in 8cm			14.75-14.90m	Boulder, very hard.				
18.02	100 in 13cm	9.0+	570	14.90-15.90m	Fine sand and silt with some clay, very dense.				
22.66	50 in 8cm	9.0+		15.90-16.90m	Fine to medium grained sandstone, very hard, cut with rockbit.				
27.24	50 in 6cm	7.0		16.90-21.56m	Gray thinly laminated clay shale, moderately hard, cut with				
31.80	50 in 10cm				rockbit to 18.16m.				
				21.56-21.76m	Black carbonaceous shale, moderately hard.				
				21.76-21.98m	Black coal bed, hard.				
				21.98-22.21m	Gray clay shale, soft, (underclay).				
				22.21-22.39m	Dark gray shaly limestone to siltstone, very hard.				
				22.39-28.89m	Gray thin to medium laminated, fine grained, calcareous,				
					micaceous silt shale, well cemented, hard.				
CORING LOG (NX Double Tube Barrel)								28.89-32.71m	Gray clay shale, thinly laminated, moderately hard.
From	To	Run	Rec	Loss	% RQD	Notes	32.71-32.94m	Black coal seam, hard.	
18.16	19.66	1.50	1.50	0.00	0.00		32.94-33.40m	Dark gray clay shale, poorly laminated, soft.	
19.66	21.16	1.50	1.50	0.00	0.00				
21.16	22.66	1.50	1.50	0.00	0.00				
22.74	24.24	1.50	1.50	0.00	0.00				
24.24	25.74	1.50	1.50	0.00	0.00				
25.74	27.24	1.50	1.50	0.00	0.00				
27.30	28.80	1.50	1.49	0.01	0.00				
28.80	30.30	1.50	1.46	0.04	0.00				
30.30	31.80	1.50	1.50	0.00	0.00				
31.90	33.40	1.50	1.50	0.00	0.00				

Persons using this information are cautioned that the materials shown are determined by the equipment noted and accuracy of the "log of materials" is limited thereby and by judgment of the operator. THIS INFORMATION IS FOR DESIGN PURPOSES ONLY:

MISSOURI DEPARTMENT OF TRANSPORTATION
Division of Materials

BORING DATA (CORE & SPT)

Sheet 15 of 18

Job No.	J4P1102					
County	Lafayette/Ray		Route	13	Design	A5664
Over	Missouri River				Skew	Right Angles
Logged by	Davis/Stevens/Dietiker				Operator	Lamberson/Wilde/Dodds
Equipment	Failing 1500				Drillers Hole No.	A-96-53
Hole Stab. by	Casing				Date of Work	10/23/96

<u>Bent</u>	<u>Boring</u>	<u>Station</u>	<u>Location</u>	<u>Barge Deck Elevation</u>
22	B-14	0+117.7	C/L	209.16
Formerly B-14		11+249	C/L	209.16

SOIL CLASSIFICATION TEST DATA				UNCONFINED COMPRESSIVE DATA			
<u>Depth, m</u>	<u>LL</u>	<u>PI</u>	<u>ASTM Class</u>	<u>Depth, m</u>	<u>Qu, kPa</u>	<u>P.P., kg/cm²</u>	
9.50		NP	SP	18.90	1907	9.0+	
				20.30	914	9.0+	
				24.20	3412	9.0+	
				26.60	7806	9.0+	
				28.60	2662	9.0+	
				29.30	1948	9.0+	
				32.10	2855	9.0+	
				33.10	423	9.0+	

SIEVE ANALYSIS (Percent Passing)
AASHTO T88

Depth, m

	9.50						
19mm	95.00						
9.5mm	95.00						
4.75mm	95.00						
2.00mm	95.00						
.850mm	94.00						
.425mm	68.00						
.300mm	26.00						
.150mm	6.00						
.075mm	3.00						

Persons using this information are cautioned that the materials shown are determined by the equipment noted and accuracy of the "log of materials" is limited thereby and by judgment of the operator. THIS INFORMATION IS FOR DESIGN PURPOSES ONLY:



Boring B-14 0+117.7 C/L
Bent 22 11/04/96

MISSOURI DEPARTMENT OF TRANSPORTATION

Division of Materials

BORING DATA (CORE & SPT)

Sheet 1 of 1

Job No.	J4P1102						
County	Ray/Lafayette		Route	13		Design	A5664
Over	Missouri River					Skew	Right Angles
Logged by	Miller					Operator	Wilde
Equipment	Failing 1500					Drillers Hole No.	H-98-62
Hole Stab. by	Casing					Date of Work	09/09/98, 09/15/98, 09/16/98
Automatic Hammer Efficiency				73	%	Drill No.	G-7888

Bent		Station		Location		Surface Elevation	LOG OF MATERIALS *	
Test Shaft #2		0+167.25		29.4m LT.		210.28	0.0-5.0m	Brown lean clay to silt.
CORING LOG (NX Double Tube Barrel)							5.0-6.20m	Gray silty clay, scattered gravel, medium stiff.
From	To	Run	Rec	Loss	% RQD	Notes	6.20-12.47m	Gray fine sand, dense.
12.80	14.15	1.35	0.70	0.65			12.47-12.95m	Granite boulder.
14.85	16.35	1.50	1.46	0.04			12.95-14.50m	Weathered shaley limestone or boulders, lost water.
16.35	17.85	1.50	1.50	0.00			14.50-15.15m	Gray clay shale.
17.85	19.35	1.50	1.50	0.00			15.15-16.77m	Gray, fine grained sandstone, moderately hard.
19.35	20.85	1.50	1.50	0.00			16.77-17.57m	Gray, calcareous, micaceous silt shale, medium hard.
20.85	22.35	1.50	1.50	0.00			17.57-18.52m	Gray fine grained sandstone, moderately hard.
22.35	23.70	1.35	1.35	0.00			18.52-22.65m	Dark gray clay shale, moderately hard.
23.70	25.20	1.50	1.50	0.00			22.65-23.02m	Black shale, hard.
25.20	26.70	1.50	1.50	0.00			23.02-23.32m	Coal.
26.70	28.20	1.50	1.50	0.00			23.32-30.15m	Gray, calcareous, micaceous silt shale, moderately hard.
28.20	29.70	1.50	1.50	0.00			30.15-32.84m	Dark gray, thinly laminated clay shale, moderately hard.
29.70	31.20	1.50	1.50	0.00			32.84-33.85m	Black shale, hard.
31.20	32.70	1.50	1.50	0.00			33.85-34.20m	Coal.
32.70	34.20	1.50	1.50	0.00			34.20-36.08m	Gray clay shale, poorly laminated, soft.
34.20	35.70	1.50	1.50	0.00			36.08-36.47m	Gray shaley limestone, thick bedded, hard.
35.70	37.20	1.50	1.50	0.00			36.47-37.51m	Black clay shale, limestone seam at 36.9m,
37.20	38.70	1.50	1.50	0.00				moderately hard.
38.70	40.20	1.50	1.50	0.00			37.51-37.96m	Coal.
40.20	41.70	1.50	1.50	0.00			37.96-40.72m	Gray clay shale, poorly laminated, soft to medium hard,
41.70	43.15	1.45	1.45	0.00				limestone seam at 39.95m.
UNCONFINED COMPRESSIVE STRENGTH TEST DATA							40.72-41.00m	Gray shaley limestone, hard.
Depth, m		Qu, kPa		P.P., kg/cm²			41.00-43.15m	Gray clay shale, poorly laminated, soft to medium hard.
26.45		2140		9.0+				
27.20		1020		9.0+				
28.40		4500		9.0+				
29.60		3650		9.0+				
31.10		2330		9.0+				
33.70		31190		9.0+				
35.20		2290		9.0+				
36.0		310		9.0+				
38.40		600		9.0+				
39.60		340		9.0+				
41.60		150		7.0				
42.30		620		9.0+				
43.10		195		9.0+				

* Persons using this information are cautioned that the materials shown are determined by the equipment noted and accuracy of the "log of materials" is limited thereby and by judgment of the operator. THIS INFORMATION IS FOR DESIGN PURPOSES ONLY:



MISSOURI DEPARTMENT OF TRANSPORTATION
Division of Materials

BORING DATA (CORE & SPT)

Sheet 19 of 40

Job No.	J4P1102					
County	Lafayette/Ray		Route	13	Design	A5664
Over	Missouri River				Skew	Right Angles
Logged by	Fennessey/Stevens				Operator	Dodds
Equipment	CME 850				Drillers Hole No.	V-98-11
Hole Stab. by	Water				Date of Work	06/03 & 04/98
Automatic Hammer Efficiency				81 %	Drill No.	G-7950

Bent		Station		Location		Surface Elevation	LOG OF MATERIALS *	
23		0+175.7		9m LT.		210.18	0.0-1.22m	Brown lean clay to silt, soft.
Boring F-39							1.22-4.72m	Light brown silty fine grained sand, very loose.
TEST DATA							4.72-10.36m	Gray-brown silt, soft, interlayered scattered fine to
Depth, m		SPT Blows/15cm		N ₆₀		Pocket Pen., kg/cm²		medium grained sand.
1.50		2-2-2		5		Sand		10.36-11.28m
4.50		2-1-2		4		0.75		Gray, medium to coarse grained sand, trace brown
7.50		4-4-5		12		Sand		lean clay seams, loose, moist.
10.50		2-3-3		8		Sand		11.88-12.28m
							12.28-12.58m	Weathered limestone.
UNCONFINED COMPRESSIVE STRENGTH								Gray, fine to medium grained limestone, fractured,
								hard.
TEST DATA							12.58-13.50m	Purple clay shale, soft to medium hard.
								13.50-14.69m
Depth, m		Qu, kPa		P.P., kg/cm²				Gray, poorly laminated clay shale, medium hard.
14.60		140		2.75				14.69-15.75m
15.80		12,255		9.0+				Gray, calcareous, micaceous silt shale, medium hard.
18.30		7520		9.0+				Gray, fine grained sandstone, moderately hard.
18.90		2060		9.0+				16.85-17.60m
20.40		2440		9.0+				Gray, calcareous, micaceous silt shale, medium hard.
21.90		1120		9.0+				17.60-18.40m
23.50		5465		9.0+				Gray, fine grained sandstone, moderately hard.
CORING LOG (NX Double Tube Barrel)							18.40-18.56m	Gray, calcareous, micaceous silt shale, hard.
From		To		Run		Rec		18.56-20.97m
12.28		13.81		1.53		0.61		Gray, slightly calcareous clay shale, hard.
13.81		15.33		1.52		1.52		20.97-22.89m
15.33		16.85		1.52		1.52		Dark gray shale, poorly laminated, hard.
16.85		18.40		1.55		1.55		22.89-23.11m
18.40		19.90		1.50		1.50		Black shale, hard.
19.90		21.21		1.31		1.31		23.11-23.24m
21.21		22.74		1.53		1.37		Black coal, hard but brittle.
22.74		24.26		1.52		1.52		23.24-24.26m
WATER TABLE OBSERVATIONS								Gray and black banded, slightly calcareous, micaceous
Date		Time Change		Depth Hole Open		Depth To Water		silt shale, medium hard.
06/09/98		5 days		5.30m		1.0m		
							**RQD on limestone portion only.	

N₆₀ - Corrected N value for standard 60% SPT efficiency.

N₆₀ = (Em/60)Nm

Em - Measured transfer efficiency in percent.

Nm - Observed N-value.

* Persons using this information are cautioned that the materials shown are determined by the equipment noted and accuracy of the "log of materials" is limited thereby and by judgment of the operator. THIS INFORMATION IS FOR DESIGN PURPOSES ONLY:



Boring F-39 0+175.7, 9m LT.
Bent 23

APPENDIX G
CONSTRUCTION AND LOAD TEST PHOTOGRAPHS FOR GRANDVIEW
TEST SITE (HNTB 2002)



G1- View of test site from North



G2- 2550 mm (72 in) bullet tooth rock auger



G3- Installing "knuckle in 2550 mm (72 in) core barrel



G4- 914 mm (36in) Core barrel



G5- Clean Out bucket



G6- Large piece of Westerville Limestone core



G7- Sonic Caliper



G8- Load frame arrives at test site



G9- Down Hole video camera



G10- Video camera monitor and controls



G11- LVWDT installed above compression device



G12- Installed sister bar Strain Gage



G13- Raising Load frame



G14- Installation of rollers/spacers along load frame



G15- Scoring CSL pipe



G16- Scored CSL pipe



G17- Lowering frame into rock socket



G18- Welding load frame to supports on temporary casing



G19- Pump truck and tremie



G20- Lowering 127mm (5 in) tremie pipe



G21- View of load test in progress



G22- Reference beam and load test in progress



G23- Top of shaft instrumented for load test

APPENDIX H
BORING LOGS AND CORE PHOTOGRAPHS FOR GRANDVIEW TEST SITE

MISSOURI DEPARTMENT OF TRANSPORTATION
Project Operations

BORING DATA (CORE & SPT)

						Sheet	15	of	17
Job No.:	J4I0766E								
County:	Jackson		Route:	I-470		Design:	A6251		
Over:	Hickman Mills Dr., Ramp S-W, Ramp S-W Detour (B), & Hickman Mills Creek (S)					Skew:	Right Angles		
Logged by:	Davis					Operator:	Murray		
Equipment:	Versa Drill 4000 TR-2, Split Spoon Sampler, NX Core Barrel					Drillers Hole No.:	Y-02-34		
Hole Stab. by:	Hollow Stem Augers					Date of Work:	04/03/02		
Automatic Hammer Efficiency:					73 %	Drill No.:	G-8641		

Bent		Station		Location		Surface Elevation	LOG OF MATERIALS*		
12		25+37		0.7' RT.		938.5	0.0-2.1'	Reddish-brown shaley lean to fat clay,	
BH9-12-2								moist, medium stiff.	
TEST DATA							2.1-6.1'	Gray shaley fat clay to clay shale, moist to	
Depth, ft.	SPT Blows/6"	N ₆₀	Pocket Pen., tsf	Est. Equiv., Qu, tsf			5.3', then dry, stiff if clay, soft if shale.		
5.0	1-5-77 in 2"	100	2.0	4.3		6.1-6.5'	Gray, fine grained, thin bedded limestone,		
11.1	4-5-9	17	3.2				moderately hard, probably a boulder.		
						6.5-15.0'	Gray and brown shaley fat clay, moist,		
							stiff to very stiff, tried to core 6.1 to 11.1'		
							with near zero recovery, back on solid shale		
							at 14.6'.		
						15.0-21.0'	Gray thinly laminated clay shale, soft.		
						21.0-26.6'	Gray, thin bedded, fine grained limestone.		
						26.6-32.6'	Dark gray thinly laminated clay shale,		
							very soft to soft.		
						32.6-33.7'	Gray, thin bedded, fine grained limestone,		
							medium hard.		
						33.7-33.9'	Dark gray thinly laminated clay shale, soft.		
						33.9-40.4'	Gray, thin bedded, fine grained limestone,		
							medium to moderately hard, unweathered.		
						40.4-42.2'	Dark gray thinly laminated clay shale, soft.		

N₆₀ - Corrected N value for standard 60% SPT efficiency.

N₆₀ = (Em/60)Nm Em - Measured transfer efficiency in percent.

Nm - Observed N-value.

* Persons using this information are cautioned that the materials shown are determined by the equipment noted and accuracy of the "log of materials" is limited thereby and by judgment of the operator. THIS INFORMATION IS FOR DESIGN PURPOSES ONLY.

MISSOURI DEPARTMENT OF TRANSPORTATION
Project Operations

BORING DATA (CORE & SPT)

						Sheet	16	of	17
Job No.:	J4I0766E								
County:	Jackson		Route:	I-470		Design:	A6251		
Over:	Hickman Mills Dr., Ramp S-W, Ramp S-W Detour (B), & Hickman Mills Creek (S)					Skew:	Right Angles		
Logged by:	Davis					Operator:	Murray		
Equipment:	Versa Drill 4000 TR-2, Split Spoon Sampler, NX Core Barrel					Drillers Hole No.:	Y-02-32		
Hole Stab. by:	Hollow Stem Augers					Date of Work:	04/02/02		
Automatic Hammer Efficiency:					73 %	Drill No.:	G-8641		

Bent		Station		Location		Surface Elevation	LOG OF MATERIALS*		
13		26+19		31.3' LT.		950.5	0.0-1.9'	Reddish-brown lean to fat clay, moist,	
BH9-13-2								medium stiff.	
TEST DATA							1.9-3.3'	Gray lean clay, moist, medium stiff.	
Depth, ft.	SPT Blows/6"	N ₆₀	Pocket Pen., tsf			3.3-6.7'	Light brown lean clay, trace gravel, medium stiff.		
5.0	4-5-9	17	2.35						
10.0	5-3-3	7	4.20			6.7-7.9'	Gray silt shale, very soft, dry.		
15.0	12-18-36	66	>9.0			7.9-12.9'	Gray calcareous silt shale, with limestone		
20.0	22-30-41	86	6.1				pockets, dry, medium hard.		
						12.9-21.8'	Gray silt shale, soft, yellow-brown mottles, thinly laminated, cut with hollow stem		
							augers, split spoon, and rockbit.		
						21.8-27.1'	Gray thinly laminated silt and clay shale, soft.		
						27.1-32.9'	Reddish-brown thinly laminated clay shale, very soft to soft.		
						32.9-34.3'	Gray thinly laminated silt shale, soft, unweathered.		
						34.3-36.0'	Gray, thin to medium bedded, fine grained limestone, moderately hard, unweathered.		
						36.0-36.8'	Gray thinly laminated clay shale, scattered limestone nodules, soft.		
						36.8-39.6'	Gray, thin bedded, fine grained limestone, medium hard, slightly weathered.		
						39.6-45.0'	Gray thinly laminated silt shale to clay shale or claystone, very soft.		
CORING LOG (NX Double Tube Barrel)									
From	To	Run	Rec	Loss	% RQD	Notes	UNCONFINED COMPRESSIVE STRENGTH		
21.8	26.8	5.0	5.0	0	0		TEST DATA		
26.8	31.8	5.0	4.1	0.9	0		Depth, ft.	Qu, tsf	P.P., tsf
31.8	36.8	5.0	5.0	0	20**		29.2	2.7	4.25
36.8	41.8	5.0	5.0	0	0**		35.3	458.3	>9.0
41.8	45.0	3.2	3.2	0	0		38.2	2.4	3.20
			**RQD on limestone portion only.						
WATER TABLE OBSERVATIONS									
Date		Time Change		Depth Hole Open		Depth To Water			

N₆₀ - Corrected N value for standard 60% SPT efficiency.

N₆₀ = (Em/60)Nm Em - Measured transfer efficiency in percent.

Nm - Observed N-value.

* Persons using this information are cautioned that the materials shown are determined by the equipment noted and accuracy of the "log of materials" is limited thereby and by judgment of the operator. THIS INFORMATION IS FOR DESIGN PURPOSES ONLY.



MISSOURI DEPARTMENT OF TRANSPORTATION
Project Operations - Materials

BORING DATA (CORE & SPT)

						Sheet	5	of	14
Job No.:	J4I0766E								
County:	Jackson		Route:	I-470		Design:	A6252		
Over:	US 71					Skew:	Right Angles		
Logged by:	Hilchen					Operator:	Wineland		
Equipment:	Failing 1500					Drillers Hole No.:	A-02-48		
Hole Stab. by:	Drilling Fluids/Casing					Date of Work:	05/02/02		
Automatic Hammer Efficiency:				72	%	Drill No.:	G-7887		

Bent		Station		Location		Surface Elevation	LOG OF MATERIALS*		
(BH8-4-2) 4		44+71		50.8' RT.		934.6	0.0-1.8'	Brown lean clay, with gravel, stiff, moist.	
							1.8-4.9'	Gray shale fill, very stiff, moist.	
TEST DATA							4.9-8.8'	Brown fat clay, stiff, moist.	
Depth, ft.	SPT Blows/6''		N ₆₀		Pocket Pen., tsf		8.8-13.9'	Light gray, fine grained, medium bedded,	
								medium hard limestone, weathered clay filled	
								seams from 8.8 to 11.1'.	
							13.9-15.8'	Olive-gray to gray shale, thickly laminated,	
								very soft rock.	
							15.8-16.8'	Dark gray thinly laminated shale, very soft	
								rock.	
							16.8-19.1'	Bluish-gray thickly laminated shale,	
								very soft rock.	
							19.1-27.7'	Light gray, fine grained, thin to medium	
								bedded, soft to moderately hard limestone,	
								with thin bluish-gray shale lenses.	
							27.7-54.5'	Dark gray thinly laminated shale,	
								very soft rock.	
							UNCONFINED COMPRESSIVE STRENGTH		
							TEST DATA		
							Depth, ft.	Qu, tsf	P.P., tsf
								12.6	410.2
								19.7	137.9
								23.9	707.3
CORING LOG (NX Double Tube Barrel)							28.1	8.4	>9.0
From	To	Run	Rec	Loss	% RQD	Notes	36.0	29.9	>9.0
4.5	8.5	4.0	1.3	2.7	0		42.0	25.6	>9.0
8.5	13.5	5.0	3.8	1.2	30		48.2	24.9	>9.0
13.5	18.5	5.0	4.7	0.3	100**		52.1	30.5	>9.0
18.5	23.5	5.0	4.7	0.3	39**				
23.5	26.5	3.0	3.0	0	70				
26.5	31.5	5.0	5.0	0	Shale				
31.5	34.5	3.0	3.0	0	Shale				
34.5	39.5	5.0	5.0	0	Shale				
39.5	44.5	5.0	5.0	0	Shale				
44.5	49.5	5.0	5.0	0	Shale				
49.5	54.5	5.0	5.0	0	Shale				
WATER TABLE OBSERVATIONS									
Date		Time Change		Depth Hole Open		Depth To Water			

N₆₀ - Corrected N value for standard 60% SPT efficiency.

N₆₀ = (Em/60)Nm Em - Measured transfer efficiency in percent.

Nm - Observed N-value.

* Persons using this information are cautioned that the materials shown are determined by the equipment noted and accuracy of the "log of materials" is limited thereby and by judgment of the operator. THIS INFORMATION IS FOR DESIGN PURPOSES ONLY.



331



333





**MISSOURI DEPARTMENT OF TRANSPORTATION
Project Operations - Materials**

BORING DATA (CORE & SPT)

						Sheet	10	of	14
Job No.:	J4I0766E								
County:	Jackson		Route:	I-470		Design:	A6252		
Over:	US 71, Ramp S-W, Ramp S-W Detour & Hickman Mills Drive and Creek(S)					Skew:	Right Angles		
Logged by:	Davis					Operator:	Hees		
Equipment:	Versa Drill 4000 TR-2, Split Spoon Sampler, NX Core Barrel					Drillers Hole No.:	Y-02-39		
Hole Stab. by:	Hollow Stem Augers					Date of Work:	04/16/02		
Automatic Hammer Efficiency:							73 %	Drill No.:	G-8641

Bent		Station		Location		Surface Elevation	LOG OF MATERIALS*		
(BH8-8-1) 8		50+34		18.6' LT.		933.7	0.0-5.1'	Brown shaley fat clay, gray and yellowish-brown mottles, moist, very stiff.	
TEST DATA							5.1-11.2'	Gray and brown shaley fat clay, scattered gravel, moist, very stiff to hard.	
Depth, ft.		SPT Blows/6"		N ₆₀	Pocket Pen., tsf				
4.0		2-2-2		5	2.15			11.2-15.4'	Gray thinly laminated clay shale, soft, weathered.
9.0		1-2-3		6	5.5			15.4-19.2'	Gray, thin to medium bedded, fine grained limestone, slightly weathered, moderately hard.
14.0		4-5-10 in 2", then 10 blows, no advance		--	4.9			19.2-26.8'	Dark gray thinly laminated clay shale, very soft.
								26.8-34.0'	Gray, thin bedded, medium to coarse grained limestone, weathered, soft to moderately hard.
								34.0-45.4'	Dark gray thinly laminated clay shale, very soft.
								UNCONFINED COMPRESSIVE STRENGTH	
								TEST DATA	
								Depth, ft.	Qu, tsf
								17.6	571.4
								23.6	11.1
								32.6	725.8
								40.8	19.4
CORING LOG (NX Double Tube Barrel)									
From	To	Run	Rec	Loss	% RQD		Notes		
15.4	20.4	5.0	3.8	1.2	42				
20.4	25.4	5.0	5.0	0	0				
25.4	30.4	5.0	5.0	0	10**				
30.4	35.4	5.0	3.6	1.4	40				
35.4	40.4	5.0	5.0	0	0				
40.4	45.4	5.0	4.6	0.4	0				
		**RQD on limestone portion only.							
WATER TABLE OBSERVATIONS									
Date		Time Change		Depth Hole Open		Depth To Water			



MISSOURI DEPARTMENT OF TRANSPORTATION
Project Operations

BORING DATA (CORE & SPT)

						Sheet	1	of	2
Job No.:	J410766D								
County:	Jackson		Route:	I-470		Design:	A6252		
Over:	Route 71					Skew:	R.A. to B/L Rte. 71		
Logged by:	Davis					Operator:	Hees		
Equipment:	Failing 1500, Split Spoon Sampler, NX Wireline Core Barrel					Drillers Hole No.:	A-103-01		
Hole Stab. by:	Casing					Date of Work:	12/17/01, 12/20/01		
Automatic Hammer Efficiency:				72	%	Drill No.:	G-7887		

Bent		Station		Location		Surface Elevation	LOG OF MATERIALS*			
		125+05		90° LT.		942.2	0.0-0.5'	Brown lean clay, soft, moist.		
							0.5-3.1'	Rock, medium hard, probably weathered		
TEST DATA								limestone.		
Depth, ft.		SPT Blows/6"		N ₆₀	Pocket Pen., tsf	Est. Equiv., Qu, tsf	3.1-3.9'	Clay seam, soft.		
20.0		40-43 in 3"		100	6.1	4.0	3.9-4.7'	Rock, soft, probably weathered shale.		
							4.7-6.5'	Brown clay, soft, wet.		
UNCONFINED COMPRESSIVE STRENGTH TEST DATA							6.5-15.5'	Gray shaley clay, soft, wet.		
Depth, ft.		Qu, tsf		Pocket Pen., tsf		Wn%	15.5-26.6'	Gray clay shale, with brown clay shale		
22.2		5.18		6.5		14.8		seams, soft, thinly laminated to		
23.9		4.61		7.2		9.9		thickly laminated, very poor quality.		
27.4		118.6		>9.0		--	26.6-32.0'	Gray, fine grained, medium to thick bedded		
32.2		14.26		>9.0		9.3		limestone, weathered, medium hard.		
36.1		2.88		5.5		12.4	32.0-33.7'	Greenish-gray thinly laminated silt shale,		
39.1		164.8		>9.0		--		medium hard.		
43.2		411.6		>9.0		--	33.7-34.4'	Black thinly laminated silt shale, soft.		
46.2		13.8		>9.0		10.1	34.4-37.7'	Gray thinly laminated silt shale, soft.		
49.5		32.7		>9.0		8.8	37.7-44.3'	Gray and yellowish-brown, medium		
51.4		18.9		>9.0		8.6		bedded, coarse grained, oolitic limestone,		
54.5		27.6		>9.0		8.8		weathered, medium hard, lost circulating		
61.1		20.7		>9.0		8.6		water at 40.1'.		
67.9		25.9		>9.0		8.6	44.3-77.2'	Greenish-gray and gray thinly laminated silt		
								and clay shale, soft to medium hard.		
							77.2-78.2'	Gray, thickly laminated to thin bedded,		
								medium to coarse grained limestone, with		
								shale lamina, medium hard, unweathered.		
CORING LOG (NX Double Tube Barrel)										
From	To	Run	Rec	Loss	% RQD	Notes	UNIT WEIGHTS			
21.0	26.0	5.0	5.0	0	0		Depth, ft.	γmoist, pcf	γsat, pcf	%sat
26.0	31.0	5.0	5.0	0	78**		22.2		139.0	100 ⁽²⁾
31.0	36.0	5.0	5.0	0	14**		23.9		146.1	100 ⁽²⁾
36.0	41.0	5.0	5.0	0	58**		27.4		166.3	N/A
41.0	46.0	5.0	4.1	0.9	30**		32.2		147.0	100 ⁽²⁾
46.0	51.0	5.0	4.2	0.8	0		36.1	138.2		93.1 ⁽²⁾
51.0	56.0	5.0	5.0	0	0		39.1		162.5	N/A
56.0	61.0	5.0	2.1	2.9	0		43.2		162.0	N/A
61.0	66.0	5.0	3.7	1.3	0		46.2		146.8	100 ⁽²⁾
66.0	71.0	5.0	3.9	1.1	0		49.5		150.1	100 ⁽²⁾
71.0	76.0	5.0	3.1	1.9	0		51.4	142.6		85.4 ⁽²⁾
76.0	78.2	2.2	1.7	0.5	0		54.5		152.0	100 ⁽²⁾
		**RQD on limestone portion only.					61.1		151.6	100 ⁽²⁾
WATER TABLE OBSERVATIONS								67.9	146.0	95.7 ⁽²⁾
Date		Time Change		Depth Hole Open		Depth To Water	(1) Assumed			
							(2) Actual			

N₆₀ - Corrected N value for standard 60% SPT efficiency.

N₆₀ = (Em/60)Nm Em - Measured transfer efficiency in percent.

Nm - Observed N-value.



APPENDIX I
CONSTRUCTION AND LOAD TEST PHOTOGRAPHS FOR WAVERLY TEST
SITE



I1- Pier 11 at Waverly site.



I2- Pier 11 at Waverly site.



I3- American 9270 Series crane with a Hain twin drill, drilling rock socket at Pier 12, existing bridge in background.



I4- Temporary outer casing, inner permanent casing, and casing clamp at Pier 12 (Pier 11 is in the background).



I-5- Pier 10 on North river bank



I6- Bullet tooth rock auger used to excavate rock socket at Waverly test site.



I7- Core Barrel used to excavate rock socket at Waverly test site.



I8- Vibratory Hammer



I9- Using vibratory hammer to set casing at Pier 12.



I10- Miniature shaft inspection device (Mini-SID) used to inspect bottom of rock sockets at Waverly bridge site.



I11- Mini-SID inspecting shaft.



I12- Rebar cage with Osterberg load cell.



I13- Portable Slurry Plant



I14- Delivering concrete to site



I-15- Using tremie to place concrete.

APPENDIX J
BORING LOGS AND CORE PHOTOGRAPHS FOR WAVERLY TEST SITE

MISSOURI DEPARTMENT OF TRANSPORTATION
Division of Materials
BORING DATA (CORE & SPT)

Sheet 21a of 35

Job No.	J2P0639						
County	Carroll/Lafayette		Route	65.00		Design	A5910
Over	Missouri River					Skew	Right Angles
Logged by	Stevens					Operator	Wineland
Equipment	Failing 1500					Drillers Hole No.	L-00-13
Hole Stab. by	Casing					Date of Work	04/25/00
Automatic Hammer Efficiency				73.00	%	Drill No.	G-7889

Bent		Station		Location		Elevation	LOG OF MATERIALS *	
11.00		95+63		28' LT.		--		Unable to position due to current.
Offset to:		95+60.4		30.1' LT.		663.20	0.0-6.1'	Barge deck.
TEST DATA						657.10	6.1-27.1'	Water.
Depth, ft.	SPT Blows/6"	N ₆₀	(N ₁) ₆₀	Pocket Pen., tsf	Est. Equiv., Qu, tsf	636.10	27.1-35.0'	Brown and gray medium to coarse grained sand, scattered fine gravel, dense.
30.0	23-27-10	45	53	Sand		628.20	35.0-47.0'	Gray coarse grained sand, scattered
40.0	6-6-6	15	15	Sand				fine gravel, medium dense.
50.0	13-13-11	29	26	Sand		616.20	47.0-52.8'	Gray fine to medium grained silty sand, dense.
73.1	82 in 5.5"	100		9.00	5.5	610.40	52.8-58.1'	Gray and purple claystone, soft.
98.7	82 in 2"	100.00		9.00+	14.4	605.10	58.1-63.1'	Greenish-gray clay shale, soft.
						600.10	63.1-64.5'	Dark gray clay shale.
						598.70	64.5-64.7'	Coal.
						598.50	64.7-67.9'	Gray claystone, poorly laminated, soft to medium hard.
						595.30	67.9-68.3'	Coal.
						594.90	68.3-68.4'	Dark brown claystone seam.
						594.80	68.4-71.5'	Gray micaceous silt shale, moderately hard, slightly calcareous.
						591.70	71.5-78.5'	Gray clay shale to claystone, soft.
CORING LOG (NX Double Tube Barrel)						584.70	78.5-85.6'	Black carbonaceous shale, moderately hard, laminated.
From	To	Run	Rec	Loss	% RQD			
53.10	58.10	5.0	4.80	0.20	Shale	577.60	85.6-90.2'	Black coal, fossiliferous, brittle, claystone seam at 88.4 to 88.5'.
58.10	63.10	5.0	4.80	0.20	Shale			
63.10	68.10	5.0	4.30	0.70	Shale	573.0	90.2-99.0'	Black carbonaceous clay shale, moderately hard.
68.10	73.10	5.0	5.0	0.00	Shale			
73.70	78.70	5.0	4.50	0.50	Shale	564.2	99.0-100.5'	Brown and gray coarse grained fossiliferous
78.70	88.70	10.0	10.0	0.00	Shale			irregularly bedded limestone, medium bedded, hard.
88.70	98.70	10.0	9.7	0.30	Shale			
98.90	103.90	5.0	5.0	0.00	80.00	562.70	100.5-103.6'	Brown and gray coarse grained sandstone, with black and white laminations, medium bedded, hard.
WATER TABLE OBSERVATIONS								
Date	Time Change	Depth Hole Open		Depth To Water				
						559.60	103.6-103.9'	Brownish-gray claystone, hard.
						559.30		Boring terminated.

N₆₀ = (Em/60)N_m N₆₀ - Corrected N value for standard 60% SPT efficiency. Em - Measured transfer efficiency in percent. N_m - Observed N-value.

(N₁)₆₀ = Normalized standardized blow count corrected for effective overburden pressure.

* Persons using this information are cautioned that the materials shown are determined by the equipment noted and accuracy of the "log of materials" is limited thereby and by judgment of the operator. THIS INFORMATION IS FOR DESIGN PURPOSES ONLY.

MISSOURI DEPARTMENT OF TRANSPORTATION
Division of Materials
BORING DATA (CORE & SPT)

Sheet 21b of 35

Job No.	J2P0639						
County	Carroll/Lafayette		Route	65.00		Design	A5910
Over	Missouri River					Skew	Right Angles
Logged by	Stevens					Operator	Wineland
Equipment	Failing 1500					Drillers Hole No.	L-00-13
Hole Stab. by	Casing					Date of Work	04/25/00
Automatic Hammer Efficiency				73.00	%	Drill No.	G-7889

Bent		Station		Location		Elevation	LOG OF MATERIALS *			
11.00		95+63		28' LT.		--				
Offset to:		95+60.4		30.1' LT.		663.20				
TEST DATA										
Depth, ft.		SPT Blows/6"		N ₆₀	(N ₁) ₆₀	Pocket Pen., tsf	Est. Equiv., Qu, tsf			
							UNCONFINED COMPRESSIVE STRENGTH TEST DATA			
								<u>Elev.</u>	<u>Depth, ft.</u>	<u>Qu, tsf</u>
									<u>P.P., tsf</u>	
								608.4	54.8	1.6
								601.8	61.4	5.3
								597.4	65.8	0.7
								594.0	69.2	9.1
CORING LOG (NX Double Tube Barrel)										
From	To	Run	Rec	Loss	% RQD			586.7	76.5	7.9
								578.0	85.2	37.2
								566.5	96.7	18.8
WATER TABLE OBSERVATIONS										
Date		Time Change		Depth Hole Open		Depth To Water				

N₆₀ = (Em/60)Nm N₆₀ - Corrected N value for standard 60% SPT efficiency. Em - Measured transfer efficiency in percent. Nm - Observed N-value.

(N₁)₆₀ = Normalized standardized blow count corrected for effective overburden pressure.

* Persons using this information are cautioned that the materials shown are determined by the equipment noted and accuracy of the "log of materials" is limited thereby and by judgment of the operator. THIS INFORMATION IS FOR DESIGN PURPOSES ONLY.



MISSOURI DEPARTMENT OF TRANSPORTATION
Division of Materials
BORING DATA (CORE & SPT)

Sheet 23a of 35

Job No.	J2P0639						
County	Carroll/Lafayette		Route	65.00		Design	A5910
Over	Missouri River					Skew	Right Angles
Logged by	Hilchen/Stevens					Operator	Lamberson
Equipment	Failing 1500					Drillers Hole No.	L-00-12
Hole Stab. by	Casing					Date of Work	04/24/00, 04/25/00
Automatic Hammer Efficiency				73.00	%	Drill No.	G-7889

Bent		Station		Location			Elevation	LOG OF MATERIALS *	
11.00		95+70		42' LT.			663.20	Inaccessible due to difficulty in positioning barge.	
Offset to:		95+64		35.5' LT.			663.20	0.0-6.1'	Barge deck.
TEST DATA							657.20	6.1-24.0'	Water.
Depth, ft.	SPT Blows/6"		N ₆₀	(N ₁) ₆₀	Pocket Pen., tsf	Est. Equiv., Qu, tsf	639.20	24.0-30.0'	Gray to tan fine to medium sand, with trace gravel.
35.0	8-8-7		18	19	Sand		633.20	30.0-38.0'	Gray fine sand, medium dense, trace black
45.0	4-6-7		16	15	Sand				lignite fines, fine gravel from 41.6 to 42.3'.
54.0	27-39-43 in 5.5"		100		9.0+	3.9	625.20	38.0-51.1'	Gray medium sand, medium dense.
75.50	82 in 5"		100.00		9.0+	6.0	612.10	51.1-58.6'	Gray and purple claystone, soft.
95.90	82 in 4"		100.00		9.0+	7.4	604.60	58.6-63.8'	Greenish-gray clay shale, soft.
							599.40	63.8-64.3'	Gray to dark gray clay shale, soft to medium hard.
							598.90	64.3-64.4'	Black coal.
							598.80	64.4-67.3'	Gray claystone, poorly laminated, soft to medium hard.
							595.90	67.3-68.1'	Black carbonaceous clay shale, medium hard.
							595.10	68.1-68.4'	Black coal, brittle.
							594.80	68.4-70.5'	Gray claystone, soft.
							592.70	70.5-78.3'	Gray claystone to clay shale, soft, coal at 74.5'.
CORING LOG (NX Double Tube Barrel)							584.90	78.3-85.9'	Black carbonaceous shale, medium hard.
From	To	Run	Rec	Loss	% RQD		582.30	85.9-87.7'	Black coal, fossiliferous, brittle, medium hard.
55.50	60.50	5.0	5.0	0.00			575.50	87.7-99.9'	Black carbonaceous shale, medium hard.
60.50	65.50	5.0	4.80	0.20			563.60	99.9-101.8'	Brown and gray medium to coarse grained, fossiliferous limestone, medium bedded, hard.
65.50	70.50	5.0	4.70	0.30					
70.50	75.50	5.0	5.0	0.00			561.40	101.8-104.9'	Brown and gray coarse grained sandstone, hard.
75.90	80.90	5.0	4.20	0.80					
80.90	85.90	5.0	5.0	0.00			556.30	104.9-105.4'	Dark brown claystone, medium hard.
85.90	90.90	5.0	2.70	2.30			557.80		Boring terminated.
90.90	95.90	5.0	5.0	0.00					
96.30	105.40	9.1	9.10	0.00					
WATER TABLE OBSERVATIONS									
Date		Time Change		Depth Hole Open		Depth To Water			

N₆₀ = (Em/60)Nm N₆₀ - Corrected N value for standard 60% SPT efficiency. Em - Measured transfer efficiency in percent. Nm - Observed N-value.

(N₁)₆₀ = Normalized standardized blow count corrected for effective overburden pressure.

* Persons using this information are cautioned that the materials shown are determined by the equipment noted and accuracy of the "log of materials" is limited thereby and by judgment of the operator. THIS INFORMATION IS FOR DESIGN PURPOSES ONLY.



L-00-12
Bent 11 95+64 35.5' Lt.
4/24/00

MISSOURI DEPARTMENT OF TRANSPORTATION
Division of Materials

BORING DATA (CORE & SPT)

Sheet 24a of 35

Job No.	J2P0639						
County	Carroll/Lafayette		Route	65.00		Design	A5910
Over	Missouri River					Skew	Right Angles
Logged by	Davis					Operator	Lamberson
Equipment	Failing 1500					Drillers Hole No.	L-00-11
Hole Stab. by	Casing					Date of Work	04/24/00
Automatic Hammer Efficiency				73.00	%	Drill No.	G-7889

Bent		Station		Location			Elevation	LOG OF MATERIALS *	
11.00		95+77		56' LT.					
Offset to:		95+78.5		55.3' LT.			663.20	0.0-6.1'	Barge deck.
TEST DATA							657.10	6.1-28.6'	Water.
Depth, ft.	SPT Blows/6"		N ₆₀	(N ₁) ₆₀	Pocket Pen., tsf	Est. Equiv., Qu, tsf	634.60	28.6-51.3'	Gray coarse grained sand, dense to very dense.
30.0	40-41 in 4"		100	118	Sand	3.9	611.90	51.3-53.2'	Gray thinly to thickly laminated silt shale,
40.0	2-3-7		12	12					weathered, soft, cut with rockbit
50.0	14-20-21		50	44					from 51.5 to 53.2'.
63.20	39-43 in 4"		100		9.0+	4.0	610.0	53.2-58.5'	Gray and purple poorly laminated
84.0	82 in 4"		100		9.0+	7.4			claystone, medium hard.
							604.70	58.5-61.7'	Greenish-gray thinly laminated clay shale,
									soft, brown claystone seam from 59.6 to 60.0'
							601.50	61.7-66.7'	Gray poorly laminated claystone,
									soft to medium hard.
							596.50	66.7-68.2'	Black bituminous coal, medium hard, brittle.
							595.0	68.2-69.8'	Gray micaceous silt shale, medium hard.
							593.40	69.8-76.2'	Gray poorly laminated claystone,
									soft to medium hard.
CORING LOG (NX Double Tube Barrel)							587.0	76.2-81.6'	Dark gray to black clay shale, medium hard
From	To	Run	Rec	Loss	% RQD				to moderately hard.
53.20	58.20	5.0	0.00	0.00			581.60	81.6-85.5'	Black, brittle, thinly bedded to thickly
58.20	63.20	5.0	0.00	0.00					laminated bituminous coal.
64.0	74.0	10.0	8.40	1.60			577.70	85.5-90.4'	Gray thinly to thickly laminated calcareous
74.0	79.0	5.0	5.0	0.00					sandy silt shale, medium hard, brittle.
79.0	84.0	5.0	4.10	0.90			572.80	90.4-99.5'	Gray thinly laminated silt shale,
84.30	89.30	5.0	4.50	0.50					soft to medium hard.
89.30	94.30	5.0	5.0	0.00			563.70	99.5-100.8'	Gray medium bedded coarse grained
94.30	99.30	5.0	5.0	0.00					limestone, moderately hard to hard.
99.30	104.30	5.0	5.0	0.00	100**		562.40	100.8-104.3'	Brown and gray coarse grained sandstone,
WATER TABLE OBSERVATIONS									medium to moderately hard.
Date	Time Change		Depth Hole Open		Depth To Water		558.90		Boring terminated.
								**RQD on limestone portion only.	

N₆₀ = (Em/60)Nm N₆₀ - Corrected N value for standard 60% SPT efficiency. Em - Measured transfer efficiency in percent. Nm - Observed N-value.

(N₁)₆₀ = Normalized standardized blow count corrected for effective overburden pressure.

* Persons using this information are cautioned that the materials shown are determined by the equipment noted and accuracy of the "log of materials" is limited thereby and by judgment of the operator. THIS INFORMATION IS FOR DESIGN PURPOSES ONLY.

MISSOURI DEPARTMENT OF TRANSPORTATION
Division of Materials

BORING DATA (CORE & SPT)

Sheet 24b of 35

Job No.	J2P0639						
County	Carroll/Lafayette		Route	65.00		Design	A5910
Over	Missouri River					Skew	Right Angles
Logged by	Davis					Operator	Lamberson
Equipment	Failing 1500					Drillers Hole No.	L-00-11
Hole Stab. by	Casing					Date of Work	04/24/00
Automatic Hammer Efficiency				73.00	%	Drill No.	G-7889

Bent	Station	Location	Elevation	LOG OF MATERIALS *			
11.00	95+77	56' LT.					
Offset to:	95+78.5	55.3' LT.					
TEST DATA							
Depth, ft.	SPT Blows/6"	N₆₀ (N₁)₆₀	Pocket Pen., tsf	Est. Equiv., Qu, tsf			
				UNCONFINED COMPRESSIVE STRENGTH TEST DATA			
					Elev.	Depth, ft.	Qu, tsf P.P., tsf
					607.2	56.0	4.1 9.0+
					601.8	61.4	4.7 9.0+
					598.2	65.0	2.1 9.0+
					592.8	70.4	10.2 9.0+
					587.2	76.0	2.9 9.0+
					570.2	93.0	9.1 9.0+
					561.7	101.5	56.7 9.0+
CORING LOG (NX Double Tube Barrel)							
From	To	Run	Rec	Loss	% RQD	SIEVE ANALYSIS (PERCENT PASSING)	
						AASHTO T88	
						Depth, ft.	
						30	40 50
						3/4"	100 100 100
						3/8"	100 99 99
						No. 4	99 99 98
WATER TABLE OBSERVATIONS						No. 10	98 98 97
Date	Time Change	Depth Hole Open	Depth To Water			No. 16	96 94 96
						No. 40	68 16 88
						No. 50	46 8 82
						No. 100	12 3 57
						No. 200	9 2 20

N₆₀ = (Em/60)Nm N₆₀ - Corrected N value for standard 60% SPT efficiency. Em - Measured transfer efficiency in percent. Nm - Observed N-value.

(N₁)₆₀ = Normalized standardized blow count corrected for effective overburden pressure.

* Persons using this information are cautioned that the materials shown are determined by the equipment noted and accuracy of the "log of materials" is limited thereby and by judgment of the operator. THIS INFORMATION IS FOR DESIGN PURPOSES ONLY.



L-00-11
Bent 11 95+78.5 55.3' Lt.
4/24/00

MISSOURI DEPARTMENT OF TRANSPORTATION
Division of Materials

BORING DATA (CORE & SPT)

Sheet 25a of 35

Job No.	J2P0639						
County	Carroll/Lafayette		Route	65.00		Design	A5910
Over	Missouri River					Skew	Right Angles
Logged by	Stevens					Operator	Wineland
Equipment	Failing 1500					Drillers Hole No.	L-00-10
Hole Stab. by	Casing					Date of Work	04/24/00
Automatic Hammer Efficiency				73.00	%	Drill No.	G-7889

Bent		Station		Location			Elevation	LOG OF MATERIALS *	
11.00		95+77		28' LT.			663.30	0.0-6.1'	Barge deck.
							657.20	6.1-25.7'	Water.
TEST DATA							637.60	25.7-47.0'	Gray medium to coarse grained sand,
Depth, ft.	SPT Blows/6"	N ₆₀	(N ₁) ₆₀	Pocket Pen., tsf	Est. Equiv., Qu, tsf				with light brown to gray silt, dense.
30.0	31-16-9	30	35			616.30	47.0-51.2'		Gray fine grained clayey sand, dense.
40.0	9-9-11	22	22			612.20	51.2-56.9'		Gray and purple claystone, soft.
50.0	4-5-17	27	24			606.40	56.9-62.7'		Greenish-gray clay shale, soft,
72.70	62-20 in 1.5"	100		9.00+	4.3				claystone seam at 60.4'.
88.40	82 in 4"	100		9.00+	7.4	600.60	62.7-67.0'		Gray to dark gray clay shale,
									soft to medium hard.
						596.30	67.0-67.7'		Black carbonaceous clay shale,
									medium hard.
						595.60	67.7-70.1'		Gray claystone, poorly laminated, soft.
						593.20	70.1-70.8'		Coal.
						592.50	70.8-73.8'		Gray silt shale to siltstone, medium hard.
						589.50	73.8-74.4'		Coal.
						588.90	74.4-78.2'		Gray clay shale, medium hard.
						585.10	78.2-85.2'		Black carbonaceous clay shale,
CORING LOG (NX Double Tube Barrel)									medium hard.
From	To	Run	Rec	Loss	% RQD	578.0	85.2-91.4'		Black coal and carbonaceous shale,
52.70	57.70	5.0	5.0	0.00					soft, brittle.
57.70	62.70	5.0	4.50	0.50		571.80	91.4-99.3'		Black carbonaceous clay shale,
62.70	67.70	5.0	5.0	0.00					moderately hard.
67.70	72.70	5.0	4.60	0.40		564.0	99.3-100.5'		Brown and gray, medium to coarse grained,
73.40	78.40	5.0	5.0	0.00					irregularly bedded, fossiliferous limestone,
78.40	83.40	5.0	5.0	0.00					hard, fair quality.
WATER TABLE OBSERVATIONS							560.80	100.5-103.8'	Gray and brown coarse grained sandstone,
Date	Time Change	Depth Hole Open		Depth To Water					thin bedded, hard, well to moderate
									cementation.
						559.50			Boring terminated.

N₆₀ = (Em/60)Nm **N₆₀** - Corrected N value for standard 60% SPT efficiency. Em - Measured transfer efficiency in percent. Nm - Observed N-value.

(N₁)₆₀ = Normalized standardized blow count corrected for effective overburden pressure.

* Persons using this information are cautioned that the materials shown are determined by the equipment noted and accuracy of the "log of materials" is limited thereby and by judgment of the operator. THIS INFORMATION IS FOR DESIGN PURPOSES ONLY.

MISSOURI DEPARTMENT OF TRANSPORTATION
Division of Materials
BORING DATA (CORE & SPT)

Sheet 25b of 35

Job No.	J2P0639						
County	Carroll/Lafayette		Route	65.00		Design	A5910
Over	Missouri River					Skew	Right Angles
Logged by	Stevens					Operator	Wineland
Equipment	Failing 1500					Drillers Hole No.	L-00-10
Hole Stab. by	Casing					Date of Work	04/24/00
Automatic Hammer Efficiency				73.00	%	Drill No.	G-7889

Bent		Station		Location		Elevation	LOG OF MATERIALS *			
11.00		95+77		28' LT.						
TEST DATA										
Depth, ft.		SPT Blows/6"		N ₆₀	(N ₁) ₆₀	Pocket Pen., tsf	Est. Equiv., Qu, tsf			
								UNCONFINED COMPRESSIVE STRENGTH TEST DATA		
								<u>Elev.</u>	<u>Depth, ft.</u>	<u>Qu, tsf</u>
									<u>P.P., tsf</u>	
								607.4	55.9	0.8
								602.8	60.5	3.6
								599.1	64.2	3.1
								585.9	77.4	3.3
								582.9	80.4	13.9
								568.4	94.9	8.1
CORING LOG (NX Double Tube Barrel)										
From	To	Run	Rec	Loss	% RQD					
83.40	88.40	5.0	3.60	1.40						
88.8	98.80	10.0	10.0	0.00						
98.8	103.8	5.0	4.50	0.50	72.00					
WATER TABLE OBSERVATIONS										
Date		Time Change		Depth Hole Open		Depth To Water				

N₆₀ = (Em/60)Nm N₆₀ - Corrected N value for standard 60% SPT efficiency. Em - Measured transfer efficiency in percent. Nm - Observed N-value.
(N₁)₆₀ = Normalized standardized blow count corrected for effective overburden pressure.

* Persons using this information are cautioned that the materials shown are determined by the equipment noted and accuracy of the "log of materials" is limited thereby and by judgment of the operator. THIS INFORMATION IS FOR DESIGN PURPOSES ONLY.



L-00-10
Bent 11 95+77 28' Lt.
4/24/00

APPENDIX K
GEOLOGY FOR SOUTH ABUTMENT AT LEXINGTON SITE

The Cherokee Group is overlain by the Marmaton Group. The Marmaton Group contains more limestone units than the Cherokee Group and was encountered in the subsurface investigation for the piers located on the bluff near the south abutment. The Marmaton Group is comprised of two subgroups, the Fort Scott Subgroup and the Appanoose Subgroup. The Fort Scott Subgroup includes four formations from the base upwards: the Excello, Blackjack Creek, Little Osage, and Higginsville: formations as described below.

Excello Formation: The Excello Shale consists of dark gray shale with green shale partings, (Thompson 1995). This formation was encountered from about elevation 201 to 201.9 m and averages about 0.8 m (2.6 ft) in thickness.

Blackjack Creek Formation: The Blackjack Creek Limestone consists of a lower and an upper unit of earthy limestone (Thompson 1995). This formation was encountered from about elevation 201.9 to 203 m and averages about 1.1 m (3.6 ft) in thickness.

Little Osage Formation: The Little Osage Formation includes a thinly laminated calcareous shale, poorly laminated clay shale, (probably underclay), the Summit Coal Bed, a black carbonaceous shale, and a gray thick bedded limestone (Houx Limestone Member), (Thompson 1995). The Houx Limestone member was encountered at about elevation 206 m. The Houx Limestone was overlain by gray to dark gray or reddish brown shale. The upper part of the Little Osage Formation was light gray and tan shale with light brown laminations. This formation was encountered from about elevation 203 to 212.1 m and averages about 9.1 m (29.9 ft) in thickness.

Higginsville Formation: The Higginsville Limestone consists of a light gray, fine grained, thin to medium bedded limestone. This formation was encountered from about elevation 212.1 to 213.6 m and averages about 1.5 m (4.9 ft) in thickness.

The subsurface investigation for the piers on the bluff south of the river encountered four of the seven widely-recognized successions of the Appanose Subgroup of the Marmaton Group. These are from the base upward: Labette Formation, Pawnee Formation, Bandera Formation, and the Altamont Formation. The Altamont Formation is overlain by about 5.5 m (18.0 ft) of eolian loess, a wind blow soil. The Labette Formation was encountered during excavation of pier 25 and the Bandera and Altamont Formations were encountered at pier 26.

Labette Formation: The Labette Formation consists of an underclay, the Alvis Coal bed, a dark gray fossiliferous shaly limestone, and the Lexington Coal Bed (Thompson 1995). The Lexington Coal Bed was mined from the 1860's to the 1920's and the end abutment (bent 26) is located directly over Riverton Mine No. 2. This formation was encountered from about elevation 213.6 to 215.8 m and averages about 2.2 m (7.2 ft) in thickness.

Pawnee Formation: The Pawnee Formation consists of a dark gray to black fissile shale (Anna Shale Member), a gray thin bedded limestone (Myrick Station Limestone Member), dark gray shale (Mine Creek Shale Member), and a medium to thick bedded Limestone (Coal City Limestone Member), (Thompson 1995). The Mulberry Coal Bed was not encountered in the borings. This formation was encountered from about elevation 215.8 to 220.8 m and averages about 5.0 m (16.4 ft) in thickness.

Bandera Formation: The Bandera Formation consists of a gray to brown shale overlain by purple shale. The purple shale is overlain by gray to brown shale to sandstone (Bandera Quarry Member), (Thompson 1995). This formation was encountered from about elevation 220.8 to 226.1 m and averages about 5.3 m (17.3 ft) in thickness.

Altamont Formation: The Altamont Formation consists of three members from the base upwards: the Amoret Limestone Member, the Lake Neosho Shale Member, and the Worland Limestone Member (Thompson 1995). Only the Amoret Limestone and the Lake Neosho Shale were encountered in the borings from about elevation 227.4 to 226.1 m. The formation averages about 1.3 m (4.3 ft) in thickness.

REFERENCES

- AASHTO, (1996). "Standard Specifications for Highway Bridges," 16th edition, American Association of State Highway Transportation Officials, Washington, D.C.
- ASTM D1143-93, "Standard Test Method for Piles Under Static Axial Compressive Load," *Annual Book of ASTM Standards*, Vol., 04.08, Soil and Rock, American Society for Testing and Materials, Philadelphia, PA, 1995 pp. 194-209
- ASTM D3967, "Standard Test Method for Splitting Tensile Strength of Intact Rock Core Specimens," *Annual Book of ASTM Standards*, Vol., 04.08, Soil and Rock, American Society for Testing and Materials, Philadelphia, PA, 1995
- Baycan, S. (1996). "Field Performance of Expansive Anchors and Piles in Rock," PhD dissertation, Department of Civil Engineering, Monash University, Clayton, Victoria, Australia, October.
- Carter, J.P. and Kullhawy, F.H. (1983). "Analysis and Design of Foundations Socketed into Rock," Research Report 1493-4, Geotechnical Engineering Group, Cornell University, Ithaca, New York, January 1987.
- Carrubba, P. (1997). "Skin Friction of large-diameter piles socketed into rock," *Canadian Geotechnical Journal*, Vol. 34, No. 2, pp. 230-240.
- Gibson, G. L. and Devenny, D. W. (1973). "Concrete to bedrock bond testing by jacking from bottom of a borehole," *Canadian Geotechnical Journal*, Vol. 10, No. 2, pp. 304-306.
- Goeke, P. M., and Hustad, P. A. (1979). "Instrumented Drilled Shafts in Clay-Shale," *Proceedings of Symposium on Deep Foundations*, E. M. Fuller, ed., ASCE National Convention, Atlanta, GA., pp. 149-164.
- Goodwin, J. W. (1993). "Bi-directional load testing of shafts to 6000 tons," *Proceedings of Geotechnical Special Publication No. 38*, Nelson, P., Smith, T., & Clukey, E., eds., ASCE, New York, NY., pp. 204-217.
- Hassan, K. M., & O'Neill, M. W. (1997), "Side Load-Transfer Mechanisms in Drilled Shafts in Soft Argillaceous Rock," *Journal of Geotechnical and Environmental Engineering*, ASCE, Vol. 123, No. 2, pp. 145-152.
- Hassan, K. M., O'Neill, M. W., Sheikh, S. A., & Ealy, C. D. (1997). "Design Method for Drilled Shafts in Soft Argillaceous Rock," *Journal of Geotechnical and Environmental Engineering*, ASCE, Vol. 123, No. 3, pp. 272-280.

Hayes, J. and Simmonds, T. (2002). "Interpreting Strain Measurements From Load Tests in Bored Piles," *Proceedings of Ninth International Conference on Piling and Deep Foundations*, Nice, France.

HNTB, (1998). "Geotechnical Investigation Report, Bridge No. A-5664 over Missouri River, Missouri Route 13, Ray/Lafayette Counties, Missouri," Consultant report produced for Missouri Department of Transportation, July.

HNTB, (1999). "Supplemental Geotechnical Investigation Report, Bridge No. A-5664 over Missouri River, Missouri Route 13, Ray/Lafayette Counties, Missouri," Consultant report produced for Missouri Department of Transportation, September.

HNTB, (2002). "Drilled Shaft Load Test and Supplemental Foundation Recommendations, Bridges A6252 and A6254, Jackson County, Missouri, Job No. J4I0766E," Consultant report produced for Missouri Department of Transportation, August 2002.

Horvath, R. G. and Kenney, T. C. (1979). "Shaft Resistance of Rock-Socketed Drilled Piers," *Proceedings of Symposium on Deep Foundations*, ASCE, pp. 182-214.

Horvath, R. G., Kenney, T. C., and Kozicki, P. (1983). "Methods of Improving the Performance of Drilled Piers in Weak Rock," *Canadian Geotechnical Journal*, Vol. 20, No. 4, pp. 758-772.

Hummert, J. B., and Cooling, T. L. (1988). "Drilled Pier Test, Fort Collins, Colorado," *Proceedings of second International Conference on Case Histories in Geotechnical Engineering*, S. Prakash, ed., University of Missouri-Rolla, Vol. 3, pp. 1375-1382.

Jackson, W. T., Perez, J. Y., and Lacroix, Y. (1974). "Foundation construction and performance for a 34-storey building in St. Louis," *Geotechnique*, Vol. 24, No. 1, pp. 63-90.

Kiehne, C. T., (1997) "Full Scale load tests of rock socketed drilled shafts," Master thesis, University of Missouri, Columbia.

Kishida, H., (1992). "Pile Testing in Osaka Amenity Park Project," Paper by Mitsubishi Co.

Kodikara, J. K., Johnston, I. W., and Haberfield, C. M. (1992). "Analytical Prediction For Side Resistance of Piles in Rock," *Proceedings of Sixth Australia-New Zealand Conference on Geomechanics*, Christchurch, New Zealand, pp. 156-162.

Kulhawy, F. H. & Phoon, K. (1993). "Drilled shaft side resistance in clay soil to rock," *Proceedings of Geotechnical Special Publication No. 38*, Nelson, P., Smith, T., & Clukey, E., eds., ASCE, New York, NY., pp. 172-183.

- Kyfor, Z. G., Schnore, A. R., Carlo, T. A., and Baily, P. F., (1992). "Static Testing of Deep Foundations," *Report No. FHWA-SA-91-042*, FHWA, Washington, DC. pp. 174.
- Lutten, R. J. (1977), "Slaking Indexes for Design and Construction of Compacted Shale Embankments," *Report No. FHWA-RD-77-1*, FHWA, Washington, DC, Vol. 3, pp. 94.
- Matich, M. A. and Kozicki, P. (1967). "Some load tests on drilled cast-in-place concrete caissons," *Canadian Geotechnical Journal*, Vol. 4, No. 4, pp. 357-375.
- McVay, M. C., Townsend, F. C., and Williams, R.C. (1992). "Design of Socketed Shafts in Limestone," *Journal of Geotechnical Engineering*, ASCE, Vol.118, No.10, pp. 1626-1637.
- Moore, W. W. (1964). "Foundation design," *Civil Engineering*, ASCE, Vol. 34 No. 1, pp. 33-35.
- Ogura, H., Sumi, M., Kishida, H., and Yoshifuka, T. (1996). "Application of the Pile Toe Test for Cast-in-Place and Precast Piles," *Foundation Drilling Magazine*, December 1996/January 1997.
- O'Neill, M. W., & Hassan, K. M. (1993). "Perimeter load transfer in drilled shafts in the Eagle Ford formation," *Proceedings of Geotechnical Special Publication No. 38*, Nelson, P., Smith, T., & Clukey, E., eds., ASCE, New York, NY., pp. 229-244.
- O'Neill, M. W., Townsend, F. C., Hassan, K. M., Buller, A., and Chan, P. S. (1996). "Load Transfer for Drilled Shafts in Intermediate Geomaterials," *Report No. FHWA-RD-95-172*, FHWA, Washington, DC., pp. 194.
- O'Neill, M. W. and Reese, L. C. (1999). "Drilled Shafts: Construction Procedures and Design Methods," *Report No. FHWA-IF-99-025*, FHWA, Washington, DC., pp. 758.
- O'Neill, M. W. (2001). "Side Resistance in Piles and Drilled Shafts," *Journal of Geotechnical and Geoenvironmental Engineering*, ASCE, Vol. 127 No.1, pp. 3-16.
- Osterberg, J. (1992). "Rock Socket Friction in Drilled Shafts: It's Greater Than You Think," *Foundation Drilling Magazine*, Vol. 21, No. 1, December/January, pp.15- 21.
- Osterberg, J. (1998). "The Osterberg Load Test Methods for Bored and Driven Piles the First Ten Years," *Proceedings of the Seventh International Conference on Piling and Deep Foundations*, Deep Foundations Institute, Vienna, Austria, pp.1-17.
- Osterberg J. (1999). "What Has Been Learned About Drilled Shafts From Osterberg Load Test," Paper presented at the Deep Foundations Institute Annual Meeting, October.

Osterberg, J. (2000). "Side Shear and End Bearing in Drilled Shafts," *Proceedings of Sessions of Geo Denver 2000- New Technological and Design Developments in Deep Foundations*, Denver, Colorado, pp. 72-79.

Pells, P. J. N., Rowe, R. K., and Turner, R. M. (1980), "An experimental investigation into side shear for socketed piles in sandstone," *Proceedings of the International Conference on Structural Foundations on Rock*, Sydney, Australia, Vol. 1, pp.291-302.

Reese, L. C., (1984), "Handbook on Design and Construction of Piles and Drilled Shafts under Lateral Load," *Report No. FHWA-IP-84-11*, FHWA, Washington, DC., pp. 386.

Reese, L. C. and O'Neill, M. W. (1988). " Drilled Shafts: Construction Procedures and Design Methods," *Report No. FHWA-HI-88-042*, FHWA, Washington, DC., pp. 564.

Rosenberg, P. and Journeaux, N. I. (1976). " Friction and End Bearing for High Capacity Socket Design," *Canadian Geotechnical Journal*, Vol. 13, No. 3, pp. 324-333.

Rowe, R. K., and Armitage, H. H. (1987). " A Design Method for Drilled Piers in Soft Rock," *Canadian Geotechnical Journal*, Vol., 24 No. 1, pp. 126-142.

Seidel, J. P., and Haberfield (1995). "Towards Understanding of Joint Roughness," *Rock Mechanics and Rock Engineering*, Department of Civil Engineering, Monash University, Clayton, Victoria, Australia, Vol. 28, No. 2, pp. 69-92.

Seidel, J. P., (1998). *Program ROCKET*, Department of Civil Engineering, Monash University, Clayton, Victoria, Australia.

Seychuck, J. L. (1970). "Load tests on bedrock," *Canadian Geotechnical Journal*, Vol. 7, No. 4, pp. 454-469.

Schmertmann, J. H., and Hayes, J. A. (1997). " The Osterberg Cell and Bored Pile Testing a Symbiosis," *Proceedings of Third International Geotechnical Conference*, Cairo Egypt.

Schmertmann, J. H., Hayes, J. A., Molnit, T., and Osterberg, J. O. (1998). " O-cell Testing Case Histories Demonstrate the Importance of Bored Pile (Drilled Shaft) Construction Technique," *Proceedings of the Fourth International Conference on Case Histories in Geotechnical Engineering*, St. Louis, Missouri, pp. 1103-1150.

Shi, L. and Brown, D. A. (2002). "Details of Osterberg Cell Finite Element Analyses," Master thesis, Department of Civil Engineering, University of Alburn, Auburn, Alabama.

Thompson, T. L., and Howe, W. B, (1995). "The Stratigraphic Succession in Missouri," Missouri Department of Natural Resources, Division of Geology and Land Survey, Vol. 40, pp. 93-116.

Thorburn, S., (1966). "Large Diameter Piles Founded on Bedrock," *Proceeding of Large Bored Piles Conference*, Institute of Civil Engineers, London, England, pp. 121-129.

URS Greiner Woodward Clyde, (2001). "Geotechnical Investigation Report, Bridge No. A6270, Missouri Route I-470, Jackson County, Missouri," Consultant report produced for Missouri Department of Transportation, April.

Williams, A. F., Johnston, I. W., and Donald, I. B. (1980). "The Design of Socketed Piles in Weak Rock," *Proceedings of International Conference on Structural Foundations on Rock*, I. A. A. Balkema, Rotterdam, The Netherlands, Vol. 1, pp. 327-347.

Williams, A. F., and Pells, P. J. N. (1981). "Side Resistance of Rock Sockets in Sandstone, Mudstone, and Shale," *Canadian Geotechnical Journal*, Ottawa, Canada, Vol. 18, No. 4, pp. 502-513.

Wood, L.E. and Deo, P. (1975), "A Suggested System for Classifying Shale Materials for Embankments," *Bulletin of the Association of Engineering Geologists*, Vol. 12, No. 1 pp. 39-55.

Zhang, L. & Einstein, H. H. (1998). "End Bearing Capacity of Drilled Shafts in Rock," *Journal of Geotechnical and Environmental Engineering*, ASCE, Vol. 124, No. 7, pp. 574-584.